Titre: Title:	Improving the Seismic Response of Tall Braced Streel Frames with Segmental Elastic Spine
Auteur: Author:	Liang Chen
Date:	2018
Type:	Mémoire ou thèse / Dissertation or Thesis
Référence: Citation:	Chen, L. (2018). Improving the Seismic Response of Tall Braced Streel Frames with Segmental Elastic Spine [Ph.D. thesis, École Polytechnique de Montréal]. PolyPublie. https://publications.polymtl.ca/3305/

URL de PolyPublie: PolyPublie URL:	https://publications.polymtl.ca/3305/
Directeurs de recherche: Advisors:	Robert Tremblay, & Lucia Tirca
Programme: Program:	Génie civil

UNIVERSITÉ DE MONTRÉAL

IMPROVING THE SEISMIC RESPONSE OF TALL BRACED STEEL FRAMES WITH SEGMENTAL ELASTIC SPINE

LIANG CHEN

DÉPARTEMENT DES GÉNIES CIVIL, GÉOLOGIQUE ET DES MINES

ÉCOLE POLYTECHNIQUE DE MONTRÉAL

THÈSE PRÉSENTÉE EN VUE DE L'OBTENTION

DU DIPLÔME DE PHILOSOPHIAE DOCTOR

(GÉNIE CIVIL)

SEPTEMBRE 2018

UNIVERSITÉ DE MONTRÉAL

ÉCOLE POLYTECHNIQUE DE MONTRÉAL

Cette thèse intitulée :

IMPROVING THE SEISMIC RESPONSE OF TALL BRACED STEEL FRAMES WITH SEGMENTAL ELASTIC SPINE

présentée par : CHEN Liang

en vue de l'obtention du diplôme de: Philosophiae Doctor

a été dûment acceptée par le jury d'examen constitué de :

M. LÉGER Pierre, Ph. D., président

M. TREMBLAY Robert, Ph. D., membre et directeur de recherche

Mme TIRCA Lucia, Ph. D., membre et codirectrice de recherche

M. BOUAANANI Najib, Ph. D., membre

M. GUIZANI Lotfi, Ph. D., membre

ACKNOWLEDGEMENTS

This thesis not only represents my work at the keyboard, but is also a milestone in my years of searching for the best seismic resistant systems. Research is never an easy task, I am glad that I have met so many great people along the way.

First and foremost, I would like to express my sincere gratitude towards my supervisor Prof. Robert Tremblay. He has been supportive since the first day I began working with him. He always encourages me to take on harder tasks and uses his immense knowledge and wisdom to guide me through the journey. He helped me come up with the thesis topic and supported me for all the years I spent on this topic. I appreciate all his contributions of time, ideas and funding to make my Ph.D. experience stimulating.

I also would like to thank my co-supervisor Prof. Lucia Tirca. She has been my supervisor since I started my graduate study. Her enthusiasm for research work has been an inspiration to me for over eight years. She is the nicest person I know, and I am really thankful for all the support she provided.

Many people have helped and taught me immensely at Ecole Polytechnique de Montreal. The technicians and researchers at structural lab: Martin Leclerc. Romain Siguier, Xavier Willem. Thanks to them for their kind assistance during the time I worked in the lab. I would also like to thank Yasaman Minouei, Ali Imanpour, Morteza Dehghani, Paul Mottier for their kindly shared research and laboratory experience.

I am grateful to all my colleagues when I worked as an intern in SBSA Experts-conseils en structure: Jeffrey Leibgott, Evan Irvine, Alessio Bernardi. They taught me what civil engineering is about with real-life examples. I will treasure this experience all my life.

I gratefully acknowledge the funding sources that made my Ph.D. work possible. The funding was provided by the National Science Engineering Research Council and the Fonds de Recherche du Quebec – Nature et Technologies. I also want to acknowledge the funding source that provided me the valuable intern experience, the Mitacs Accelerate program.

Lastly, I would like to thank my family for all their love, encouragement and support. For my parents who raised me with a love of science and supported me in all my pursuits. And most of all

for my loving, supportive, encouraging, and patient wife Xuan Qin whose faithful support during this rugged but fruitful journey is much appreciated. Love you.

Liang Chen

Ecole Polytechnique de Montreal

August 2018

RÉSUMÉ

Les cadres contreventés en acier conventionnels sont largement utilisés comme systèmes de résistance à la force latérale contre les tremblements de terre pour leur réponse sismique légère et ductile. Cependant, de nombreuses études ont prouvé que les cadres à contreventement concentrique (CBF) et les cadres à contreventement excentré (EBF) sont enclins à un mécanisme d'effondrement à étage mou. Les dommages sont susceptibles de se concentrer sur un seul étage après le début de la production de l'élément de dissipation d'énergie (entretoise ou maillon) à l'étage correspondant.

De nombreuses configurations structurelles innovantes ont été proposées au cours des dernières décennies pour empêcher l'effondrement des cadres à ossature en acier, le cadre à contreventement excentré (TBF) étant l'un d'entre eux. TBF est développé basé sur EBF conventionnel. Des liens élastiques sont ajoutés pour attacher les liens ductiles des étages adjacents. Ainsi, les liens, les colonnes, le faisceau à l'extérieur des liens, et les entretoises forment une colonne élastique continue le long de la hauteur du bâtiment, pour forcer un mécanisme d'effondrement global. Bien que des performances sismiques remarquables soient obtenues avec les TBF, les demandes de force dans les éléments structurels croissent exponentiellement avec le nombre croissant d'étages dans la structure. En conséquence, il devient rentable de concevoir et de construire un tel système dans des bâtiments plus hauts.

Un nouveau type de configuration structurelle appelé structures contreventées de treillis élastique segmentés (SESBF) est proposé et étudié dans cette recherche. Ce système évolue à partir des EBF et TBF conventionnels tout en combinant les avantages des deux systèmes, à savoir le poids léger et la demande sismique réduite des EBF et la performance sismique améliorée des TBF. Un cadre entièrement attelé excentré est divisé en plusieurs segments le long de la hauteur du bâtiment, et les liens entre les segments sont retirés. Par conséquent, le moment fléchissant de l'épine élastique continue est libéré au niveau des articulations entre les segments. Une série d'analyses numériques est menée pour examiner la réponse sismique du système de segment rachidien élastique avec EBF et TBF conventionnels comme références. Il est prouvé que le système d'élasticité segmentaire élastique, s'il est conçu correctement, peut atteindre une performance sismique optimale sans augmentation significative en termes de coût. L'accent d'un design approprié est mis en avant car

une tendance du développement de segment mou est prévisible pour les bâtiments élevés dans des conditions de charge sismique extrêmes.

Afin de développer une méthode de conception pratique et robuste, une combinaison d'approches analytique et numérique est employée. Un groupe de SESBFs allant de 8 à 24 étages avec différentes longueurs de segments est conçu avec les résultats obtenus à partir d'analyses de l'historique de la réponse temporelle non linéaire. La demande en forces de chaque élément structural et la réponse sismique des structures sont étudiées à la fois dans le domaine temporel et dans le domaine fréquentiel. Une analyse modale est également effectuée pour ces structures. On observe que la réponse post-élastique où les composantes principales se sont plastifiées à un effet significatif sur la demande de force maximale des membres des épines élastiques. Avec ces résultats, une méthode de conception qui utilise la technique de superposition modale est proposée et vérifiée numériquement pour déterminer la demande de force des membres structurels dans les fermes élastiques avec des sections de liaison données. Une analyse de spectre de réponse modifiée est utilisée pour prédire la demande de force des éléments élastiques en raison de modes de vibration plus élevés.

Pour aider à déterminer la longueur et la configuration optimales des segments, une procédure complète pour la conception préliminaire et l'optimisation du SESBF est également développée. Cette procédure est basée sur un modèle numérique simplifié. Ce modèle regroupe la rigidité de cisaillement et la rigidité à la flexion de chaque segment dans les SESBFs en un ressort de cisaillement et une colonne élastique. Des équations et des procédures pour estimer ces raideurs sont également développées. Ainsi, les concepteurs peuvent effectuer à la fois l'analyse de spectre et l'analyse de l'historique temporel pour une configuration particulière d'intérêt, sans connaître les propriétés exactes de la trame. Une fois qu'un niveau de performance cible est sélectionné, une configuration optimale peut être déterminée à l'aide de quelques itérations de l'analyse de l'historique temporel. Cette procédure est vérifiée numériquement, une bonne corrélation entre le modèle simplifié et le modèle complet est atteinte. L'application de la procédure proposée est démontrée pour un SESBF de 24 étages.

Un programme d'essais expérimental est également développé à l'aide du simulateur de tremblement de terre du Laboratoire d'ingénierie structurelle de la Polytechnique de Montréal. Un

cadre à chevrons de 8 étages conçu sur la base du NBCC de 1980 et un SESBF de 8 étages à deux segments conçus avec les exigences de force résultant d'une analyse de l'historique temporel non linéaire sont conçus et réduits à 30%. Le cadre mis à l'échelle et le cadre original sont analysés par analyse numérique pour valider le modèle mis à l'échelle. Des tests de mise en forme en temps réel seront effectués sur les trames mises à l'échelle pour confirmer les prédictions obtenues à partir de l'analyse numérique et valider l'adéquation de la procédure de conception proposée et la réponse sismique prédite du SESBF.

ABSTRACT

Conventional steel braced frames are widely used as lateral force resisting systems against earthquakes for their light weight and ductile seismic response. However, numerous studies have proven that both concentrically braced frames (CBFs) and eccentrically braced frames (EBFs) are prone to soft-storey collapse mechanism. Damage is likely to concentrate on a single storey after the energy dissipating component (brace or link) at corresponding storey starts to yield.

Many innovative structural configurations were proposed in the past decades to prevent the soft-storey collapse of steel braced frames, tied eccentrically braced frame (TBF) being one of them. TBF is developed based on conventional EBF. Elastic ties are added to tie the ductile links of adjacent storeys together. Thus, the ties, the columns, the beam outside of links, and the braces form a continuous elastic spine along the building height, to force a global collapse mechanism. Although remarkable seismic performance is achieved with the TBFs, the force demands in structural members grow exponentially with the increasing number of storeys in the structure. As a result, it becomes cost-inefficient to design and construct such system in taller buildings.

A new type of structural configuration named braced frame with segmental elastic spine (SESBF) is proposed and studied in this research. This system evolves from conventional EBF and TBF while combines the advantages of both systems, i.e. the light weight and reduced seismic demand of the EBFs and the enhanced seismic performance of the TBFs. A fully tied eccentrically braced frame is divided into several segments along the building height, and the ties between segments are taken out. Consequently, the bending moment of the continuous elastic spine is released at the joints between segments. A series of numerical analyses are conducted to examine the seismic response of the segmental elastic spine system with conventional EBF and TBF as references. It is proven that the segmental elastic spine system, if designed properly, can achieve optimum seismic performance without a significant increase in terms of cost. The emphasize of a proper design is brought up because a tendency of soft-segment development is foreseeable for tall buildings under extreme seismic loading conditions.

To develop a practical and robust design method, a combination of analytical and numerical approach is employed. A group of SESBFs ranging from 8- to 24-storey SESBFs with various length of segments is designed with the results obtained from nonlinear time history analyses. The

forces demand of each structural member and the seismic response of the structures are studied both in time domain and frequency domain. Modal analysis is also performed for these structures. It is observed that the post elastic response where the main yielding components that are yielded has a significant effect on the maximum force demands on the members of the elastic spines. With these findings, a design method that utilizes modal superposition technique is proposed and verified numerically for determining the force demand of structural members within the elastic trusses with given link sections. A modified response spectrum analysis is utilized to predict the force demand of the elastic members because of higher vibration modes.

To help determine the optimum length and configuration of the segments, a complete procedure for the preliminary design and optimization of the SESBF is also developed. This procedure is based on a simplified numerical model. This model lumps the shear stiffness and flexure stiffness of each segment in the SESBFs into one shear spring and one elastic column. Equations and procedures to estimate these stiffnesses are also developed. Thus, designers can perform both spectrum analysis and response time history analysis for a particular configuration of interest in a timely fashion without knowing the exact properties of the frame. Once a target performance level is selected, an optimum setup of SESBF can be determined through a few iterations of time history analysis. This procedure is verified numerically and good correlation between the simplified model and the full model is achieved. The application of the proposed procedure is demonstrated for a 24-storey SESBF.

An experimental test program is also developed using the earthquake simulator at the Structural Engineering Laboratory at Polytechnique de Montreal. Shake table test will be performed on a 30% scaled model of an 8-storey chevron braced frame designed based on 1980 NBCC to confirm the deficiencies identified by nonlinear dynamic analysis. The experimental program includes a second test that will be performed on an 8-storey SESBF with two-segment (SESBF-2) which is designed as retrofit solution for the existing frame. Both the scaled and the original frame are analyzed through numerical analysis to validate the scaling process. The shake table tests will confirm the accuracy of the numerical analysis used to predict the seismic response of both the existing CBF and the SESBF systems and validate the adequacy of the proposed design procedure for the SESBF system. The test will also confirm the possibility of using SESBFs as a rehabilitation scheme to retrofit existing sub-standard structures.

TABLE OF CONTENTS

ACKNOWLEDGEMENTS III

RÉSUMÉ V

ABSTRACT VIII

LIST OF TABLES XVI

LIST OF FIGURES XXII

LIST OF SYMBOLS AND ABBREVIATIONS XXVII

LIST OF APPENDICES XXX

CHAPTER 1 INTRODUCTION 1

1.1 Background 1

1.2 Problem definition 4

1.3 Objectives and Scope of the Study 5

1.4 Methodology 6

1.5 Thesis structure 6

CHAPTER 2 LITERATURE REVIEW 8

2.1 Soft storey mechanism 8

2.2 Soft storey mechanism in concentrically braced frames 9

2.3 Soft storey mechanism in eccentrically braced frames 10

2.3.1 Discussion of seismic response of EBFs in the 1990s 11

2.3.2 Seismic response of Modern EBFs 14

2.4 Existing structural systems to prevent soft-storey mechanism 16

2.4.1 Zipper braced frame 16

2.4.2 Dual braced frame (Strongback system) 22

2.4.3 Tied braced frame....29
2.4.4 Rocking frames....33
CHAPTER 3 DEVELOPMENT OF BRACED FRAME WITH SEGMENTAL ELASTIC TRUSSES SYSTEM....38
3.1 Understanding of soft-storey mechanism in CBFs and EBFs....38
3.1.1 The soft-storey mechanism in CBFs....38
3.1.2 The soft-storey mechanism in EBFs....41
3.2 Braced frames with fully tied systems....43
3.2.1 Elastic zipper braced frame (EZBF)....44
3.2.2 Suspended zipper braced frame (SZBF)....46
3.2.3 Tied EBF (TBF)....48
3.2.4 Seismic response of fully tied braced frames....49
3.3 Development of segmental systems with elastic trusses....49
3.4 Seismic response of braced frame with segmental elastic trusses....52
3.4.1 Typical response of braced frame with segmental elastic trusses....52
3.4.2 Potential improvement for a braced frame with segmental elastic trusses....53
3.5 Design of braced frame with segmental elastic trusses....55
3.5.1 Capacity design approach....56
3.5.2 Frequency analysis....57
3.5.3 Modal superposition....58
3.5.4 Inelastic vibration modes....59
3.5.5 Determination of inelastic vibration modes....60
3.5.6 Design of SESBFs....61
3.5.7 Additional Validation of the proposed design method....61

3.6 Optimum design of braced frame with segmental elastic trusses 65
3.6.1 Simplified structural model 66
3.6.2 Validation of the simplified model 68
3.7 Proposed design methodology 70
3.7.1 Determine the best configuration for a SESBF 71
3.7.2 Design the SESBF with selected configuration 72
3.8 Experimental test program 74
3.8.1 Purpose of the test program 74
3.8.2 Test setup 75
CHAPTER 4 ARTICLE 1: MODULAR TIED ECCENTRICALLY BRACED FRAMES FOR IMPROVED SEISMIC RESPONSE OF TALL BUIDLINGS 76
4.1 Introduction 76
4.2 Building and Framing Systems Studied 79
4.2.1 Buildings studied 79
4.2.2 Design of the structures 80
4.2.3 Design of the vertical elastic trusses 84
4.3 Seismic Analysis 86
4.3.1 Numerical Model 86
4.3.2 Nonlinear Static (Pushover) Analysis 89
4.3.3 Selection and Scaling of Ground Motions 91
4.3.4 Analysis Results for the Structures 92
4.3.5 Residual drift responses for the 8-storey and 16-storey frames 102
4.3.6 Collapse assessment using incremental dynamic analysis (IDA) 104
4.4 Conclusions 106

CHAPTER 5 ARTICLE 2: PRACTICAL SEISMIC DESIGN PROCEDURE FOR STEEL BRACED FRAMES WITH SEGMENTAL ELASTIC SPINES 113

5.1 Introduction 113

5.2 Analysis and Design Methods 117

5.2.1 Modal superposition method 117

5.2.2 Proposed design procedure 126

5.3 Case Study 127

5.3.1 Buildings studied 127

5.3.2 SESBF Design 128

5.3.3 Validation of the method through nonlinear dynamic analysis 138

5.4 Conclusions 156

CHAPTER 6 ARTICLE 3: DETERMINATION OF OPTIMUM CONFIGURATIONS FOR STEEL BRACED FRAMES WITH SEGMENTAL ELASTIC SPINES 164

6.1 Introduction 165

6.2 Proposed Methodology 167

6.2.1 Simplified structural model (SM) 167

6.2.2 Stiffness and strength properties 169

6.3 Detailed Procedure 173

6.3.1 Selection of a truss segment configuration 174

6.3.2 Determining initial SM properties using ESFP 174

6.3.3 Construct the SM model and perform RSA 177

6.3.4 Verification of the fundamental period and seismic drifts 178

6.3.5 Verification of the wind drifts 179

6.3.6 Performing NLRHA 179

6.3.7 Verification of NHLRA results 179
6.3.8 Comparison with other truss segment configurations 180
6.3.9 Final Design 180
6.4 Design Example 180
6.4.1 Buildings studied 181
6.4.2 Preliminary design 182
6.4.3 NLRHA 184
6.4.4 Final Design 190
6.5 Conclusion 195
CHAPTER 7 EXPERIMENTAL TEST PROGRAM 200
7.1 Introduction 200
7.2 Test program 200
7.2.1 Overview 200
7.2.2 Design of original frames 201
7.2.3 Scaling of testing frames 208
7.2.4 Selection of ground motions 212
7.3 Numerical models and simulation results 213
7.3.1 Modeling details 213
7.3.2 Modeling of connections 215
7.4 Expected results 216
7.4.1 Possible failure modes: 216
7.4.2 Seismic response of the scaled models 218
CHAPTER 8 GENERAL DISCUSSION 221

CHAPTER 9 CONCLUSIONS AND RECOMMENDATIONS 223

9.1 General 223

9.2 Summary and conclusions 224

9.3 Recommendations for future studies 227

BIBLIOGRAPHY 229

APPENDICES 237

LIST OF TABLES

Table 3-1: Calibration of ductile link model 42

Table 3-2 Suggested fundamental periods by the code and fundamental periods obtained from dynamic analysis 62

Table 3-3 CMR of structural systems 65

Table 4-1 Building periods, steel tonnage and maximum seismic base shears (/frame). 83

Table 4-2 Test results used for the calibration of link beam elements 88

Table 4-3 Drift concentration factors (DCF) from NSA for the 8- and 16-storey frames. 91

Table 4-4 Values of response parameters for the 8-storey and 16-storey braced frames. 93

Table 4-5 DCF values for the 8-storey and 16-storey braced frames. 94

Table 4-6 Evaluation of collapse safety of the 16-storey buildings according to FEMA P695 ... 106

Table 5-1 Elastic and inelastic modal properties for the 8-storey SESBF-1 configuration 121

Table 5-2 Design spectrum ordinates for site class C in Vancouver, BC 129

Table 5-3 Parameters used to calculate the design base shear 129

Table 5-4 Periods (s) of the elastic and inelastic vibration modes of the 8-storey SESBFs 130

Table 5-5 Periods (s) of the elastic and inelastic vibration modes of the 16-storey SESBFs 131

Table 6-1 Design spectrum ordinates for Site Class C, Vancouver 183

Table 6-2 selected ground motions 186

Table 6-3 Characteristics and storey drift response of the SESBF configurations 194

Table 7-1 Periods of structures (sec) 205

Table 7-2 Member sections of selected CBF 206

Table 7-3 Member sections for 8-storey SESBF with 2 segments 207

Table 7-4: Scaling factors for shaketable specimens 209

LIST OF FIGURES

Figure 1-1: Typical soft-storey response of CBFs 1

Figure 1-2: U.S. -Japan EBF Test Structure (Popov, Ricles, & Kasai, 1992) 2

Figure 1-3: Braced frame systems proposed to prevent soft-storey response 3

Figure 1-4: 8-storey segmental braced frame with 2 segments: a) segmental ZBF; b) segmental TBF 5

Figure 2-1: Maximum response and schematic diagram of Olive View Medical Center under 1971 San Fernando earthquake (Mahin, Bertero, Chopra, & Collins, 1976) 8

Figure 2-2: Braced hysteresis loop and different zones (Chen, 2011) 9

Figure 2-3 Chevron braced frame configuration and its failure mechanism (Bruneau et al. 2005) 10

Figure 2-4: Typical configuration and yielding mechanism of EBFs 10

Figure 2-5: Response of six-storey EBF (Popov, 1992) 12

Figure 2-6: Seismic response of thirteen-storey EBF (Popov, Ricles, & Kasai, 1992) 13

Figure 2-7: Zipper braced frame configuration and its yielding mechanism (Chen, 2011) 17

Figure 2-8: Behaviour of zipper braced frame system with weak zipper column (Tirca & Tremblay, 2004): a) zipper yields in tension; b) zipper buckles in compression 17

Figure 2-9: Mechanisms and lateral load distributions adopted for design with brace buckling initiating at the: a) upper floors; b) lower floors (Tremblay & Tirca, 2003) 18

Figure 2-10 Computed peak axial loads in zipper columns for 4-, 8-, 12-storey buildings (Tirca & Tramblay, 2004) 19

Figure 2-11 Axial force in zipper columns obtained from nonlinear dynamic time-history analyses of 4-, 8-, 16-story buildings (Tirca & Chen, 2012) 20

Figure 2-12 Maximum compression and tension forces in zipper columns of 12-storey zipper frame under regular, near-field and Cascadia ground motions (Chen, 2011) 21

Figure 2-13: BRB with elastic truss (Tremblay & Merzouq, 2004; Tremblay & Poncet, 2007)...23

Figure 2-14 Elevation views of six different bracing configurations: (a) V6; (b) X6; (c) X6-3; (d) SB6-3; (e) SB6-3B; (f) SB6-3 L (Lai & Mahin, 2015).....24

Figure 2-15 Schematic drawing of strongback test specimen (Simpson & Mahin, 2018).....25

Figure 2-16 Elevation drawing of the Heinz Avenue Building (Panian, Bucci, & Janhunen, 2015) 26

Figure 2-17 BRBM frame elevation (Panian, Bucci, & Janhunen, 2015) 27

Figure 2-18 Concept of stiff rocking core rehabilitation technique (Pollino, Slovenec, Qu, & Mosqueda, 2017).....28

Figure 2-19 Hybrid analytical substructuring (Slovenec, Sarebanha, Pollino, Mosqueda, & Qu, 2017).....29

Figure 2-20: Force combinations for member design proposed by (Rossi, 2007).....31

Figure 2-21: Results of non-linear dynamic analysis in terms of maximum lateral displacement (Rossi, 2007) 32

Figure 2-22: Axial forces of braces, beam segments, ties and columns for analyzed structures (Rossi, 2007) 33

Figure 2-23 Rocking frame (Roke et al., 2009) 34

Figure 2-24 FBF with multiple BRB columns and the axial forces in the columns (Tremblay et al. 2004).....36

Figure 2-25 Rocking frame with load reducing fuses (Wiebe et al., 2012) 37

Figure 2-26 Shear force envelopes and storey drift distributions (Wiebe et al., 2012) 37

Figure 3-1: Comparisons between simulated brace response and experimental test results.....39

Figure 3-2: Interstorey drift profiles 4-, 8- and 12-storey CBF buildings under subduction and crustal record sets (Tirca, Chen, & Tremblay, 2015).....40

Figure 3-3: a) Replaceable link beams with end plate connections and proposed ties to link connection detail; b) Calibration of the numerical hysteretic link model in OpenSees (Chapter 4).....41

Figure 3-4: Ductile link OpenSees model.....41

Figure 3-5: Result of time-history analyses for 8- and 16-storey EBFs (Chapter 4).....43

Figure 3-6: Structural configurations and their failure mechanisms: a) elastic zipper frame; b) suspended zipper frame; c) TBF.....44

Figure 3-7: Expected global yielding mechanisms for the framing systems studied.....46

Figure 3-8: Brace or link induced forces for the design of: a) Exterior columns in ZBFs, b) Zipper columns in E-ZBFs; c) Zipper columns in S-ZBFs; d) Hat truss and exterior column in S-ZBF; e) Zipper column and hat trusses in M-S-ZBF; and f) Exterior column in TBF.....46

Figure 3-9: Interstorey drift profile for 8-storey EZBF, SZBF and TBF.....49

Figure 3-10: Seismic response of 16-storey EZBF, SZBF and TBF.....50

Figure 3-11: Structural configuration and yielding mechanisms of segmental SZBF and segmental TBF.....51

Figure 3-12: Seismic response of segmental SZBF and segmental TBF.....52

Figure 3-13: Seismic response of 8-storey EBF, TBF and SESBF (2 segments) (Chapter 4).....53

Figure 3-14: Structural configurations for SESBFs with energy dissipative devices (EDs) (Tremblay et al, 2014).....54

Figure 3-15: Storey drift profile of SESBFs with dissipative devices (Tremblay et al, 2014).....55

Figure 3-16: Snapshots of forces in main structural members obtained from time-history analysis 57

Figure 3-17: Power spectral of axial forces in 1st floor braces.....58

Figure 3-18: Elastic and inelastic vibration modes of the 16-storey braced frame with segmental elastic trusses: a) elastic modes; b) inelastic modes.....60

Figure 3-19 Spectrum of scaled ground motions 62

Figure 3-20 IDA curves of 8-, 9- and 10-SESBFs 63

Figure 3-21 IDA curves of 12-, 15- and 16-SESBFs 64

Figure 3-22 a) Conventional EBF; b) Simplified model 66

Figure 3-23: 8-storey 2- segments SESBF and spring-mass models: a) SESBF; b) shear-spring model; c) rotational spring model; d) proposed model 68

Figure 3-24: Comparison of pushover analysis results between discrete model and shear spring model 69

Figure 3-25: a) structural model; b) Comparison of shapes of inelastic vibration modes; c) Comparison of roof deflection from time-history analysis 70

Figure 3-26: Design flowchart for SESBF: a) preliminary design with simplified model; b) detailed design with finite element model 74

Figure 4-1 Mitigation of soft-storey response in multi-storey steel braced frames: a) Concentration of inelastic deformations in EBFs; b) Tied braced frame (TBF); c) Dual-BRBF configuration; d) Higher mode response in TBF; and e) Modular tied braced frame (M-TBF). 79

Figure 4-2 a) Floor plan of the building studied; b) Elevation of 8-storey framing systems; c) Elevation of 16-storey framing systems. 80

Figure 4-3 Factored link shear forces Vf and factored link shear resistance to shear force Vr/Vf ratios for: a) 8-storey building; and b) 16-storey building. 84

Figure 4-4 Anticipated inelastic response of the 16-storey TBF: a) Inelastic vibration modes; b) Design forces in truss members. 85

Figure 4-5 Design forces in the braces, columns and tie members of the 16-storey TBF. 86

Figure 4-6 a) Replaceable link beams with end plate connections and proposed tie-to-link connection detail; b) Calibration of the numerical hysteretic link model in OpenSees (Test 4C). 87

Figure 4-7 Deformed shape of the 8-storey braced frames from NSA: a) EBF; b) TBF; and c) M-TBF.....90

Figure 4-8 Deformed shape of the16-storey braced frames from NSA: a) EBF; b) TBF (CL design); c) M-TBF-1; and d) M-TBF-2. 90

Figure 4-9 Lateral load-displacement responses from NSA for the 8-storey and 16-storey braced frames. 91

Figure 4-10 Design spectrum and 5% damped absolute acceleration spectra of the ground motion records suites: a) 8-storey frame scaled for 0.4-2.0 s; b) 16-storey frame scaled for 0.6-4.0 s 92

Figure 4-11 Storey shears, storey drifts, axial force in columns and tie members of the 16-storey braced frames. 95

Figure 4-12 Comparison of the 84th percentile storey shears, storey drifts, and axial loads in columns and tie members of the 16-storey braced frames. 96

Figure 4-13 Storey drift time histories at the 8th and 16th storeys and horizontal displacement profiles for the 16-storey braced frames under Ground motion # 776. 96

Figure 4-14 Time history of the roof displacement and storey drift at first and top levels of the 16-storey braced frames and profiles of storey drifts and tie axial forces under Ground motion # 776. 98

Figure 4-15 Time history of the roof displacement and storey drift at first and top levels of the 16-storey braced frames and profiles of storey drifts and tie axial forces under Ground motion no. 767. 99

Figure 4-16 Storey shears, storey drifts, and axial loads in columns and tie members of the 8-storey braced frames. 101

Figure 4-17 Storey shears, storey drifts, axial loads in columns and tie members of the 24-storey braced frames. 102

Figure 4-18 Residual *vs* peak inelastic storey drifts (90th percentile) for 8-storey and 16-storey: a) EBF; b) TBF; c) M-TBF-1; and d) M-TBF-2 104

Figure 4-19 IDA curves of 16-storey frames subjected to the selected record set: a) EBF, b) TBF-CL, c) MTBF-1, d) MTBF-2 105

Figure 5-1 Deflected shape of braced frames: a) conventional EBF, b) Dual-BRBF by Tremblay (2003), c) Tied EBF (TBF) by Martini et al. (1990) and Ghersi et al. (2000), d) Modular tied EBF (M-TBF) by Liang et al. (2012). 117

Figure 5-2 Yielding mechanisms and lateral load patterns illustrated for the 8-storey EBF and 8-storey SESBF-1 configuration. 118

Figure 5-3 Vibration modes of the 8-storey SESBF-1 configuration: a) Elastic modes; b) Inelastic modes with reduced link stiffness ($\alpha = 0.01$). 121

Figure 5-4 Likely yielding pattern cases for a 12-storey SESBF-3 configuration. 124

Figure 5-5 Mode shapes and periods of 8-storey SESBF-2 configuration: a) Elastic modes; b) Inelastic modes, Case1: links yielding in both segments; c) Inelastic modes, Case 2: links yielding in bottom segment; and d) Inelastic modes, Case 3: links yielding in second segment only ($\alpha = 0.01$). 126

Figure 5-6 Building studied: a) Plan view; b) Elevation of 8-storey configurations SESBF-1 and SESBF-2; and c) Elevation of 16-storey configurations SESBF-2 and SESBF-4. 128

Figure 5-7 Calculation of the Set I member forces for the 8-storey frames assuming an inverted triangular lateral load pattern: a) SESBF-1 configuration; b) SESBF-2 configuration. 133

Figure 5-8 Comparison between inverted triangular and RSA lateral load patterns used for the calculation of Set I member forces for the 8-storey SESBF-2 configuration: a) Lateral load patterns; b) Brace axial forces; c) Tie axial forces. 133

Figure 5-9 Comparison between inverted triangular and RSA lateral load patterns used for the calculation of Set I member forces for the 16-storey SESBF-2 configuration: a) Lateral load patterns; b) Brace axial forces; c) Tie axial forces. 134

Figure 5-10 Truncated design spectra for: a) 8-storey SESBF-1 configuration; and b) 8-storey SESBF-2 configuration. 135

Figure 5-11 Set II axial forces in braces, ties and columns for cases i = 1, 2, and 3 for: a) 8-storey SESBF-2 configuration; and b) 16-storey SESBF-2 configuration. 136

Figure 5-12 Influence of reduced link stiffness on Set II forces of 8-storey SESBF-2 configuration. 136

Figure 5-13 Axial forces in braces, ties, and columns of 8-storey seismic force resisting system: a) SESBF-1 configuration; and b) SESBF-2 configuration. 138

Figure 5-14 Scaled response spectra and the scenario-specific period range for each ground motion suite for Vancouver, Site Class C: a) crustal suite, b) subduction inslab (SIS) suite, and c) subduction interface (SIF) suite 139

Figure 5-15 Time-history response series of 8-storey SESBF-2 configuration under ground motion SIF3: a) Segment drifts; b) Link shear forces; c) Axial force in brace at 7th floor; d) Axial force in tie at 7th floor; e) Axial force in brace at 3rd floor; and f) Axial force in tie at 3rd floor. 145

Figure 5-16 Time-history responses of 8-storey SESBF-2 configuration under ground motion C2: a) Segment drifts; b) Link shear forces; c) Axial force in brace at 7th floor; and d) Axial force in tie at 7th floor. 145

Figure 5-17 Peak values of storey shears, drifts, and axial forces in braces, columns, and ties along the height of the 8-storey SESBF-2 configuration. 147

Figure 5-18 Peak values of storey drifts and axial forces in braces, columns and ties for the 8-storey SESBF-2 configuration under: a) Crustal records; b) SIS records; and c) SIF records. 148

Figure 5-19 Spectra and member forces from records C2, SIS1, and SIF4 for the 8-storey SESBF-2 configuration: a) Response spectra; b) Axial forces in ties; c) Axial forces in braces. 149

Figure 5-20 Peak values of storey drift, shears, and axial forces in braces, columns, and ties along the height of the 8-storey SESBF-1 configuration. 150

Figure 5-21 Peak values of storey drifts, storey shear, and axial forces in braces, columns and ties along the height of the 16-storey SESBF-2 configuration. 152

Figure 5-22 Peak values of storey drifts, storey shears, and axial forces in braces, columns and ties along the height of the 16-storey SESBF-4 configuration. 153

Figure 5-23 Shear force time-history in the links of the upper segment of SESBF-2 configuration under C5 ground motion. 154

Figure 5-24 Shear force time-history developed in links of upper segment of SESBF-2 configuration under Mexico City, 1985, ground motion. 155

Figure 5-25 Design spectrum and response spectrum of the 1985 Mexico City earthquake (SCT, S00E record).....156

Figure 5-26 Peak values and distribution of axial forces in braces, columns and ties along the height of 16-storey SESBF-2 configuration under the 1985 Mexico City earthquake (SCT, S00E record). 156

Figure 6-1 Evolution of braced frame systems to mitigate the soft-storey response: a) Eccentrically braced frames prone to damage concentration; b) TBF; c) SESBF 166

Figure 6-2 Typical lumped mass-spring structural model for 4-storey frame 168

Figure 6-3 SESBF-2 system and its deformed shape: a) Actual frame; b) Simplified model (SM) 169

Figure 6-4 Vertical distribution of seismic storey shears from NBCC and ASCE 7 ESFPs and RSA. 172

Figure 6-5 Comparison between stiffness values from preliminary design (SM) and after final design (F): a) Flexural stiffness; and b) Shear stiffness. 172

Figure 6-6 Flowchart of the preliminary design process for SESBFs using the SM 173

Figure 6-7 Storey shear distribution pattern for the 24-storey SESBF-6 configuration. 177

Figure 6-8 T_d/T_a for braced frames in past studies.....178

Figure 6-9 Plan view and specified loads of the building studied. 181

Figure 6-10 The studied SESBF-*n* configurations of the 24-storey building 182

Figure 6-11 Storey shear distributions for the SESBF-8 configuration: a) From ESFP; b) From RSA using the SM.....183

Figure 6-12 Acceleration response spectra of the scaled ground motion records.....185

Figure 6-13 Storey drift profiles from NLRHA with the SM for the SESBF-8 configuration.....187

Figure 6-14 Storey drift profiles from SM NLRHA for configurations: a) SESBF-6; b) SESBF-4; c) SESBF-3; and d) SESBF-5. 188

Figure 6-15 Peak storey drifts and drift concentration factor (DCF) from SM NLRHA.....190

Figure 6-16 Link overstrength for the SESBF-6, SESBF-4, SESBF-5 and SESBF-3 configurations. 191

Figure 6-17 Axial force demands in truss members for configurations: a) SESBF-6; and b) SESBF-4.....193

Figure 6-18 Storey drift profiles from FM NLRHA for configurations: a) SESBF-6; b) SESBF-4; c) SESBF-3; and d) SESBF-5. 195

Figure 7-1 Structural laboratory (website) 201

Figure 7-2: Plan view and elevation view of prototype structures.....202

Figure 7-3: Comparison between storey shear of buildings of different configurations 204

Figure 7-4 Storey drift profile of 8-storey chevron braced frame: a) Class C site; b) Class E site 206

Figure 7-5 Drawing of the composite beam.....210

Figure 7-6: ABAQUS model of the scaled beam.....211

Figure 7-7 Detail of the link assembly.....212

Figure 7-8: Ground motion scaling 212

Figure 7-9 Spectrum of scaled ground motion records 213

Figure 7-10: Result of column analysis.....214

Figure 7-11: Modeling of connections 215

Figure 7-12: Deformed shape.....217

Figure 7-13 Storey drift profile of the scaled 8-storey CBF 218

Figure 7-14 Storey drift profile of the scaled 8-storey SESBF-2.....219

Figure 7-15 Axial forces of ties and braces.....220

LIST OF SYMBOLS AND ABBREVIATIONS

Symbols

A	cross-sectional area of section
Ag	Brace cross-sectional area
C_x	Lateral force distribution coefficient
C_u	Probable compressional resistance
C'_u	Probable post-buckling resistance
d	Depth of section
E	Young's modulus
F_a	Acceleration-based site coefficient
F_v	Velocity-based site coefficient
F_y	Yielding stress of steel
h_n	Total height of the structure
h_i	Height of the i^{th} storey in a structure
I	Moment of inertia
I_E	Earthquake importance factor of the structure
P	column axial load for P-Δ effect calculation
r	Radius of gyration
r_g	Force demand in members due to gravity load
r_I	Force demand in members due to Set I modes effect
r_{II}	Force demand in members due to Set II modes effect
R_d	Ductility related force modification factor
R_o	Overstrength related force modification factor

S_a	Spectrum acceleration
T_a	Fundamental period of vibration of the structure
V_d	Storey shear obtained by dynamic spectrum analysis
V_{design}	Design storey shear
V_{static}	Storey shear obtained with static equivalent method
W	Seismic weight
φ	Resistance factor

Abbreviations

2D	2-Dimensional
AISC	American Institute of Steel Construction
ASCE	American Society of Civil Engineers
BF	Braced frame
BRB	Buckling restrained frame
CBF	Concentrically braced frame
CSA	Canadian Standards Association
DCF	Damage concentration factor
EBF	Eccentrically braced frame
ED	Energy dissipating devices
HSS	Hollow Square Section
IDA	Incremental dynamic analysis
MD	Moderately ductile
MRF	Moment resisting frame

NBCC	National Building Code of Canada
NLRHA	Nonlinear response history analysis
OpenSees	Open system for earthquake engineering
TBF	Tied braced frame
ESFP	Equivalent static force procedure
SESBF	Braced frame with segmental elastic spines
SRC	Stiff rocking core
SZBF	Suspended zipper frame
UHS	Uniform hazard spectrum
ZBF	Zipper braced frame

LIST OF APPENDICES

Appendix A – Drawings for test specimens.....235

CHAPTER 1 INTRODUCTION

1.1 Background

Steel braced frames are considered as one of the most efficient, economical and versatile structural systems against earthquake excitations. However, most conventional steel braced systems do not exhibit satisfactory performance when subjected to large earthquake forces primarily due to the concentration of deformations in a single storey which leads to premature dynamic instability of the structure. Both concentrically braced frames (CBFs) and eccentrically braced frames (EBFs), median- to high-rise, are prone to this so-called soft-storey collapse mechanism. This collapse mechanism of steel braced frames is studied extensively in the past decades.

In CBFs, input energy is designed to be dissipated through inelastic behaviour of braces, such as yielding and buckling. Due to the lack of ability of conventional CBFs to redistribute the inelastic demand over the building height, brace inelastic action often creates a soft-storey in terms of both stiffness and strength in the structure and leads to a concentration of deformation and eventually collapse of the structure as shown in Figure 1-1.

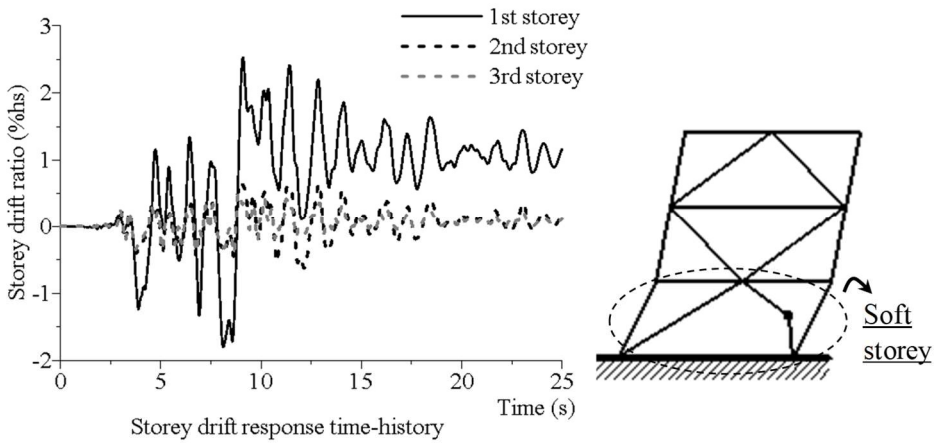

Figure 1-1: Typical soft-storey response of CBFs

In EBFs, links act as the primary energy dissipating components, and they are generally considered preferable given their substantial energy dissipating capacity and symmetric hysteretic loops. However, the yielding of link members may still create a soft storey in the structure due to the low post yielding stiffness as shown in Figure 1-2.

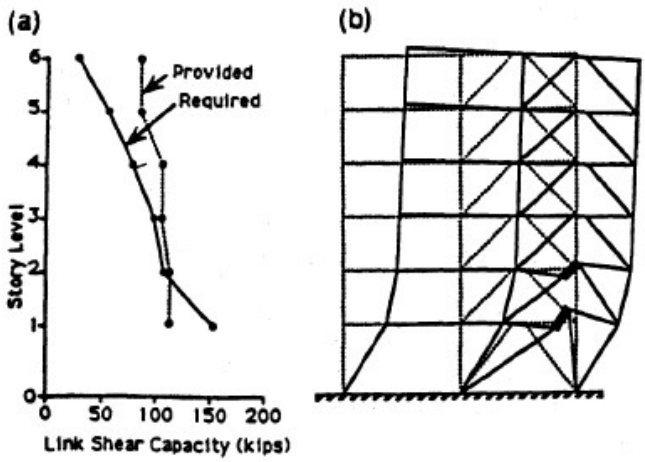

Figure 1-2: U.S. -Japan EBF Test Structure (Popov, Ricles, & Kasai, 1992)

During the last decades, to mitigate the soft storey response of high-rise braced frames, the braced frame system has evolved from classical CBFs and EBFs toward more complex systems such as zipper braced frames (ZBFs), tied eccentrically braced frames (TBFs), dual braced frames (DBFs), rocking braced frames (RBFs), and others.

Figure 1-3 shows the aforementioned structural systems and their global yielding mechanisms. In the ZBF system, the addition of zipper columns aims to utilize braces and beams at all storeys during an earthquake event to spread energy dissipation over the entire height of the structure. Better performance is observed when the zipper columns are specifically designed to remain elastic (EZF in Figure 1-3). In the S-ZBF configuration, an elastic hat truss is introduced at the top level. All unbalanced vertical components of the brace forces are collected in the zipper columns up to the roof level and distributed to the edge columns through the braces of the elastic truss. This configuration aims to avoid a full-height inelastic mechanism with loss of lateral strength after buckling of the compression braces.

In TBF systems, vertical ties are added to the conventional EBFs to tie together the ends of all ductile links in order to engage all the links when yielding initiates from one of them. Similar to ZBF, when the ties are designed to remain elastic, the global yielding mechanism is naturally achieved. From a different perspective, the TBFs can also be considered as two elastic brace sub-trusses connected by energy dissipating links, where the sub-trusses act as a vertical spine to the structure to prevent soft-storey formation.

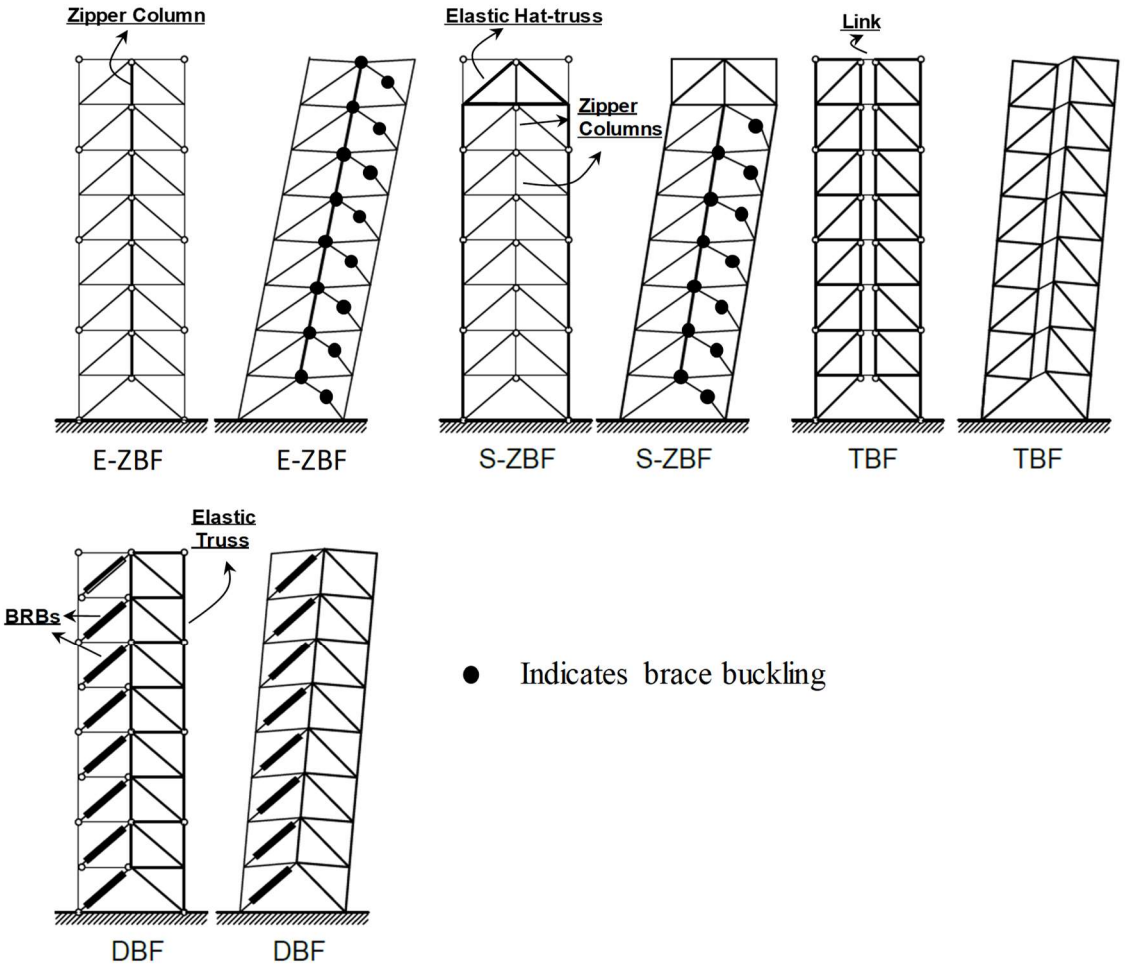

Figure 1-3: Braced frame systems proposed to prevent soft-storey response

In DBFs, the structural system consists of one elastic vertical brace sub-truss and Buckling Restrained Braces (BRBs) or conventional bracing members on the other side. Input energy is dissipated through yielding of BRBs or braces while vertical continuity of the system is kept by the elastic truss(es). In rocking systems (RBFs), the frame is designed to allow uplift from its support at the base-of-column to foundation interface under strong earthquake excitations. The soft-storey formation is prevented because all structure members are expected to remain elastic during the entire earthquake event. Energy dissipation of RBFs is achieved by introducing hysteretic or viscous energy dissipating devices that are activated upon base rocking.

Most of the structural systems developed to eliminate the soft-storey collapse mechanism introduce a vertical truss or column to the original system. The truss or column is designed strong

enough to remain elastic while forcing the directly connected dissipating members on different floors to act simultaneously. This type of structure systems is categorized as the “Strongback” system.

1.2 Problem definition

Current solutions for soft-storey failure mechanism prevention utilize a full elastic back-bone/link system that attracts tremendous forces when the number of storeys increases. The large sections required to build such system make it less economical and sometimes impossible to construct. Without such systems, however, there are no viable ways to stop damage concentration in a ductile framing system, especially in medium to high seismicity regions.

Previous work also showed that partially relaxing the constraint on lateral deformation could reduce the force demand in the structure while maintaining adequate seismic performance. For instance, this is the case when allowing rocking to occur at several locations along the building height. Member forces due to overturning moments produced by higher vibration modes can then be controlled along the building height.

In this research, this approach will be examined further by introducing the concept of segmental braced frames. In this configuration, the braced frames are broken into vertical modules that extend over a number of storeys along the building height so that some flexibility is introduced in the system when deforming in the inelastic range. In each segment, soft-storey response is prevented by means of elastic truss or vertical ties, but overall frame deformation can take place at the junctions between the modules. This concept is particularly suitable for the ZBF, TBF and DBF systems. An example is given in Figure 1-4 for an 8-storey TBF. As shown, 4-storey segments are used with the ties being interrupted between each of the segment. Very limited data exits on the seismic performance of such segmental braced frame systems and no design provisions have been proposed yet to achieve the intended seismic response.

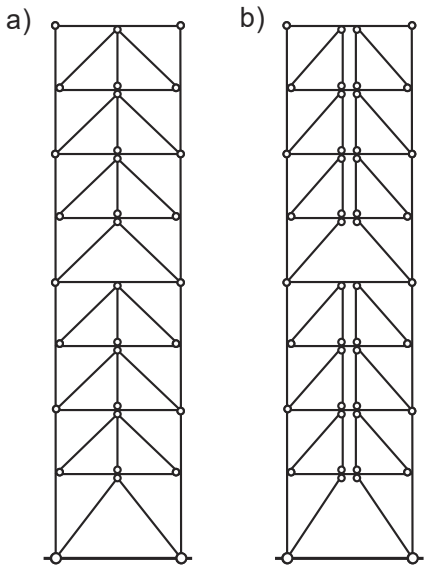

Figure 1-4: 8-storey segmental braced frame with 2 segments: a) segmental ZBF; b) segmental TBF

1.3 Objectives and Scope of the Study

The ultimate goal of this doctoral research is to develop sufficient knowledge on the seismic response of the segmental braced frame structural system and propose a seismic design method for these systems. The study focuses on segmental braced frame systems adopted for mid- to high-rise building structures.

In this light, the main objective of the study is four-fold:

1. Develop an efficient and economic seismic resisting system that is preventive to the soft-storey formation, which is named Segmental Elastic Spine Braced Frames (SESBFs).
2. Develop a robust and simple design methodology for such system. The proposed design method will be tightly connected to the current Building Code Provisions to make it easy to apply in for Canadian applications.
3. Verify the newly developed system and design method with numerical analysis.
4. Develop an experimental test program to validate the proposed design method. The experimental program will include a test on a sub-standard CBF and a test on a SESBF. The objective is to confirm the deficiencies of the sub-standard CBF and verify if the newly

proposed system can be used as a seismic retrofit strategy. The test program will be conducted for buildings located in Montreal, Quebec.

1.4 Methodology

Main steps to fulfill aforementioned objectives were as follows:

1) Review the past researches. Great efforts have been devoted by various researchers trying to prevent damage concentration in braced frames. Existing structural configurations were examined and compared.
2) Based on previous comparison, innovative structural configurations were proposed. Prototype structural models were designed and built for these structural configurations. Nonlinear time-history analyses were performed with these models to evaluate and compare the benefits of the systems and identify their limitations.
3) The most beneficial structural system, the SESBFs, was selected and its seismic response was studied through extensive numerically simulations.
4) A practical design method was developed and validated through extensive nonlinear time-history seismic analyses.
5) An easy-to-apply procedure was developed for the determination of the optimum configurations for SESBFs at the preliminary design stage. The method was also validated through numerical simulations.
6) An experimental program was designed to qualify the seismic performance of the SESBF system while exploring the potential of the system to be used as a retrofit strategy for seismically deficient steel braced frames.

1.5 Thesis structure

This PhD dissertation is presented in 9 chapters. It is composed of the journal articles that have been written based on the results of the doctoral research.

Chapter 1 introduces the background information of the existing problem and outlines the objectives and the main activities of the research.

Chapter 2 reviews the past studies conducted by other researchers to understand and examine the existing braced frame systems which have been proposed to prevent soft-storey formation. Past researches regarding numerical simulations are also reviewed and criticized.

Chapter 3 discusses the methodologies and approaches taken to fulfill the research objectives in detail.

Chapters 4, 5, 6 present the following three articles that have been submitted for publication in scientific journals:

1) Modular tied eccentrically braced frames for improved seismic response of tall buildings.
2) Practical seismic design procedure for steel braced frames with segmental elastic spines.
3) Determination of optimum configurations for steel braced frames with segmental elastic spines.

Chapter 7 describes the proposed experimental program.

A general discussion regarding the research process and findings is presented in Chapter 8. Finally, Chapter 9 concludes this doctoral research and highlights the main original contributions. A list of recommendations for future research is also given in this chapter.

CHAPTER 2 LITERATURE REVIEW

This chapter presents the studies conducted in the past regarding the soft-storey mechanism in braced frames and various structural configurations that have been proposed to eliminate the formation of soft-storeys in such frames. Both the conclusions and limitations of these studies are discussed to evaluate the benefits and disadvantages of each structural system in terms of seismic performance.

2.1 Soft storey mechanism

The soft-storey phenomenon is used to describe undesired structural response under ground motion excitation when large deformation is concentrated at a single floor level. The input energy, in its nature, will search for a breakthrough point in the structure, which is usually created by sudden changes in stiffness, strength and ductility. This phenomenon was observed in numerous major earthquake events, such as 1971 San Fernando earthquake, 1989 Loma Prieta earthquake, 1994 Northridge earthquake and 1995 Kobe earthquake. Figure 2-1 shows the deformation and the deformed shape of Olive View Medical Center during 1971 San Fernando earthquake.

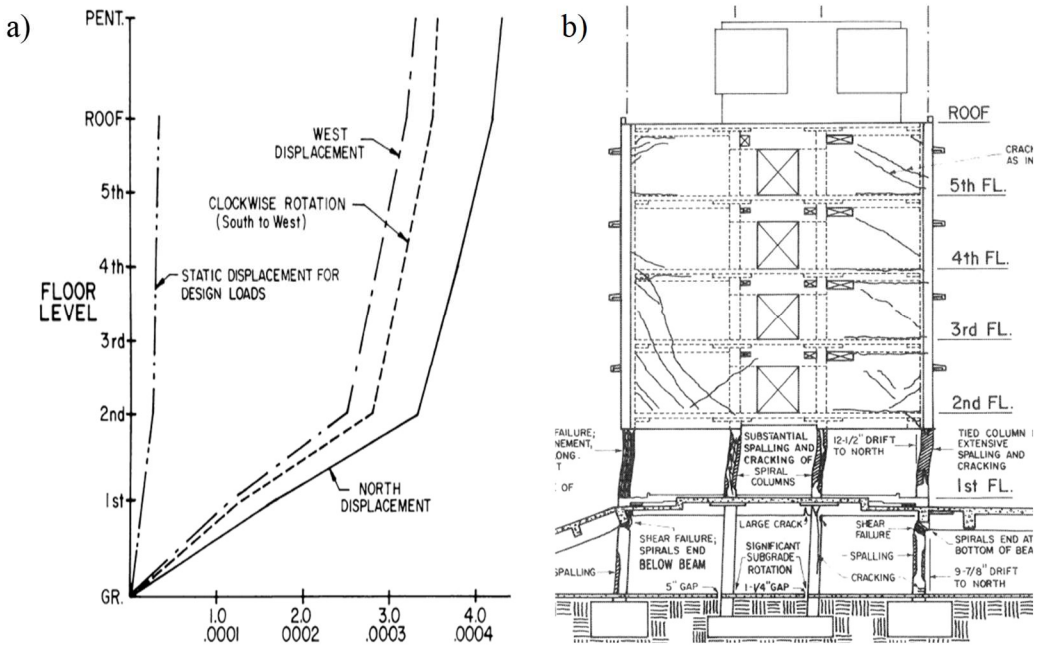

Figure 2-1: Maximum response and schematic diagram of Olive View Medical Center under 1971 San Fernando earthquake (Mahin, Bertero, Chopra, & Collins, 1976)

Mahin, Bertero, Chopra, & Collins (1976) have concluded that the discontinuation of the shear walls in the bottom two storeys was the main reason, which caused the side-way collapse of the structure. Further studies (Cassis & Cornejo, 1996; Alekar, Jain, & Murty, 1997; Kanitkar & Kanitkar, 2004; Hejazi et al., 2011) also emphasized the direct relationship between structure stiffness/strength irregularities and the formation of soft-storey response.

2.2 Soft storey mechanism in concentrically braced frames

With the increasing popularity of steel frames, various steel configurations (MRFs and BFs) are also found to be prone to the soft-storey mechanism Khatib, Mahin, & Pister (1988). In this thesis, the discussion will focus mainly on the braced frames.

Braced frames are found weak against soft-storey mechanism, especially CBFs (Chen & Mahin, 2012). In conventional CBFs, energy is expected to be dissipated primarily through the inelastic actions of diagonal braces, such as buckling and yielding. The brace hysteresis response can be divided into four hysteresis zones: elastic zone, plastic zone, yielding zone and buckling zone as shown in Figure 2-2 (Chen, 2011).

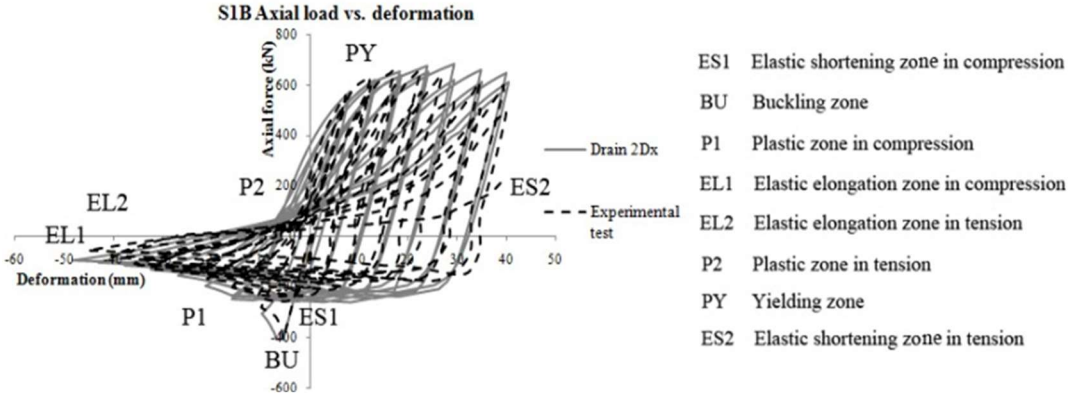

Figure 2-2: Braced hysteresis loop and different zones (Chen, 2011)

Due to the unsymmetrical hysteretic behaviour of the brace, there is deterioration of the building lateral load behaviour after buckling of braces in terms of both stiffness and strength, which creates a soft-storey at the buckling location. The difference in brace compression and tension resistances results in unsymmetrical brace hysteretic response. Under cyclic loading, the brace compressive strength also progressively reduces, and the brace accumulates permanent elongation upon yielding

in tension, which further accentuates the dissymmetry in brace response and leads to progressive degradation of storey shear resistance. Typical failure mechanism of CBFs are illustrated in Figure 2-4.

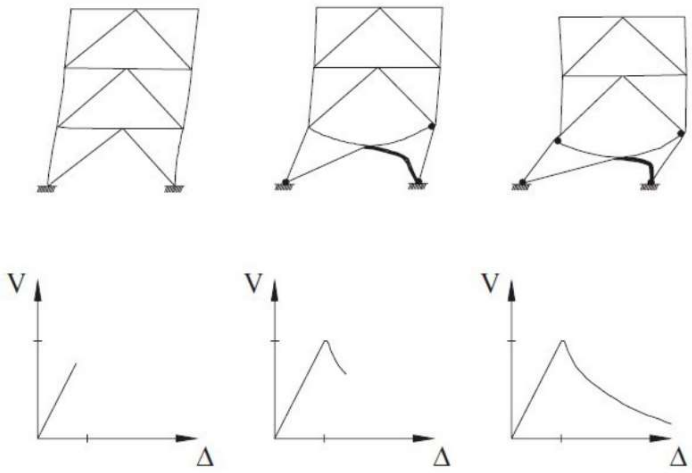

Figure 2-3 Chevron braced frame configuration and its failure mechanism (Bruneau et al. 2005)

2.3 Soft storey mechanism in eccentrically braced frames

Eccentrically braced frame (EBF) has been widely used as a seismic load resisting system in North America. Conventional EBFs consist diagonal braces, beams, columns and specially designed ductile link elements. The system relies on yielding of these link beams to dissipate seismic energy. A typical configuration of a 2-storey conventional EBF is shown in Figure 2-4. The link beam can yield either in bending or in shear depending on the length of the link.

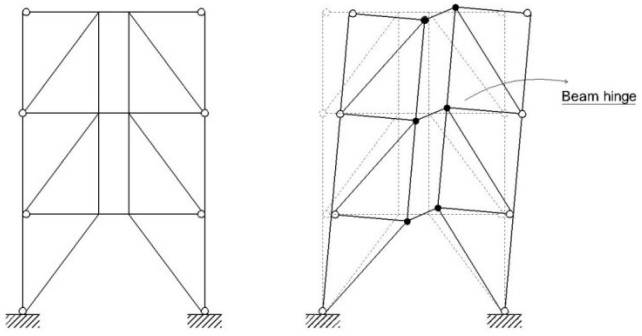

Figure 2-4: Typical configuration and yielding mechanism of EBFs

In EBFs, seismic input energy is essentially dissipated through shear and/or flexural yielding of the ductile link beam segments depending on the length of the segments. This translates into symmetrical and stable inelastic hysteresis response.

2.3.1 Discussion of seismic response of EBFs in the 1990s

Foutch (1989) presented a full-scale six-storey eccentrically braced dual frame building being tested in Large-Size Testing Facilities. The frame was designed with three-times the required capacity based on the 1979 and 1982 UBC provisions. Some of the results are shown in Figure 2-5. He pointed out that the response of the system was reasonably good due to the large capacity, and the energy was mostly dissipated by the yielding links. However, the damage was concentrated within the first three floors. The conclusion was made based on three dynamic tests that were conducted in the research program. They included an elastic test (very small drift), an inelastic test (maximum storey drift of 0.5%) and a series of three sinusoidal tests simulating the “first mode” response of the building to sinusoidal base excitation. The first two tests produced little to no damage to the structure with the largest storey drift of 0.5%. Majority of the observations were made solely based on the third test, which only excited the first mode of the structure. Even though, the structure performed poorly in terms of damage distribution.

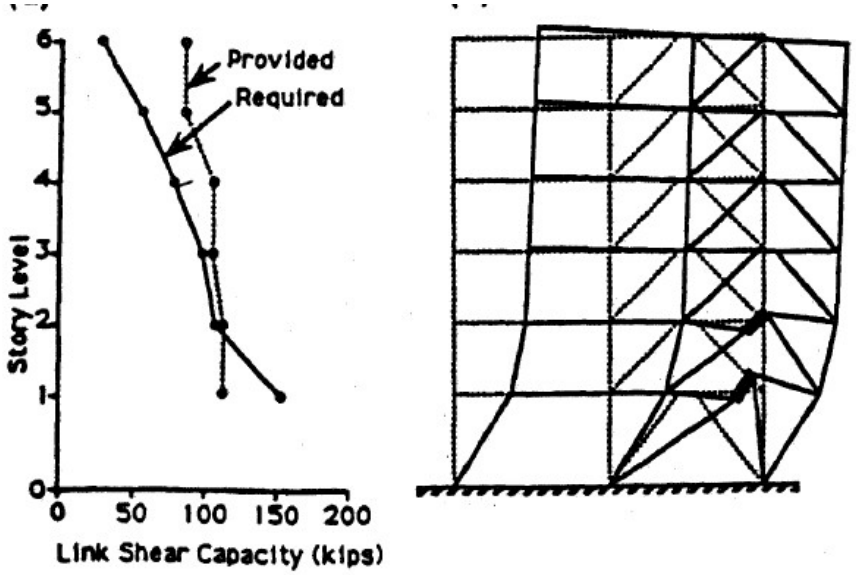

Figure 2-5: Response of six-storey EBF (Popov, 1992)

Martini (1990) also demonstrated that EBFs are susceptible to a concentration of excessive inelastic link deformation at particular storey levels with a 13-storey model. The result is shown in Figure 2-6b. He proposed to use tie elements to connect the links vertically to force a global failure mechanism in the structure as shown in Figure 2-6c.

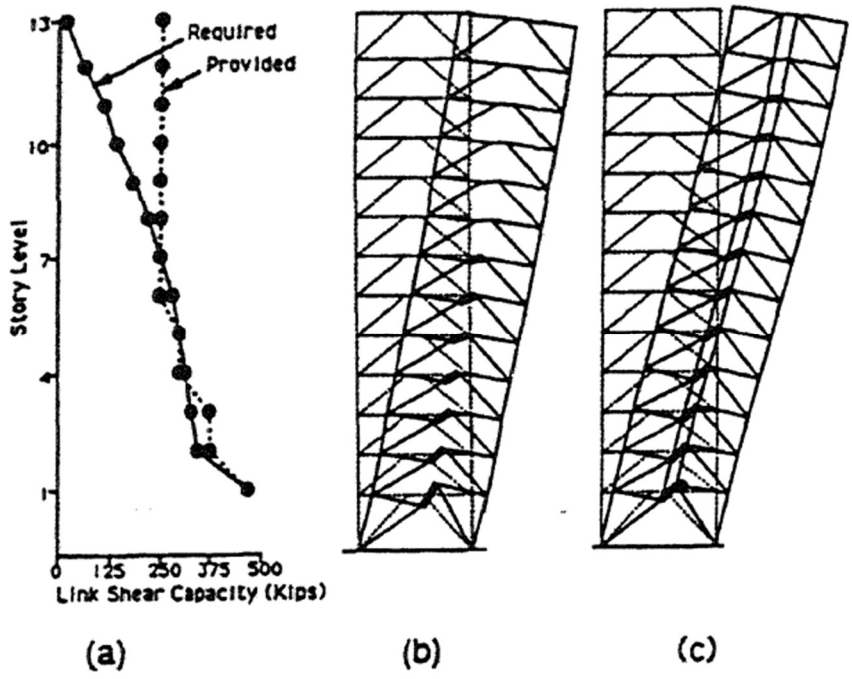

Figure 2-6: Seismic response of thirteen-storey EBF (Popov, Ricles, & Kasai, 1992)

Later, Popov, Ricles, & Kasai (1992) pointed out that incorrectly designed link elements may lead to an undesired seismic response, which is the reason for the poor performance of EBFs observed in the previously mentioned tests. A design method for proportioning links was hence proposed by the authors. The method emphasized on choosing the link sections to have a uniform value for link over-strength throughout the frame height.

Several studies were carried out by Popov (1992) to examine this proposed design methodology, including redesigned EBFs that was presented by Foutch (1989) and Martini (1990) and a series of inelastic time-history analyses for 4, 6, 10 and 20-storey EBFs. He concluded that the main reason for soft storey mechanism to form in EBFs is the overly strengthened links. If all links are proportioned closely to the link shear force required by the code, EBF up to 10 storeys develops uniformly distributed inelastic link deformation over the building height. For EBFs with more than 10 storeys, if the static design forces are calibrated by elastic dynamic vibration modes, the proposed method can further improve their seismic inelastic performance.

He also emphasized that EBFs, for which the links are designed proportional to the NEHRP static design forces, are prone to the concentration of inelastic deformation. It is crucial to include 2nd

and 3rd vibration modes in determining the static story shear design forces. This opinion is widely accepted nowadays; most design guidelines require dynamic analysis to be performed in designing taller EBFs. When evaluating the EBF designed in the paper by Martini (1990), Popov specifically pointed out that the links located on the upper storeys have much larger over-strength comparing with rest of the structure and hence caused the failure of the 13-storey EBF. He modified the design of link sections of the structure according to its elastic vibration modes combination with CQC method and obtained satisfactory results (Popov, 1992).

The results presented by Popov, Ricles, & Kasai (1992) depicted that EBF response is very sensitive to the vertical distribution of the over-strength ratio of ductile links in the structure. A 50% over-strength ratio of links at upper storeys as used in the example illustrated by Martini (1990) dramatically changed the dynamic response of the building and lead to a concentration of damage in the lower floors. Although the modified design method proposed by Popov can reduce the likelihood of soft storey formation, one has to realize that material properties may vary. Considering the material strength factor of link sections are ranging from 1.1 to 1.5 as found by Okazaki et al. (2004), the over-strength created by material variation alone could put conventional EBFs at risk. Moreover, link selection is also restricted by their availabilities. More often than not, the links at higher storeys of buildings are stronger than required to meet the maximum link rotation criteria, especially for structures having lower seismic demand.

2.3.2 Seismic response of Modern EBFs

Eccentrically braced frame (EBF) is a relatively new structural concept. The first recorded seismic event which pushed modern EBFs to the inelastic range was the Christchurch earthquake series of 2010/2011 in New Zealand.

Clifton, Nashid, Ferguson, Hodgson, & Seal (2012) summarized the performance of the EBFs during this event. In general, he concluded, the EBFs in New Zealand demonstrated excellent seismic resistance during said events. He also noted, data collected during the Christchurch earthquake event evidenced the adequacy of a capacity design procedure for EBF as a design method for members outside of ductile links. It was observed that all inelastic demand was concentrated into the active links as required by the procedure.

Although there were still limited number of cases where structure experienced more severe damage, the damage was more likely caused by poor detailing.

However, several major differences between building code in New Zealand and Canada must be realized.

1) All column connections including gravity column connections are required to be rigid according to P3404:2009 in New Zealand. In Canada, columns in braced frames are only required to be continuous for at least two storeys, and no rigid connection is required for any columns (CISC, 2016).

2) For buildings with weak ground floor such as parking lots, columns on ground floor are fixed to foundation with reinforced connections in New Zealand. Most of the structures examined belong to to this category. This connection detail greatly increased the lateral stiffness of the ground floor, thus reducing the possibility of soft-storey formation at this floor.

These differences could potentially change the response of EBFs in Canada compared with the response illustrated in Christchurch event. Firstly, all columns in EBFs are required to be rigidly connected throughout the building height, including gravity columns. Secondly, all columns, including gravity columns are fixed to the foundation in most of the structures examined. When the ground floor is used for the parking lots, reinforcement was added to ensure the rigidity of the connections. The impact of these modifications to conventional EBFs in North American is two-fold. The fixity of ground floor columns greatly increases the lateral stiffness of ground floor. All the rigidly connected columns also serve as connections between storeys to redistribute induced lateral loads.

In addition, the authors also noted that several link sections in the structure studied (Clifton, 2012) were fractured due to miss-alignment of link stiffeners and the connected braces. This finding indicates that failure of links could also happen due to construction errors, which could potentially lead to the formation of a soft-storey in a EBF without continuous columns.

2.4 Existing structural systems to prevent soft-storey mechanism

2.4.1 Zipper braced frame

For the chevron bracing configuration, Khatib, Mahin, & Pister (1988) proposed to link the braces to beam joints of adjacent storeys with zipper column to form a zipper braced frame (ZBF), with the aim of utilizing the stiffness of all beams and remaining braces against concentrated lateral force. The zipper columns are presented in the structure to transfer the unbalanced brace force produced upon brace buckling to adjacent levels, and thus, to force the braces located on those levels to buckle. As illustrated in Figure 2-7, the zipper frame mechanism is formed when all braces on half span experienced buckling, few braces of the other side experience yielding, and beams hinges are possibly developed at their mid-span. They proposed a design method and demonstrated the potential of the system for a 6-storey braced frame. The zipper braced frame (ZBF) was introduced in the Commentary of the AISC Seismic Provisions for Structural Steels (AISC, 1992) as an alternative means to improve the response of multi-storey braced frames. Afterwards, many studies regarding this structural system had been conducted. Sabelli (2001) designed and analyzed a 3- and 6-storey zipper braced frames. The zipper columns were selected to have the same section as the braces of the level below. Considering the vertical projection of the unbalanced load could not be greater than the brace capacity, the selections of zipper sections were conservative. The author concluded that the zipper braced frames has great potential to uniformly distribute the damage over the building height. However, while the analysed 3-storey zipper frame exhibited the expected response, the zipper columns in the 6-storey ZBF experienced non-linear behaviour that was amplified by the effects of higher modes (as illustrated in Figure 2-8), which raised the concern that the zipper columns may not be sufficiently strong to remain elastic throughout the ground excitations due to the effect of higher modes.

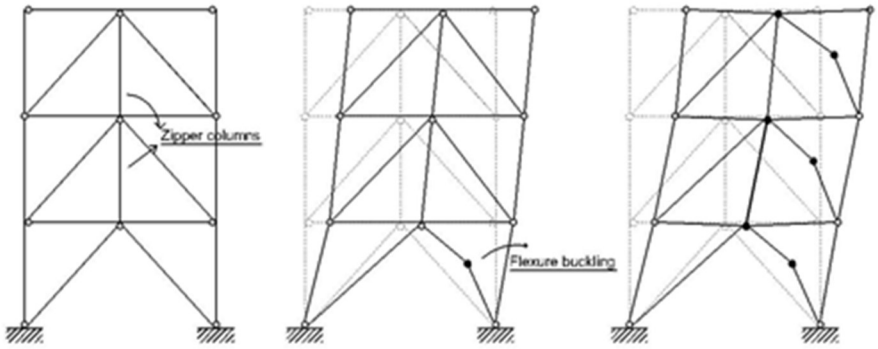

Figure 2-7: Zipper braced frame configuration and its yielding mechanism (Chen, 2011)

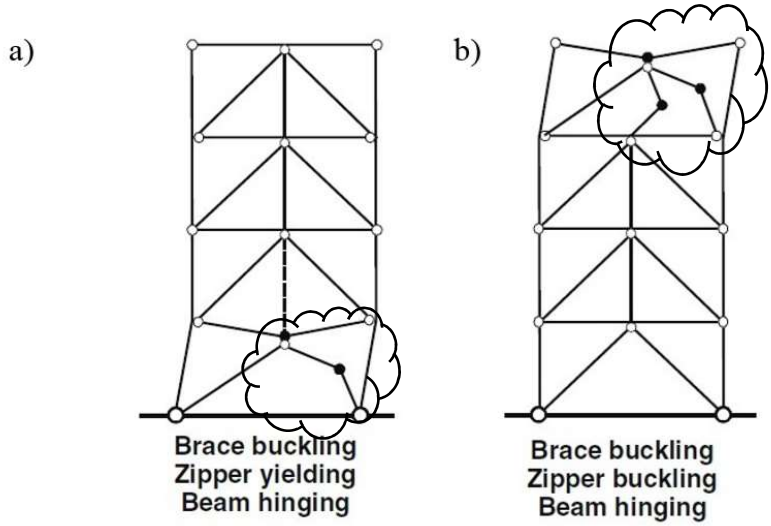

Figure 2-8: Behaviour of zipper braced frame system with weak zipper column (Tirca & Tremblay, 2004): a) zipper yields in tension; b) zipper buckles in compression

2.4.1.1 Elastic zipper braced frame

Tremblay & Tirca (2003) proposed a strong zipper column design procedure for the ZBF system to ensure that the zipper column will respond in the elastic range while transferring brace forces after brace buckling or yielding. This procedure suggested including higher modes effect in the zipper design by adopting a serial of lateral force distribution patterns representing the force redistribution after brace buckling. All structural members in the zipper frame, with the exception of zipper columns, are designed in accordance with the existing building code for moderate ductile

chevron braced frames. The so-designed ZBF system, labelled E-ZBF, ensures the development of a full-height zipper mechanism. Triangular lateral load patterns representing lateral inertia force occurring after brace buckling and yielding are used to predict the maximum possible forces that will be induced in the zipper columns. Several different lateral load patterns are applied upon buckling of every brace member to capture the redistributed shear force. Furthermore, two scenarios are considered depending on whether brace buckling is initiated from the top or the bottom of the frame, as shown in Figure 2-9.

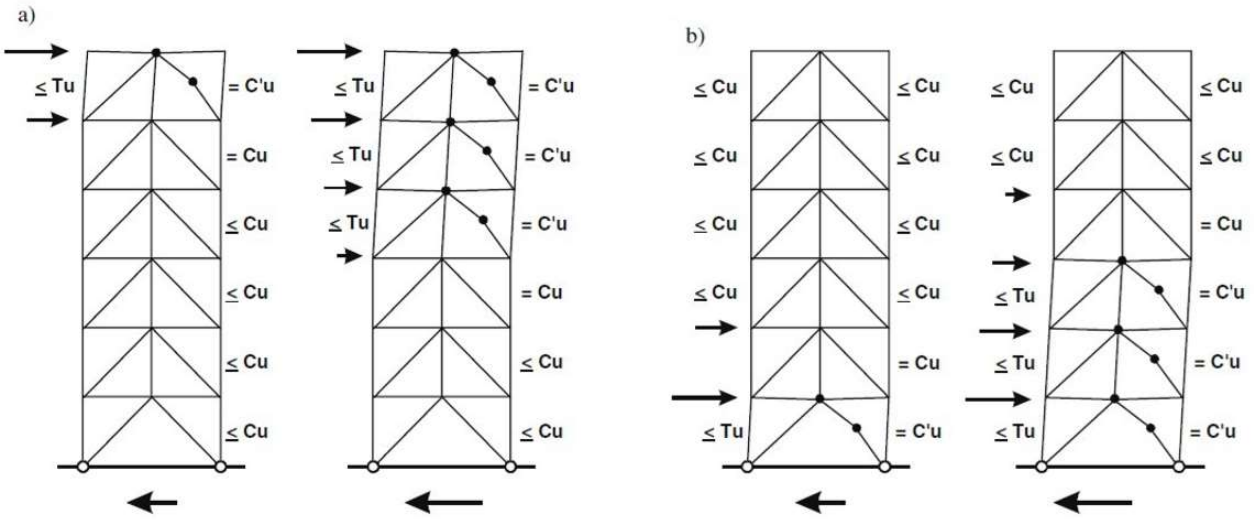

Figure 2-9: Mechanisms and lateral load distributions adopted for design with brace buckling initiating at the: a) upper floors; b) lower floors (Tremblay & Tirca, 2003)

The lateral force was assumed to be at the maximum level at the bottom/top where the brace buckling first occurred. This force linearly diminished to zero at the level above/below the storey where the brace just buckled. In this respect, the lateral forces are redistributed mostly to the levels with reduced lateral stiffness due to inelastic behaviour, i.e. brace buckling. Based on this load distribution pattern, maximum compression and tension demands in the zipper columns were enveloped, and the zippers can be designed accordingly.

With the zipper columns being designed to remain elastic, the axial forces induced by the braces can be effectively transferred across the entire structure and inelastic response can be achieved over the entire structure height. Additional numerical analyses conducted for a 4-, 8- and 12- storey structures located in Victoria, B.C. (Tirca &Tremblay, 2004) under various ground motion types

confirmed the adequacy of the aforementioned design method with only a few exceptions for the design tension force as shown in Figure 2-10. In this research the ground motions were scaled to much the UHS at the fundamental period of the building, while the numerical analyses were conducted using Drain 2DX (Allahabadi, 1988).

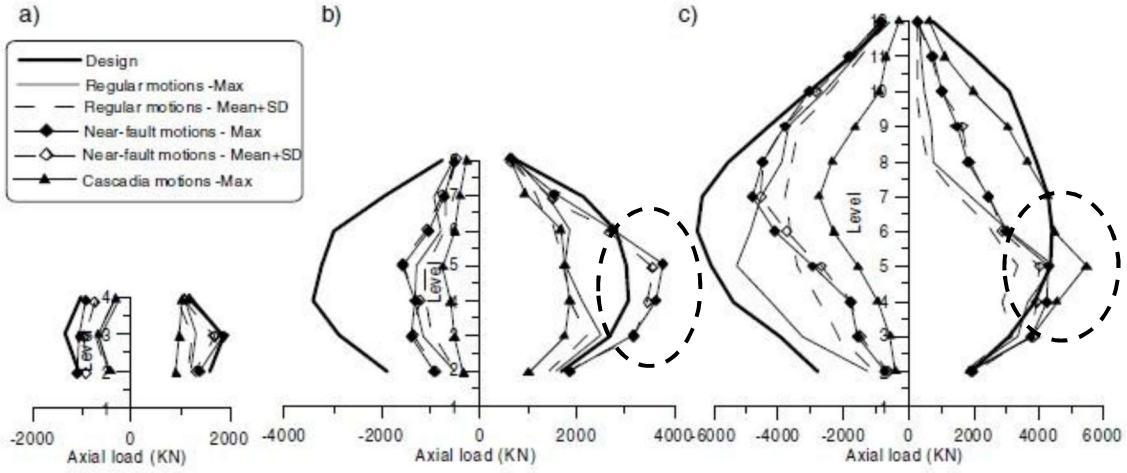

Figure 2-10 Computed peak axial loads in zipper columns for 4-, 8-, 12-storey buildings (Tirca & Tramblay, 2004)

To achieve a more accurate prediction of the axial forces that may develop in the zipper columns, the design method proposed by Tremblay and Tirca was further refined by Chen (2011) and Tirca and Chen (2012). The authors added six different load distribution patterns as recommended in FEMA 356 and it was concluded that slightly larger tensile force demand can be obtained if a parabolic distribution is considered for designing the zipper columns compared to the originally proposed triangular lateral force distribution patterns. Estimating the maximum compressive force triggered in the zipper column using triangularly distributed lateral loads was found to be adequate and maintained. E-ZBFs for 4-, 8- and 12-storey buildings located in the Victoria region were designed according to these revised criteria and tested under three ground motion ensembles: crustal, subduction and near-field. Although near-field ground motions are not expected in Canada, this ensemble was selected in order to examine the system behaviour under such earthquakes. The results shown in Figure 2-11 illustrate that the maximum axial force demand experienced by the zipper columns were well predicted by the revised design method. At mean time, it is also clearly shown that the sections required for zipper columns increased greatly with the number of storeys.

To withstand the force demand in the zipper strut of a 12-storey system designed for Victoria, BC, a large cross-section (2HSS254x254x13.0) was required and the size increased to W360x347 for the16-storey E-ZBF building (Z Chen, 2012). It became unrealistic to apply this system to high-rise steel structures.

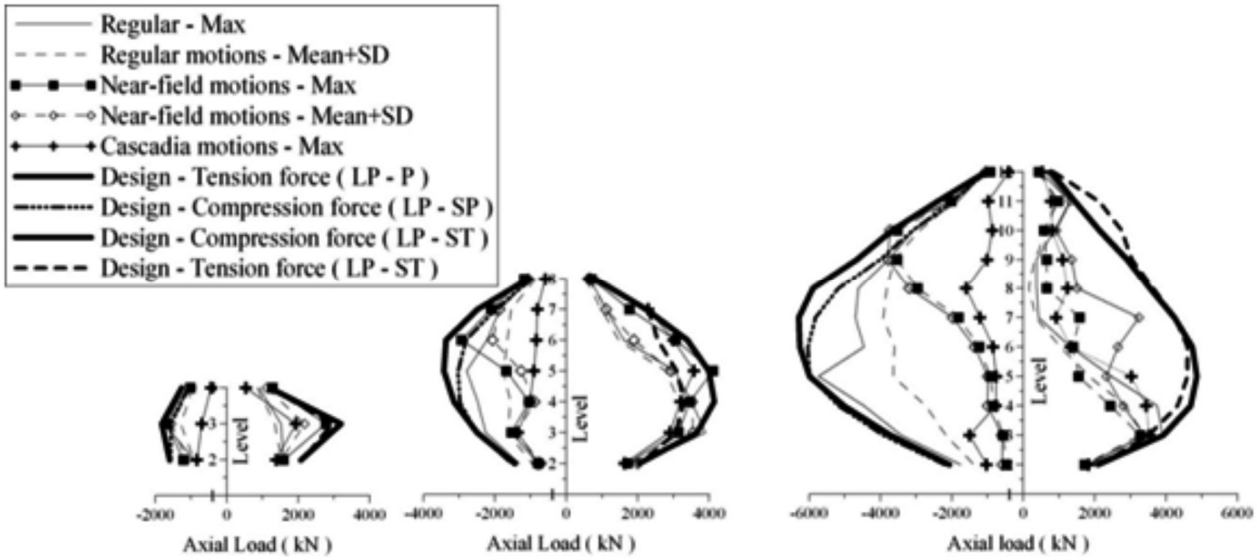

Figure 2-11 Axial force in zipper columns obtained from nonlinear dynamic time-history analyses of 4-, 8-, 16-story buildings (Tirca & Chen, 2012)

Furthermore, as depicted from Figure 2-12, that maximum compression is expected in the zipper column in the upper floors while maximum tension is expected in the lower floors. This behaviour was observed in all buildings. In the taller buildings, however, compression was lower than predicted in the bottom levels and tension was lower than expected in the upper floors. This means that the probability of having all braces to behave inelastically at the same time over the full building height diminishes when the number of storeys is increased. This is due to the fact that the structure response naturally tends to be dominated more by higher vibration modes, rather than first mode in taller buildings. It leads to a question that if it is necessary or realistic for the modern structure to be designed for a full-height mechanism.

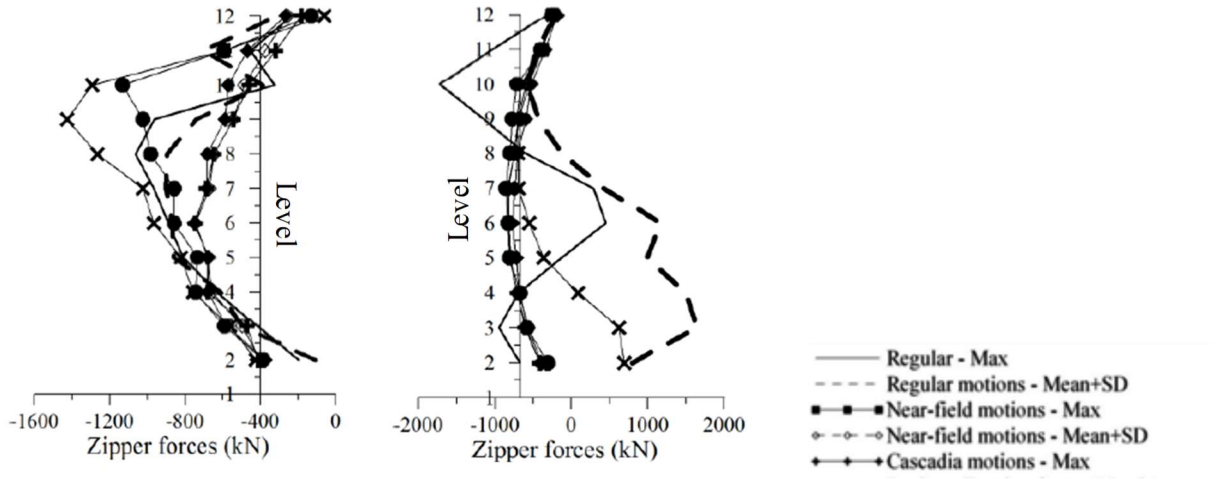

Figure 2-12 Maximum compression and tension forces in zipper columns of 12-storey zipper frame under regular, near-field and Cascadia ground motions (Chen, 2011)

On the other hand, under extreme ground excitations, the 4-storey E-ZBFs responded more in the first mode in the inelastic range, with the formation of a full-height zipper mechanism characterized by brace inelastic response developing simultaneously in all floors at the same time. This led to excessive storey drifts, greater than 2% of storey height. Tremblay (2003) reported similar response for an 8-storey ZBF frame: the structure experienced large lateral displacements and reached near collapse condition all braces had buckled and lost part of their compressive resistance.

2.4.1.2 Suspended zipper braced frame

Leon and Yang (2003) proposed a different concept for ZBF structures. They introduced an elastic hat truss at the top floor of conventional ZBFs to vertically anchor the zipper column and limit the lateral deformations and mitigate the risk of dynamic instability of the structure after the formation of the full-height zipper mechanism. It was therefore suggested that the hat truss be designed to behave elastically under the maximum anticipated zipper column force corresponding to the sum of the brace unbalanced forces developing over the full building height. The structure is then labelled as suspended zipper braced frame (S-ZBF). S-ZBF offers a relatively clear load transfer path. Unbalanced brace forces were collected by the zippers and transferred to the elastic hat truss and then the energy columns of the frame were taking these forces down to the foundation. Therefore, capacity design concept was adopted; the zippers were designed to be able to resist the accumulated differences between the tension capacity and the post-buckling capacity of braces. To

ensure the elasticity of the hat truss, it was designed for both the forces transferred from zipper columns as well as 1.8 times the lateral shear force at the specific storey.

This suspended zipper braced frame system was validated numerically for structures up to 20 storeys (Yang et al., 2008) and experimentally through shake table and quasi-static cyclic tests performed on three-storey models (Schachter and Reinhorn, 2006; Yang et al., 2010). Analytical 2D and 3D models was also built by Yang (2006) who concluded that "the suspended zipper frame configuration is able to overcome the instability and full collapse problems of a full-height zipper mechanism and achieve a more uniform distribution of damage over its height without the use of overly stiff beams". However, the main drawback of this system was also highlighted by Yang (2006): the force demand in the elastic hat truss increased rapidly with more storeys in the system, which significantly reduce the feasibility of this system in high-rise buildings.

2.4.2 Dual braced frame (Strongback system)

Tremblay et al. (1997) first proposed a dual braced frame with vertical elastic truss to improve the response of X-bracing with tension-only conventional braces. When compared to reference conventional steel braced frames for 4- and 8-storey buildings, the addition of the vertical elastic truss eliminated the concentration of inelastic demand along the structure height. Moreover, the benefits were more pronounced when higher R values were used in the calculation of the seismic design loads, suggesting that higher ductility factors could be specified for DBFs.

Tremblay (2003) then proposed the dual configuration with buckling restrained bracing members as illustrated in Figure 2-13. Various configurations of DBFs with BRB members were examined by Tremblay & Poncet (2007). For an 8-storey braced frame, the dual system was found to exhibit more uniform storey drift demand compared to the BRB frame. Tremblay and Merzouq (2004) proposed a design method for the elastic truss members of the DBF system with BRB members. They performed incremental dynamic analysis to compare the seismic performance and resistance to collapse of BRB frames and DBFs with BRB members for buildings having 8 to 24 storeys in height. Reduced peak storey drifts, more uniform ductility demand, and more robust performance against collapse could be achieved in all cases with the dual system. Tremblay and Merzouq (2005) refined the DBF design procedure based on time history response of the framing system, including

empirical expressions for predicting the design forces for the elastic truss members. Merzouq and Tremblay (2006) verified the seismic performance against collapse when applying these refined design guidelines for 8- to 24-storey buildings. Design procedure was proposed and proven to be adequate for crustal and sub-crustal earthquakes as well as subduction ground motions. Tremblay and Poncet (2007) examined the seismic response of conventional CBFs, BRB frames and DBFs with BRB members. For the 12- and 16-storey buildings, the seismic performance was significantly improved when using the dual system. It is noteworthy that the number of buckling restrained braces is reduced by half compared to the common chevron BRB frame configuration, which may represent an economic incentive for the system. The DBF system with BRB members was used for a 3-storey frame in California (Mar, 2010).

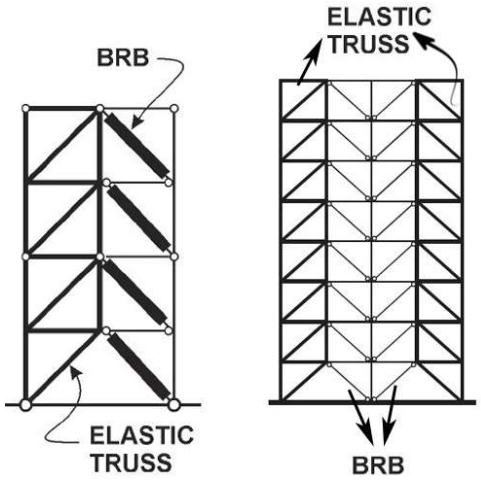

Figure 2-13: BRB with elastic truss (Tremblay & Merzouq, 2004; Tremblay & Poncet, 2007)

Similar concepts were investigated by a number of other researchers and practical engineers on alternative bracing configurations (Lai & Mahin, 2015; Panian, Bucci, & Janhunen, 2015; Pollino, Slovenec, Qu, & Mosqueda, 2017; Slovenec, Sarebanha, Pollino, Mosqueda, & Qu, 2017; Simpson & Mahin, 2018; Pollino, Sabzehzar, Qu, & Mosqueda, 2013; Qu, Sanchez-Zamora, & Pollino, 2014).

Lai & Mahin (2015) compared the seismic performance and cost of the 3 different variations of the frame with strongback systems to that of conventional chevron bracing system and “X” bracing systems, as shown in Figure 2-14. It is found that the strongback system can effectively prevent

the soft-storey mechanism in the braced framing systems with 13% to 18% less cost. With the addition of BRBs, the peak storey drifts and residual displacements can be further reduced.

However, with the code-specified over-strength factor of 2.0, it is inadequate to ensure that the members in the vertical elastic truss remain elastic under design-level seismic forces. Limited yielding is observed near the top of the strongback systems. Thus, Lai and Mahin (2015) noted further investigation is needed for this simple over-strength factor design approach.

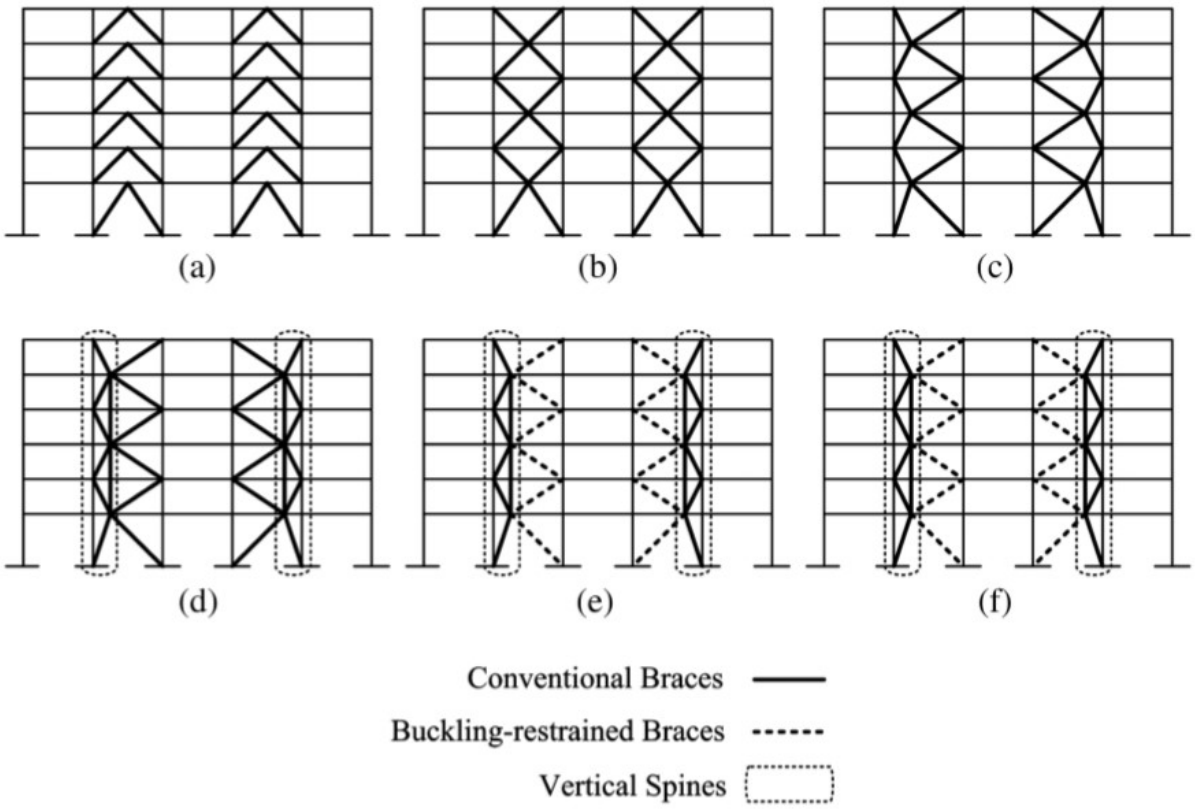

Figure 2-14 Elevation views of six different bracing configurations: (a) V6; (b) X6; (c) X6-3; (d) SB6-3; (e) SB6-3B; (f) SB6-3 L (Lai & Mahin, 2015)

Cyclic testing of a nearly full-scale two-storey one-bay specimen was conducted by Simpson & Mahin (2016) to investigate the viability of the strongback system as shown in Figure 2-15. The test specimen represented a retrofit scheme for a two-storey chevron braced frame that was designed according to older code standards. A weak storey was formed for the original chevron braced frame due to local buckling and fracture of brace. The retrofit scheme kept the original

beams and columns. The column, half of the beam and the newly added braces formed the elastic strongback. A BRB was added to the left side of the frame as the primary energy-dissipating devices. The strongback brace members were sized based on the maximum capacity of the BRB. The strongback system was found to successfully prevent the soft-storey formation. An evenly distributed storey drift profile was achieved for the specimen.

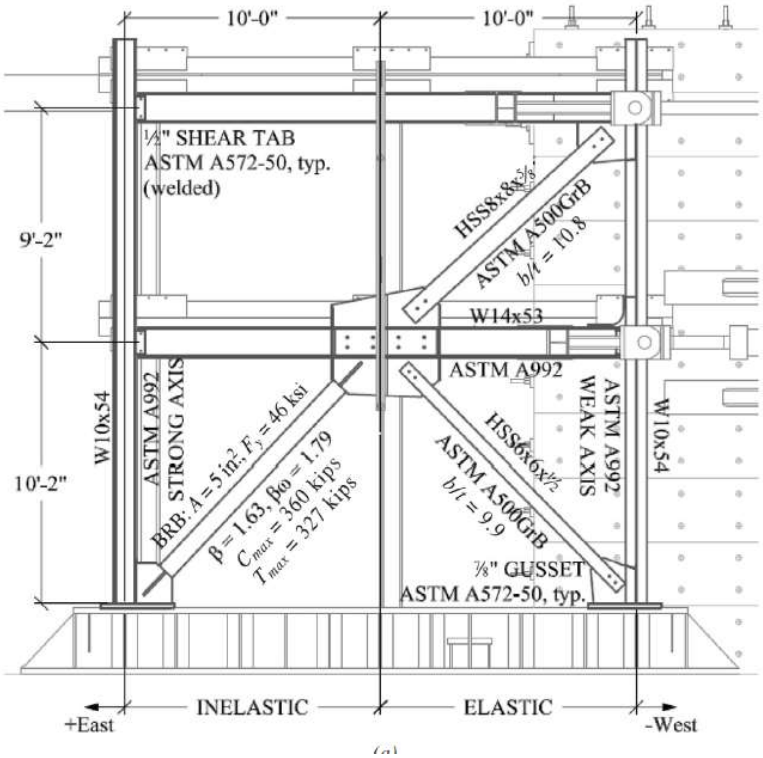

Figure 2-15 Schematic drawing of strongback test specimen (Simpson & Mahin, 2018)

A four-storey laboratory building was constructed with a buckling restrained braced mast frame (BRBM) (Panian, Bucci, & Janhunen, 2015). The elevation drawing is shown in Figure 2-16. The BRBM consisted of a BRB located on each floor of the frame and a vertical elastic mast that was continuous over the entire height of the structure, as shown in Figure 2-17. The BRBs were designed to have equal capacity at all storeys. The members of the elastic mast were designed with nonlinear time history analysis, capacity design principles, and an overstrength factor of 2.0. The elastic mast was able to force a first-mode rocking displaced shape and led to reduced overall damage. In addition, the number of BRBs required for such system was greatly reduced comparing to that of a conventional BRB frame.

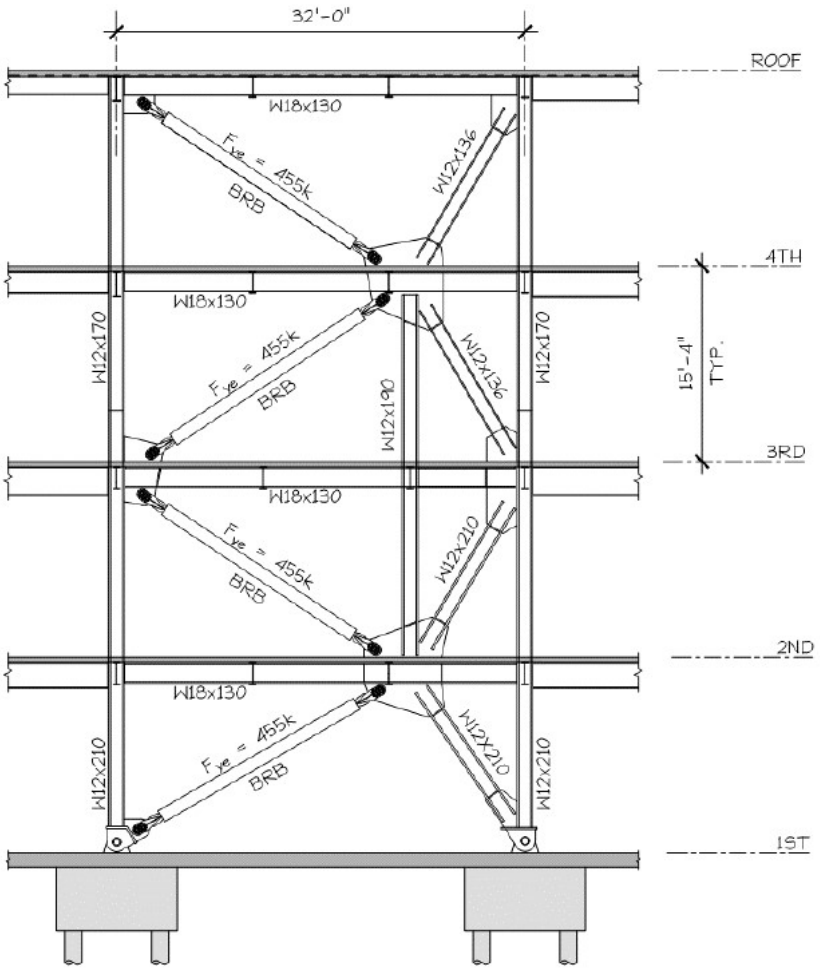

Figure 2-16 Elevation drawing of the Heinz Avenue Building (Panian, Bucci, & Janhunen, 2015)

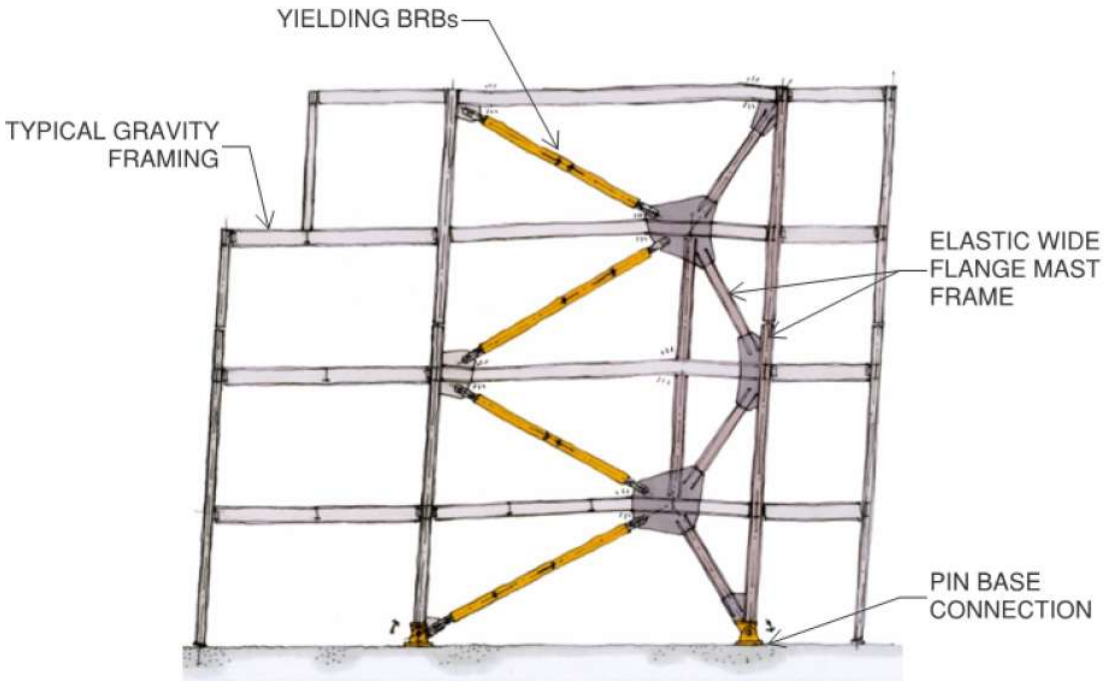

Figure 2-17 BRBM frame elevation (Panian, Bucci, & Janhunen, 2015)

Pollino et al. (2013) proposed a stiff rocking core (SRC) system for rehabilitating sub-standard buildings. The concept of this technique is shown in Figure 2-18. A continuous elastic trussed mast (rocking core) was added to the under-performed structure to prevent soft-storey formation. Steel yielding links can also be added to further improve the seismic performance of the retrofitted structure and increase its energy dissipation capacity.

A performance-based design method was proposed by Pollino et al. (2017) for the design of steel yielding links. The SRC members were designed based on two components. The first component is the differential shear between the shear forces back calculated from a uniformly distributed storey drift combined with an inverted triangular lateral force distribution pattern and the lateral force capacity of the braces. The second component is shear forces resulted by higher modes combined with a square root of the sum of squares (SRSS) rule. The system was numerically proven to successfully mitigate the soft-storey mechanism, and the addition of steel yielding links could help the frame to achieve a target performance level in terms of maximum drift for 3-storey buildings. However, it was also pointed out that the design method is overly conservative for building with 3 floors.

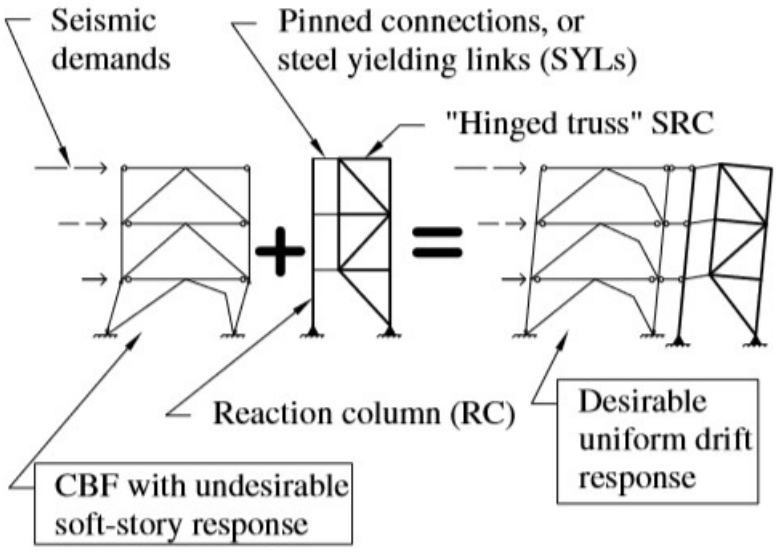

Figure 2-18 Concept of stiff rocking core rehabilitation technique (Pollino, Slovenec, Qu, & Mosqueda, 2017)

Slovenec et al. (2017) presented a hybride test the SRC rehabilitation technique. A 3-storey physical specimen and a 6-storey model consisted of the 3-storey physical specimen and another 3 storey of analytical model were tested under dynamic loading as shown in Figure 2-19. The SRC was designed according to the method presented in Pollion et al. (2017). These tests demonstrated the efficiency of the SRCs in terms of preventing soft-storey formation. But it was also noted that steel yielding links were required to guarantee a desired seismic performance level due to the low energy dissipation of the old CBFs.

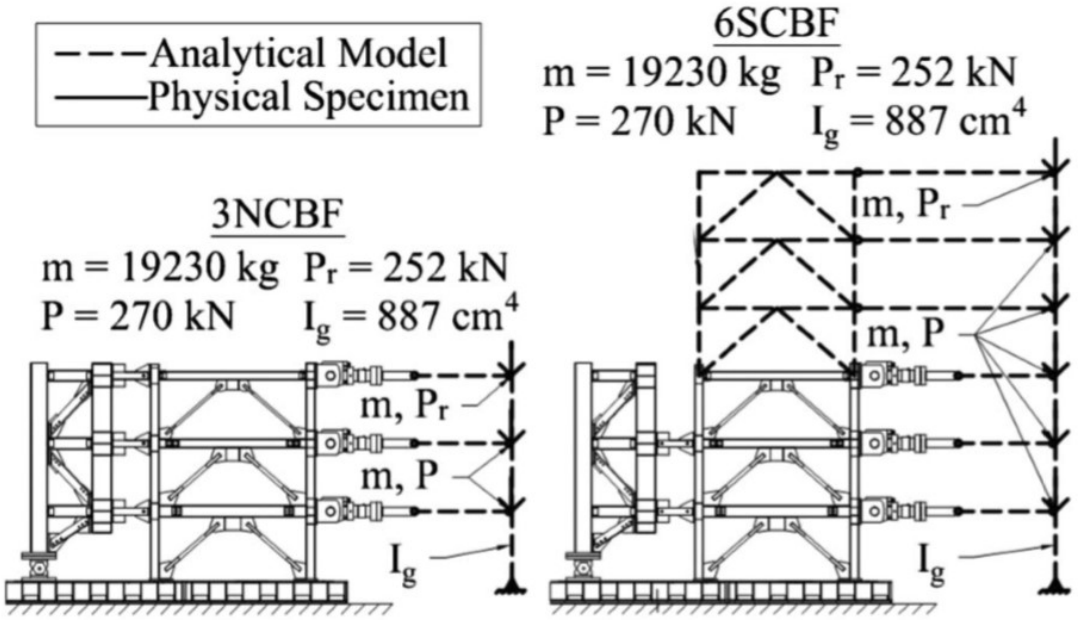

Figure 2-19 Hybrid analytical substructuring (Slovenec, Sarebanha, Pollino, Mosqueda, & Qu, 2017)

Simpson (2016) and Liu (2017) thoroughly reviewed the development of the strongback system. The functionality of the strongback system in terms of soft-storey prevention was highlighted in both papers.

However, although these studies regarding the strongback system are extensive and sophisticated, no design method is found to be able to accurately predict the force demand of structural members. In addition, majority of the tests are performed on 2- to 6-storey buildings, the influence of the total height of the structure on the force demand of members are therefore not yet observed nor discussed.

2.4.3 Tied braced frame

As mentioned in the previous section, Martini (1990) proposed to use vertical ties to connect all ductile links together in a conventional EBF to ensure uniform plastic demand distribution throughout building height. This tied braced frame system, labelled TBF, was further studied by Ghersi et al. (2000, 2003, 2006), Rossi (2007) and Bosco and Rossi (2009). Regarding the influence

of the link overstrength factor in the EBF behaviour, Bosco & Rossi (2009) claimed that after extensive investigation on a large set of traditional eccentrically braced structures, the link overstrength factor was found to play an important role; however, it did not guarantee that larger plastic deformations of links at all floors may occur prior to a concentration of these deformations in a few storeys. Ghersi et al. (2003) and Rossi (2007) further developed and validated a design method for the TBF configuration. The authors employed mode superposition method in the design process of TBF assuming inelastic (reduced) first mode response and elastic second mode response. The design of the systems is acquired through displacement-based approach, whereas the ultimate lateral displacements and maximum lateral displacements were computed following the methodology proposed by Roeder and Popov (1978) regarding traditional EBFs. The total rotation of the structure is calculated as the sum of all deformative contributions. The entire design of tied braced frame is a serial of iterative processes. All the links are designed to have approximately the same plastic rotational capacity. After the link design, the force demands of rest structural members are calculated with mode superposition method based on the forces imposed by the strain hardened links. In the mode superposition method, the lateral forces corresponding to the first vibration mode are reduced by the ductility factors whereas the forces resulted from second vibration mode are not modified by ductility factors and over-strength factors. Rossi and Ghersi proposed to add a force reduction factor to the forces generated from second and higher modes based on knowledge gained from past researches and experiments as shown in Figure 2-20.

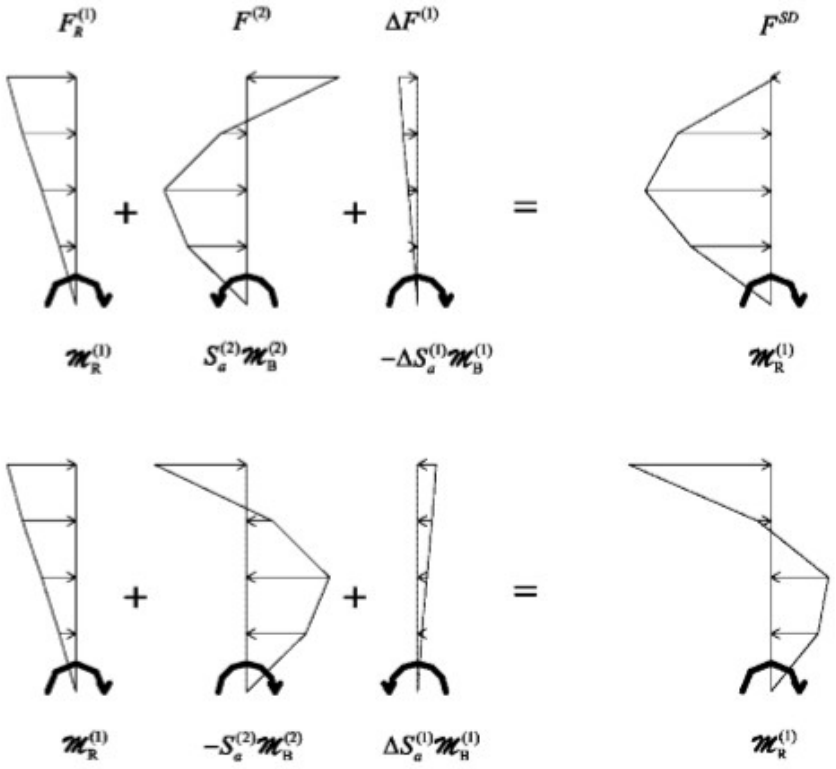

Figure 2-20: Force combinations for member design proposed by (Rossi, 2007)

The proposed method demonstrated accurate prediction of forces demand in the structural members. Further, Bosco and Rossi (2009) confirmed that this system, even without carefully proportioned links, was able to produce large plastic rotations of the links at all storeys. The design methodology proposed for the TBF system was developed in agreement with Eurocode 8 and Eurocode 3 requirements. Buildings up to 16 storeys designed with the proposed design method responded adequately under ground motion excitations, as shown in Figure 2-21.

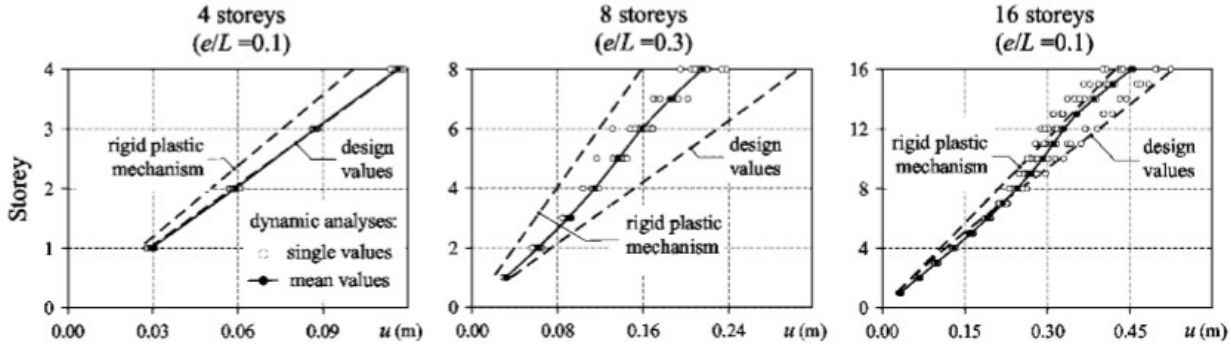

Figure 2-21: Results of non-linear dynamic analysis in terms of maximum lateral displacement (Rossi, 2007)

A uniformly distributed inter-storey drift profile was achieved by using the proposed design method, which led to a preferred global collapse mechanism for examined structures. In the meantime, the cost to achieve this design was also significant. The member forces obtained from numerical simulations are shown in Figure 2-22. Take the 16-storey TBF for example, the maximum forces in the ties reached almost 7000 kN, which is twice as much as the axial forces in the bottom brace of the structure and is close to the axial forces in the columns on the first floor. The amount of forces attracted to the tie members is significant, which led to huge sections for the tie members. The difficulty for connection detailing is foreseeable.

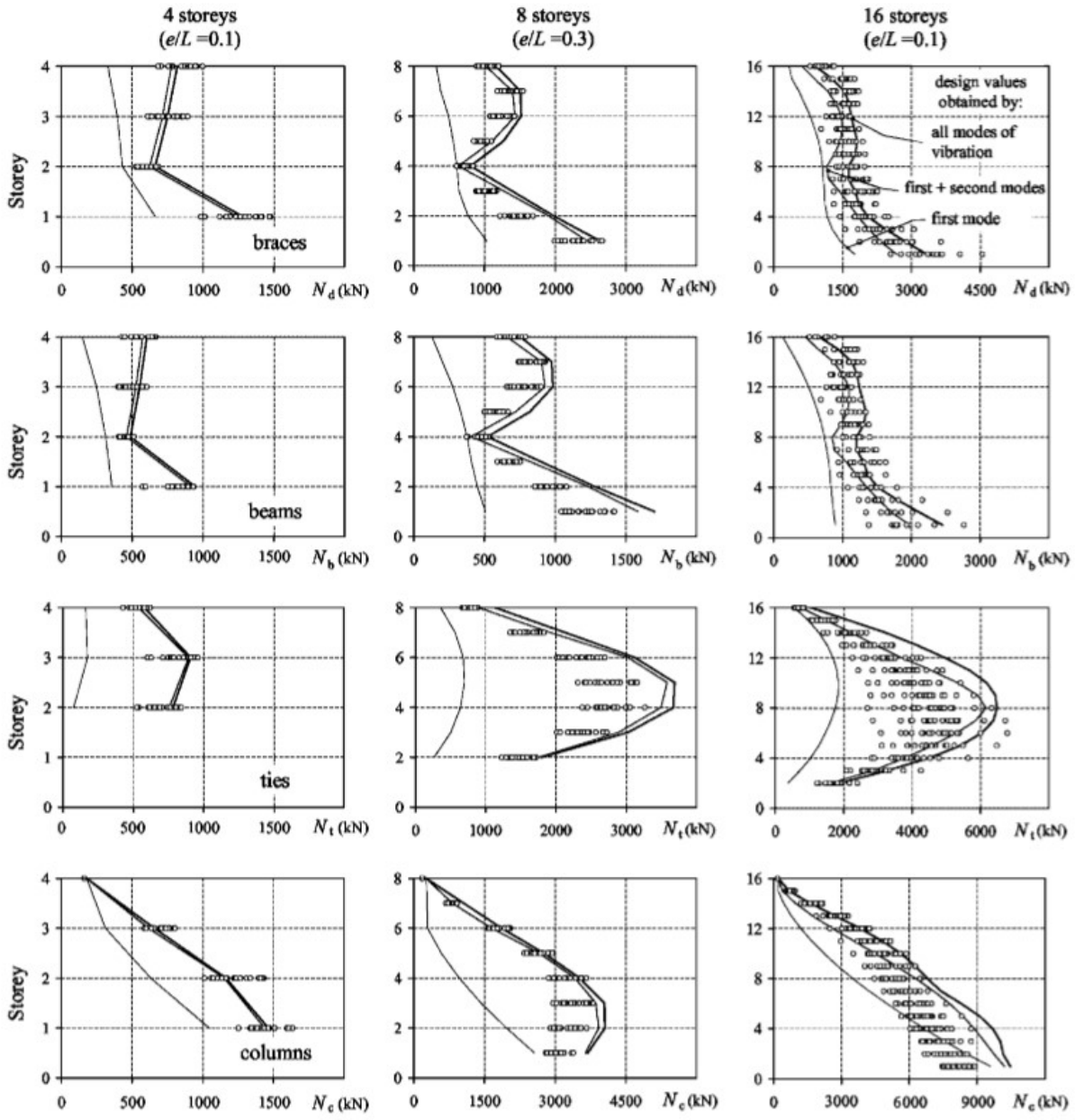

Figure 2-22: Axial forces of braces, beam segments, ties and columns for analyzed structures (Rossi, 2007)

2.4.4 Rocking frames

This idea was originally introduced by Beck & Skinner (1974) and Kelly & Tsztoo (1977) to concrete structures and steel structures. The controlled rocking frame allows buildings to sway with the motion of earthquakes and returns to their original position at the end of earthquake in order to

reduce the force demands in the frame members that are sized to remain elastic. Supplemental forces resisting overturning and energy dissipaters can be added to further enhance the performance of the system. Alternative approach aiming to mitigate soft-storey formation in steel structures, labelled as rocking frame and showed in Figure 2-23, was proposed and tested by Roke et al. (2009). Extensive studies were also conducted by Eatherton et al. (2010) to the controlled rocking system. The behaviour of this system was characterized as a combination of two actions, uplifting of the frame and elongation of post-tension strands. While combined with a fuse system, the whole system characterized a flag shape hysteretic response.

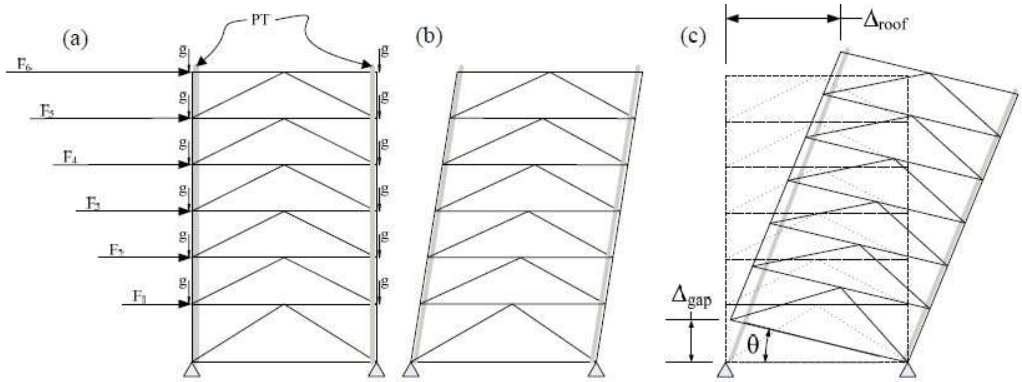

Figure 2-23 Rocking frame (Roke et al., 2009)

Eatherton et al. (2009) has compared an ordinary concentrically braced frame with a rocking frame. The rocking frame was designed for a higher response modification factor (R=3.25) while preventing the premature yielding of braces before rocking. However, with the expected higher ductility of the rocking system, the force demand in the brace may not be reduced but increased, as stated by Roke et al. (2009). In fact, Roke et al. have highlighted that the actual force demand in the braces can reach as high as 4 times the design strength. Therefore, the rocking frame has to be designed to account for higher mode demands, i.e. the member force demands are computed as the sum of first mode forces and higher mode forces.

As Roke proposed in the paper, the first mode forces should be calculated based on the mass distribution of first mode, which is calculated from the modal participation factor and mode shape, as follow:

$$\{s_1\} = \Gamma_1[\mathrm{m}]\{\phi_1\}$$

Then, the overturning moment resulted from first mode forces are derived as:

$$OM_1 = \{h\}^t\{s_1\}\mathrm{g}$$

The higher mode forces did not influence the overturning moment of the structure. However, they had large contributions in the base shear. Spectral acceleration values for each mode modified with a load factor obtained from probabilistic analysis were suggested to use for design purposes. Therefore, the design member forces of each mode in global response can be quantified with these factored design effective pseudo accelerations. Then the design forces of each member can be obtained using the complete quadratic combination (CQC) method.

Tremblay et al. (2008) studied rocking braced frames with viscous dampers placed between the column bases and the foundations. Restoring force was provided by the gravity loads supported by the columns. Numerical simulations were performed on 2 to 6-storey frames and shake table testing was conducted on a half scale model of a two-storey frame. The tests showed that the response could be easily predicted by commercially available computer programs. The numerical simulations showed that the member forces increased with the number of storeys, relative to the reduced forces used for regular CBFs. Roke et al. (2009), Deierlein et al. (2011) and Weibe et al. (2012) studied RBF systems in with vertical pre-tensioned tendons were used to re-center the structure after column uplift. In the first and third system, friction was used to dissipate energy upon rocking. Yielding was adopted in the RBF by Deierlein et al. (2011). The performance of the systems studied by Weibe et al. and Deierlein et al. was verified through shake table testing. Slow hybrid testing of a 6-storey frame specimen was performed by Roke et al. (2009).

In the 8-storey frame tested by Weibe et al. (2012), rocking was permitted at the base as well as the frame mid-height. The second rocking interface aimed at reducing member forces due to higher mode response. In addition, a self-centering bracing member was used at the structure base to conrol storey shear forces.

Tremblay et al. (2004) has proposed to use BRBs as columns on selected floors to form global flexural hinges along the height of braced frame labelled Flexural Braced Frame (FBF) system. All other frame members besides the BRBs are designed to remain elastic. The frame response is similar to a braced frame with multiple rocking bases. With limited number of BRBs, a significant amount of energy can be dissipated with proper configuration. The authors also highlighted that in

high-rise applications multiple storeys can be selected with the placement of BRB columns to reduce base shear resulted from higher mode effects as shown in Figure 2-24.

Wiebe et al. (2012) tested an 8-storey rocking steel frame with shake table test. Test results showed the rocking frame exhibited uniformly distributed damage even at very high ground motion intensity. However, storey shear forces as well as the over turning moment induced into the structure increased greatly with the intensity of the ground motion due to higher mode effect. The author proposed the addition of a second rocking interface to mitigate the great forces created by higher modes effect as well as secondary fuses to limit the base shear of the studied structure (Figure 2-25). These additions led to pronounced results as the storey forces due to higher modes effect were greatly reduced and base shear of the structure was halved while the storey drift and its distribution were not disturbed. (Figure 2-26).

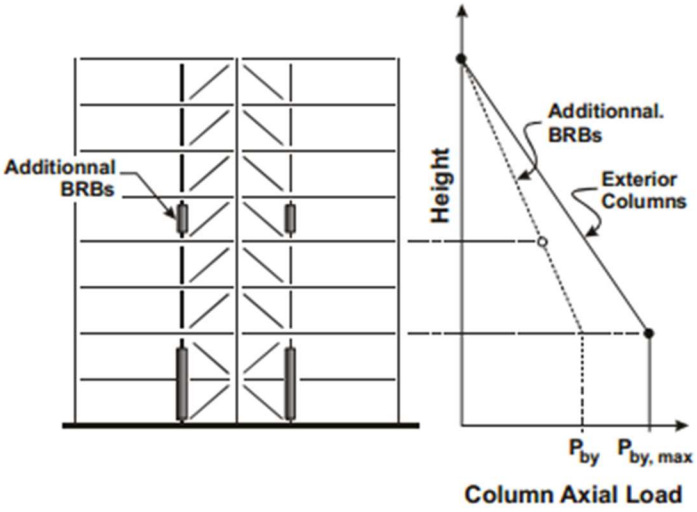

Figure 2-24 FBF with multiple BRB columns and the axial forces in the columns (Tremblay et al. 2004)

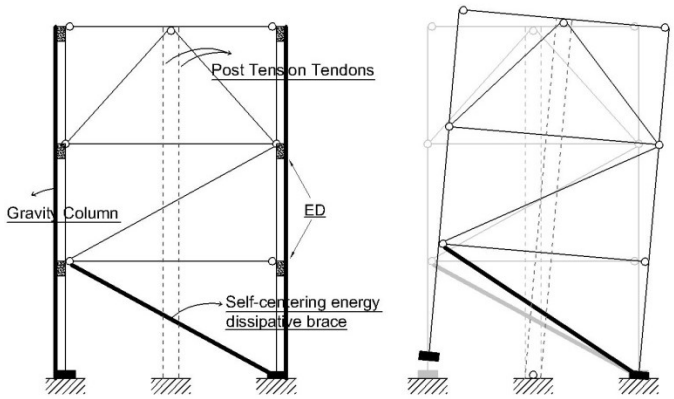

Figure 2-25 Rocking frame with load reducing fuses (Wiebe et al., 2012)

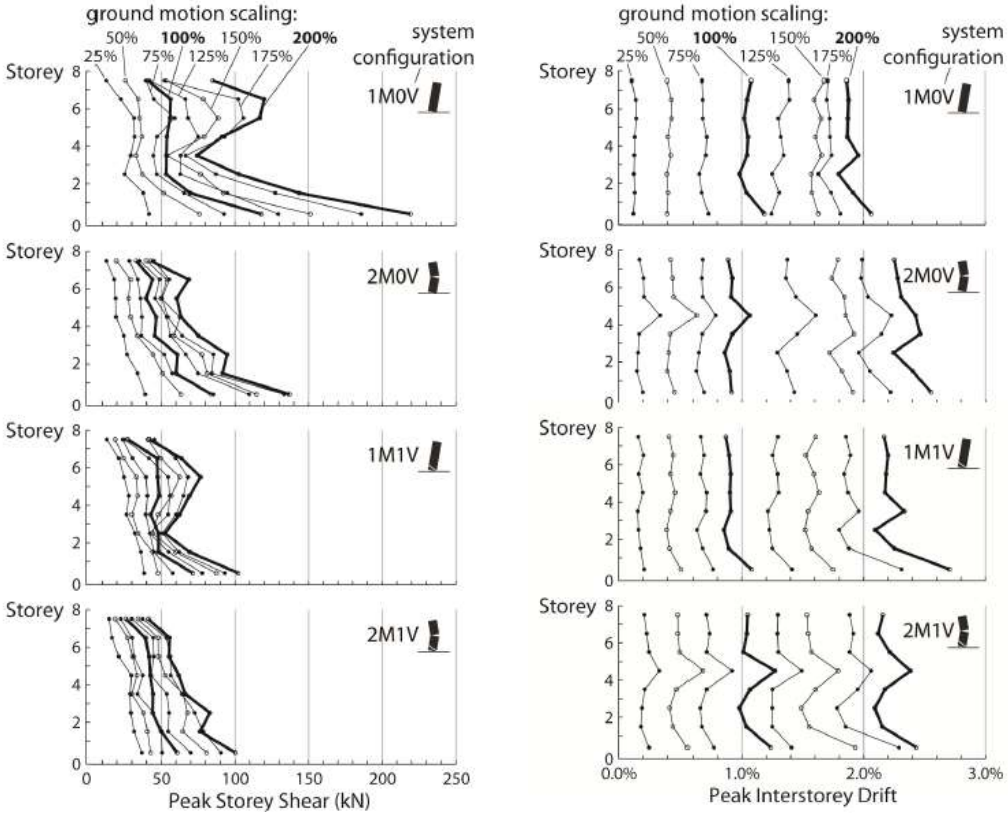

Figure 2-26 Shear force envelopes and storey drift distributions (Wiebe et al., 2012)

CHAPTER 3 DEVELOPMENT OF BRACED FRAME WITH SEGMENTAL ELASTIC TRUSSES SYSTEM

Seismic hazard contains a lot of randomnesses. It is very hard for a building to be designed and constructed to survive all kinds of earthquakes without being damaged. Understanding this, in the past decades, researchers and designers started to switch from elastic design to ductile design. Nowadays, structures are designed to dissipate input energy with specifically designed elements to avoid damage to other structural and non-structural members. As a result, these elements are designed with less strength but greater ductility, so they can dissipate more energy while guaranteeing the healthiness of other members. However, this design philosophy introduces another problem. When a ductile member in a certain storey starts to yield, the stiffness of the corresponding storey reduces drastically, which in turn creates a soft-storey in the building.

Many previous studies have shown that a system which is able to transfer inelastic demand vertically within the structure can effectively eliminate the formation of soft-storey collapse mechanism. This is especially needed in steel braced frames since most of the columns are pinned connected in these type of structures, which offers no resistance for the soft-storey mechanism.

As mentioned in the previous chapter, some countries with high seismicity have stricter requirements for braced frame structures and are proven to positively affect the seismic performance of these systems. However, a simpler and more controllable approach is still preferred.

3.1 Understanding of soft-storey mechanism in CBFs and EBFs

To provide a solution for the soft-storey collapse mechanism in braced frames, a proper understanding of the problem is needed as a first step. A series of analyses were performed to address the soft-storey mechanism in both CBFs and EBFs.

3.1.1 The soft-storey mechanism in CBFs

A 4-storey, 8-storey and 12-storey moderately ductile CBF buildings are designed and analyzed numerically with both crustal and subduction ground motions. These models are constructed in the Open System for Earthquake Engineering Simulation platform (OpenSees, 2003). It is noted that to properly assess the collapse risk of CBFs, it is crucial to correctly model the buckling and fatigue failure of steel braces.

3.1.1.1 Buckling steel bracing model

Hallow steel sections (HSS) is commonly used as bracing members in CBFs due to their superior compression performance. An OpenSees inelastic brace model incorporating low-cycle fatigue material is calibrated with past experimental data. This model uses inelastic beam column elements in OpenSees which is constructed with an iterative force formulation. Plastic deformation is distributed along the length of the elements. Parametric study is performed, and all parameters related to brace definition in OpenSees are studied and calibrated to match the results obtained from past experimental tests. Comparisons of calibrated brace model responses and experimental test results are shown in Figure 3-1 (Tirca & Chen, 2014).

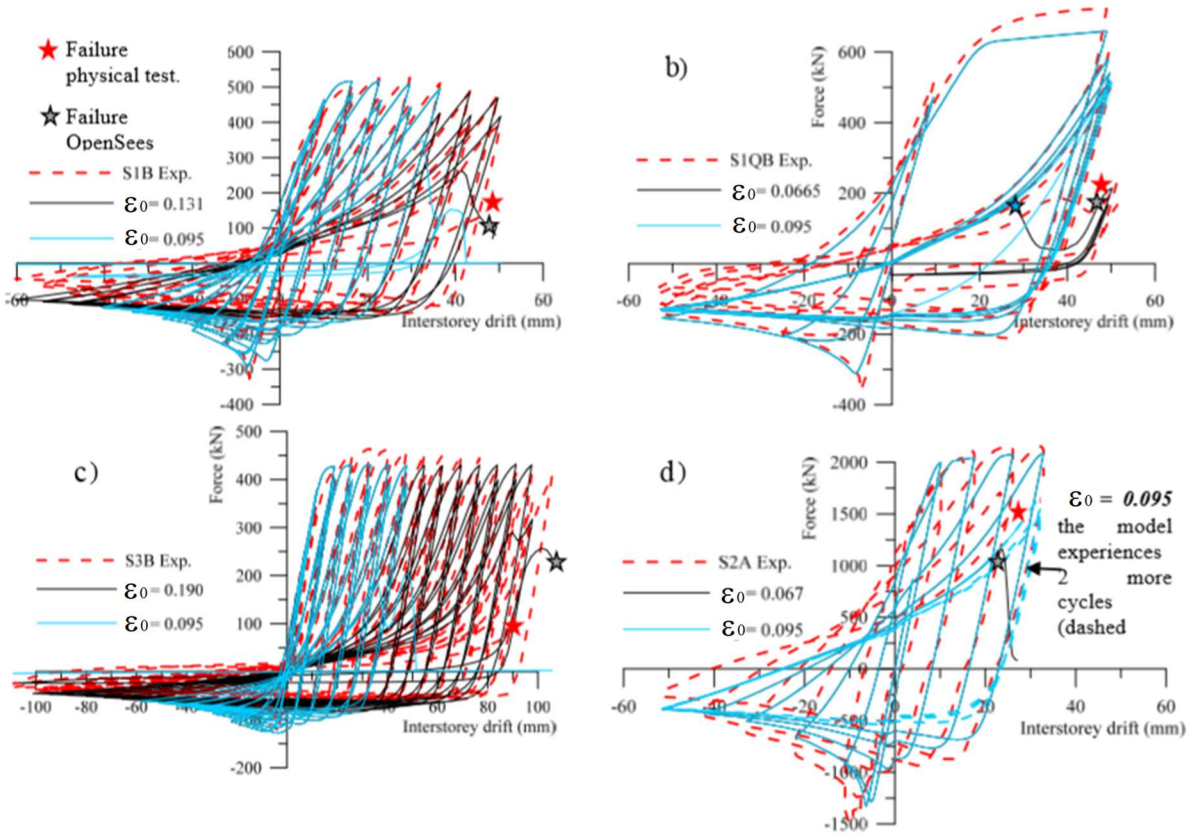

Figure 3-1: Comparisons between simulated brace response and experimental test results

More detailed calibration process is presented in (Tirca & Chen, 2014).

3.1.1.2 Influence of earthquake characteristics to CBF response

Two different sets of minimum 7 ground motion records are selected and scaled to meet the target design spectrum. One set is selected from crustal ground motions, and the other set is selected from Tohoku subduction ground motions. Ground motion records from both sets are selected to match the geotechnical profile of the target region. The interstorey drift profiles of all models are presented in Figure 3-2.

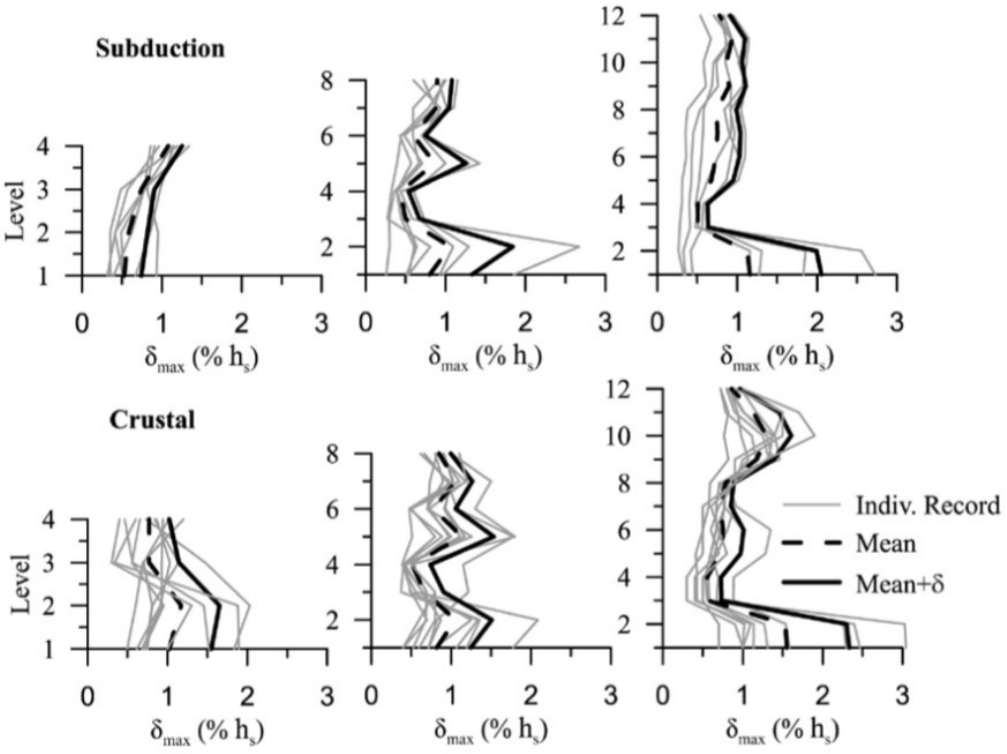

Figure 3-2: Interstorey drift profiles 4-, 8- and 12-storey CBF buildings under subduction and crustal record sets (Tirca, Chen, & Tremblay, 2015)

It can be depicted from the figure that the concentration of inelastic demand increases with increasing number of storeys in both cases.

Incremental dynamic analyses are also performed to understand the influence of ground motion intensity to CBF performance. It is noticed that when increasing the scaling factor of some ground motion records, the critical floor shifts within the structure. This suggests that the weak storey is a relative term which associates with the magnitude and characteristics of the seismic event.

3.1.2 The soft-storey mechanism in EBFs

3.1.2.1 Ductile shear link model

Ductile links are the energy dissipation components in EBFs. To properly simulate the response of EBFs, numerical hysteretic link model in OpenSees is calibrated. The link configuration and calibration are shown in Figure 3-3. The model setup is presented in Figure 3-4. The ductile link model is constructed with an elastic beam-column element and two springs in parallel that are connected to one end of the beam-column element.

The elastic beam column element is defined using the E & I of the link to simulate the flexure response of the link. The shear spring is defined with Steel02 material that is calibrated to mimic the shear deformation of the link. A min-max material is added in parallel with the shear spring to disconnect the link when the total rotation reaches a certain threshold. This value is determined from the average of experimental data, as shown in Table 3-1.

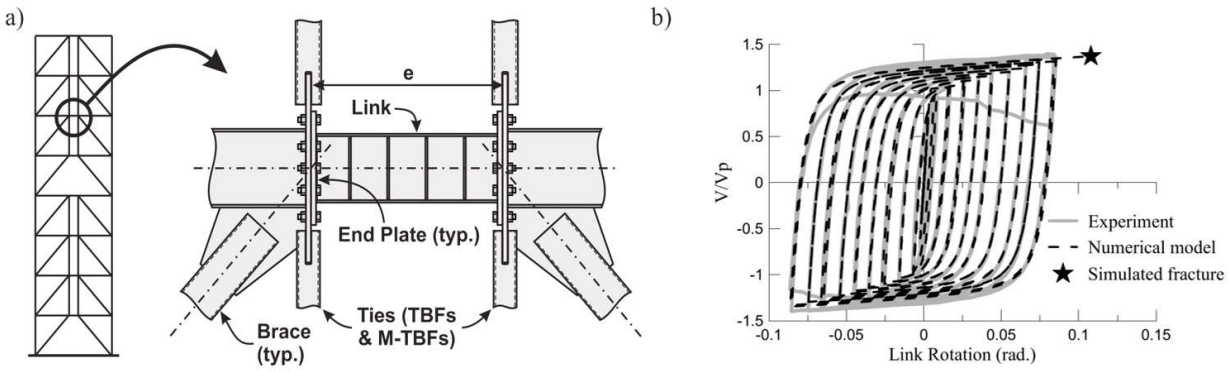

Figure 3-3: a) Replaceable link beams with end plate connections and proposed ties to link connection detail; b) Calibration of the numerical hysteretic link model in OpenSees (Chapter 4)

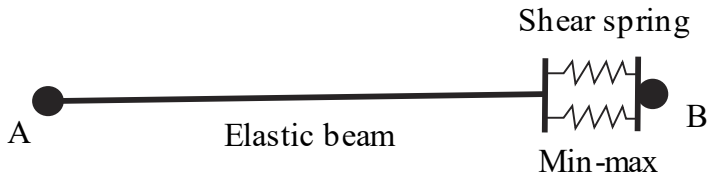

Figure 3-4: Ductile link OpenSees model

Table 3-1: Calibration of ductile link model

ID	Section	RyFy (MPa)	e (mm)	Vp (kN)	Vmax/Vp	Rmax
1A	W10X19	405	584	371	1.15	0.157
1B	W10X19	405	584	371	1.27	0.096
1C	W10X19	405	584	371	1.3	0.090
4C	W10X33	421	584	423	1.4	0.086
8-RLP	W16X36	392	930	652	1.43	0.120
12-SEV	W18X40	393	584	787	1.34	0.075
12-RAN	W18X40	393	584	787	1.59	0.129
				Average	1.35	0.108
				Max	1.59	0.157
				C.O.V.	1.18	1.45

3.1.2.2 EBF performance under earthquake excitation

An 8- and 16-storey EBFs located in Vancouver region are designed and analyzed with a set of 18 historical ground motion records. The ground motion records are selected from the PEER database (PEER 2011) to reflect the magnitude-distance scenarios that dominate the hazard at the site studied. The results of the time-history analyses are shown in Figure 3-5.

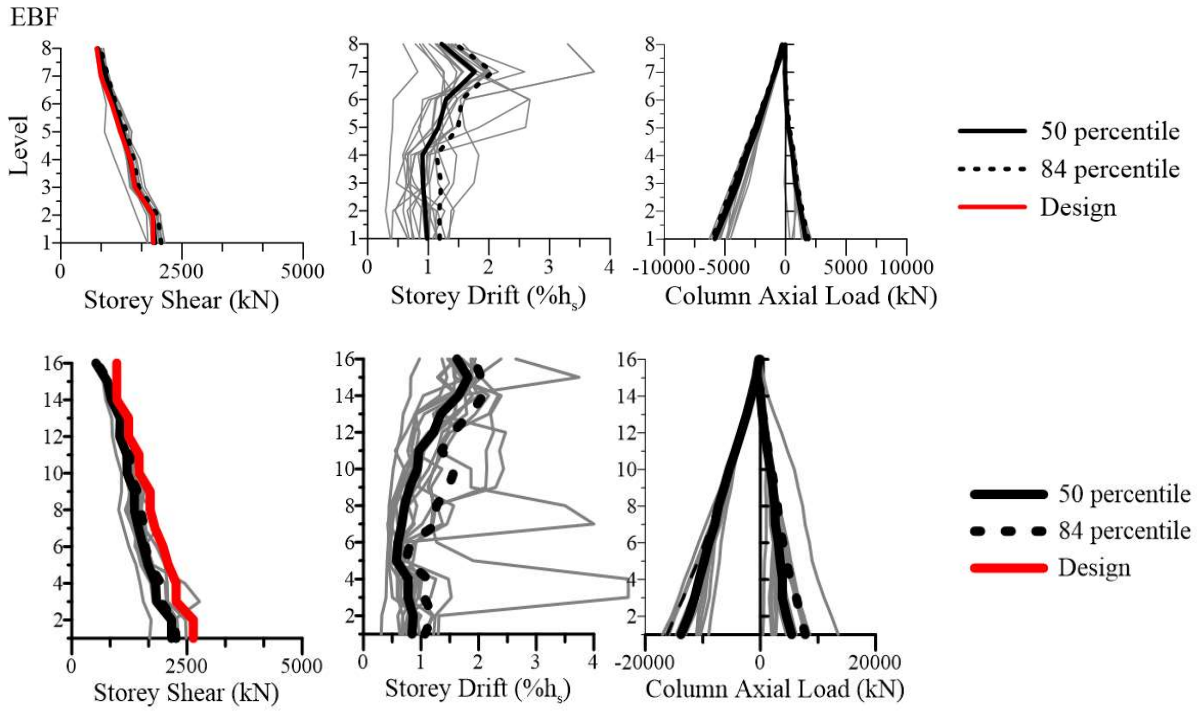

Figure 3-5: Result of time-history analyses for 8- and 16-storey EBFs (Chapter 4)

In general, the average response in terms of interstorey drift satisfies the code requirements (NRCC 2010, 2015). However, large peaks indicating damage concentration are observed for both frames.

3.2 Braced frames with fully tied systems

The first systems that are studied in this research program are the ones which are proposed by other researchers: zipper frame, zipper frame with elastic hat-truss and tied eccentrically braced frame (EBF). These configurations and their yielding mechanisms are shown in Figure 3-6.

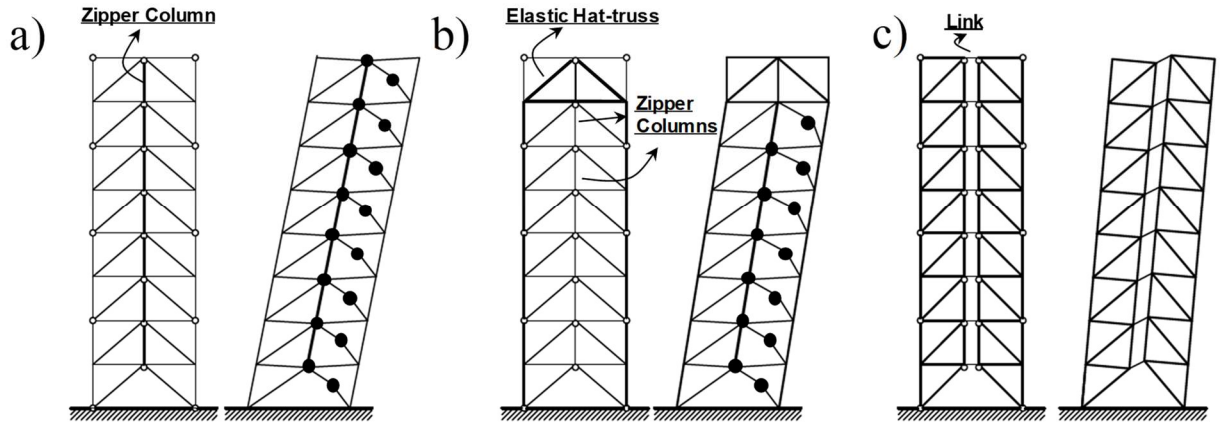

Figure 3-6: Structural configurations and their failure mechanisms: a) elastic zipper frame; b) suspended zipper frame; c) TBF

3.2.1 Elastic zipper braced frame (EZBF)

Khatib et al. (1988) proposed to add a zipper column between floors to distribute the inelastic demand that develops in braces over the frame height. For this system, Tremblay and Tirca (2003) proposed a design procedure to account for higher mode response and ensure that zipper columns remain essentially elastic upon brace buckling and yielding (Figure 3-6a). This design methodology for elastic zipper columns (E-ZBF system) was further refined by Tirca and Chen (2012).

As illustrated in Figure 3-7, the seismic input energy in zipper braced frames is intended to be dissipated mainly through inelastic buckling and tension yielding of the bracing members. Following capacity design procedure for steel braced frames, the brace members are selected first to resist axial forces from load combinations including code specified seismic loads. Adjacent members are then designed to carry gravity loads while resisting forces induced by the braces reaching their axial resistances in the inelastic range. This is illustrated in Figure 3-8a where the braces attain their probable yield tensile strength, T_u, and compressive resistances, C_u. Column forces in tension (T_e) and compression (C_e) for this condition are obtained by cumulating the

vertical components of brace forces in the levels above the level under consideration. Zipper columns are designed to resist the unbalanced vertical forces that develop at the brace-to-beam intersection points after buckling of the braces, i.e., when the compression braces exhibit their reduced post-buckling compressive resistance, C'_u.

For the elastic zipper braced frame (E-ZBF) system studied herein, brace induced forces in the zipper columns are determined using the approach proposed by Tremblay and Tirca (2003) and refined by Tirca and Chen (2012). As shown in Figure 3-8b, the compression forces in the zipper columns, C_z, are determined to start from the top level and to propagate downwards following the assumed brace buckling sequence, while tension forces T_z are computed from the first level. Zipper columns so-designed are expected to remain essentially elastic under a severe earthquake such that they can effectively distribute the inelastic response over the building height after brace buckling and yielding has initiated at one level. Brace axial loads induced in beams are determined from the lateral load patterns and brace axial loads considered for the design of zipper columns. In Figure 3-8b, beam hinging may occur in E-ZBFs as the zipper columns are not connected to any fixed vertical support. The extent of beam yielding mainly depends on the storey drift demand and, thereby, the level of inelastic demand experienced by the bracing members.

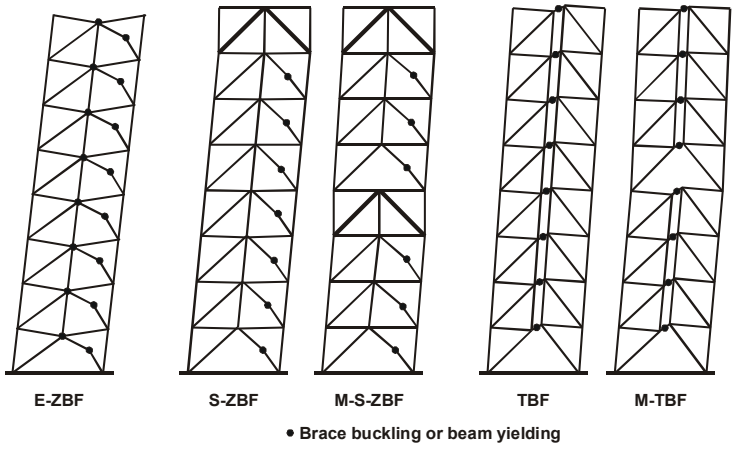

Figure 3-7: Expected global yielding mechanisms for the framing systems studied

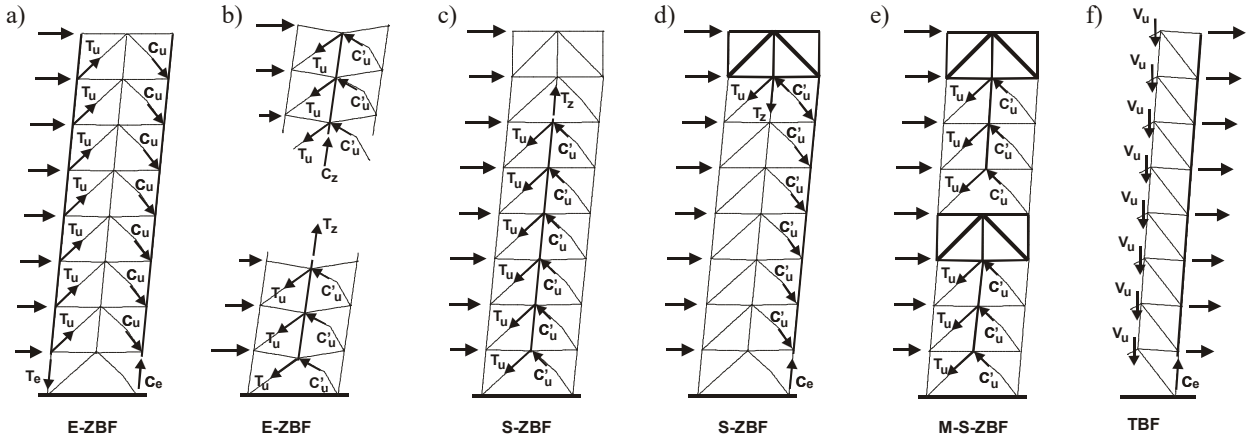

Figure 3-8: Brace or link induced forces for the design of: a) Exterior columns in ZBFs, b) Zipper columns in E-ZBFs; c) Zipper columns in S-ZBFs; d) Hat truss and exterior column in S-ZBF; e) Zipper column and hat trusses in M-S-ZBF; and f) Exterior column in TBF

3.2.2 Suspended zipper braced frame (SZBF)

As an alternative to improve the robustness of the original zipper braced frame system, Leon and Yang (2003) suggested introducing an elastic hat truss at the building top level to vertically anchor the zipper column (Figure 3-6b). The response of this suspended zipper braced frame system (S-ZBF) was validated numerically for structures up to 20 stories (Yang et al., 2008) and

experimentally through shake table and cyclic tests performed on three-storey models (Schachter and Reinhorn, 2006; Yang et al., 2010).

In the suspended zipper (S-ZBF) system, the zipper column is vertically anchored at its upper end to the hat truss formed by the beams and braces at the top level. Hence, it only needs to be designed to resist the cumulated tension force from the unbalanced brace forces that develop in the brace post-buckling range starting from the first level (T_z in Figure 3-8c). Except at the hat truss level, the brace and beam designs for the S-ZBFs and E-ZBFs systems are identical. The braces of the hat truss are designed for 170% of the design storey shear plus the forces imposed by the zipper columns (Figure 3-8d), as recommended by Yang et al. (2008) to account for the system overstrength resulting from brace yielding and buckling. The beams are sized to resist additional axial forces due to truss action. Compared to E-ZBFs, exterior columns in S-ZBFs must also be verified in compression for the post-buckling brace condition, as they must resist the vertical reactions imposed at the hat truss ends in addition to gravity loads and cumulated brace post-buckling compression forces (Figure 3-8d). The expected inelastic mechanism for S-ZBFs is illustrated in Figure 3-7. Contrary to E-ZBFs, beam plastic hinging is prevented because the beams are vertically supported by the zipper columns. However, for a given storey drift, this stiffer vertical response at beam mid-spans is likely to result in higher inelastic demand in the bracing members.

In tall buildings, the cumulated tension force in the zipper columns can become significant, requiring large sections for the zipper column and hat truss members as well as large exterior column sizes to resist the hat truss end reactions. For such structures, a modular suspended zipper brace frame (M-S-ZBF) configuration, where additional hat trusses are introduced along the building height, may represent a more effective solution because the unbalanced braced forces are

only cumulated over a few storeys in the zipper columns and need not be entirely taken up to the roof level before being redirected down to the foundations (Figure 3-8e). For instance, for the 8-storey braced frame studied herein, the design tension load in the zipper column at the 7th level reduces from 7490 kN in the S-ZBF configuration to 2390 kN when inserting an intermediate hat truss at the 4th level to form an M-S-ZBF system.

3.2.3 Tied EBF (TBF)

Martini et al. (1990) proposed to vertically tie together the ductile links of any two consecutive floors of EBFs to achieve more uniform yielding demand in the links (Figure 3-6c). This tied EBF (TBF) system was studied by Ghersi et al. (2000). Later, Ghersi et al. (2003, 2006) and Rossi (2007) developed and validated a design method for the proposed TBF system.

In tied eccentrically braced frames (TBFs), the vertical ties are expected to resist tension or compression axial loads, depending upon the relative strength of the links and the storey drift demand imposed by the motion. The design procedure by Ghersi et al. (2006) and Rossi (2007) was adopted in this study. The links are sized first to resist the code specified seismic forces. Short links, 600 mm long, yielding in shear were selected at every level for all structures. Design link shear forces were obtained from response spectrum analysis. All other members, including beam segments outside the links, braces, ties and columns were designed to resist the combined effects of gravity loads, the forces induced by shears developing in the strain hardened links, V_u, assuming first mode response (Figure 3-8f), and the forces due to second mode response. This last set of forces was obtained from elastic response analysis and reduced to account for a nonlinear response as proposed by Rossi (2007).

3.2.4 Seismic response of fully tied braced frames

8-storey buildings located on Class C site in Vancouver region are designed with aforementioned structural systems (EZBF, SZBF and TBF). The seismic response of these systems is analyzed numerically, and the results in terms of inter-storey drift are shown in Figure 3-9.

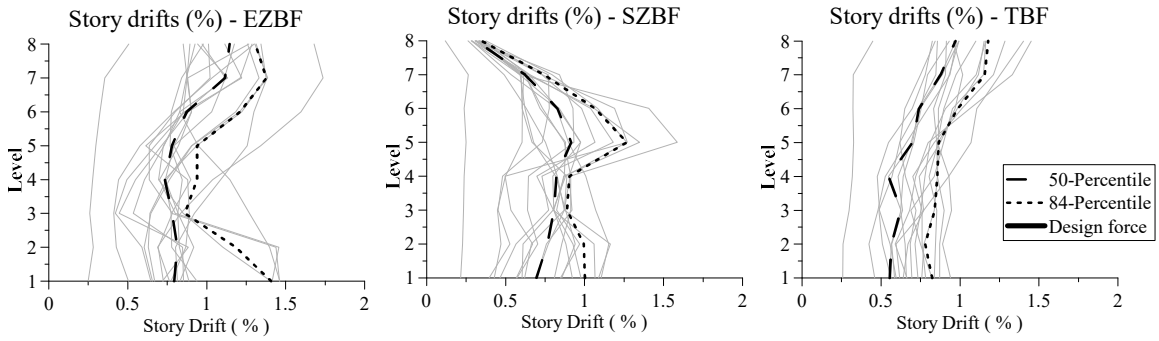

Figure 3-9: Interstorey drift profile for 8-storey EZBF, SZBF and TBF

EZBF and TBF are developed with a similar concept, that is to add elastic vertical links to connect the yielding components of adjacent storeys in the structure. The purpose of this addition is to help the structure to distribute inelastic demand vertically when ductile members yield. Comparably speaking, adding ties to EBF resulted in a better system. That is because the elastic trusses formed by the ties, beams and columns in TBFs worked as a continuous elastic backbone in the system. That is not the case in EZBF. Both braces located on any floor of the EZBF can buckle in compression and yield in tension. The zippers can only transfer the unbalanced load to adjacent storeys, but there are no strong trusses to force a global collapse mechanism. In case of SZBF, the super strong hat-truss on the roof of the system reduces the storey drift on the upper levels dramatically. As a result, the floors away from the hat truss suffer more damage. Overall, all three systems performed very well with a maximum storey drift of less than 2% storey height in extreme cases.

3.3 Development of segmental systems with elastic trusses

Because the systems studied previously show great potential, the only drawback is that the internal forces in the elastic trusses quickly become excessive and less efficient for structures with increasing number of storeys, as shown in Figure 3-10.

It has to be noted, for EZBF and SZBF systems, the forces in the zipper columns are calculated assuming all associated braces are yielded/buckled. Thus, the design forces determined based on such assumption can be excessive as the assumed condition is hard to achieve in high-rise buildings. This is also the reason for the large design compression forces in the columns of SZBF, as it is assumed that all the forces collected by the zipper columns are transferred to the energy columns. For the TBF, a reduction factor is proposed by Rossi (2009) to design the ties. The proposed design procedure is able accurately predict the maximum axial forces in the ties but underestimates the axial forces of braces on the upper levels of the 16-storey building.

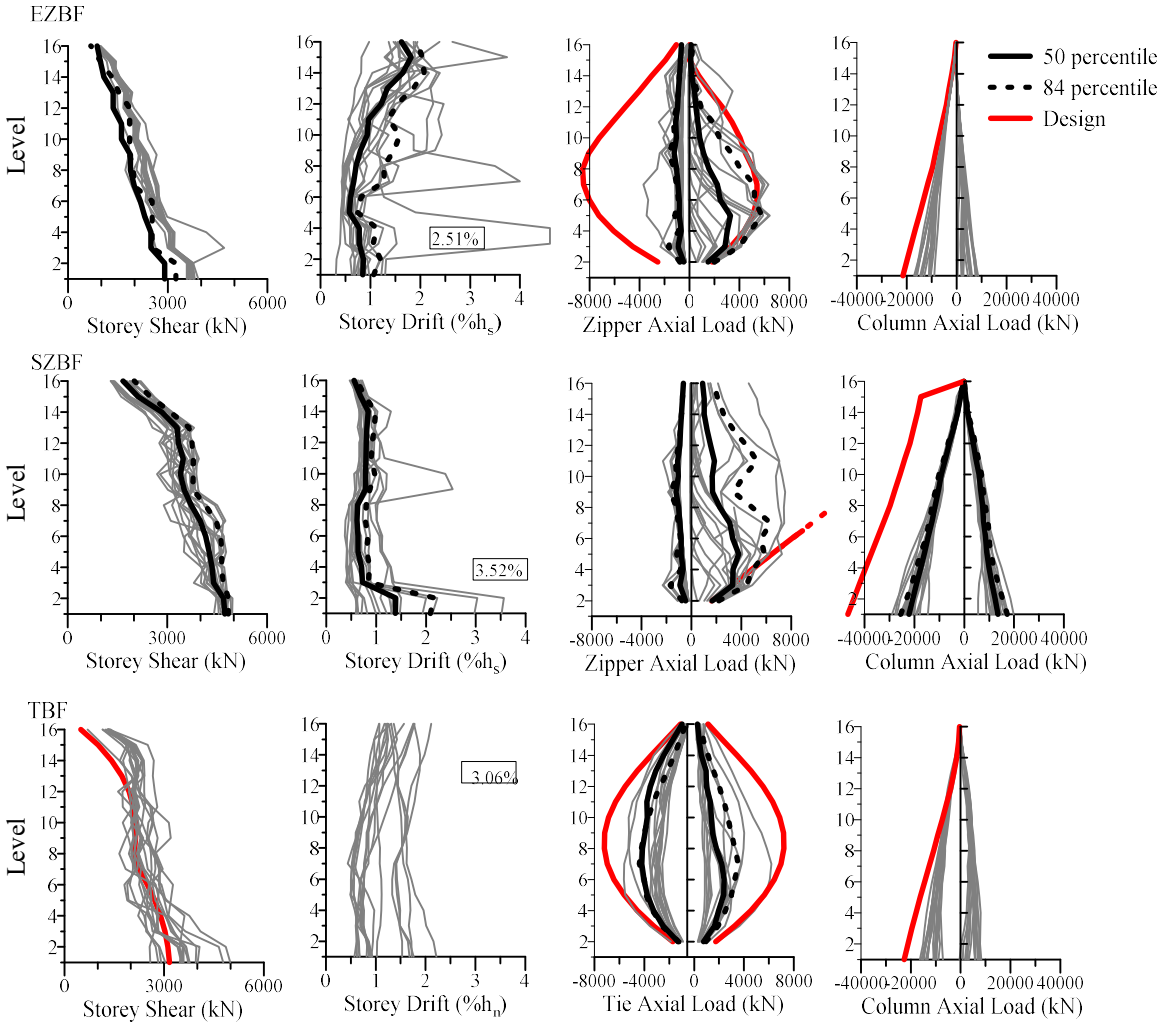

Figure 3-10: Seismic response of 16-storey EZBF, SZBF and TBF

To achieve higher efficiency, an attempt was made to break the whole system into segments, as shown in Figure 3-7.

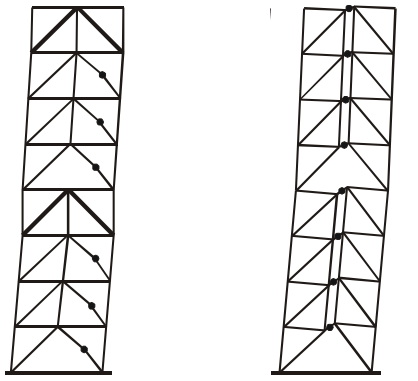

Figure 3-11: Structural configuration and yielding mechanisms of segmental SZBF and segmental TBF

Analyses were performed for all three types of systems. Typical results are shown in Figure 3-12. Both segmental SZBF and segmental TBF performed relatively good in terms of storey drift. But the problem remains for SZBF. When putting in segments, it introduces multiple stiff trusses within the structure. The floor directly on top of the truss is likely to experience excessive storey drift. This is because the elastic truss attracts large lateral forces, however, the energy is not dissipated within the storey. The energy naturally seeks an exit from adjacent floors, and the floor directly on top is also weaker due to the absence of zipper columns.

It is observed during the analyses that both TBF and segmental TBF is capable of reducing the maximum residual drift of the structure. This is because that in TBF and segmental TBF systems a number of storeys are linked together. Storeys with less permanent deformation help the other storeys to reduce their residual drifts. This observation is discussed and studied in Section 4.3.5. It is understood that accurate prediction of residual drift of structures is very difficult even with a sophisticated finite element model as the one used in this study due to the small magnitude. But the tendency of TBFs and segmental TBFs reducing maximum drift stays true.

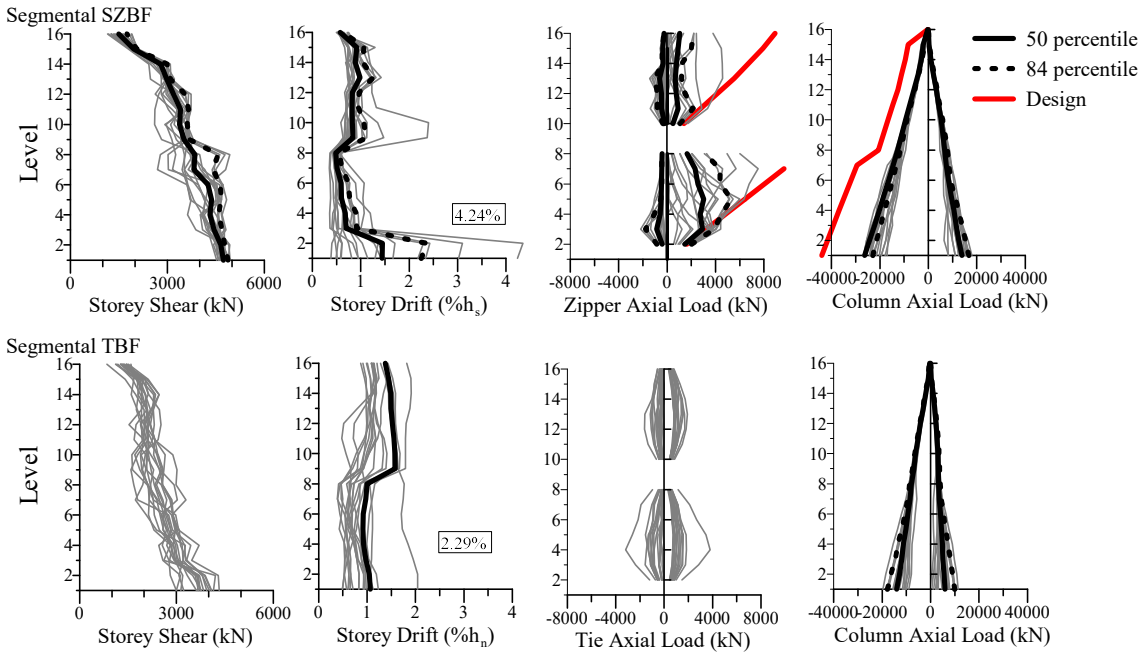

Figure 3-12: Seismic response of segmental SZBF and segmental TBF

3.4 Seismic response of braced frame with segmental elastic trusses

3.4.1 Typical response of braced frame with segmental elastic trusses

As discussed in the previous section, segmental TBF offers the better performance comparing with EZBF and SZBF. Therefore, the main subject of our research is set to segmental TBF, which is renamed to the braced frame with segmental elastic trusses (SESBF) to emphasis the importance of the elastic trusses formed by ties, beams and columns.

Article 1 that will be presented in Chapter 4 compares the performance and cost for the three types of structural configurations: conventional EBF, fully tied EBF and SESBF. Typical results obtained from the time-history analysis are presented in Figure 3-13. For better comparison, Incremental Dynamic analyses (IDAs) are performed for the 16-storey frames of each system, the Collapse Margin Ratios (CMR) of each system are compared. The results of these analyses are also presented in Chapter 4.

The study shows the great potential of SESBF with different numbers of segments. When the system consists only one segment (i.e. the TBF), seismic response of the frame is greatly enhanced.

When a SESBF with more segments are selected, notable improvement is observed based on the length of each segment. Shorter segments bring comparably less enhancement while adding minimum cost to the structure. Longer segments can reduce the possibility of soft segment formation at the cost of exponentially increased member forces.

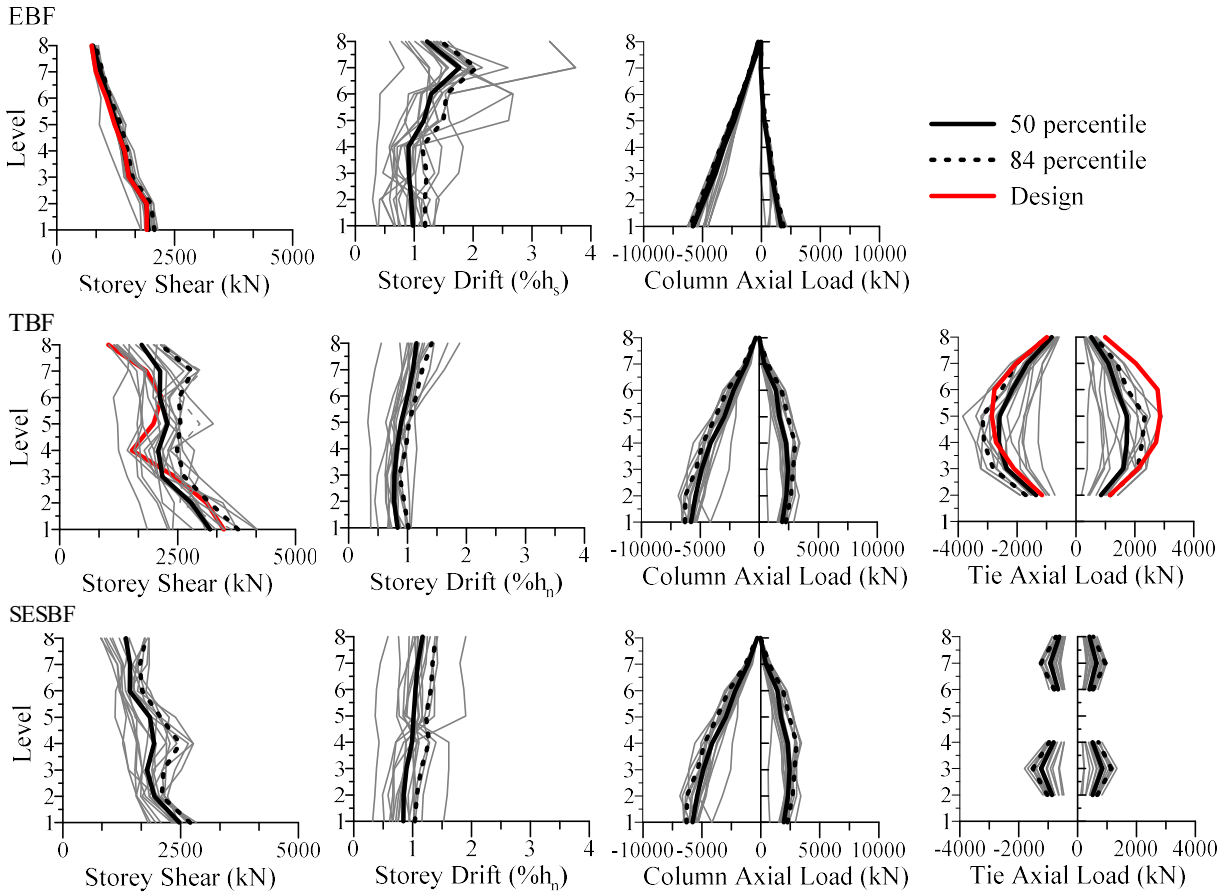

Figure 3-13: Seismic response of 8-storey EBF, TBF and SESBF (2 segments) (Chapter 4)

3.4.2 Potential improvement for a braced frame with segmental elastic trusses

To further improve the performance of SESBF, a study is conducted to add popular dissipative devices such as friction dampers (FD), buckling restrained braces (BRBs) and self-centering energy dissipative braces (SCEDs) to 16-storey SESBFs with 2 or 4 segments. The configurations for these systems are shown in Figure 3-14. And the response of these systems in terms of storey drift is shown in Figure 3-15. The energy dissipative devices are placed vertically to connect the elastic

trusses of different segments. These are the locations where largest axial deformation is induced for a given inter-segment drift ratio. The findings of this study are published in Tremblay, Chen, and Tirca (2014). The study concluded that adding energy dissipative devices can further enhance the seismic performance of SESBFs and significantly reduces the probability of formation of soft-segment.

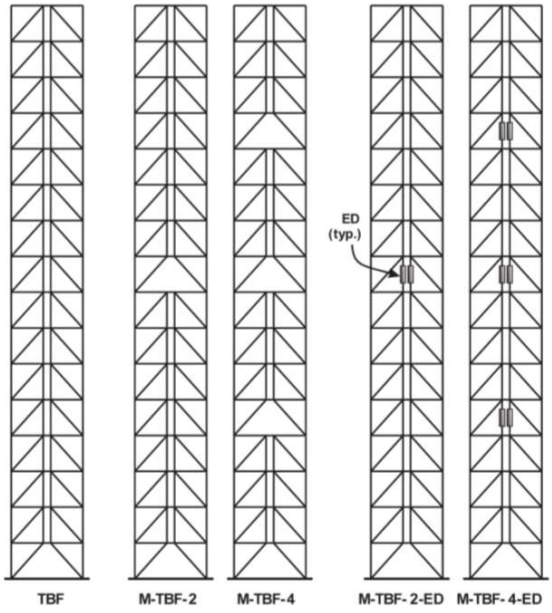

Figure 3-14: Structural configurations for SESBFs with energy dissipative devices (EDs) (Tremblay et al, 2014)

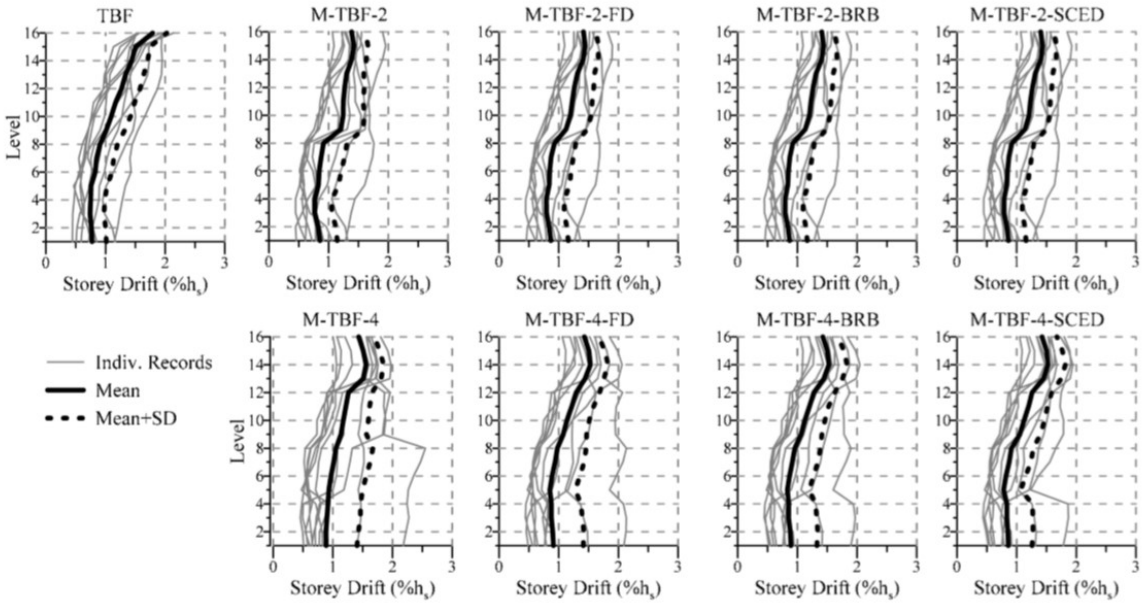

Figure 3-15: Storey drift profile of SESBFs with dissipative devices (Tremblay et al, 2014)

3.5 Design of braced frame with segmental elastic trusses

With studies discussed in the previous sections, a basic understanding of the seismic performance of braced frame with segmental elastic trusses is established. This structural system is both efficient and economical, and it can withstand relatively large ground motion excitations if designed properly without excessive damage concentration. Furthermore, the system can work flawlessly with all the energy dissipating devices for enhanced performance. At this point, the task remaining is to find a robust design method.

Article 2 that will be presented in Chapter 5 explicitly explains the proposed design method. The method combines the modal superposition technique with the capacity design approach. Firstly, inelastic vibration modes of a SESBF are defined as the vibration modes of the structure when ductile links are yielded. These vibration modes are categorized into two categories: the modes governed by the yielding of links and the modes that induces bending in the segmental elastic trusses, which are noted as Set I modes and Set II modes respectively. Forces induced by Set I modes, noted as Set I forces, are calculated with the capacity of the ductile links in each segment, while the Set II forces are obtained with response spectrum analysis using a modified spectrum

that only includes the spectrum acceleration coordinates of corresponding vibration modes. The Set I and Set II forces combined with gravity load gives a somewhat conservative and accurate prediction of the total force demand in the structural members. Detailed design procedure incorporating with current building code (NBCC 2015) is presented in 5.2.2. Design examples of 8-storey and 16-storey SESBFs with various segmental configurations as well as the seismic response of these structures that validates the proposed design method are presented in 5.3.

Although the proposed method is both simple and straightforward, the road leading to the method is rough. Major milestones along the road is demonstrated in the following sections.

3.5.1 Capacity design approach

Because the segmental trusses need to remain elastic in order to transfer the inelastic demand within the structure throughout the entire earthquake event, the first idea comes to mind is the capacity design approach. The maximum possible loads in each member need to be understood and captured to perform a capacity design. A fully tied 8-storey tied EBF is used to conduct this study. The model is built in SAP2000. Elastic steel material is assigned to all structural members except the ductile links. The structural model was subjected to various ground excitations, and the forces at each specific time period were plotted and analyzed. Some snapshots of the forces in main structural members are demonstrated in Figure 3-16. The forces in the members are normalized to their respective maximum forces. Red and blue colors represent respectably tensile and compressive axial forces.

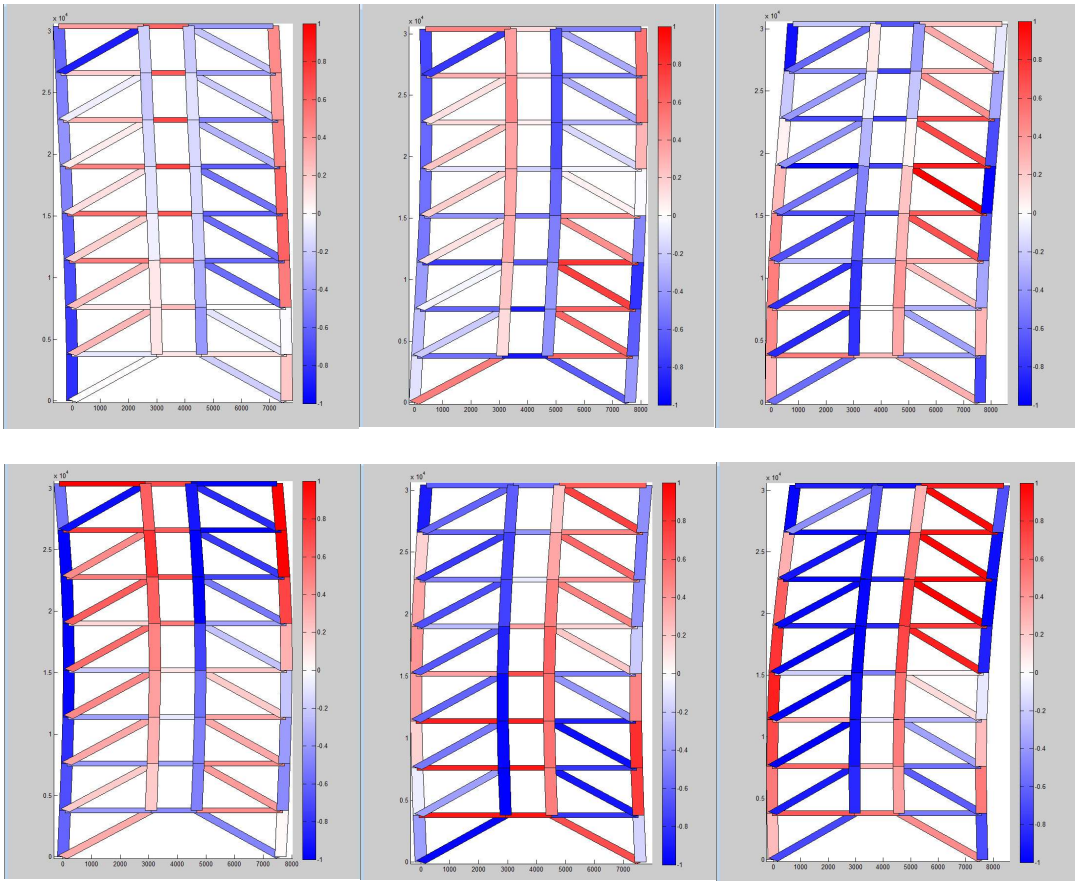

Figure 3-16: Snapshots of forces in main structural members obtained from time-history analysis

Analyzing similar snapshots of buildings with various height and configuration, several observations are made. The ties are activated when corresponding sub-trusses are bent. The maximum tie axial forces are not related to the level of shear forces in the ductile links. On the other hand, maximum axial forces in braces and column happen simultaneously with the maximum shear forces in the links. These observations suggest that it is not possible to determine the maximum tie forces based on the capacities of connected links. However, the maximum axial forces in braces and columns are directly related to the capacities of the links.

3.5.2 Frequency analysis

To further understand the response of braced frames with segmental elastic trusses, frequency analysis is performed. The time-history response of interstorey drifts, axial member forces for 8-

storey TBF and STF are converted to the frequency domain through Fast Fourier Transformation (FFT). Some of the results are shown in Figure 3-17.

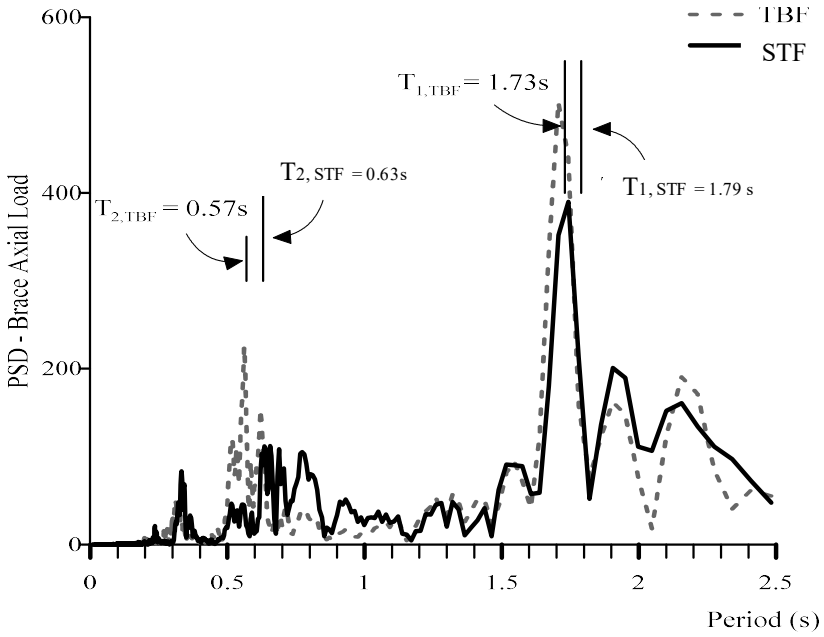

Figure 3-17: Power spectral of axial forces in 1st floor braces

The figure shows that the response in terms of interstorey drifts and brace axial forces in governed by the first two vibration modes in the TBF, and first 3 vibration modes in the SESBF. Influence of the third vibration mode in TBF is very minimum compared to the influence of the second vibration mode. On the other hand, in 8-storey SESBF, the influence of the third vibration mode is greatly increased while the influence of second vibration mode is reduced.

This result suggests the forces of members in TBF is a combination of loads induced by the first and second vibration modes in TBF, which agrees with the conclusion made by Rossi (2007). In addition, the segmental configuration with 2 segments introduces another set of loads that is resulted from the third vibration mode. The mode shapes of these vibration modes are illustrated in Chapter 5.

3.5.3 Modal superposition

With the help of frequency analysis presented in the previous section, it is concluded that the member forces of 2 segments SESBFs comes from 3 sources, which are the first three vibration

modes. In additional to the elastic vibration modes, many noises are also noticed in frequency domain, which indicates that inelastic vibration modes are also important when predicting the member forces of a SESBF.

3.5.4 Inelastic vibration modes

After failure to obtain the correct member forces with modal superposition method using elastic vibration modes for brace frame with segmental elastic trusses, I realized that the problem is not the method itself, but the vibration modes that were used in the superposition.

The differences between conventional frame and frames with elastic trusses are presented in the following section.

For conventional frames, a simplified global collapse mechanism is normally assumed in the design phase. Under this assumption, the inelastic vibration modes can then be determined as having the same shape as elastic vibration modes but much longer period. Therefore, when designing a conventional frame, a ductility factor D can be used to transfer elastic forces to inelastic forces.

In a system with elastic trusses changes the response of the system after the energy dissipating components in the structure yield. The elastic and inelastic mode shapes of frames with segmental elastic trusses are shown in Figure 3-18.

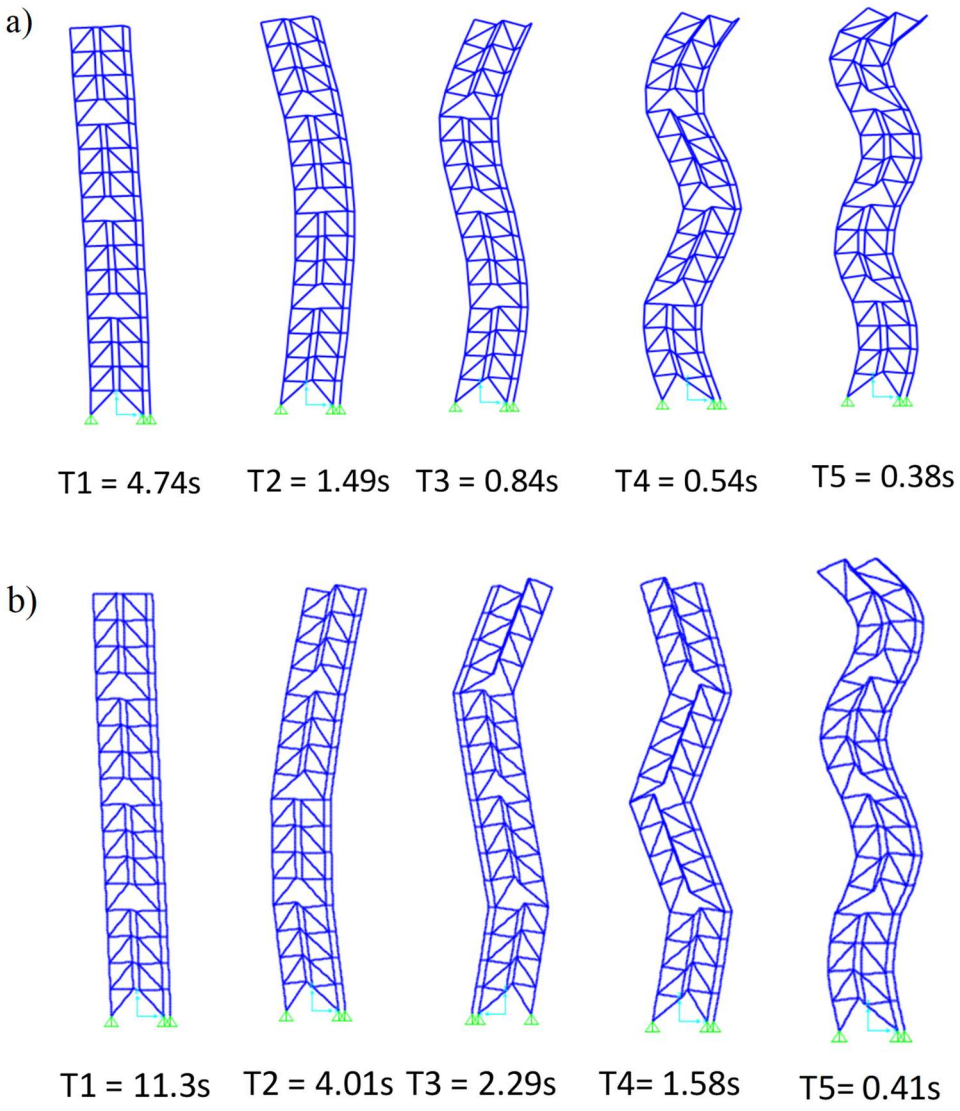

Figure 3-18: Elastic and inelastic vibration modes of the 16-storey braced frame with segmental elastic trusses: a) elastic modes; b) inelastic modes

The differences between elastic and inelastic vibration modes created a significant error in the previous calculation of maximum load demands in structural members.

3.5.5 Determination of inelastic vibration modes

Upon understanding the differences between elastic and inelastic vibration modes for the proposed system, the development of design method comes down to a single task, that is to determine the inelastic vibration modes.

To make the design method easily accessible, a general-purpose finite element software SAP2000 is used to determine the inelastic vibration modes of the SESBF systems.

To obtain the inelastic vibration modes, all the links are assigned to their post-yielding stiffness, which is the stiffness comes from strain hardening of the material. Parametric study is also carried out to quantify the influence of the post-yielding stiffness of links. It concludes that when the post-yielding stiffness of the link is lower than 5% of its elastic stiffness, the exact value has little to no impact on the force distribution nor the magnitude of the structural members.

3.5.6 Design of SESBFs

Detailed design method is presented in Section 5.2. Design examples of 8- and 16-storey SESBFs of one, two and four segments are illustrated in Section 5.3.

3.5.7 Additional Validation of the proposed design method

The design examples presented in Section 5.3 has proven that the proposed design method is able to accurately predict the maximum forces in the structural members of SESBFs. Meanwhile, the 8- and 16-SESBFs designed with the proposed method demonstrated a satisfactory response under the design level earthquakes in terms of maximum storey drift and drift distribution. In this section, the collapse possibilities of SESBFs designed with the proposed method is assessed with incremental dynamic analyses (IDAs).

8-, 9-, 10-, 12-, 15-, 16-storey SESBFs with various number of equal length segments with the same geometry as the one presented in 5.2 are designed. The suggested fundamental periods of the structures by the code, $T_a = 2 \times 0.025 \times h_s$, and those obtained from dynamic analyses are presented in Table 3.2. A k-storey SESBF with n segments are noted as k-n herein.

Table 3-2 Suggested fundamental periods by the code and fundamental periods obtained from dynamic analysis

Systems		8-1	8-2	9-3	10-2	12-3	12-4	15-3	15-5	16-2	16-4
T_a (code)	(s)	1.52	1.52	1.71	1.90	2.28	2.28	2.85	2.85	3.04	3.04
T_1 (dyn.)	(s)	1.95	2.25	2.6	2.9	3.45	3.43	3.81	4.27	4.59	4.65

Five ground motions that induce the most damage in the system shown in Chapter 5 are selected for the IDAs. The five interface subduction ground motions are therefore selected herein. The spectrum of the selected ground motions and their mean spectrum are plotted in Figure 3-19. As shown, the mean spectrum of the selected ground motion records is almost identical to the design spectrum of Vancouver region (NBCC 2015), which is plotted in red in the figure.

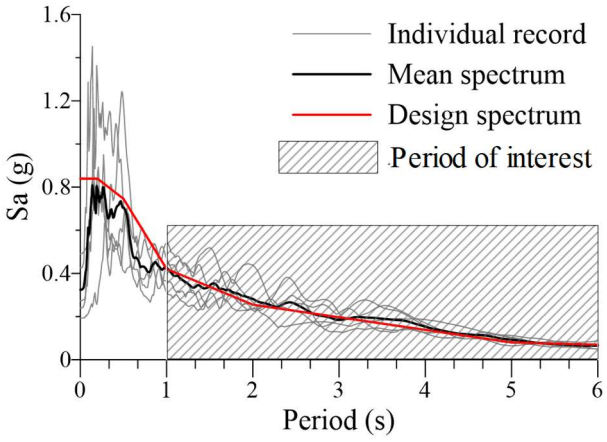

Figure 3-19 Spectrum of scaled ground motions

The results of the IDAs are illustrated in Figure 3-20 and Figure 3-21. The collapse margin ratio (CMR) of a structure, according to FEMA P695 (FEMA, 2009), is defined as the ratio of the spectrum acceleration at collapse and the spectrum acceleration corresponding to the design level. The CMR values for the studied structures are shown in Table 3-3. In general, all the structures examined in this study exhibit acceptable performance in terms of CMR, which suggests that even 3-storey segments can enhance the seismic response of the structure. In the meantime, longer

segments further improve the seismic performance of the same structure. 8-storey segments greatly reduce the maximum storey drift of the structure comparing with 4-storey segments, while significantly increases the CMR. SESBFs with shorter segments (3-, 4-, 5-storeys) while are more beneficial in terms of cost, possess higher collapse potential. Thus, due to this nature of SESBFs, the best segmental configuration is highly case-dependent. Designers have to select a suitable segmental configuration for each real-life case, and a method to help them make such decision is still needed.

The results also suggest that the structures that undergo less maximum story drift when subjected to design level earthquake tend to have greater CMR. In other words, the collapse potential of a SESBF system can be predicted based on its maximum storey drift under design level ground motion records.

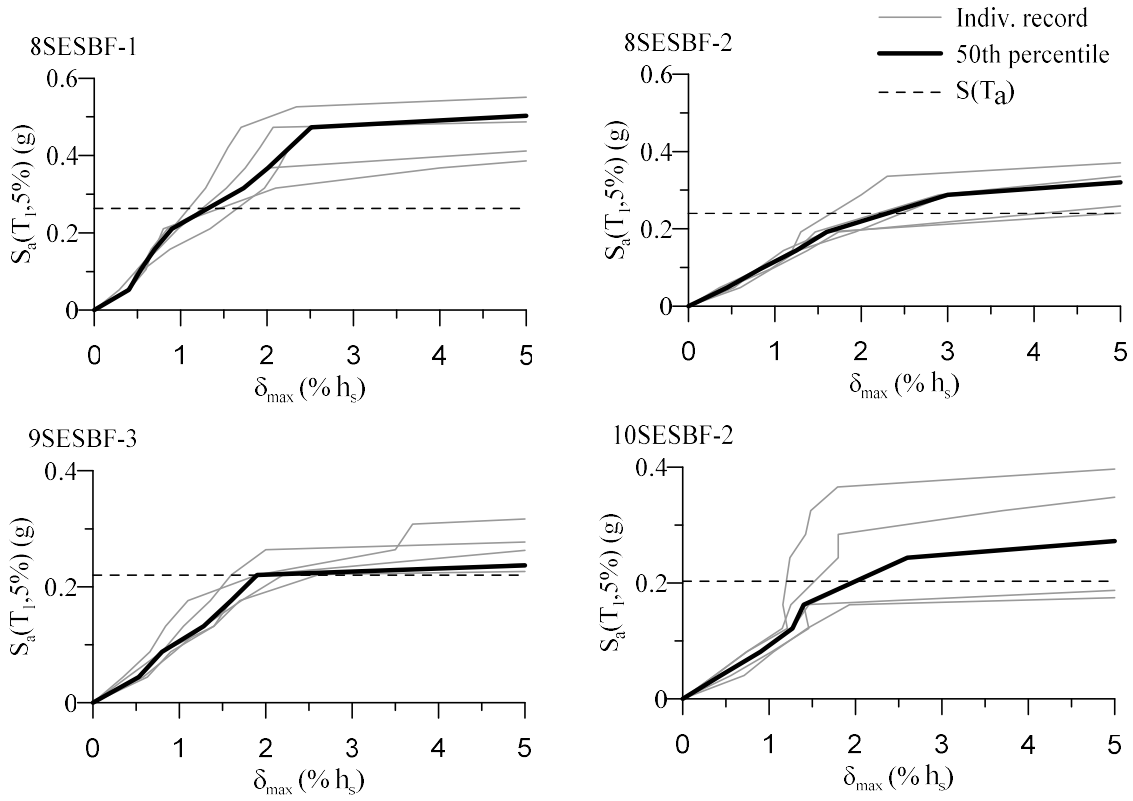

Figure 3-20 IDA curves of 8-, 9- and 10-SESBFs

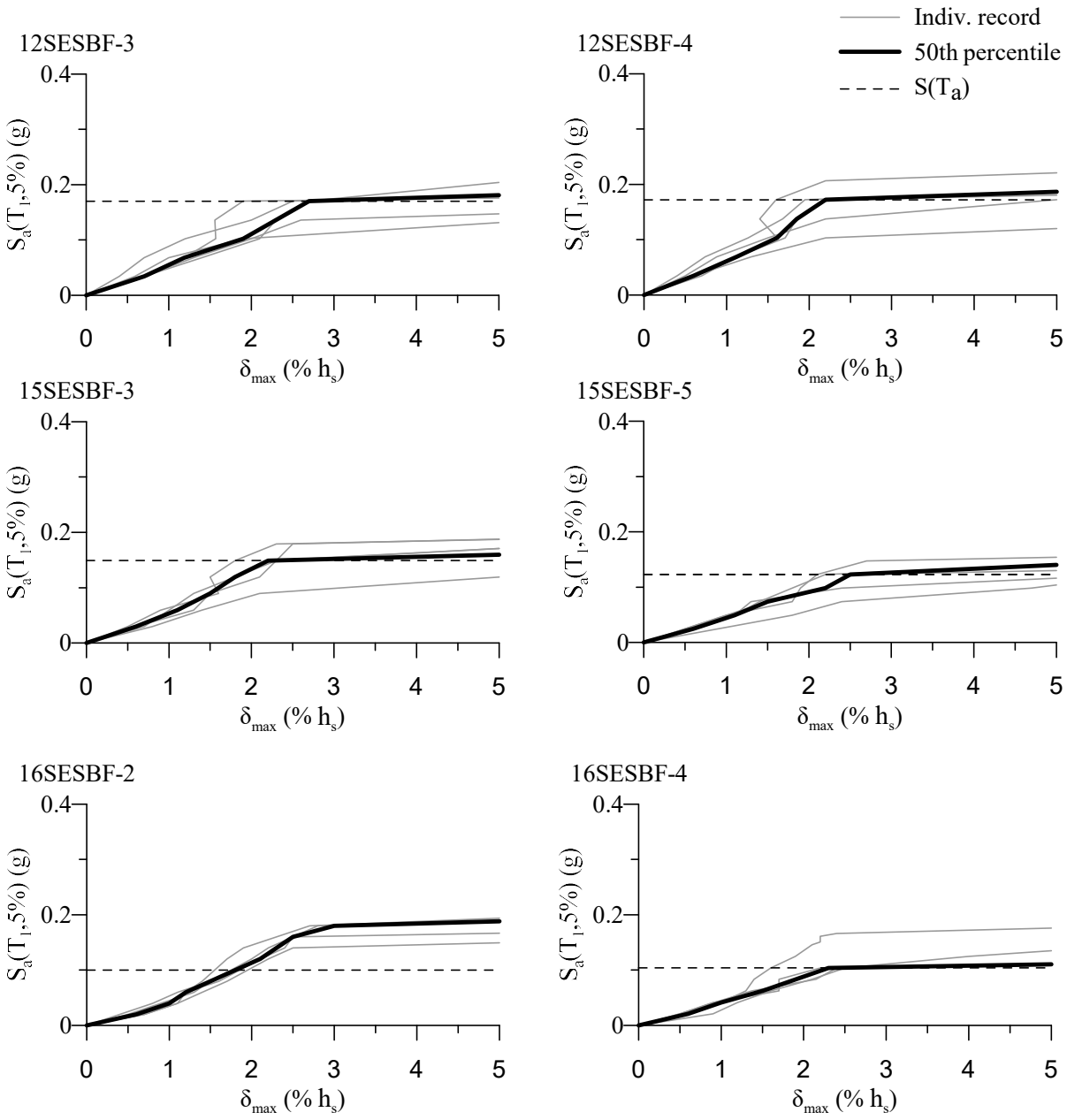

Figure 3-21 IDA curves of 12-, 15- and 16-SESBFs

Table 3-3 CMR of structural systems

Systems		8-1	8-2	9-3	10-2	12-3	12-4	15-3	15-5	16-2	16-4
$S_a(\bar{T}_1)$	(g)	0.263	0.24	0.22	0.203	0.17	0.172	0.149	0.123	0.1	0.104
CMR	-	1.81	1.20	1.16	1.18	1.06	1.10	1.08	1.10	1.75	1.11

3.6 Optimum design of braced frame with segmental elastic trusses

After the design method for SESBFs is developed, it was found that even for a properly designed SESBF, a soft-segment is still possible to form. This is expected as there is no additional system exists in the structure after all the ductile links of a segment yield to support the structure, particularly the segment. When the intensity of an input ground motion exceeds a certain level, that segment is likely to undergo large deformation. Therefore, it is necessary to develop a method that is able to predict the possible formation of a soft segment for a given SESBF. As stated, the formation of soft segments is directly related to the intensity and characteristics of individual earthquake. Therefore, the easiest option is to run time history analysis with a set of ground motion records that includes all the representative ground motions for a given region. In addition, since the design of SESBFs is a relatively long process, it would be very helpful to be able to determine the arrangement of the segments of a SESBF being designed. To fulfill these requirements, a simplified numerical model built with a commercially available finite element software is in need.

Article 3 that will be presented in Chapter 6 introduced a simple method to determine the optimum segmental configuration for a target SESBF. The method utilizes a simplified structural model to predict the seismic response of the corresponding structure. Properties of the elements that are used to build the simplified model can be obtained through static calculations and some iterations of spectrum analysis. The simplified model is able to replicate the inelastic seismic response of the structure with good accuracy. A design example of a 24-storey SESBF, presented in Section 6.4, demonstrates the entire process of the selection of segmental configuration. Maximum storey drift values and dynamic drift concentration factors (DCFs) are adopted to assess the performance of

each configuration. Designers can choose the suitable configuration for their buildings knowing that enhancement of seismic performance is coupled with exponentially increased member forces.

3.6.1 Simplified structural model

The idea of building a simplified model to predict the seismic performance of the corresponding structure is promising. Mass-spring models are widely used for such purpose due to their simplicity. The system, in the case of M-TBF, has concentrated ductile response, which is generally achieved by yielding of ductile links. In the meantime, the rest of the structure remains elastic. This seismic response makes the mass spring model a perfect candidate to replicate the seismic response of the structure.

The characteristics of a SESBF is very similar to that of the conventional EBFs. Thus, the realization of the simplified model shall start with a conventional EBF.

3.6.1.1 Simplified model for conventional EBF

The total deformation of conventional EBF is contributed by six components: the flexure and axial deformation of beams, the axial deformation of braces, the shear deformation of ductile links, the global flexure deformation due to the shortening and elongation of columns and the P-Delta effect. These deformations can be categorized into three categories: the shear deformation and the flexure deformation of the frame and the secondary effect which is the P-Delta effect. To include all three components, the simplified model for a 1-storey EBF is constructed with a nonlinear shear spring, an elastic column and a P-Delta column as shown in Figure 3-22b.

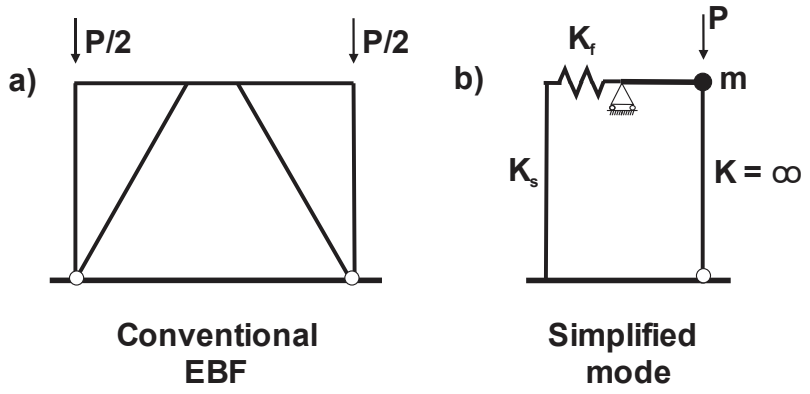

Figure 3-22 a) Conventional EBF; b) Simplified model

The simplified model capture both elastic and inelastic characteristics of the original SESBF system:

1. When the links behave elastically, the total deformation of the system consists of these components: global bending deformation due to elongation and shortening of exterior columns, shear deformation of ductile links, deformation of elastic trusses (axial deformation of beams, braces and ties), deformation due to p-Delta effect.
2. When the links behave inelastically, the momentum created by exterior columns is disconnected, while the other three components remain.

Figure 3-23 shows the three options considered for the simplified model: shear spring model, rotational spring model, combined model.

The shear spring model presented in Figure 3-23b neglects the deformation within each segment, only the displacement of the roof of each segment is considered. This model lumps all the masses on each floor to a single mass, rigid bar connects the masses while all the deformation of the segment is modelled by a shear spring located at the bottom of the segment. As a result, the deformation resulted from P-delta effect and truss bending action is neglected. On the bright side, the only parameters required to build this model are the stiffness and capacity of the links and value of storey masses.

The rotational spring model is demonstrated in Figure 3-23c. This model is very similar to the shear spring model except that instead of a shear spring, a rotational spring that combines both shear stiffness and flexure stiffness of the segment is utilized. This model requires both stiffness and capacity of ductile links as well as the stiffness of the elastic trusses to be constructed. Comparing to the shear spring model, the rotational spring model is able to capture the global flexure and shear response of the system. However, because the rotational angle of each segment is only controlled by the rotational spring, the global flexure response can not be captured.

To retain both the elastic and inelastic characteristics of the structure, a more sophisticated model is proposed. As shown in Figure 3-23d, the proposed model consists of two parts: a lumped mass rigid bar system that reproduces a more accurate deformation pattern for P-Delta effect calculation

and a shear-spring elastic bar system that accounts for both the flexure and shear stiffness of the structure. The two parts are laterally constrained at the roof level of each segment.

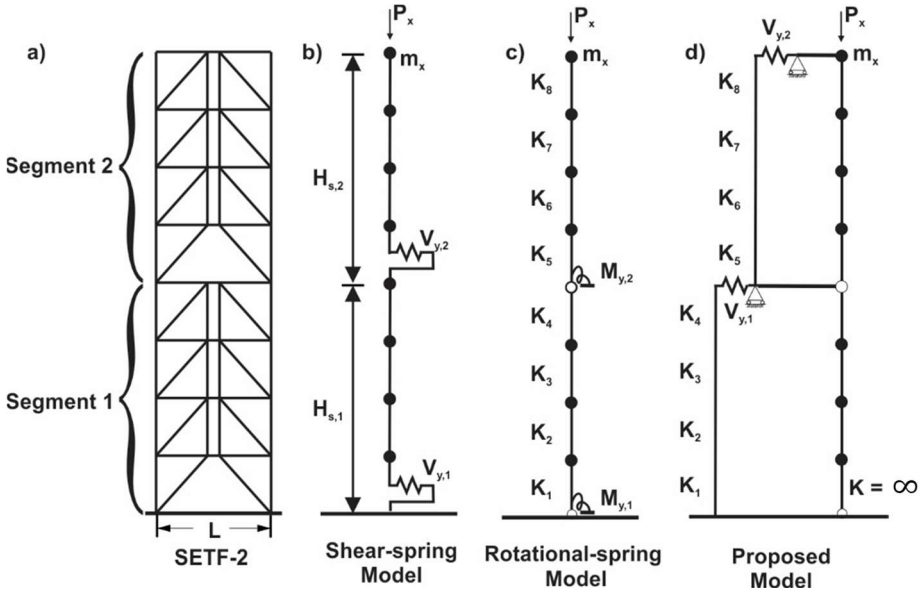

Figure 3-23: 8-storey 2- segments SESBF and spring-mass models: a) SESBF; b) shear-spring model; c) rotational spring model; d) proposed model

The properties of proposed models can be derived from the designed structures; however, it would destroy the purpose of having these models. Therefore, to make these models easy to use and build without going through the detailed design phase for each and every segmental configuration the designers want to investigate, it is important to be able to estimate these properties with sufficient accuracy with simple analyses and calculations.

An iterative procedure is proposed herein. The iterations initiate with static calculations and update all the spring properties after each spectrum analysis based on seismic induced lateral loads at each segment.

The detailed procedure to obtain the properties of the springs used in the SM is discussed in Section 6.2.2.

3.6.2 Validation of the simplified model

To validate the proposed SM, structures with various heights and different segmental configurations are designed with the proposed approach. Full models (FM) of these structures are

built in SAP2000. Static and dynamic analyses are performed on both SM and FM, the results obtained from these analyses are demonstrated in the following section.

1) Push-over analysis

Static pushover analysis is performed on the SM and FM of a 4-storey SESBF-1. In general, during a static pushover analysis, only the weakest segment in SESBF will yield, therefore, the analysis was not performed on SESBFs with more than one segment. The result of the pushover analysis is shown in Figure 3-24. The SM possesses very similar stiffness and strength as the FM. In addition to the pushover analysis, the stiffness values of the SM are also directly compared with that of the FM for a 24-storey SESBF with various configurations. The result of the comparison is discussed in Section 6.2.2.

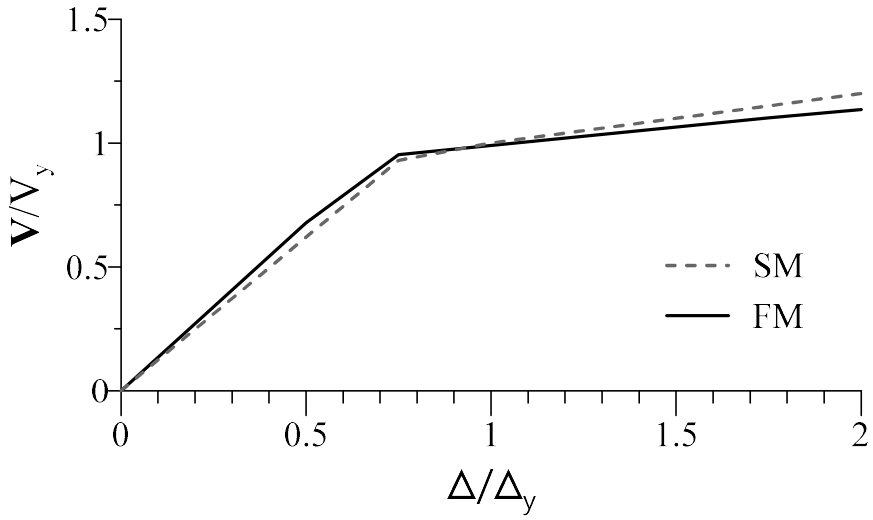

Figure 3-24: Comparison of pushover analysis results between discrete model and shear spring model

2) Dynamic analysis

Modal analysis and nonlinear time-history analyses are performed on a 24-storey SESBF-4. The FM of the frame is shown in Figure 3-25a. The inelastic vibration modes of both SM and FM are shown in Figure 3-25b. The time-history of the roof displacement of both SM and FM under ground motion is shown in Figure 3-25c. The results illustrated the proposed SM can adequately replicate the dynamic properties of the FM. The displacement time-history shows that the SM can accurately mimic the elastic response of the FM.

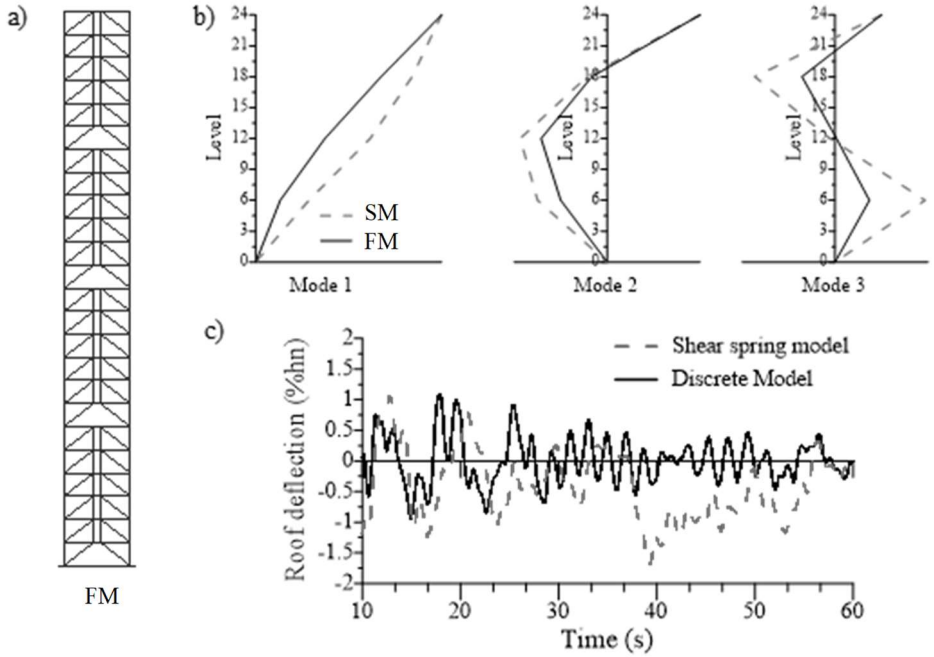

Figure 3-25: a) structural model; b) Comparison of shapes of inelastic vibration modes; c) Comparison of roof deflection from time-history analysis

3) Additional verifications

More detailed verifications of the SM in terms of stiffness and seismic response are presented in Section 5.3.3.

3.7 Proposed design methodology

With all the knowledge gained throughout previous studies, a robust and easy-to-use design method is proposed. The general design process for SESBFs is expressed as a flowchart in Figure 3-26. The preliminary design when the optimum segment arrangement is selected is performed using a simplified structural model following the approach that is presented in Chapter 6. When the desirable configuration is determined, detailed design is performed according to the procedure presented in Chapter 5. Both sections of the design procedure can be performed with most commercial finite element software, such as SAP2000. These steps will be briefly explained herein:

3.7.1 Determine the best configuration for a SESBF

As explained in the previous sections, the procedure consists of two major sections as shown in Figure 3-26. The first section is to determine the most appropriate segmental configuration for the target structure as illustrated in Figure 3-26a. Different segmental configurations shall be examined in this section. Designers have to keep in mind that SESBFs with longer segments perform better in earthquakes in general. In exchange, the force demands in the truss members, especially in the ties, increase exponentially. It is recommended that the designer shall aim at the configuration(s) with shortest segments while having acceptable performance.

The following steps shall be executed for each configuration.

1. Selection of truss configurations

As mentioned, the configurations to be examined are selected based on the length of segments. In general, designers are recommended to select a configuration that consists segments covering 2 or 3 storeys, and gradually increase the length of segments depending on the performance.

2. Determine the initial segment strength and stiffness

Knowing the static base shear and storey force distribution pattern, the characteristics of the springs used in simplified model of the corresponding configuration can be calculated directly.

3. Build the simplified model (SM) in SAP2000

SAP2000 is a general-purpose finite element software that is widely used in the industry. The simplified model described in 3.6.1.1 is built with the properties calculated previously. Modal analysis is performed with the SM to verify the fundamental period T_a of the SM. If the T_a does not agree with the empirical fundamental period of a conventional EBF of the same height, the stiffness of the SM shall be adjusted.

4. Run Response spectrum analysis (RSA) with the simplified model

The initial properties of the springs are calculated from static equivalent method. Most building codes today require dynamic analysis to design mid- to high-rise structures. Thus, knowing that the SM is able to replicate the response of a SESBF frame, elastic response spectrum analysis is performed with the SM. The seismic drift should meet the drift requirement in the code. In case the

requirement is not met, inertia of the elastic columns in the SM shall be increased to reduce the seismic drifts.

The storey shear distribution obtained from Step 4 will be used to calculate and update the spring properties of the SM. Step 2 to 4 is repeated until the storey shear distribution obtained from last iterations converge (match with acceptable tolerance).

5. Check wind load and drift requirement

Additional adjustment shall take place if the SM cannot withstand the code specified wind load. The code also imposes a $1/400h_s$ drift limit for the structures under wind loading, stiffness of the SM shall be further adjusted to accommodate such requirement.

6. Perform nonlinear time-history analysis with the SM

A set of ground motion records shall be selected and scaled to reflect the geological condition and the design spectrum of the target site. Nonlinear time-history analysis can then be performed with the SM to predict the seismic response of the frame with the respective segmental configuration.

7. Determine the preferable segmental configuration

The time-history response of the SMs is analyzed according to the performance criteria set by the designer. A preferable segmental configuration is selected which is normally the configuration with shortest segments that assures acceptable seismic performance.

3.7.2 Design the SESBF with selected configuration

Once the segmental configuration is selected, the respective SESBF can be designed with the procedure described in Chapter 5. A brief description is given below:

8. Design of ductile links

The shear strength of the shear springs of the SM is collected and used to design the ductile links.

9. Preliminary design of structural members

As the links are designed, force component r_l, which is determined by the strength of the strain hardened links, can be calculated. The calculations can be done by hand or with pushover analysis.

A preliminary design can be performed with only the force component r_I and r_g, which is the gravity component.

10. Build detailed finite element model

A detailed structural model can be built in SAP2000 with sections obtained from the preliminary design.

11. Calculate force component r_{II}

Force component r_{II} can be obtained through RSA performed on the structural model with modified spectrum, which includes the spectral accelerations of the modes that induce bending on the segmental elastic trusses. The ductile links in the structural model is simulated to reflect their post-yielding stiffness.

Force component r_{II} is then added to the combination of r_I and r_g to obtain the total force demand of the members. The member sizes of the preliminary design are adjusted for the updated force demand.

12. Check member resistance

Steps 10 and 11 are repeated until the members in the preliminary design are able to resist the updated force demand.

13. Check seismic and wind drift

The detailed finite element model with updated member sections are then used to perform checks on the drift limits. Member sections must be further adjusted until the maximum storey drifts under seismic load and wind load meet their respective code requirements.

14. Final design

The final design is obtained when all the checks return satisfactory results.

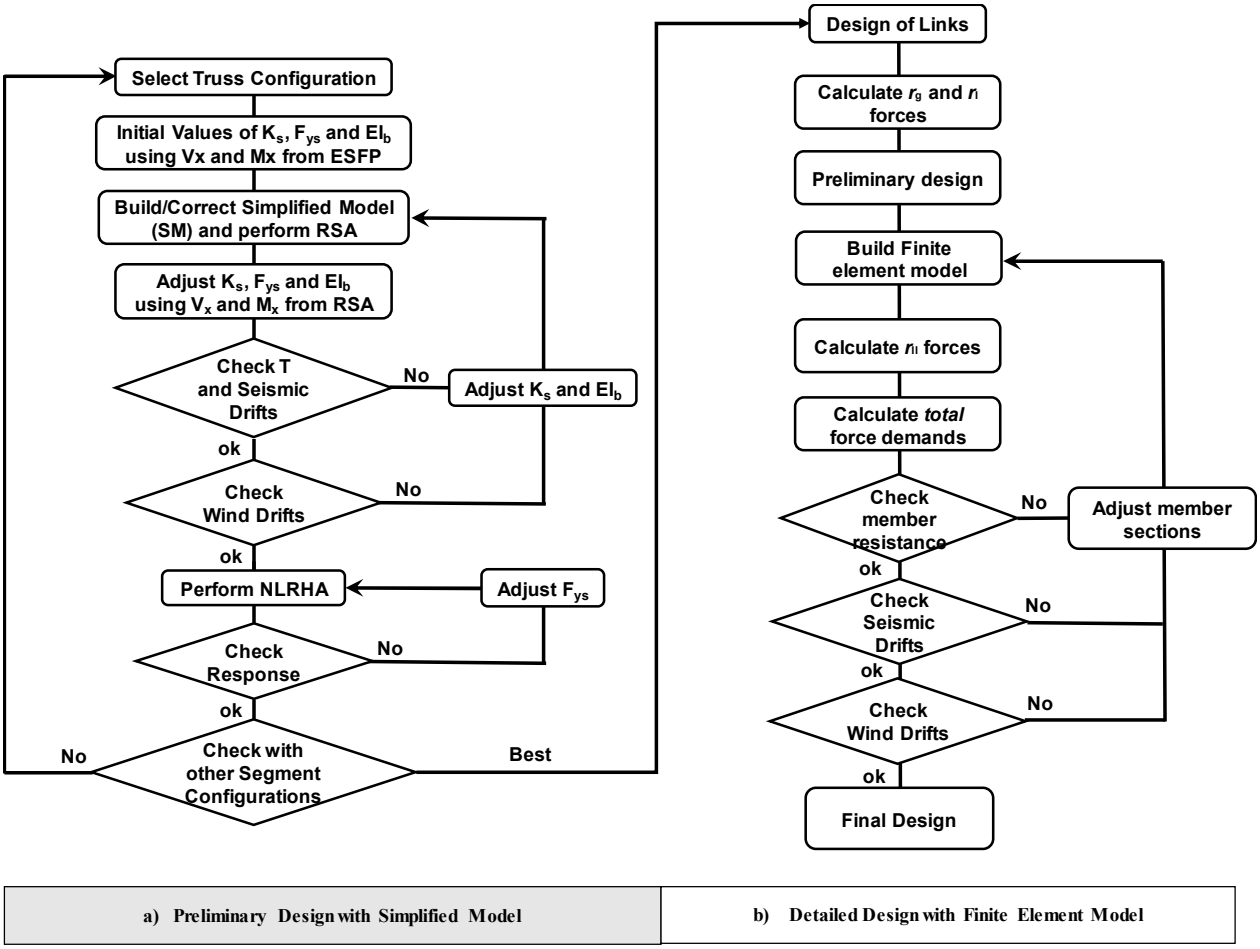

Figure 3-26: Design flowchart for SESBF: a) preliminary design with simplified model; b) detailed design with finite element model

3.8 Experimental test program

3.8.1 Purpose of the test program

The goal of the test program is three folds:

1) To examine the seismic performance of existing chevron braced frame that is designed based on 1980 code.
2) To study the seismic response of SESBF with 2 segments as a new system as well as a retrofit strategy for existing buildings.
3) Verify the proposed design method for SESBFs.

3.8.2 Test setup

The test program is designed to utilize the shaketable that is available in the structural laboratory of Ecole Polytechnique de Montreal. The details regarding the experimental test will be discussed in Chapter 7.

CHAPTER 4 ARTICLE 1: MODULAR TIED ECCENTRICALLY BRACED FRAMES FOR IMPROVED SEISMIC RESPONSE OF TALL BUIDLINGS

Liang Chen[1], Robert Tremblay[1] and Lucia Tirca[2]

[1]Polytechnique de Montreal, Quebec, Canada

[2]Concordia University, Quebec, Canada

The article was submitted to the *Journal of Constructional Steel Research* on April 7, 2018.

Abstract

To improve the vertical distribution of seismic storey drifts and inelastic demands in multi-storey steel eccentrically braced frames (EBFs) two alternative braced frame configurations are examined: the tied braced frame (TBF) system and the modular tied braced frame (M-TBF) system. In TBFs, the concentration of inelastic deformation is prevented by connecting all ductile links over the frame height with vertical tie members. In the M-TBF configuration, the ties are interrupted at one or more locations along the frame height to reduce member forces while achieving the same objective. The performance of each bracing configuration is investigated through nonlinear response history analysis of 8-storey and 16-storey prototype structures. Both the TBF and M-TBF systems could mitigate the soft-storey response and reduce residual deformations observed in the reference EBFs. The TBFs exhibited the smallest and most uniform storey drift demand, as well as the smallest permanent drifts. However, this enhanced response was obtained at the expense of high axial force demands in the tie members. Member forces diminished significantly when adopting a modular tied braced frame configuration, which led to a reduction in the required steel tonnage with limited increases in peak and residual drift demands.

Keywords: eccentrically braced frame; tied braced frame; modular; storey drift; residual drift

4.1 Introduction

The eccentrically braced frame (EBF) system can exhibit large lateral stiffness properties while displaying high ductility through yielding in shear and/or bending in the ductile beam segments

when subjected to seismic ground motions. Nowadays, the seismic design codes include specific design and detailing provisions to achieve this intended inelastic seismic performance. In particular, capacity design provisions have been implemented such that the link beams can reliably sustain the anticipated inelastic deformations while the beam segments outside the links, braces and columns possess sufficient strength to remain essentially elastic.

Despite their appealing characteristics, past experimental and numerical studies have shown that the link inelastic deformations of multi-storey EBFs may concentrate in only a few floors, especially when the ratio of the shear force demand to the yield strength of the links is not uniformly distributed over the building height (Witthaker et al. 1987; Ricles and Popov 1987; Popov et al., 1992, Chao and Goel, 2005). As illustrated in Figure 4-1a, inter-storey drift and high link rotation demands tend to concentrate at the bottom and upper levels of tall EBF structures (Martini et al., 1990; Ricles and Bolin 1990; Chao and Goel 2005; Richards and Uang 2006; Bosco and Rossi 2009; Koboevic and David 2010; Koboevic et al. 2012). This behaviour is attributed to the limited capacity of the system to redistribute inelastic demand in the non-yielding storeys. In extreme cases, this may lead to excessive link rotations and a tendency to form soft-storey response (AISC 2010). In Canada and the U.S., height limits are not prescribed for EBFs, which may represent a concern for tall frames located in high seismic regions.

To overcome this drawback and achieve more uniformly distributed yield demands in EBF links of multi-storey buildings, it was proposed to vertically tie all ductile links over the structure height, so that all links will be activated after yielding initiates in one link (Martini et al. 1990; Whittaker et al. 1990). This tied EBF system, referred to herein as TBF, is illustrated in Figure 4-1b. The TBFs were further studied by Ghersi et al. (2000). Ghersi et al. (2003, 2006) and Rossi (2007) developed and validated a design method for TBFs. Bosco and Rossi (2009) compared the response of traditional EBFs and tied EBFs. The TBFs, in fact, consist of a pair of elastic vertical trusses connected by yielding shear links. Such an elastic truss, spine, mast or strongback system has been used to improve the seismic response of concentrically braced frames and braced frames with buckling restrained braces (BRBs) (Tremblay et al. 1997; Tremblay 2003; Merzouq and Tremblay 2006; Tremblay and Poncet 2007; Mar 2010; Qu et al. 2014; Lai and Mahin 2015, Simpson and Mahin 2018). An application with BRB members (dual BRB frame) is illustrated in Figure 4-1-1c. In all these systems, higher mode response induces shear and flexural demand on the elastic vertical

trusses, which may result in high force demands on the truss members that must be considered in design (Figure 4-1d).

A modular tied braced frame (M-TBF) configuration was proposed by the authors to reduce the forces in the elastic truss members (Chen et al. 2012, Tremblay et al. 2014). The proposed configuration is illustrated in Figure 4-1e. Force demands on truss members are reduced because bending of the elastic trusses is decreased by breaking the continuity of the vertical ties. Tie continuity is however maintained over a minimum of storeys within each module to keep preventing the soft-storey response. In this article, the nonlinear seismic response of the proposed M-TBF system is examined compared to that of EBFs and TBFs. Herein, the capacity of the M-TBF system to achieve uniform inelastic drift response while reducing the force demands compared to TBFs is verified. Nonlinear seismic analysis is performed on M-TBFs employed for 8-storey and 16-storey buildings located in southwest British Columbia, a seismic active region situated along the west coast of Canada. The response parameters of interest are the peak storey drifts and, for the tied systems, peak axial forces in the truss members. Residual storey drifts are also examined, and the steel tonnages for each system are compared to assess their cost-effectiveness. In the last section of the article, the M-TBF system is applied to a 24-storey building to verify its potential for taller braced frames.

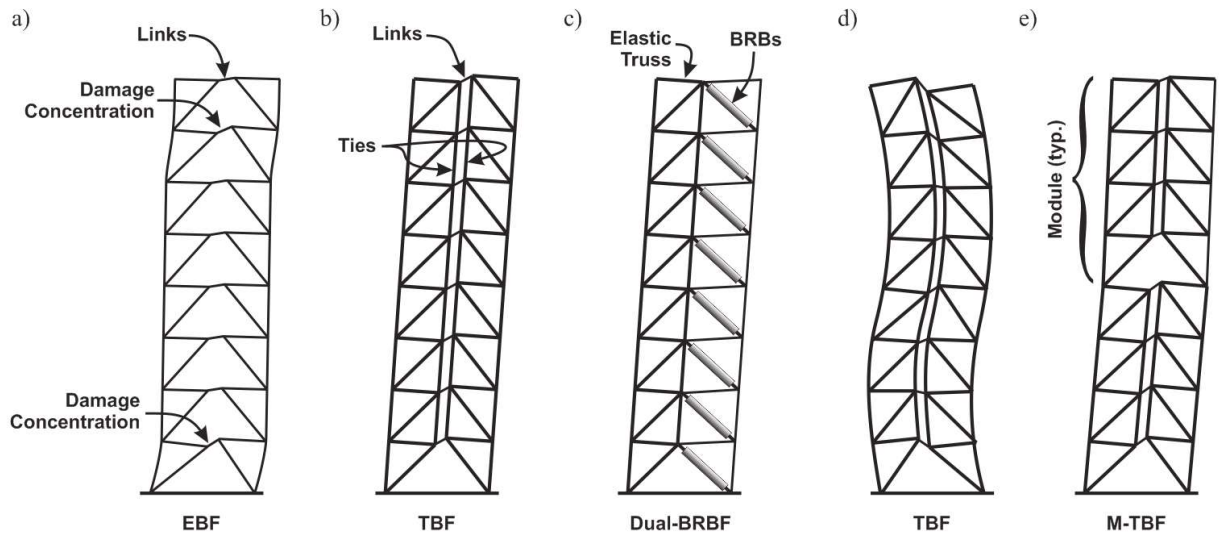

Figure 4-1 Mitigation of soft-storey response in multi-storey steel braced frames: a) Concentration of inelastic deformations in EBFs; b) Tied braced frame (TBF); c) Dual-BRBF configuration; d) Higher mode response in TBF; and e) Modular tied braced frame (M-TBF).

4.2 Building and Framing Systems Studied

4.2.1 Buildings studied

The 8-, 16-, and 24-storey prototype buildings are regular office buildings located on a Site Class C in Victoria, British Columbia. All buildings have the same floor plan as shown in Figure 4-2a. The roof dead and snow loads are respectively equal to 3.4 and 1.48 kPa. The floors support 4.5 kPa dead load and 2.4 kPa occupancy live load. The weight of the exterior cladding is 1.2 kPa. The lateral resistance along both orthogonal directions is provided by individual braced frames. One of the four identical braced frames acting in the E-W direction is studied herein. As indicated, EBF, TBF, and M-TBF configurations are examined. These configurations are illustrated in Figure 4-2b and Figure 4-2c for the 8-storey and 16-storey buildings, respectively. For the 8-storey building, two modules of the M-TBF spanning over 4 consecutive storeys are considered. For the 16-storey structure, M-TBFs with 8-storey modules (M-TBF-1) and 4-storey modules (M-TBF-2) are studied. The latter was included to investigate the effects of releasing further the continuity of the vertical truss. For the 24-storey building, only one M-TBF configuration with six 4-storey modules

is studied.

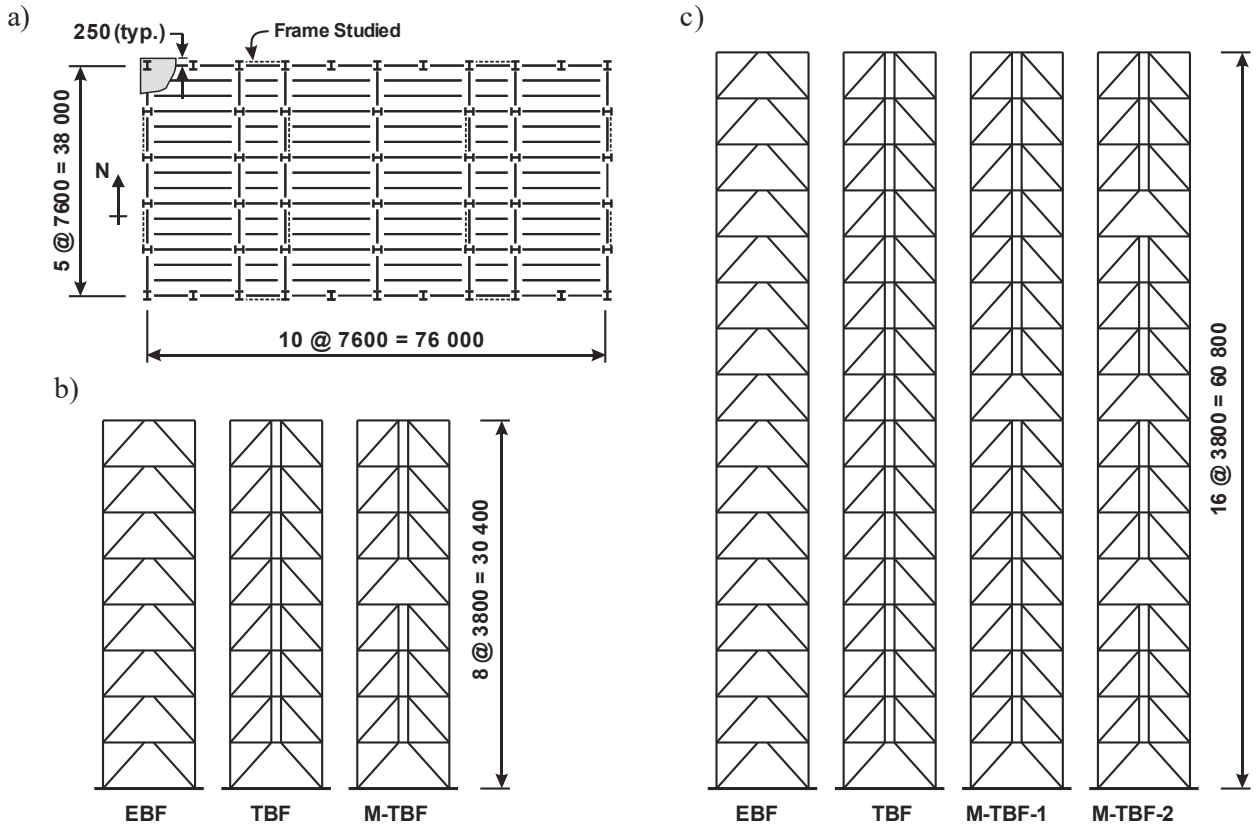

Figure 4-2 a) Floor plan of the building studied; b) Elevation of 8-storey framing systems; c) Elevation of 16-storey framing systems.

4.2.2 Design of the structures

The structure design was performed in accordance with the provisions of NBCC 2010 (NRCC 2010) and the CSA S16-09 (CSA 2009) design standard for steel structures. The braced frames were first designed for earthquake resistance and then verified for wind loading conditions. In CSA S16, link beams in EBFs can be regular links that are part of roof and floor beams or replaceable links that are bolt connected to the beams. In this study, replaceable link beams with bolted end plate connections as proposed by Mansour et al. (2011) and depicted Figure 4-6a were used for all frames studied. The links were made of ASTM A992 W shapes with F_y = 345 MPa. The length of the links (e) was adjusted to yield in shear (short link behaviour) while maintaining link plastic rotations within the code prescribed limit of 0.08 radians. Following capacity design principles, the

link beams were sized first to resist the code specified seismic forces as obtained from response spectrum analysis. All other members were designed to remain essentially elastic under the forces induced by the links reaching their probable resistances including strain-hardening effects combined with concomitant gravity loads effects. Braces and vertical ties were square tubing conforming to ASTM A500, grade C (F_y = 345 MPa) whereas beams and columns were ASTM A992 W shapes. For the columns, the same section was kept for two consecutive floors, as commonly done in practice.

In the NBCC, the seismic design base shear V is determined from:

$$V = \frac{S(T_a)M_V I_E W}{R_d R_o} \quad (1)$$

where S is the design spectrum based on uniform hazard spectrum (UHS) ordinates established for a probability of exceedance of 2% in 50 years, T_a is the structure fundamental period, M_V accounts for higher mode effects on base shear, I_E is the importance factor, W is the seismic weight, and R_d and R_o are the ductility- and overstrength-related force modification factors, respectively. For the site studied, S is equal to 1.20 for $T_a \leq 0.2$ s and 0.09 for $T_a \geq 4$ s. The other values are: S(0.5 s) = 0.82, S(1.0 s) = 0.38, and S(2.0 s) = 0.18. For intermediate periods, S is linearly interpolated. For the structures investigated, M_V = 1.0 and the buildings were assumed to be of the normal importance category with I_E = 1.0. For all three framing configurations, the values R_d = 4.0 and R_o = 1.5 were used, as specified in NBCC for steel eccentrically braced frames. For design, the period T_a can be taken equal to the computed structure fundamental period except that it cannot exceed 0.05 h_n for braced frames, where h_n is the building height (in meters). The upper limits on T_a for the calculation of V were, therefore, equal to 1.52, 3.04, and 4.56 s, respectively, for the 8-storey, 16-storey and 24-storey buildings.

The final periods from the modal analysis for the first three lateral modes, T_1, T_2, and T_3, are given in Table 4-1. As shown, T_1 exceeded the code upper limit on T_a for all frames. The upper limit, therefore, governed the value of V. In addition, as per NBCC, V should not be less than the value determined for T_a = 2.0 s, which applies to the studied 16-storey and 24-storey buildings. For all frames, the response spectrum analysis (RSA) was used to determine the seismic induced storey

shears from which link shears were calculated. When using the RSA method, NBCC requires that the analysis results be scaled up by the ratio $0.8V/V_d$ when V_d is less than $0.8V$. Herein, V_d is the dynamic base shear resulted from the RSA. The aforementioned correction applies to all studied structures. Values of $0.8V$ were equal to 3.68% W for the 8-storey frames and 2.4% W for the 16-storey and 24-storey frames. In NBCC and CSA S16, seismic storey shears used to design the links must be further increased to account for P-delta effects and notional load effects.

For all EBFs, the links were designed individually to resist the shear forces obtained from the analysis. For the TBF system, identical links designed for the average link shear force computed over the entire building height were used at all levels (CL = constant link), as proposed by Rossi et al. (2007). For the 16-storey TBFs, a second design was performed where links were designed individually to resist the link shear forces from the analysis (VL = variable links). Constant link (CL) design was also adopted for the M-TBFs in anticipation of uniform inelastic response within each module. Hence, the same section was used for all links in a module; that section is determined to resist the average shear force demand over the height of the module. Values of the design factored link shears V_f including stability effects that were used in all frames are plotted in Figure 4-3. The resulting link factored shear capacity-to-demand ratios, V_r/V_f, are also presented in the figure. As shown, the ratios are close to 1.0 for all frames except at the roof level of the EBF structures due to minimum detailing requirement governing the design of lightly loaded links.

The design of the truss members for frames with elastic vertical trusses is described in the next section. After completion of the design for seismic resistance, seismic storey drifts including inelastic effects were verified against the NBCC limit of $2.5\%h_s$, where h_s is the storey height. No change was needed for the 8-storey and 16-storey structures. For the three 24-storey frames, the code limit was exceeded in the EBF top levels. Thus, to reduce the overall bending, the column sizes at the bottom ten storeys were increased and to satisfy the 2.5% h_s limit, larger brace sections were required at levels 7 to 10.

Table 4-1 Building periods, steel tonnage and maximum seismic base shears (/frame).

Structure Height	Structure Type	T_1 (s)	T_2 (s)	T_3 (s)	Steel Tonnage (t)	84th V/W from NLHRA (%)
8-Storey	EBF	2.27	0.77	0.42	21.7	7.19
	TBF-CL	2.03	0.65	0.33	25.7	13.2
	M-TBF	2.10	0.72	0.35	23.7	9.39
16-Storey	EBF	4.34	1.50	0.87	73.6	4.43
	TBF-CL	4.34	1.40	0.69	90.0	7.21
	TBF-VL	4.18	1.40	0.77	91.1	7.44
	M-TBF-1	4.34	1.45	0.72	76.9	6.90
	M-TBF-2	4.36	1.41	0.78	76.3	6.59
24-Storey	EBF	7.88	2.46	1.34	171	3.40
	TBF-CL	7.67	2.34	1.19	219	4.07
	M-TBF	7.82	2.39	1.26	183	3.80

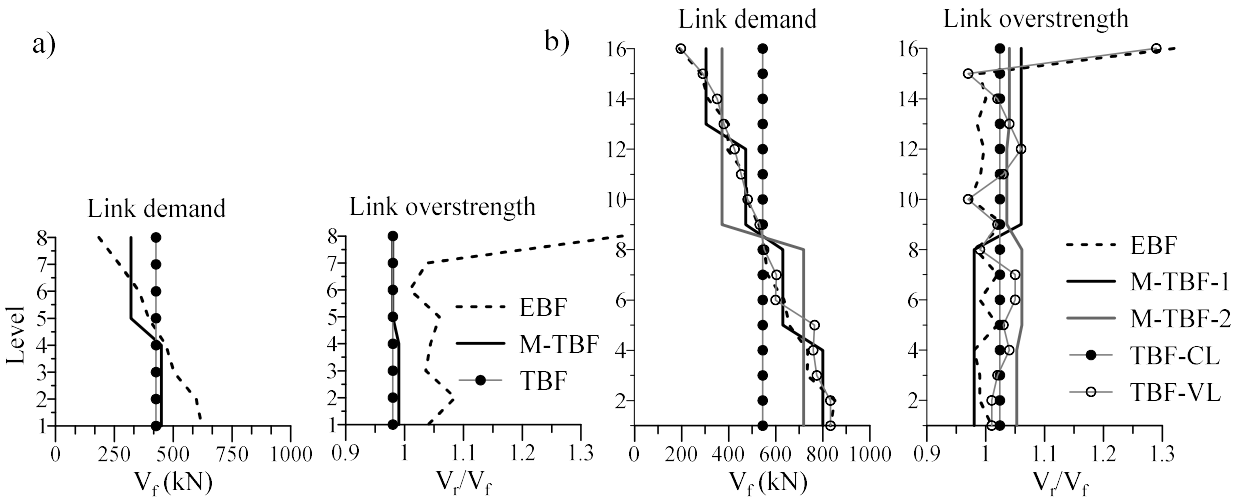

Figure 4-3 Factored link shear forces Vf and factored link shear resistance to shear force Vr/Vf ratios for: a) 8-storey building; and b) 16-storey building.

The reference wind pressure at the site is 0.57 kPa for a return period of 50 years. Because the structure periods are longer than 1.0 s, wind loading was determined using the dynamic analysis procedure of NBCC in which the gust factor depends on the building dynamic properties. In the calculations, urban exposure conditions and a critical damping ratio of 1% were considered. For all structures, forces from factored wind loads were less than seismic induced forces, and maximum wind deflections were lower than the limit of 1/400 h_s prescribed for these structures. Hence, wind loading did not influence the braced frame designs.

4.2.3 Design of the vertical elastic trusses

While code specified capacity design provisions were applied for the design of beams outside of links, braces and columns of frames with vertical elastic trusses should be designed to resist additional forces to that resulted from the first mode response when all links develop their strain hardened strength. These additional forces are that induced by shear and bending resisted by the elastic trusses when the structure responds in its second and higher modes when links yield in shear. The first and second mode responses are illustrated in Figure 4-4a for the 16-storey TBF structure. The two modes were obtained by reducing the shear stiffness of the links to their post-yielding value, simulating the inelastic response of the frame upon yielding of the links. Deflected shapes

in these 1st and 2nd inelastic modes are similar to their elastic counterpart, except for the amplified link deformations. In the first inelastic mode, all links are yielding, and the flexural demand on the vertical truss is limited. Truss bending response is essentially mobilized in the second mode. As proposed by Rossi (2007), design forces for the vertical truss members can then be estimated by adding the contribution from both modes (Figure 4-4b). First mode forces were assumed equal to those induced by all links reaching their probable hardened resistance, V_u, neglecting flexural truss response, as is done when performing capacity design for conventional EBFs. Additional member forces were obtained from the second elastic mode response multiplied by a reduction factor $\alpha = 0.90 - 0.04n_s$ to account for inelastic response, where n_s is the number of storeys. Member forces from gravity loads are added to those resulted from seismic loads. The relative contribution from gravity loads, first mode response and reduced second mode response are illustrated in Figure 4-5 for the braces, columns, and ties of the 16-storey TBF.

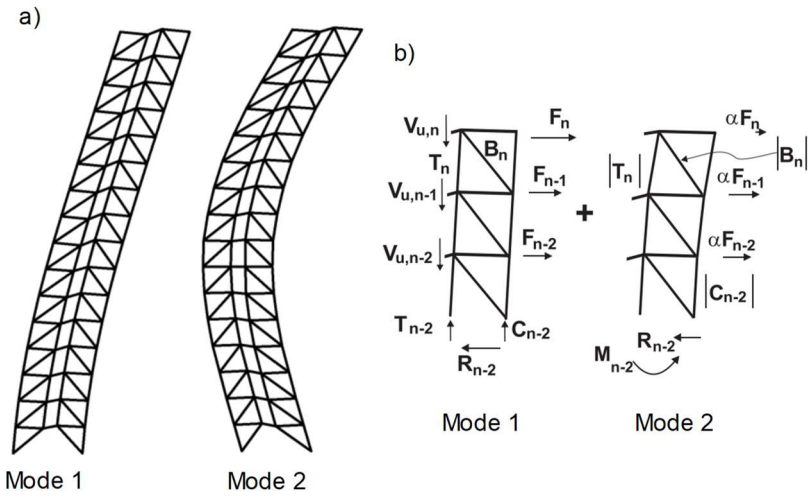

Figure 4-4 Anticipated inelastic response of the 16-storey TBF: a) Inelastic vibration modes; b) Design forces in truss members.

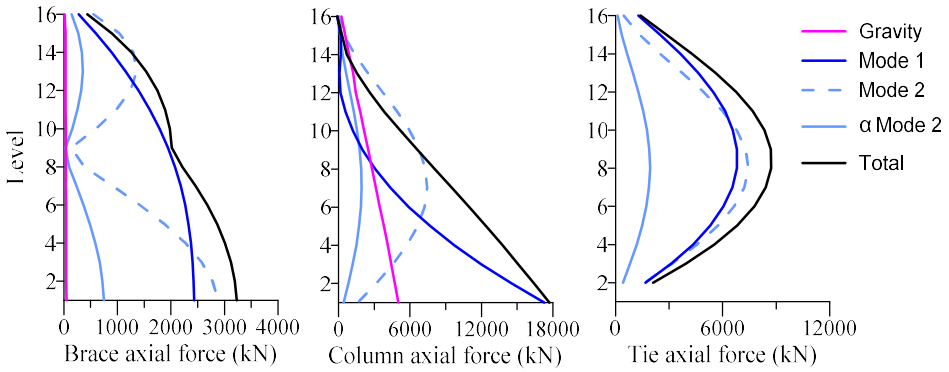

Figure 4-5 Design forces in the braces, columns and tie members of the 16-storey TBF.

In the absence of existing guidance for the force demand in vertical truss members of M-TBFs, member forces in beams outside the links, ties, braces and columns for these frames were determined from nonlinear dynamic time history analyses using an iterative analysis-design process until convergence on member sizes was reached. Time history analysis is described in the next section. In the process, the 84th percentile force values from the analysis were used.

Frame properties are summarized in Table 4-1. Tied braced frames are slightly stiffer than their corresponding EBFs. Using a modular configuration instead of a fully continuous system has limited effect on building lateral stiffness and periods. As expected, the steel tonnage is maximum for TBFs for all three building heights. On average, TBFs require 23% more steel than the conventional EBFs. Using the TBF-CL versus TBF-VL for the 16-storey building it had virtually no impact on steel consumption. When using M-TBFs, this increase is reduced to 6%. Similarly, for the 24-storey building, there is nearly no difference in steel tonnage between the M-TBF-1 (8-storey modules) and M-TBF-2 (4-storey modules) structures.

4.3 Seismic Analysis

4.3.1 Numerical Model

Nonlinear time history dynamic analysis was performed using the OpenSees platform (McKenna and Fenves, 2004). The analyses were carried out on a 2-D model that included one of the four bracing bents acting in the E-W direction. The shear links were modelled using elastic beam-

column elements with a zeroLength element reproducing elastic and inelastic shear responses of the links (Rozon et al., 2012). The Steel02 material was assigned to the zeroLength element to reproduce the link hysteretic response, together with the Min-Max material to capture the link failure. The model was calibrated against the results from seven tests conducted on short links by Okazaki & Engelhardt (2006). Description of the selected test specimens is given in Table 4-2 where e is the length of the link, V_p is the plastic shear strength, V_{max} is the maximum shear including strain hardening experienced in the tests, and γ_{max} is the maximum rotation experienced by the specimen before the occurrence of strength degradation. Proper calibration of the Steel02 parameters permitted to reproduce kinematic and isotropic hardening responses of the links, as illustrated in Figure 4-6b for Specimen 4C. As shown in Table 4-2, the average and maximum rotation computed for the selected 7 tests is 0.108 rad. and 0.157 rad., respectively. As recommended in ASCE/SEI 41-13 (2013), the average value was used to set the limits for the Min-Max material used to detect a link failure.

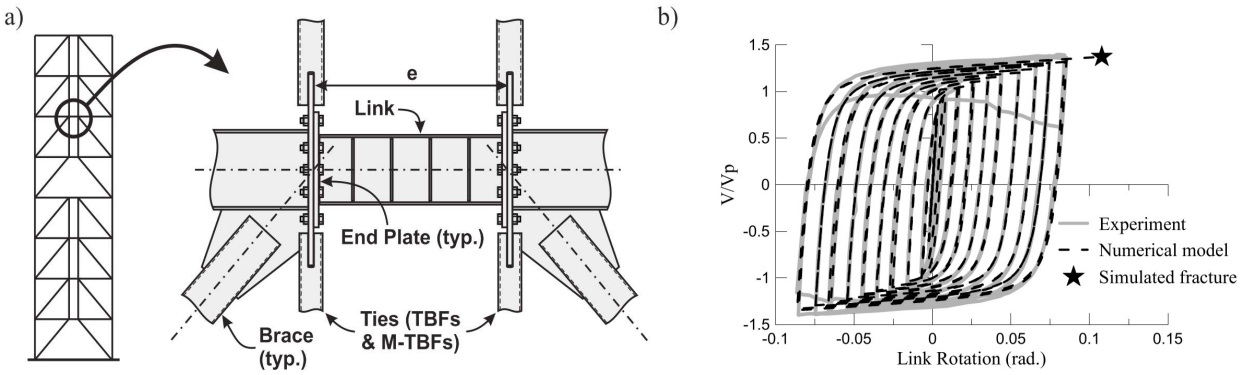

Figure 4-6 a) Replaceable link beams with end plate connections and proposed tie-to-link connection detail; b) Calibration of the numerical hysteretic link model in OpenSees (Test 4C).

Table 4-2 Test results used for the calibration of link beam elements

Test ID	Section	R_yF_y (MPa)	e (mm)	V_p (kN)	V_{max}/V_p	γ (rad.)
1A	W10X19	405	584	371	1.15	0.157
1B	W10X19	405	584	371	1.27	0.096
1C	W10X19	405	584	371	1.30	0.090
4C	W10X33	421	584	423	1.40	0.086
8-RLP	W16X36	392	930	652	1.43	0.120
12-SEV	W18X40	393	584	787	1.34	0.075
12-RAN	W18X40	393	584	787	1.59	0.129
				Average	1.35	0.108
				Max	1.59	0.157

Although braces, beam segments outside the links, ties, and columns were designed to remain elastic, nonlinear models were used for all components to detect and account for potential ultimate limit states in the analysis. The braces and ties were modelled using nonlinear beam-column elements with distributed plasticity and fiber discretization of the cross-section. The Steel02 material with properties suggested by Aguero et al. (2006) was assigned to the fibers, and initial out-of-straightness of 1/500 of the brace lengths was considered to reproduce the buckling strength of braces. Rotational end restraints induced by the gusset plates were also considered and defined in zeroLength elements connecting the braces to rigid links that simulated part of column cross-section and connection. Beams outside of links and columns were also modelled with fiber-base nonlinear beam-column elements. The material yield strength of 385 MPa for I-shapes and 460 MPa for HSS members were assigned to steel materials in the model.

In the model, 3% of critical damping was specified with Rayleigh method in the first and third modes of vibration for the 8-storey structures and the first and fifth modes for the 16-storey and 24-storey structures. Stiffness proportional damping was assigned to the frame members, not to the zeroLength elements used in the shear links. Geometric nonlinearities were considered in the analyses by including a P-delta column representing the leaning gravity columns supported by the braced frame studied (shaded area in Figure 4-2a) and applying gravity loads consisting of the dead load plus 50% of the live load and 25% of the roof snow load.

4.3.2 Nonlinear Static (Pushover) Analysis

Nonlinear static (pushover) analysis (NSA) was conducted to verify and obtain a first insight into the inelastic response of the studied structures. In these analyses, the nonlinear lateral load pattern of ASCE/SEI 7-10 (2010) was applied to the structures, and the lateral displacement at the roof level was gradually increased until failure occurred in one of the links when the rotation reached 0.108 rad. The deformed shape of different frames of the 8-storey and 16-storey buildings are shown in Figure 4-7and Figure 4-8, respectively. The lateral load-deformation responses of these frames are presented in Figure 4-9, where V_{static} is equal to $0.8V$ used in the design of the frames. Similar results were obtained for the 24-storey frames.

Non-uniform shear yielding in both conventional EBFs resulted in limited roof drift values when link rotations reached the limit in the critical storey. Conversely, TBFs exhibited evenly distributed inelastic deformation of links over the building height, which resulted in larger roof drift upon the occurrence of link failure as illustrated in Figure 4-7 and Figure 4-8. In terms of lateral capacity, the TBF-VL design outperformed the TBF-CL design for the 16-storey, but the latter exhibited slightly higher lateral deformation capacity. The significant difference in behaviour between EBFs and TBFs can be appreciated by comparing their drift concentration factors (DCF), i.e. ratios between the largest storey drift to the average storey drift over the building height at the end of the analysis. As shown in Table 4-3, the DCFs for the TBFs are close to unity whereas those for the EBFS are much higher. As expected, links in each of the modules of the M-TBFs experienced uniform rotation, which resulted in uniform storey drifts in the modules. The M-TBFs, therefore, displayed an intermediate response compared to the former two types in terms of lateral deformation capacity and DCF values. For the 16-storey building, among the two M-TBF designs, M-TBF-1 with 8-storey modules showed better response with larger lateral displacement capacity and lower DCF compared to the M-TBF-2 with 4-storey modules.

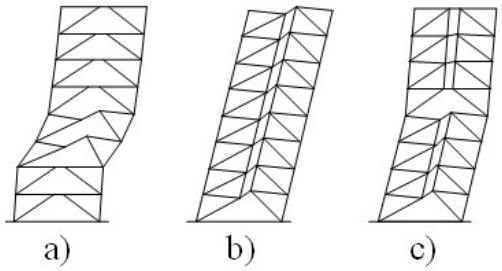

Figure 4-7 Deformed shape of the 8-storey braced frames from NSA: a) EBF; b) TBF; and c) M-TBF.

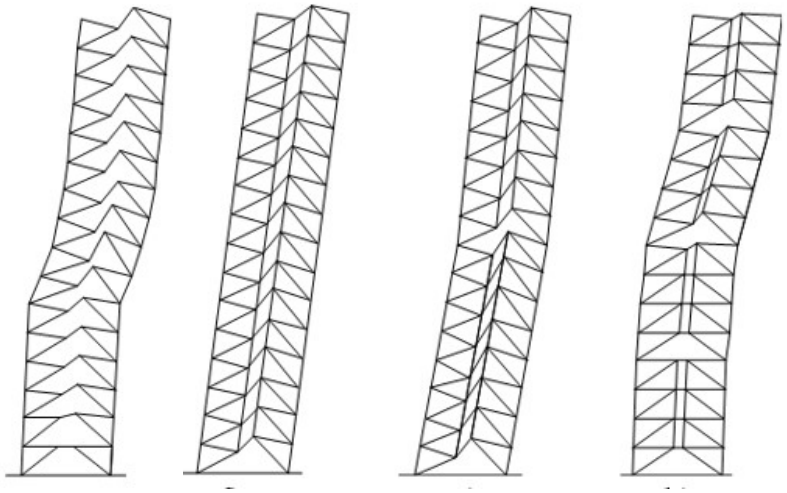

Figure 4-8 Deformed shape of the16-storey braced frames from NSA: a) EBF; b) TBF (CL design); c) M-TBF-1; and d) M-TBF-2.

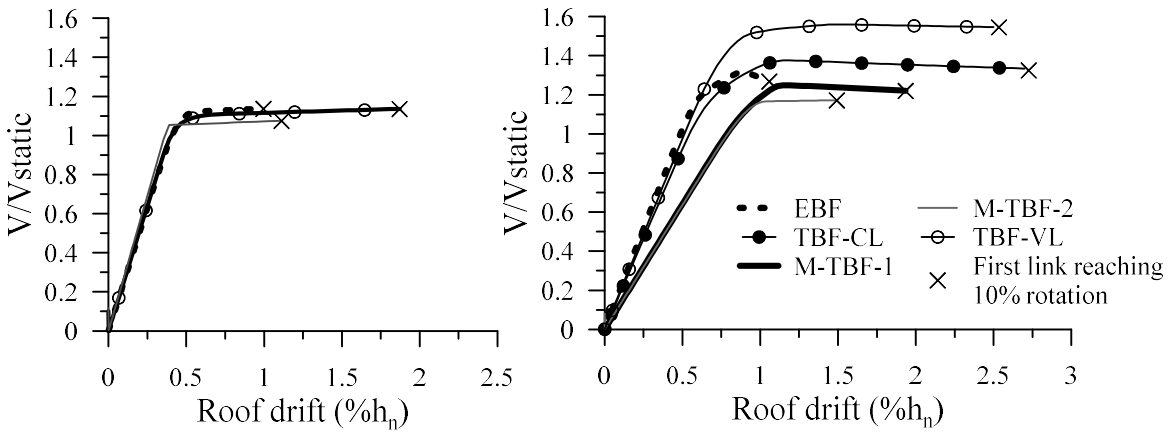

Figure 4-9 Lateral load-displacement responses from NSA for the 8-storey and 16-storey braced frames.

Table 4-3 Drift concentration factors (DCF) from NSA for the 8- and 16-storey frames.

	8-storey			16-storey				
Type	EBF	TBF	M-TBF	EBF	TBF-CL	TBF-VL	M-TBF-1	M-TBF-2
DCF	2.6	1.1	1.5	2.4	1.1	1.3	1.3	2.2

4.3.3 Selection and Scaling of Ground Motions

The 8-storey structures were subjected to a suite of 18 historical ground motion records that were selected from the PEER database (PEER 2011) to reflect the magnitude-distance scenarios that dominate the hazard at the site studied. The records were linearly scaled to match, on average, the design spectrum within the 0.4-2.0 s period range, representative of the first and second mode periods of the structures (Figure 4-10a). A second suite of 17 ground motions was considered for the 16-storey frames. As shown in Figure 4-10b, the emphasis for the selection and scaling of these additional records was built on matching the design spectrum for longer periods to cover the periods in the first three modes contributing to 90% mass participation for these taller frames (Figure 4-10b).

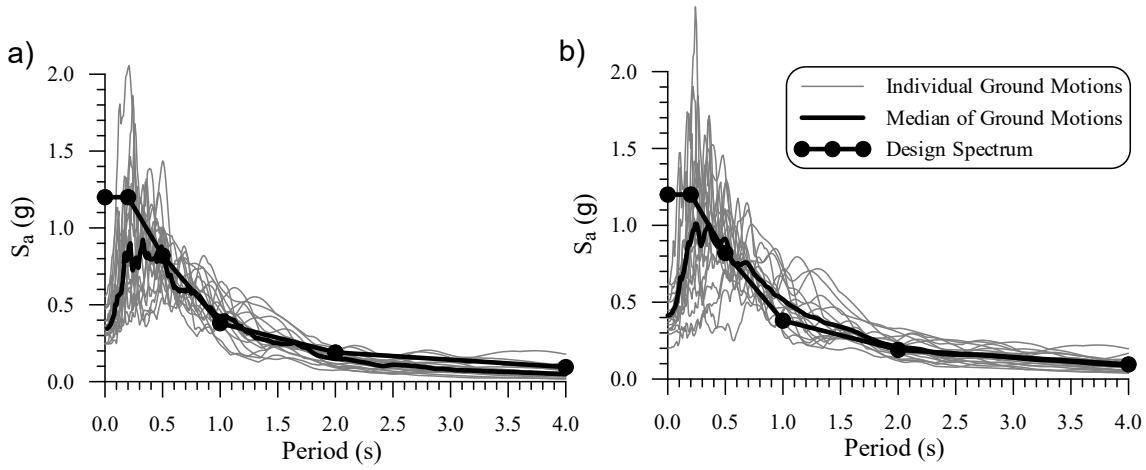

Figure 4-10 Design spectrum and 5% damped absolute acceleration spectra of the ground motion records suites: a) 8-storey frame scaled for 0.4-2.0 s; b) 16-storey frame scaled for 0.6-4.0 s

4.3.4 Analysis Results for the Structures

Peak values of the response parameters for the 16-storey frames are presented in Figure 4-11. The 50th and 84th percentile values of these peak response parameters are given in Table 4, and a comparison of the 84th percentile member force values is presented Figure 4-12. The number of link failures due to excessive link plastic rotations and the number of ground motion records that caused these failures are also given in Table 4-4.

Table 4-4 Values of response parameters for the 8-storey and 16-storey braced frames.

Struct.	Structure Type	Drift (% h_s)		Residual Drift (% h_s)		Link Rotation (% rad.)		No. of link failures	No. of ground motions with link failure
		50th per.	84th per.	50th per.	84th per.	50th per.	84th per.		
8-St.	EBF	1.76	2.06	0.54	0.77	3.05	4.94	2	1
	TBF	1.15	1.41	0.20	0.30	1.63	2.69	0	0
	M-TBF	1.17	1.39	0.24	0.49	1.70	2.66	0	0
16-St.	EBF	1.65	1.87	0.10	0.50	2.70	3.84	6	3
	TBF-CL	0.99	1.59	0.09	0.43	0.35	3.57	0	0
	TBF-VL	1.13	1.63	0.15	0.32	0.36	3.26	0	0
	M-TBF-1	1.02	1.52	0.12	0.32	1.14	3.75	0	0
	M-TBF-2	1.01	1.59	0.18	0.39	1.90	3.67	0	0
24-St.	EBF	1.48	2.50	0.37	0.90	2.66	6.80	11	7
	TBF-CL	1.42	1.73	0.18	0.37	1.66	3.77	0	0
	M-TBF	1.11	1.41	0.18	0.38	1.67	3.80	0	0

In the case of 16-storey EBF, the soft-storey response was observed under 3 out of 17 ground motions that drove the six links to failure (Figure 4-11). In Tables 4 and 5, the 16-storey EBF shows limited capability to redistribute the concentrated large inelastic demands along the building height.

This is also reflected by the peak storey drift and the DCF values. However, this behaviour is not observed for the TBFs and M-TBFs which display more evenly and less scattered the storey drift among floors. When examining Figure 4-11 and Figure 4-12 together with the storey drift and DCF values given in Tables 4-4 and 4-5, the TBF is the most effective system for drift control, especially in the case when constant link (CL) configuration as recommended by Rossi (2007) is employed. Similar peak storey drifts and DCF statistics were however obtained with the two M-TBFs. Nonetheless, storey drift distributions for these systems show variations between modules as was expected because of the flexural discontinuities introduced in the vertical elastic trusses. As expected, the M-TBF-1 with longer (8-storey) elastic truss segments shows a more uniform drift response.

Table 4-5 DCF values for the 8-storey and 16-storey braced frames.

Percentile	8-storey			16-storey				
	EBF	TBF	M-TBF	EBF	TBF-CL	TBF-VL	M-TBF-1	M-TBF-2
50th	2.04	1.40	1.34	2.11	1.36	1.70	1.46	1.54
84th	2.60	1.50	1.62	2.69	1.70	2.00	1.69	1.81

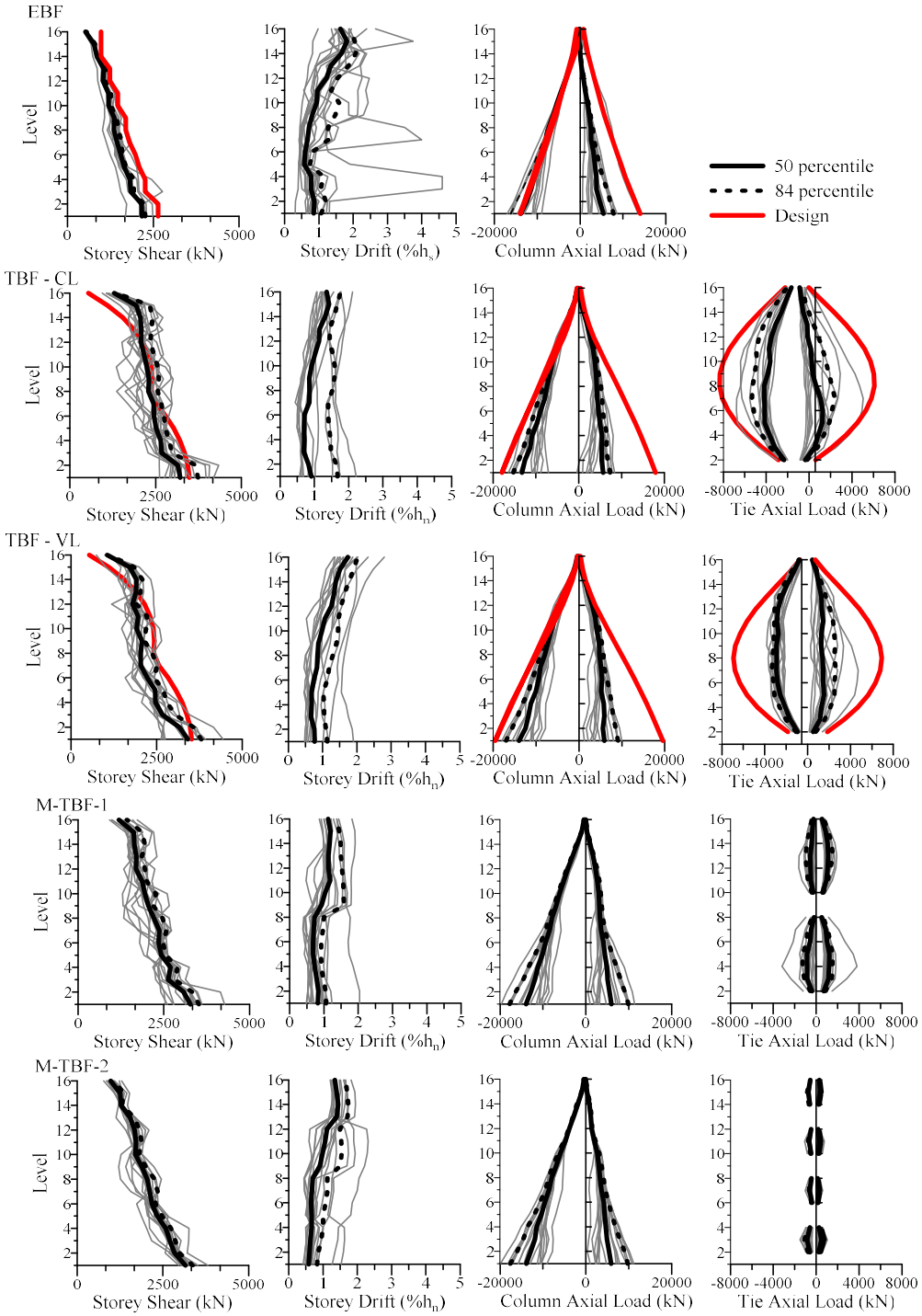

Figure 4-11 Storey shears, storey drifts, axial force in columns and tie members of the 16-storey braced frames.

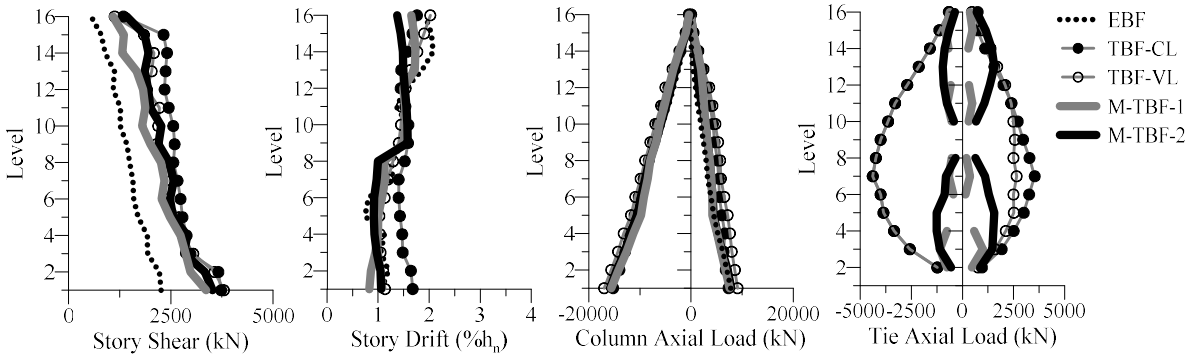

Figure 4-12 Comparison of the 84th percentile storey shears, storey drifts, and axial loads in columns and tie members of the 16-storey braced frames.

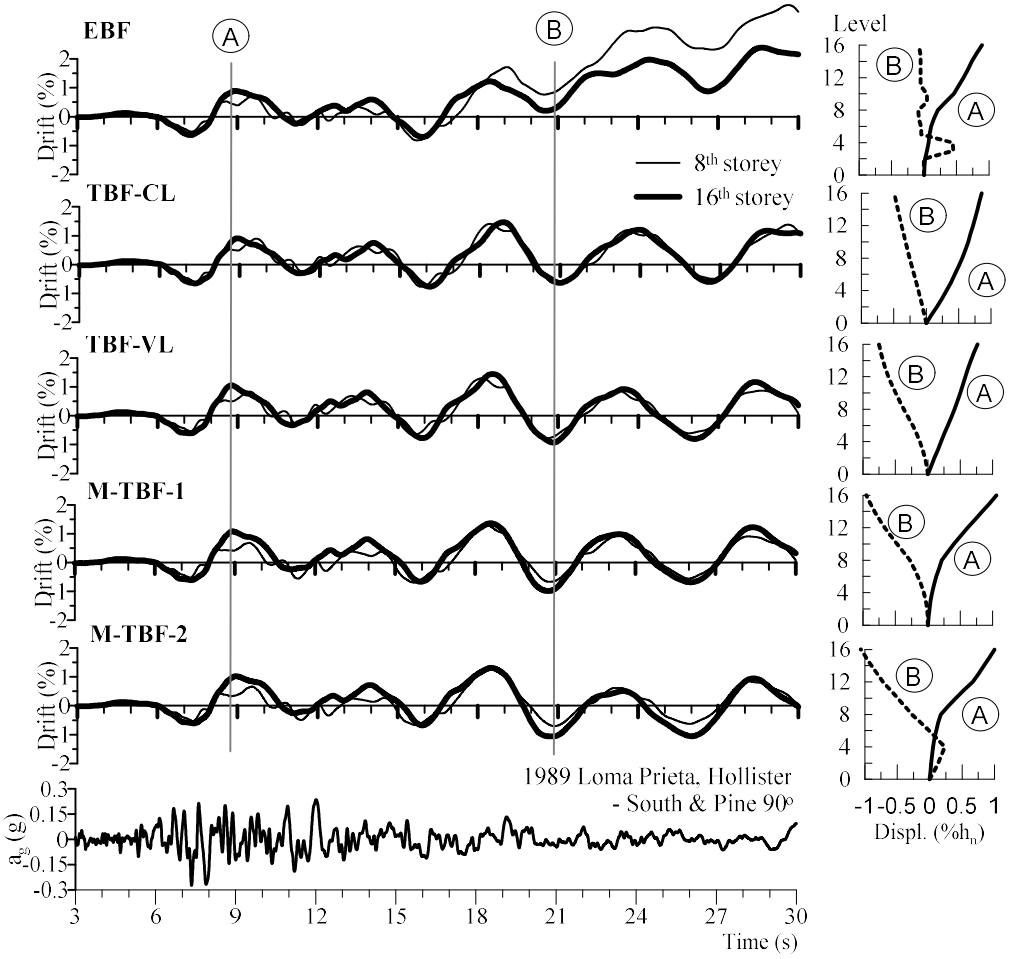

Figure 4-13 Storey drift time histories at the 8th and 16th storeys and horizontal displacement profiles for the 16-storey braced frames under Ground motion # 776.

Time histories of drift series at the 8th and 16th storeys of all framing systems resulted under a ground motion recorded during the 1989 Loma Prieta earthquake are plotted in Figure 4-13. Displacement profiles at two selected time steps are also given in the figure. Under this record, the EBF structure experienced pronounced storey drift concentrations at levels 3 and 4 as well as at 7 and 8. The EBF frame also developed progressive drifting during the ground motion excitation. Conversely, the response of all TBF and M-TBF systems generally followed the first-mode deflected shape with storey drifts at the 8th and 16th levels are overlapping nearly perfectly for the duration of the ground motion. For the M-TBF-2 structure, however, the first two modules showed independent responses during some period intervals of earthquake shaking.

Time histories of roof displacement and storey drifts at the first and top storeys of all frames under the same ground motion are plotted in Figure 4-14. Variations over the frame height of storey drifts and tie axial forces at time sequence "A" which corresponds to the occurrence of maximum roof displacements are also illustrated in the same figure. As illustrated, roof displacements are dominated by the first-mode response with oscillations at periods close to T_1 periods of structures that are given in Table 4-1. As shown, for the 16-storey EBF, this response is maintained and even amplified after the strong ground shaking. This is explained by the long period content of the ground motion signal as revealed by low-pass filtering. Storey drift at the first and roof levels are also governed by the first mode, except for the EBF and M-TBF-2 structures for which the ground motion signals contain higher frequency oscillations due to higher mode response. The TBF and M-TBF-1 structures show smooth drift profiles at the peak lateral displacements (time step "A") whereas the EBF and to a lesser extent the M-TBF-2 systems show larger variations of storey drifts at the same time sequence. In the bottom right graph, the tie force profiles resulted in the two TBFs clearly show that achieving the desirable drift profiles at maximum roof displacement required a considerable effort from the elastic trusses in bending. Partially interrupting the continuity of the elastic trusses in the M-TBF-1 and M-TBF-2 systems markedly reduced that contribution, as evidenced in the same graph. The same response parameters are presented in Figure 4-15 when the frames were subjected to a ground motion characterized by a single acceleration pulse. In this case, all frames behaved similarly, exhibiting a time lag between the storey drift at the first floor and the response at the roof level as the shear wave induced by the ground motion travelled up the building. At peak roof displacement, after the ground motion pulse, all frames exhibit an "S" deformed shape

typical from this type of demand. Again, the TBF and M-TBF-1 systems exhibited the smother deformation profiles while some variations can be observed for the other two systems. The flexural demand imposed by elastic trusses mimics the deformed shape, as revealed by the tie force pattern at time “A”.

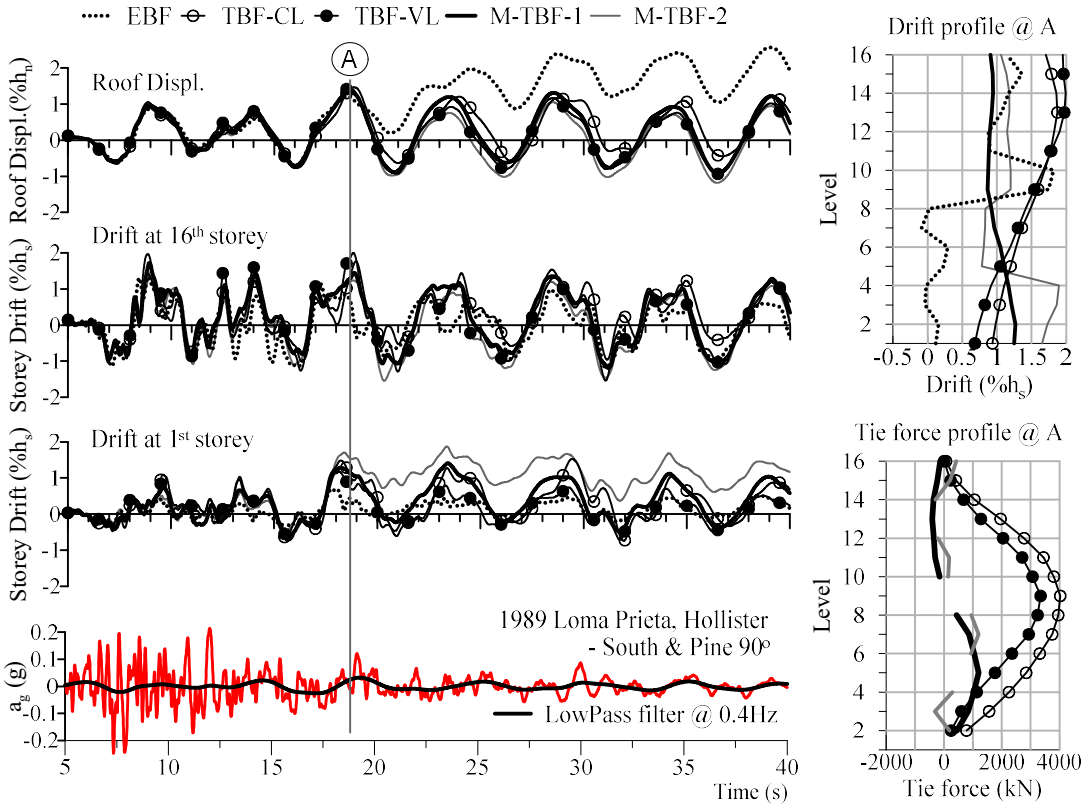

Figure 4-14 Time history of the roof displacement and storey drift at first and top levels of the 16-storey braced frames and profiles of storey drifts and tie axial forces under Ground motion # 776.

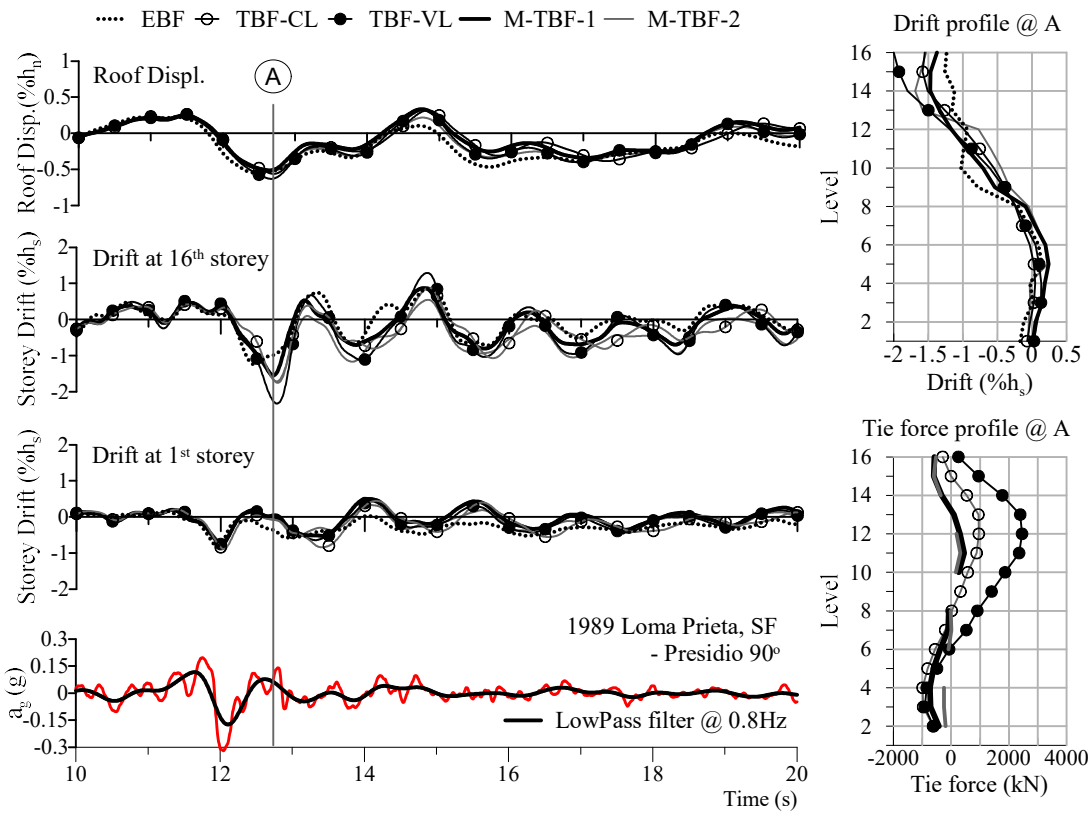

Figure 4-15 Time history of the roof displacement and storey drift at first and top levels of the 16-storey braced frames and profiles of storey drifts and tie axial forces under Ground motion no. 767.

Amplitudes of member forces resulted for the 16-storey braced frames are illustrated in Figure 4-11 and 4-12. These exhibit similar trends among the studied structural systems. Hence, minimum force demands are obtained with the EBF system while member forces in the TBFs and M-TBFs generally increase as more constraint is imposed on the frame response by increasing the number of storeys linked by ties (e.g. TBFs *vs.* M-TBFs, M-TBF-1 *vs.* M-TBF-2). To a lesser extent, uniformizing the link resistances over the frame height (TBF-CL *vs.* TBF-VL) the force demand is slightly reduced. As it was observed for the 16-storey frames, the variability in storey shears reduces considerably when changing from the TBF-CL system to the less constraining M-TBF-2 design. As illustrated in Figure 4-12, reductions in storey shears between these two extreme cases are more pronounced in the upper half of buildings height. Meanwhile, for the M-TBF-2 system, reductions in tie member forces are more significant when compared to the TBF system. The axial

loads in the columns do not vary much among all 16-storey framing systems, including the EBF, and the TBF design proposed by Rossi (2009) tends to overestimate the force demands on the ties while providing better storey shear predictions.

When examining the response of the M-TBF solutions, the M-TBF-1 with two 8-storey modules performed nearly as well as the original TBF in terms of storey drifts. As illustrated in Figure 4-12, this modular configuration permitted to reduce significantly the tie forces from a maximum of 4400 kN at the 7th storey of TBF-CL to 1550 kN at the 5th storey of M-TBF-1. Storey shears are also reduced, especially from levels 9 to 15. Introducing greater discontinuity in the elastic trusses with 4-module, the M-TBF-2 design resulted in even lower axial loads in the tie members with a maximum of 1000 kN at the 3rd storey. This less constrained structural system experienced no greater storey drifts, as shown in Table 4-4. However, the results presented in Figure 4-11 and 4-12 indicate that increasing the number of modules or reducing the number of storeys per module, could eventually lead to severe drift concentrations in a single module. For this frame example, relatively larger drifts were developed in the base module of M-TBF-2 suggesting that this configuration is probably the lower limit beyond which the response would become close to that of the conventional EBF system. Thus, for multi-storey buildings, the M-TBFs solution is the optimum that likely exists to reduce member forces without compromising uniformity in the deformation response. As proposed by Tremblay et al. (2014), the design might be further refined by replacing some of the ties, that are removed from the TBF configuration to create the M-TBF, with energy dissipating elements that would partially restrain relative rotations between the elastic truss segments without inducing much additional forces in the truss members.

In general, the seismic response of 16-storey buildings is in agreement with that observed for the 8-storey buildings. All studied systems demonstrated acceptable seismic performance through nonlinear time history analysis. In comparison, the EBF system is the least preferable due to the possible occurrence of concentrated inelastic deformation which causes link failure. The chance of damage concentration in EBFs increases in taller buildings. The TBFs are capable of redistributing the inelastic demand within the system. Similar to the 8-storey building, the 16-storey TBFs experienced no damage concentration. The storey drifts are evenly distributed along the building height. The M-TBFs demonstrated compatible performance comparing to TBFs in terms of storey

drift distribution and DCF values. In addition, from the results of M-TBF-1 and M-TBF-2, it was reflected that the length of modules has a noticeable impact on the seismic performance of the structure. The M-TBF-1 with 8-storey modules experiences less peak storey drift as well as less DCF compared to the M-TBF-2 with 4-storey modules.

Similar observations are made for the 8-storey and 24-storey frames. Peak values of the storey shears, storey drifts, column axial loads, and tie axial loads are given in Figure 4-16 for the 8-storey EBF, TBF, and M-TBF systems. For 24-storey buildings, the results are plotted in Figure 4-17.

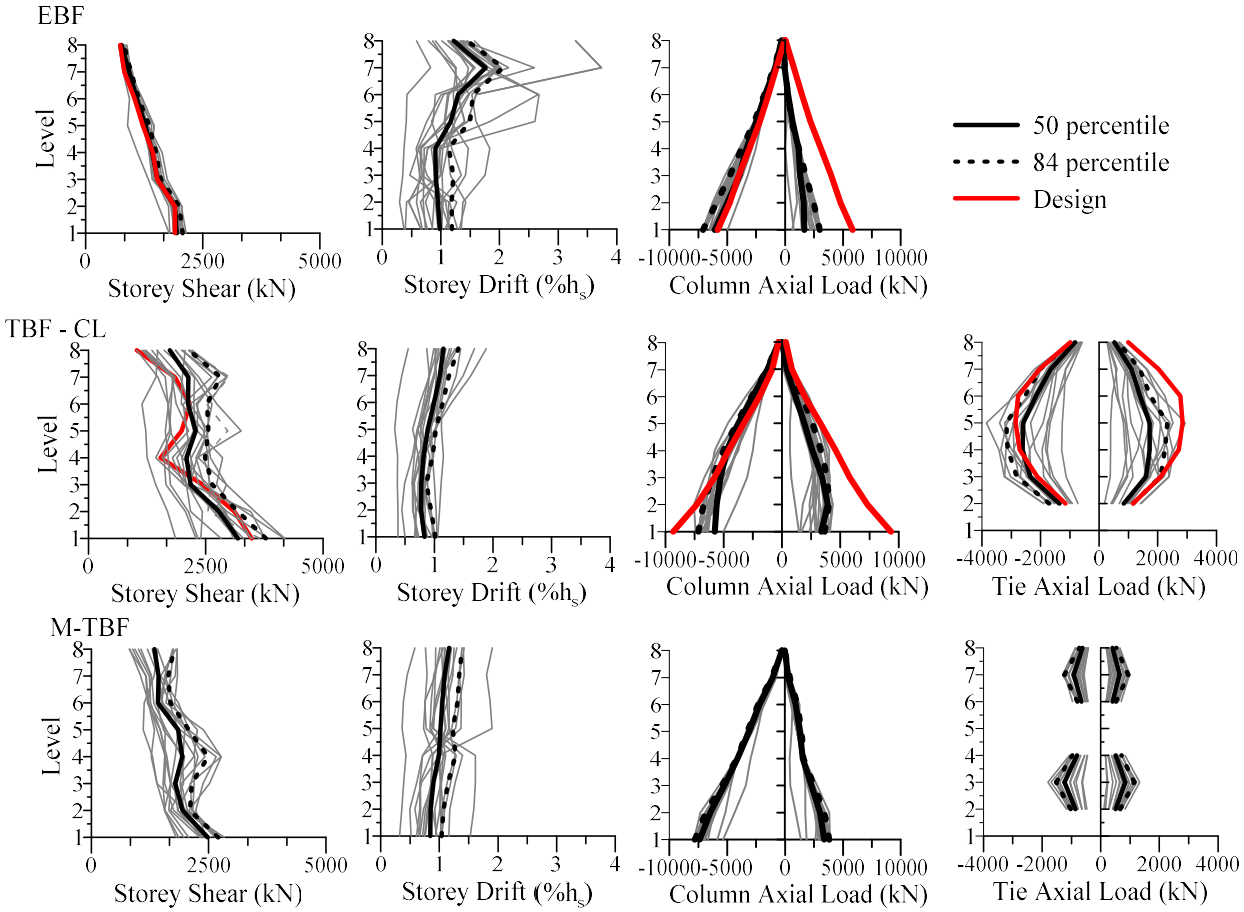

Figure 4-16 Storey shears, storey drifts, and axial loads in columns and tie members of the 8-storey braced frames.

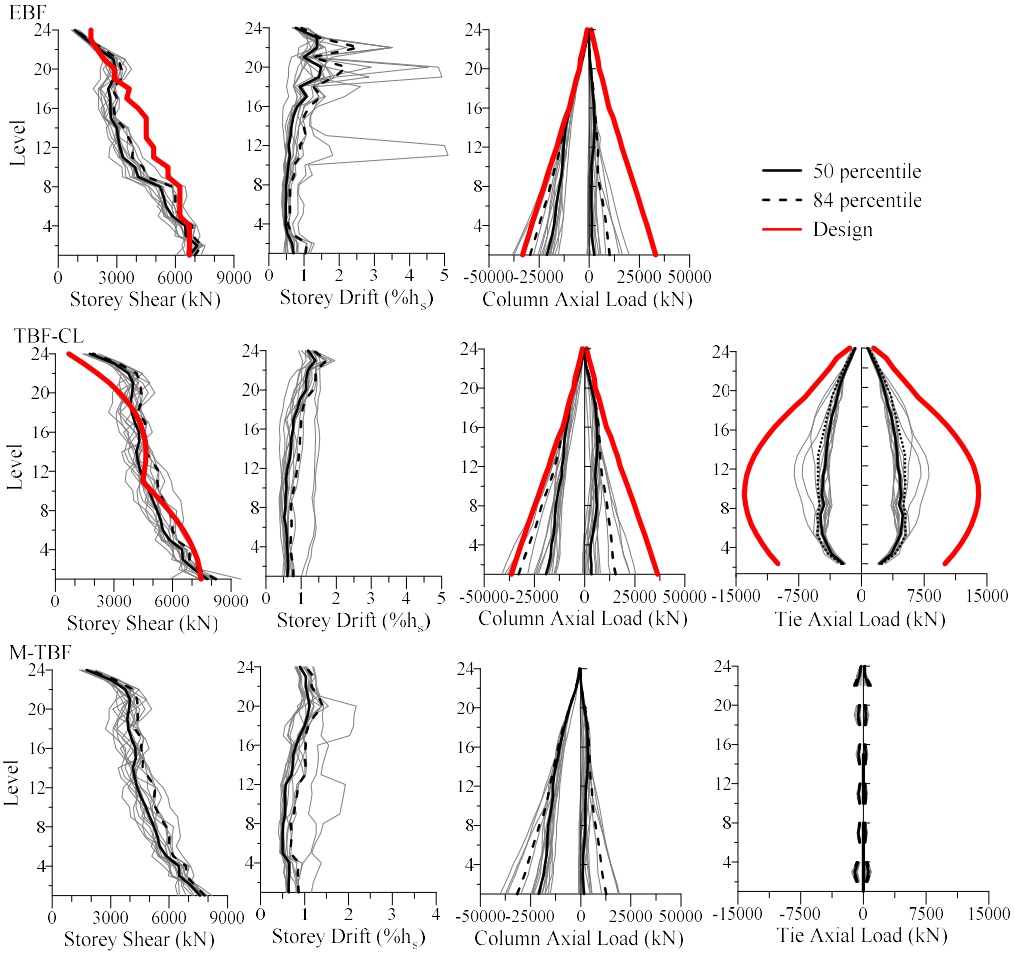

Figure 4-17 Storey shears, storey drifts, axial loads in columns and tie members of the 24-storey braced frames.

4.3.5 Residual drift responses for the 8-storey and 16-storey frames

Residual drifts are becoming an important parameter in seismic design, and it was of interest to examine the impact of using M-TBF on permanent deformations. Erochko et al. (2011) demonstrated the relationship between residual storey drifts (Δ_r) and maximum storey drifts (Δ_{max}) for both moment frames (MFs) and buckling restrained braced frames (BRBFs) assuming recoverable elastic drifts of 0.8% and 0.25% *h* for both systems, respectively. A similar approach is used here for the 8-storey and 16-storey EBF, TBF and M-TBF systems. Values of peak residual storey drifts and peak inelastic storey drifts as obtained for each ground motion record in the nonlinear dynamic analysis are plotted in Figure 4-18a for the two conventional EBFs. As shown,

these values can be bounded by the 1:1 line as was found by Erochko et al. for moment frames and buckling restrained braced frames. For these structures, the recoverable elastic storey drifts ranged from 0.3% to 0.7% h_s. These values are comparable with those found for MFs and BRBFs.

Pairs of residual *vs.* inelastic storey drifts for the TBFs and M-TBFs are presented in Figure 4-18b to d. As shown, for both the TBFs and M-TBF-1 systems, values can be enveloped by a 0.5:1.0 straight line indicating the reduced residual drift response for these frames. This enhanced behaviour is attributed to the elastic vertical trusses which contribute to returning a structure with yielding links to its original position after each oscillation cycle. Although less pronounced, a similar benefit was also observed when adopting an M-TBF-2 configuration. For all three systems with elastic trusses used in the 8-storey to 24-storey buildings examined in this article, the 84th percentile values of the residual drifts in Table 4 range between 0.3 and 0.43% h_s at the end of the earthquakes, which represents an excellent performance for such tall ductile systems. In counterpart, values for the EBFs vary between 0.5 and 0.9% h_s for the EBFs.

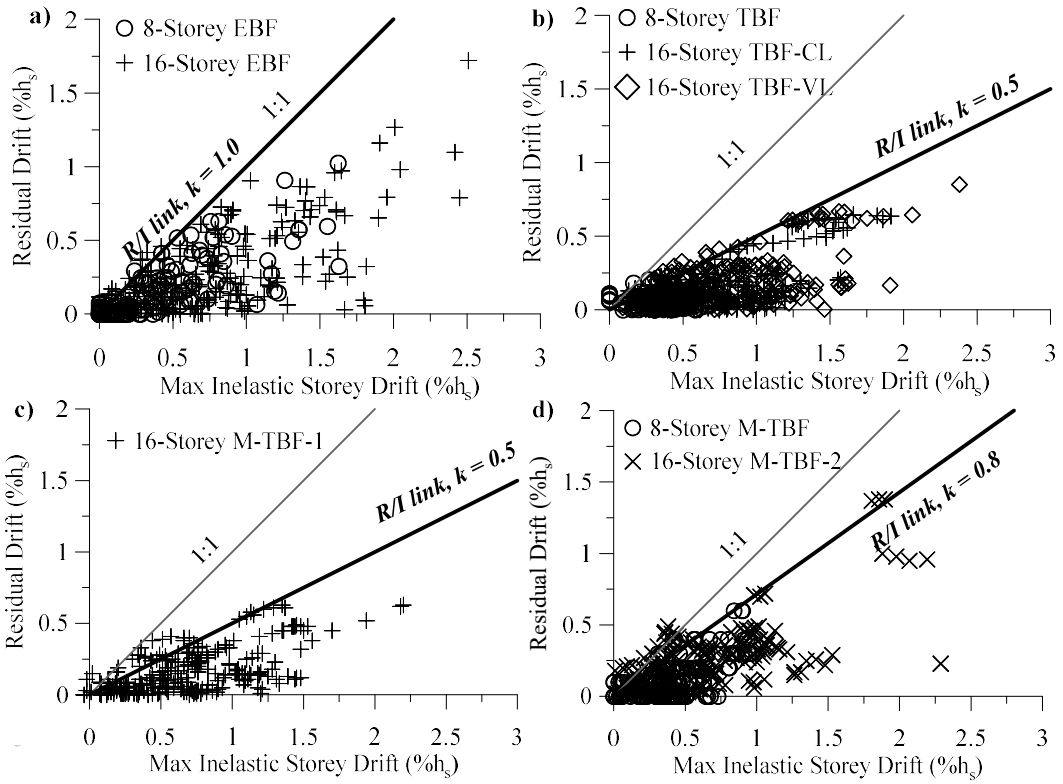

Figure 4-18 Residual *vs* peak inelastic storey drifts (90th percentile) for 8-storey and 16-storey: a) EBF; b) TBF; c) M-TBF-1; and d) M-TBF-2

4.3.6 Collapse assessment using incremental dynamic analysis (IDA)

To further assess the seismic performance of the three type of systems, incremental dynamic analyses are performed. Due to the similar characteristics demonstrated by structures with various heights, the 16-storey frames are selected to show the potential of each system. The results of IDAs are illustrated in Figure 4-19. The mean spectrum of the ground motion set is scaled with respect to the spectral acceleration at the fundamental period of the structure, $S_a(T_1)$. All the records in the set are scaled accordingly. The maximum storey drift values for the respective $S_a(T_1)$ are plotted in the figure. A sudden increase in terms of maximum storey drift indicates collapse of the system.

For the EBF, collapse occurs soon after the ground motion reaches design level if not before. But the 50th percentile value shows that the majority of the records causes collapse of the structure only when their intensities are above design level. For the TBF, most records show a smooth curve until collapse, which suggests a preferable global collapse mechanism. For the M-TBFs, the set of records shows two types of response. When the ground motion records can create a weak module

in the system, the collapse of the system occurs very soon. For other ground motions, the system is able to withstand stronger shake before collapse happens.

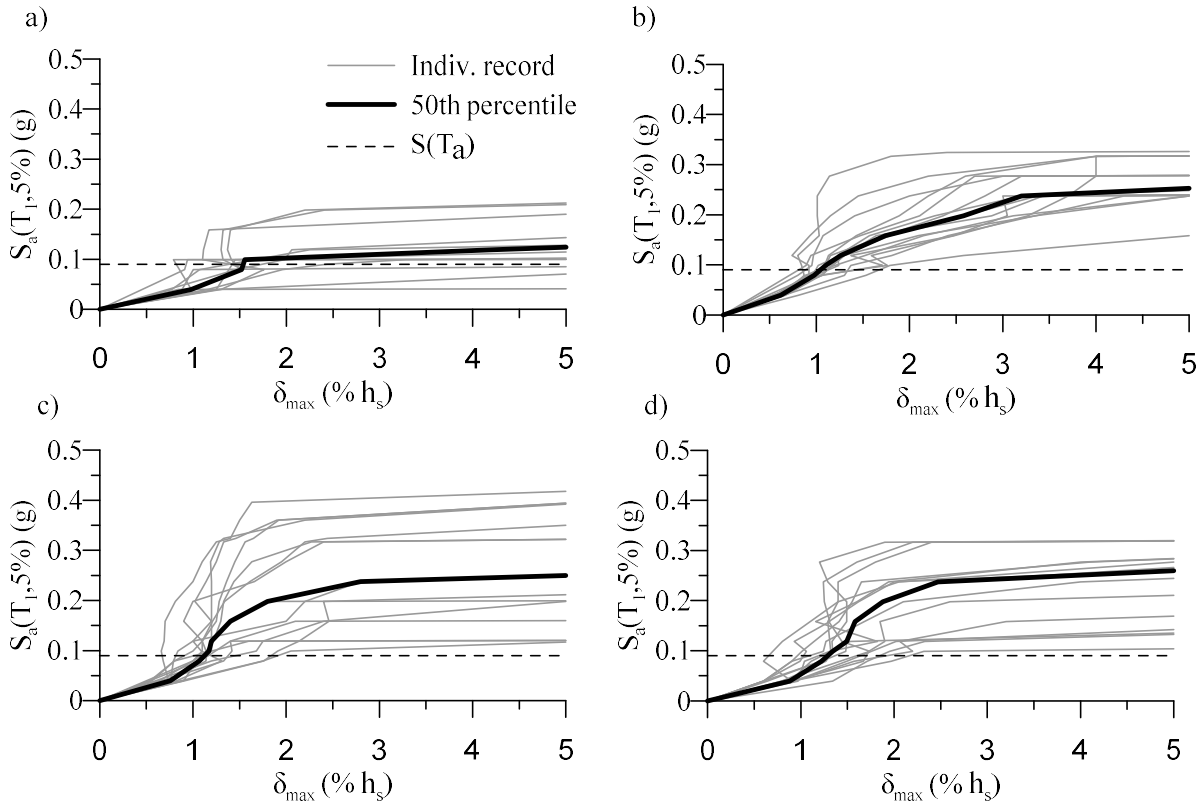

Figure 4-19 IDA curves of 16-storey frames subjected to the selected record set: a) EBF, b) TBF-CL, c) MTBF-1, d) MTBF-2

For a quantitative comparison, the following parameters of the systems are listed in Table 4-6: the median collapse capacity,$S_a(\bar{T}_1)$, the collapse margin ratio, CMR, and the adjusted collapse margin ratio ACMR. $S_a(\bar{T}_1)$ is defined as the spectral acceleration when 50% of the ground motions causes collapse of the system. The CMR is calculated as the ratio between the $S_a(\bar{T}_1)$ and $S_a(T_1)$, where the $S_a(T_1)$ is the 2%/50 years spectral acceleration at the fundamental period of the structure. In case of 16-storey frames, the $S_a(T_1)$ equals to 0.09 g. The ACMR is computed as the product of the CMR and a spectral shape factor SSF. The calculation of SSF is suggested by FEMA P695.

Table 4-6 Evaluation of collapse safety of the 16-storey buildings according to FEMA P695

Parameters	EBF	TBF-CL	M-TBF-1	M-TBF-2
$S_a(\bar{T}_1)$ (g)	0.1188	0.216	0.234	0.208
CMR	1.32	2.40	2.60	2.31
ACMR	1.85	3.86	3.93	3.72
$ACMR_{10\%}$	1.90	1.90	1.90	1.90

As shown in Table 4-6, comparing to the EBF, both the TBF and the M-TBF are able to reduce the possibility of collapse significantly. Although EBF is not acceptable in term of ACMR, but the difference is not significant. Meanwhile, the ACMR values for TBF and M-TBFs greatly exceeded the acceptable value, which indicates the design force of TBF and M-TBFs can be reduced accordingly to avoid unnecessary cost. In terms both CMRs and ACMRs, the M-TBF-2 system exhibits comparable seismic response as the TBF and M-TBF-1. Incorporating with the low cost, the M-TBF-2 system is demonstrated to be a cost-efficient and robust system.

4.4 Conclusions

Nonlinear time history seismic analysis was performed on 8-storey to 24-storey prototype buildings to evaluate and compare the seismic response of three steel eccentrically braced frame systems such as the conventional EBFs, the EBFs with elastic vertical trusses labelled TBFs and the modular system, M-TBF. The latter two were designed with vertical elastic trusses to mitigate storey drift concentrations along the building height. The structures were assumed to be in Victoria, BC, and were designed using Canadian code seismic provisions. The method proposed by Rossi (2007) was used to design the elastic truss members of the TBFs. In the M-TBFs, the vertical trusses were segmented into multi-storey modules to reduce the force demand on the elastic truss members. The M-TBF vertical trusses were designed using nonlinear time history analysis results. The following conclusions can be drawn from this study:

- All three types of braced frames studied exhibited satisfactory, stable seismic response, with no structural collapse detected in any of the analyses.

- As observed in past studies, EBFs exhibited concentrations of inelastic response along their heights, which led to marked variations in peak storey drifts with occurrences of excessive plastic rotation demands in links. The TBF system experienced reduced and more uniform peak storey drifts, which came at the expense of higher member forces and larger steel tonnage. In particular, the continuous vertical ties that are needed to form the vertical trusses have to be designed to resist high axial forces induced by higher mode frame response. The design procedure of the TBF system was found to be effective, although conservative for the vertical tie members for the 16-storey and 24-storey buildings.

- The proposed M-TBF system exhibited uniform drift response within each module, but variations in drift responses were observed between modules. Peaks storey drift values were comparable to those obtained with the TBF system. Dividing the elastic vertical trusses of the TBF system into modules significantly diminished the axial forces in the vertical ties. Storey shear forces and column axial loads also reduced when using the M-TBF configuration, which resulted in steel tonnage values comparable to those required for the conventional EBFs. The results indicated that the modules must contain a minimum number of storeys to prevent storey drift concentrations in one of the modules.

- Both the TBF and M-TBF systems were found to have higher re-centring capabilities compared to conventional EBFs. For the structures studied, the 84^{th} percentile values of the residual storey drifts were less than 0.43% h_s.

- The results of IDAs show that although collapse probability of EBFs is slight higher than the acceptable value (10%), the difference is insignificant. Both TBFs and M-TBFs greatly reduces the collapse probability of the systems. M-TBF-2 is proven to be the most economical and reliable system. The results also suggest that the design load for the TBFs and M-TBFs can be reduced to further improve the efficiency of the system.

Additional work is needed to further study the behaviour of modular tied EBFs and develop an effective design methodology for the system. In addition to predicting axial forces in the elastic trussed members, the design approach should provide guidance for determining M-TBF configurations that properly prevent from the soft-storey response with the least steel tonnage.

Acknowledgements

Financial support for this project was provided by the Natural Sciences and Engineering Research Council of Canada and the Fonds de recherche Nature et technologies (FRQNT) of the Government of Québec.

References

Aguero, A., Izvernari, C., and Tremblay, R. (2006). "Modelling of the Seismic Response of Concentrically Braced Steel Frames using the OpenSees Analysis Environment." *Int. J. of Advanced Steel Construction*, 2, 3, 242-274.

AISC. (2010a). *Specification for structural steel buildings, AISC/ANSI 360-10*, American Institute of Steel Construction (AISC), Chicago, IL.

AISC. (2010b). *Seismic provisions for structural steel buildings, AISC/ANSI 341-10*, American Institute of Steel Construction (AISC), Chicago, IL.

ASCE. (2013). *Seismic Evaluation and Retrofit of Existing Buildings, ASCE/SEI 41-13*, American Society of Civil Engineers (ASCE), Reston, VA.

ASCE. (2010). *Minimum Design Loads for Buildings and Other Structures, ASCE/SEI 7-10*, American Society of Civil Engineers (ASCE), Reston, VA.

Bosco, M., and Rossi, P.P. (2009). "Seismic performance of eccentrically steel braced frames," *Engineering Structures*, 31, 664-679.

CSA. (2009). *CSA S16-09, Design of Steel Structures*. Canadian Standards Association (CSA), Toronto, ON.

CSI. (2009). *SAP2000 - Integrated Software for Structural Analysis and Design*. Computer & Structures, Inc., Berkeley, CA.

Chao, S.-H., and Goel, S. (2005). *Performance-based seismic design of eccentrically braced frames using target drift and yield mechanism as performance criteria*. Report UMCEE-05-05, University of Michigan, Ann Arbor, MI.

Chen, L., Tremblay, R., and Tirca, L. (2012). "Seismic Performance of Modular Braced Frames for Multi-Storey Building Application." *Proc. 15th World Conf. on Earthquake Eng*., Lisbon, Portugal, Paper No. 5458.

Erochko, J., Christopoulos, C., Tremblay, R., Choi, H. (2011). "Residual Drift Response of SMRFs and BRB Frames in Steel Buildings Designed according to ASCE 7-05". *Journal of Structural Engineering*, 137(5), 589-599.

Ghersi, A., Neri, F., Rossi, P.P., and Perretti, A. (2000). "Seismic response of tied and trussed eccentrically braced frames." *Proc. Stessa 2000 Conf.,* Montreal, Canada, 495-502.

Ghersi, A., Pantano, S., and Rossi, P.P. (2003). "On the design of tied braced frames." *Proc. Stessa 2003 Conf.,* Naples, Italy, 413-429.

Ghersi, A., Marino, E.M., and Rossi, P.P., (2006). "Innovative design criteria, based on ductility control for earthquake resistant steel structures." in *Innovative Steel Structures for Seismic Protection of Buildings*, Monza, Italy: Polimetrica International Scientific Publisher, 155-207.

Koboevic, S., Rozon, J., and Tremblay, R. (2012). Seismic performance of low-to-moderate height eccentrically braced steel frames designed for North-American seismic conditions. *J. Struct. Eng.,* 138(12), 1465-1476.

Koboevic, S., David, S.O. (2010). Design and seismic behaviour of taller eccentrically braced frames. *Canadian Journal of Civil Engineering*, 37(2), 195-208.

Mansour, N., Christopoulos, C., and Tremblay, R. 2011. Experimental validation of replaceable shear links for eccentrically braced frame. J. Struct. Eng., ASCE, 137, 10, 1141-1152.

Lai, J.-W., and Mahin, S.A. (2015). "Strongback System: A Way to Reduce Damage Concentration in Steel-Braced Frames," *J. Struct. Eng.*, *ASCE*, 141(9). DOI: 10.1061/(ASCE)ST.1943-541X.0001198.

Mar, D. (2010). "Design examples using mode shaping spines for frames and wall buildings." *Proc. 9th U.S. National Conf. and 10th Canadian Conf. on Earthquake Engineering.* Toronto, ON, Paper No. 1400.

Martini, K., Amin, N., Lee, P.L., and Bonowitz, D. (1990). "The Potential Role of Nonlinear Analysis in the Seismic Design of Building Structures." *Proc. 4th National Conf. on Earthquake Eng.*, Palm Springs, CA, 2, 67-76.

McKenna, F. and Fenves, G.L. 2004. *Open System for Earthquake Engineering Simulation (OpenSees)*. Pacific Earthquake Engineering Research Center (PEER), University of California, Berkeley, CA. (http://opensees.berkeley.edu/index.html)

Merzouq, S., and Tremblay, R. (2006). "Seismic Design of Dual Concentrically Braced Steel Frames for Stable Seismic Performance for Multi-Storey Buildings." *Proc. 8th U.S. National Conference on Earthquake Eng.*, San Francisco, CA, Paper 1909.

NRCC. (2010). National Building Code of Canada, 13th ed., National Research Council of Canada, Ottawa, ON.

Okazaki, T., and Engelhardt, M.D. (2006), "Cyclic Loading Behaviour of EBF links constructed of ASTM A992 Steel." *Journal of Construction Steel Research*, 63, 751-765.

Pollino, M. and Bruneau, M. (2007), "Seismic Retrofit of Bridge Steel Truss Piers Using a Controlled Rocking Approach." *J. of Bridge Eng.*, 12, 5, 600-610.

Popov, E.P., Ricles, J.M., and Kasai, K. (1992). "Methodology for optimum EBF link design." *Proc. 10th World Conf. on Earthquake Engineering*, 7, 3983-3988.

Popov, E.P., Takanashi, K., and Roeder, C.W. (1976). *Structural steel bracing systems: Behavior under cyclic loading*. Report No. EERC 76-17, Earthquake Engineering Research Center, Univ. of California at Berkeley, Berkeley, CA.

Qu, B., Sanchez-Zamora, F., and Pollino, M. (2014). "Mitigation of inter-story drift concentration in multi-story steel concentrically braced frames through implementation of rocking cores," *Engineering Structures*, 70, 208-217.

Richards, P. W. and Uang, C. M. (2006). "Testing protocol for short links in eccentrically braced frames". *Journal of Structural Engineering*, ASCE, 132(8), 1183-91.

Ricles, J.M., and Bolin, S.M. (1990). "Energy dissipation in eccentrically braced frames." *Proc. 4th National Conf. on Earthquake Eng.*, Palm Springs, CA, 2, 309-318.

Ricles, J. M., and Popov, E. P. (1987). *Dynamic analysis of seismically resistant eccentrically braced frames.* Report No. ERCC 87-07, Earthquake Engineering Research Center, Univ. of California at Berkeley, Berkeley, CA.

Rossi, P.P. (2007). "A design procedure for tied braced frames." *Earthquake Engineering and Structural Dynamics*, 36, 2227–2248.

Simpson, B.G., and Mahin, S.A. (2018). "Experimental and Numerical Investigation of Strongback Braced Frame System to Mitigate Weak Story Behavior," *J. Struct. Eng.*, 144(2). DOI: 10.1061/(ASCE) ST.1943-541X.0001960.

Tremblay, R. (2003). "Achieving stable inelastic seismic response for multi-story concentrically braced steel frames", *Eng. J.,* 40(2), 111-129.

Tremblay, R., Robert, N., and Filiatrault, A. 1997. "Tension-Only Bracing: A Viable Earthquake-Resistant System for Low-Rise Steel buildings?" *Proc. SDSS '97 Fifth Int. Colloquium on Stability and Ductility of Steel Structures*, Nagoya, Japan, 2, 1163-1170.

Tremblay, R., and Tirca L. (2003). "Behaviour and design of multi-storey zipper concentrically braced steel frames for the mitigation of soft-storey response." *Proc. STESSA 2003 Conf.*, Naples, Italy, 471-477.

Tremblay, R., and Poncet, L. (2007). "Improving the Seismic Stability of Concentrically Braced Steel Frames." *Eng. J.*, 44(2), 103-116.

Tremblay, R., Chen, L., and Tirca, L. (2014). "Enhancing the seismic performance of multi-storey buildings with a modular tied braced frame system with added energy dissipating devices." *International Journal of High-Rise Buildings*, 3(1), 21-33.

Whittaker, A., Uang, C.-M., and Popov, E. P. (1987). *Earthquake Simulation Tests and Associated Studies of a 0.3-Scale Model of a Six-Story Eccentrically Braced Steel Structure*. Report No. UCB/EERC-87/02, Earthquake Engineering Research Center, University of California, Berkeley, CA.

Whittaker, A., Uang, C.M., and Bertero, V.V. (1990). *An Experimental Study of the Behaviour of Dual Steel Systems*. Report no. UCB/EERC-88/14, Earthquake Engineering Research Center, University of California, Berkeley, CA.

CHAPTER 5 ARTICLE 2: PRACTICAL SEISMIC DESIGN PROCEDURE FOR STEEL BRACED FRAMES WITH SEGMENTAL ELASTIC SPINES

Liang Chen[1], Robert Tremblay[1] and Lucia Tirca[2]

[1]Polytechnique de Montreal, Quebec, Canada

[2]Concordia University, Quebec, Canada

The article was submitted to the *Journal of Constructional Steel Research* on August 7, 2018.

Abstract

A practical seismic design method is proposed for tall steel braced frames with segmental elastic trussed spines (SESBFs) used to achieve uniform storey drift response. The method combines the forces arising from yielding of ductile elements along the braced frame height to the forces resulting from higher modes involving flexural dynamic response of the elastic truss segments. The first set of forces is obtained from static analysis whereas response spectrum analysis is used for the second one. The method is applied and validated for 8-storey and 16-storey SESBFs created from conventional EBFs. SESBF configurations including one, two and four elastic truss segments were examined. The structures were located in Vancouver, BC, and their behaviour was examined through NLRHA. The method generally provided excellent predictions of the peak force demand imposed on the truss members. Elastic flexural response of the truss segments is not bounded by yielding of the frame ductile elements and was found to be sensitive to ground motion signatures and damping assumptions. For taller frames with long truss segments, complete yielding of the individual segment as assumed in design was not observed in the analyses, and the proposed method resulted in conservative member force predictions.

Key words: Braced frames, Elastic truss spine, Drift concentration, Higher modes.

5.1 Introduction

Steel braced frames such as concentrically braced frames (CBFs), eccentrically braced frames (EBFs), and buckling restrained braced frames (BRBFs) represent effective structural systems to

resist lateral loads due to winds and earthquakes for low- and medium-rise buildings. However, as illustrated in Figure 5-1a for an EBF, these systems are prone to drift concentrations along their height and have the tendency to develop soft-storey response in taller applications (Khatib et al. 1988, Tremblay 2000, 2003, Sabelli 2001, Chen and Mahin 2012, Lai and Mahin 2015, Speicher and Harris 2016, Pollino et al. 2017, Zaruma Ochoa 2017).

Among the several strategies that have been proposed to address this problem, modifying the braced frame configuration to include an elastic vertical truss forming a stiff spine, back-bone or strong back is a promising approach to achieve enhanced seismic performance with uniform storey drift demand for tall braced frames (Martini 1990, Whittaker et al. 1990, Tremblay et al. 1997, Ghersi et al. 2000 2003, Tremblay 2003, Tremblay and Merzouq 2004, Merzouq and Tremblay 2006, Rossi 2007, Tremblay and Poncet 2007, Takeuchi et al. 2015, Pollino et al. 2017). Two configurations are shown in Figure 5-1: a dual BRBF system in which an elastic truss is formed by adding vertical ties connecting the upper ends of the braces of adjacent floors (Figure 5-1b) and a tied EBF (TBF) system in which two so-formed elastic trusses are connected by the ductile link beams (Figure 5-1c). In the inelastic range, the elastic spines enforce a first mode response to mobilize inelastic response in the BRBs or links over several consecutive storeys, leading to more uniform drift response, greater energy dissipation capacity and superior redundancy for the seismic force resisting system. The concept has been implemented in actual constructions in Japan (Aoki et al. 1998, Taga et al. 2004, Takeuchi et al. 2015) and California (Mar 2010, Panian et al. 2015, 2017). Laghi et al. (2017) examined the application of the concept to steel moment frames. Physical testing has been recently completed on a full-scale two-storey frame by Simpson and Mahin (2018).

Early studies on the system revealed that the elastic vertical truss is subjected to forces from yielding braces or links reaching their yield strength as the frame deforms in its first mode plus forces induced by shear and bending of the elastic truss responding elastically in its higher vibration modes. A design methodology for elastic trussed spines has not been proposed yet to account for the complex dynamic response of the system and ensure that the spine can achieve the intended behaviour. From nonlinear response history analyses (NLRHA) conducted on dual BRB frames shown in Figure 5-1b, Tremblay and Merzouq (2005) proposed BRB axial load patterns that could be considered to determine peak forces in ties, braces, columns and beams forming the elastic truss. NLRHA showed that the approach could predict well design forces for 8- to 24-storey frames. For

the TBF system of Figure 5-1c, Rossi (2007) proposed to design the truss members for forces induced by all links reaching their yield strength simultaneously over the frame height plus the forces obtained from the structure elastic second mode response. A reduction factor was applied to the second mode contribution to reflect the energy dissipated by links responding in that mode. NLRHA showed that storey shears were generally well predicted by the method except that forces in the tie members were overestimated for 16- and 24-storey structures (Chen et al. 2018). For the retrofit of existing 2- and 6-storey seismically deficient braced frames, Pollino et al. (2017) proposed using an elastic vertical truss to form a stiff rocking core connected to the existing frames by ductile link beams at each level. Forces in the truss members were determined from storey shears contributed by the existing braces and the yielding links reaching their capacities assuming uniform drift (first mode) profile plus shears from the SRSS (square root of the sum of the squares) combination of the second and higher elastic modes. The design method was validated through NLRHA and hybrid simulation was used to verify the seismic response of the system (Slovenec et al. 2017).

The response of steel braced frames with elastic truss spines is similar to that of cantilevered reinforced concrete shear walls that can develop large shear forces and bending moments from higher mode response while forming a plastic hinge at their bases as a result of first mode response (Blakeley et al, 1975). A solution proposed to predict these shears and moments is to combine the demand from first mode response, as reduced to account for yielding, to the demand from the elastic second and higher modes (e.g., Eibl and Keitzel 1988, Eberhard and Sozen 1993, Priestley and Amaris et al. 2002, Sullivan et al. 2008). Design approaches that combine elastic higher mode effects with inelastic first mode demand have also been used for other lateral load resisting systems or response parameters for buildings (e.g., Rodriguez et al. 2002, Chopra and Goel 2004). The approach has also been implemented to seismically isolated bridges (Buckle et al. 2011, AASHTO 2014, CSA 2014).

Past studies on braced frames with elastic truss spines showed that significant forces can develop in the spine members. Chen et al. (2012, 2018a) proposed a modular version of the tied EBF system in which the vertical elastic trusses are cut into multi-storey modules or segments along the building height. This M-TBF system is shown in Figure 5-1d. Interrupting the flexural continuity of the spine significantly reduced the force demand on the truss members while maintaining the capacity

of the system to prevent drift concentration and soft-storey response. M-TBFs from 8- to 24-storey frames could achieve similar peak storey drift responses with substantially reduced steel tonnage compared to their TBF counterpart. For this M-TBF system, Tremblay et al. (2014) showed that linking the truss segments with properly sized energy dissipating elements could partially restore the continuity of the elastic truss and increase energy dissipation capacity to improve the frame response while still controlling the force demands on the elastic truss components. Balazadeh-Minouei et al. (2017) showed that an M-TBF system could represent a cost-effective seismic retrofit solution for a 10-storey building with non-ductile chevron braced frames.

In this article, a practical approach is proposed for the seismic design of steel braced frames with segmental elastic spine trusses. Forces associated to first mode response are obtained from simple plastic analysis of the structure assuming that all ductile elements have yielded and attained their strain hardened capacities. Effects from higher mode response are determined from multi-mode response spectrum analysis using a truncated response spectrum to eliminate first mode contribution and a structure model in which reduced stiffness is assigned to the yielding elements. In the article, the design method is presented and validated for TBFs and M-TBFs with short links yielding in shear as shown in Figure 5-1c&d, but the method equally applies any other SESBFs, i.e., braced frames with segmental elastic spines. In the first part of the article, the method is described and illustrated for an 8-storey frame with one and two-segment elastic truss. The method is then verified against NLRHA results for 8- and 16-storey frames. The structures studied are located in Vancouver, British Columbia, a region where the seismic hazard is contributed by shallow crustal earthquakes, subduction inslab earthquakes and subduction interface earthquakes, allowing the design approach to be validated for three different ground motion types.

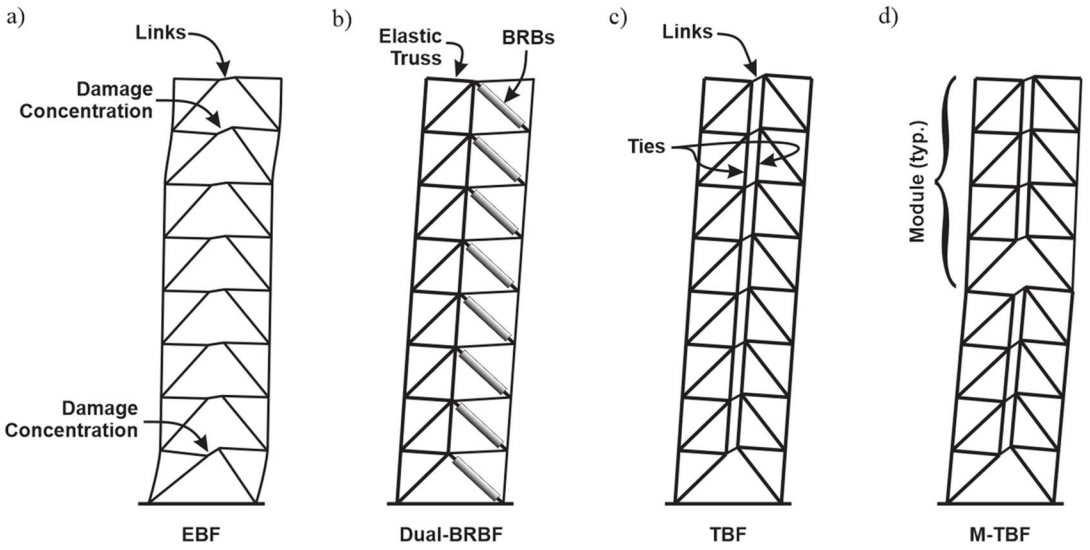

Figure 5-1 Deflected shape of braced frames: a) conventional EBF, b) Dual-BRBF by Tremblay (2003), c) Tied EBF (TBF) by Martini et al. (1990) and Ghersi et al. (2000), d) Modular tied EBF (M-TBF) by Liang et al. (2012).

5.2 Analysis and Design Methods

5.2.1 Modal superposition method

The main distinctive feature of SESBFs versus conventional braced frames is the capacity of the vertical elastic truss to trigger simultaneous yielding in all links or braces over the height of the truss segments. This beneficial property has been confirmed through numerous nonlinear static and dynamic analyses performed in past studies. As a result, the deformed profile and vibration modes of SESBFs responding in the inelastic range can be easily predicted as they are firmly constrained by the stiff elastic spine. This is not the case for conventional braced frames which can exhibit complex, highly variable and unpredictable drift profiles when responding in the inelastic range to seismic excitations. However, the ability of SESBFs to achieve uniform and predictable drift response comes at the expense of bending moments and shear forces that must be resisted by the elastic truss in addition to the forces imposed by the ductile yielding elements.

The expected yielding patterns for 8-storey EBF and SESBF-1 systems subjected to strong ground motion are illustrated in Figure 5-2 (SESBF-1 is a SESBF built with a single segment elastic truss). For the EBF, lateral loads inducing maximum storey shears and overturning moments at any floor along the frame height are limited by the plastic shear resistances V_{PL} of all links located the level under consideration. Maximum forces in the EBF columns, braces, and beams outside the links are therefore bounded by the links shear strength and can be easily determined from static analysis, as is done in capacity design. Conversely, lateral inertia forces generated in the SEBSF in Figure 5-2b are not bounded by the yield strength of the links because of the additional moment M_{Truss} that can develop in the elastic vertical trusses. Hence, lateral inertia forces can be larger than those expected in EBFs, which can lead to larger storey shears (V_{truss}) that must be resisted by beams and braces. Additional axial forces are also induced in the columns and vertical tie members by moments M_{Truss}. The same response is observed in braced frames with segmented vertical trusses except that the truss flexural continuity is interrupted between segments and its effects on inertia forces only develop within each truss segment. Inertia forces are therefore smaller and member forces reduce accordingly. The main challenge encountered in the design of SESBFs is to predict the additional inertia forces and the resulting member forces in the vertical elastic truss members.

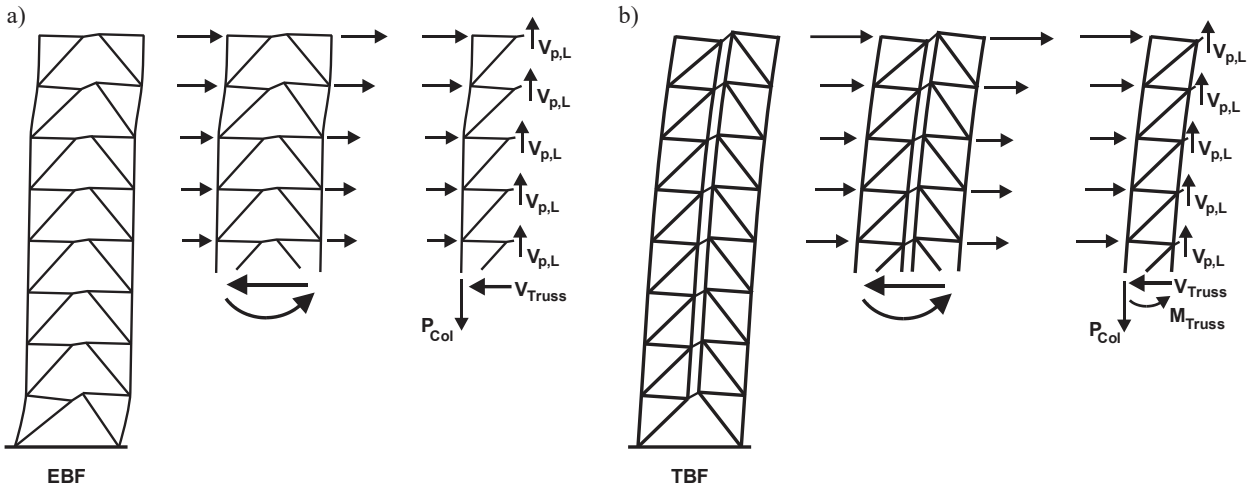

Figure 5-2 Yielding mechanisms and lateral load patterns illustrated for the 8-storey EBF and 8-storey SESBF-1 configuration.

In conventional EBFs, storey shears and overturning moments along the frame height reach their maximum when the structure responds in its first mode and yielding develops in all ductile links. This loading condition is generally adopted in capacity design to obtain upper bound estimates of the forces that can be attained in columns, braces and beams upon yielding of the links. Well-proportioned SESBFs are intended to enforce this first mode response and it is therefore expected that simultaneous yielding of all links will occur over long periods of time and for several times under severe earthquake ground motions. For SESBFs with segmented elastic trusses, that same response will develop over the height of the individual segments, forcing inelastic response in all links of the segments. As the braced frame laterally deforms during these yielding excursions, lateral dynamic response is also expected to develop along the length of the truss segments due to the horizontal floor masses present along the truss segments and the flexibility of the truss segments. This dynamic response is essentially governed by the flexural and shear stiffness of the vertical elastic trusses, as the stiffness of the yielding ductile links is reduced to their post-yield stiffness. This assumption forms the basis of the analysis method proposed in this article to predict design forces in spine members. The method consists in a modal superposition method in which the contribution of individual modes to any response quantities r_n, such as spine member forces, are summed up to obtain the total response or force demand, r, (Chopra 2001):

$$r(t) = \sum_{n=1}^{N} r_n(t) \qquad (1)$$

Modal superposition gives an accurate solution if the modal properties of the structure are known and a sufficient number of modes is considered. Eq. (1) applies to both elastic and inelastic systems, as long as the modal properties of the system can be computed. For SESBFs, inelastic modal properties can be obtained by assigning a reduced stiffness to yielding links that simulates their kinematic strain hardening responses. In Figure 5-3, elastic and inelastic mode shapes and periods are compared for the 8-storey SESBF-1 system that will be presented later. The analyses were performed using the SAP2000 computer program (CSI 2017) and the figure shows the numerical model used with the leaning column that was included to account for P-delta effects. In the figure, periods of the inelastic modes were obtained using a reduced link stiffness equal to αk_L where α =

0.01 and k_L is the elastic (initial) link stiffness. As shown, the elastic and inelastic mode shapes are nearly identical. The periods are influenced by links stiffness but this effect is more pronounced for the first mode dominated by link deformations and gradually reduces for the higher modes when elastic truss deformations contribute more to the mode shapes.

In Figure 5-3, the inelastic mode 1 presents no interest for design purpose because it corresponds to the deformation pattern associated with uniform yielding of all links and member forces induced by this mode can be obtained from simple static analysis. In the proposed analysis method, only the second and higher inelastic modes need to be considered in the multimode response analysis as it is the response in these modes that produce the additional inertia loads and member forces that are sought. Inelastic modal properties of the frame assuming a reduced stiffness for the links calculated with $\alpha = 0.001$, 0.01, and 0.05 are presented in Table 5-1. Modal properties of the elastic system are also given for comparison purposes. As shown, for the higher modes, the differences between the elastic and inelastic modes and their associated periods are small. This means that the influence of the reduced links stiffness is limited and the analysis will not be sensitive to the reduced stiffness values that are assigned to the links to establish inelastic modal properties.

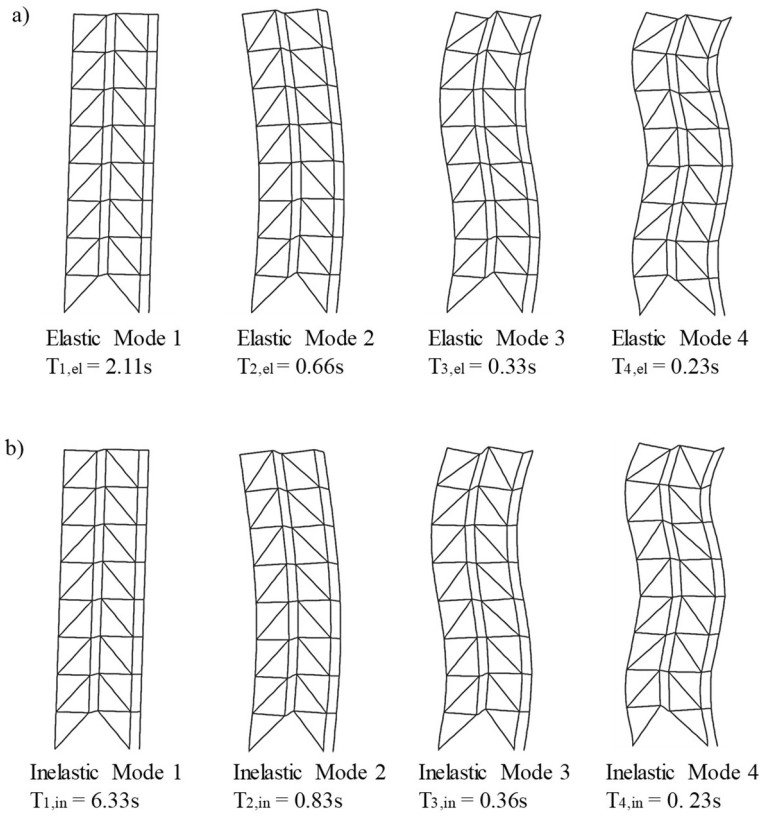

Figure 5-3 Vibration modes of the 8-storey SESBF-1 configuration: a) Elastic modes; b) Inelastic modes with reduced link stiffness ($\alpha = 0.01$).

Table 5-1 Elastic and inelastic modal properties for the 8-storey SESBF-1 configuration

α	T_1 (s)	M_1 (%)	T_2 (s)	M_2 (%)	T_3 (s)	M_3 (%)	T_4 (s)	M_4 (%)
1.0 (elastic)	2.11	0.72	0.66	0.19	0.33	0.047	0.23	0.021
0.05	3.53	0.78	0.79	0.15	0.35	0.038	0.23	0.017
0.01	6.33	0.79	0.83	0.14	0.36	0.035	0.23	0.017
0.001	12.4	0.79	0.83	0.14	0.36	0.035	0.23	0.017

The analysis method therefore consists in combining the force demand from yielding links in the first inelastic mode with the additional forces resulting from the dynamic response in the second and higher inelastic modes. The two sets of forces are labelled r_{I} and r_{II}, respectively. For design purposes, only a conservative estimate of the maximum expected value of $r(\mathrm{t})$ is needed and the simple absolute sum combination can be used to obtain the design values:

$$|r(t)|_{max} = |r_I(t)|_{max} + |r_{II}(t)|_{max} \tag{2}$$

This combination rule is also justified by the marked difference that exists between the structure first mode period and the periods of the higher inelastic modes of Set II. This difference is generally sufficient to permit the attainment of the peak forces from Set II while the frame is experiencing large yielding excursions in its fundamental mode and Set I forces are also maximum.

As discussed, Set I forces r_{I} can be obtained from static analysis considering that all links have reached their probable (or expected) strain hardened resistance and this set will be referred to as $r_{\mathrm{I,stat}}$. Forces $r_{\mathrm{I,stat}}$ can be obtained from hand calculations or by means of a nonlinear static (pushover) analysis, as done in capacity design. In both cases, a lateral load pattern must be adopted which can vary from a simple inverted triangular distribution to a more refined distribution obtained from storey shears determined with elastic response spectrum analysis. This aspect is further discussed in the example presented below. In these calculations, link resistances are computed using probable or expected material yield strength and considering strain hardening effects.

Forces for Set II (r_{II}) are obtained from modal response spectrum analysis performed with the numerical model with reduced stiffness for the shear links. To eliminate the first mode response from the analysis, the design spectrum is truncated for periods longer than the inelastic second mode period, $T_{2,\mathrm{in}}$, i.e., the spectrum used in the analysis is set to zero for periods $T > T_{2,\,\mathrm{in}}$. Forces for Set II can be obtained using an SRSS combination rule as modes from elastic truss response are generally well separated. This response spectrum analysis considering only the contribution of the inelastic modes obtained with the inelastic (reduced) link stiffness is referred to IRSA. Gravity load effects r_{g} must also be included to obtain design forces for the elastic truss members, r_{design} and Eq. 2 becomes:

$$r_{design} = r_g + r_{I,Stat} + r_{II,IRSA} \quad (3)$$

Gravity load induced forces r_g are obtained from a static analysis performed on the structure model with reduced link stiffness so that redistribution of gravity loads upon yielding of the ductile links is taken into account and gravity induced forces are obtained for the same conditions as Set I and II forces.

For the design of SESBFs with two or more segments, the design method must be modified to account for the fact that link yielding may not develop in all segments at the same time, which results in various yielding patterns that must be considered in design. For an SESBF system with *n* segments, the total number of yielding pattern cases, *m,* is equal to 2^n. In theory, all these possible yielding pattern cases should be examined to identify the one generating the maximum force in any of the vertical truss members. In practice, however, the number of yielding patterns for design can be reduced by examining only the yielding sequences that are more likely to occur in the frame. Link yielding in multi-segment SESBFs generally starts in a given segment and then propagates upwards or downwards until links of all segments reach yielding. For a frame with *n* segments, considering the cases where any *k* adjacent segments yield ($1 \leq k \leq (n-1)$), the total number of yielding pattern cases can be reduced from 2^n to the n^{th} partial sum, i.e., $m = n\,(n+1)/2$ cases. This is illustrated in Figure 5-4 for a 12-storey SESBF-3 system. For this frame, the total number of cases reduces from $m = 2^n = 8$ to $m = 3(3+1)/2 = 6$. IRSA is then performed for each of the 6 cases by assigning a reduced stiffness to the yielding links for the pattern and the Set II force for the design of a given member is the maximum value out of the 6 values obtained from the 6 analyses. For SESBFs with two or more segments, Eq. 3 is then rewritten to obtain the maximum forces arising from cases $i = 1$ to m:

$$r_{design} = r_g + r_{I,Stat} + \max_m \left[r^i_{II,IRSA}\right] \quad (4)$$

In Figure 5-4, it is noted that Set I forces $r_{\text{I,stat}}$ would in fact be different for each of the yielding pattern cases. For consistency, that forces $r^i_{I,Stat}$ should therefore be computed for each case *i* and added to Set II forces $r^i_{II,IRSA}$ of the same case *i*. This approach was not retained because the forces in the elastic, non-yielding links for cases $i = 2$ are unknown and it would not be possible to calculate forces $r^i_{I,Stat}$ for these cases. Eq. 4 as proposed is therefore expected to result in

conservative force estimates as Set I forces $r^1_{I,Stat}$ represent maximum values that may not be reached in the other cases.

For multi-segments SESBFs, it must also be noted that the number of inelastic modes that need not be considered in IRSA increases from 1 (one segment) to n (n = number of segments). This is illustrated in Figure 5-5 presenting the elastic and inelastic modes for an 8-storey SESBF-2 system for which the number of yielding pattern cases m = 3. As shown, both inelastic modes 1 and 2 involve deformations concentrating in the yielding links with reduced stiffness. Only modes 3 and higher are of interest for IRSA as those modes involve flexural deformations of the elastic trusses. For this frame, Set II forces would therefore be obtained from IRSA performed with a design spectrum truncated for periods longer than $T_{3,\text{in}}$ to exclude the contributions from inelastic modes 1 and 2. The figure also shows that shapes and periods in modes 3 and higher do not vary much between the three different yielding pattern cases m = 1 to 3, which means that similar Set II forces are expected from the three cases.

.

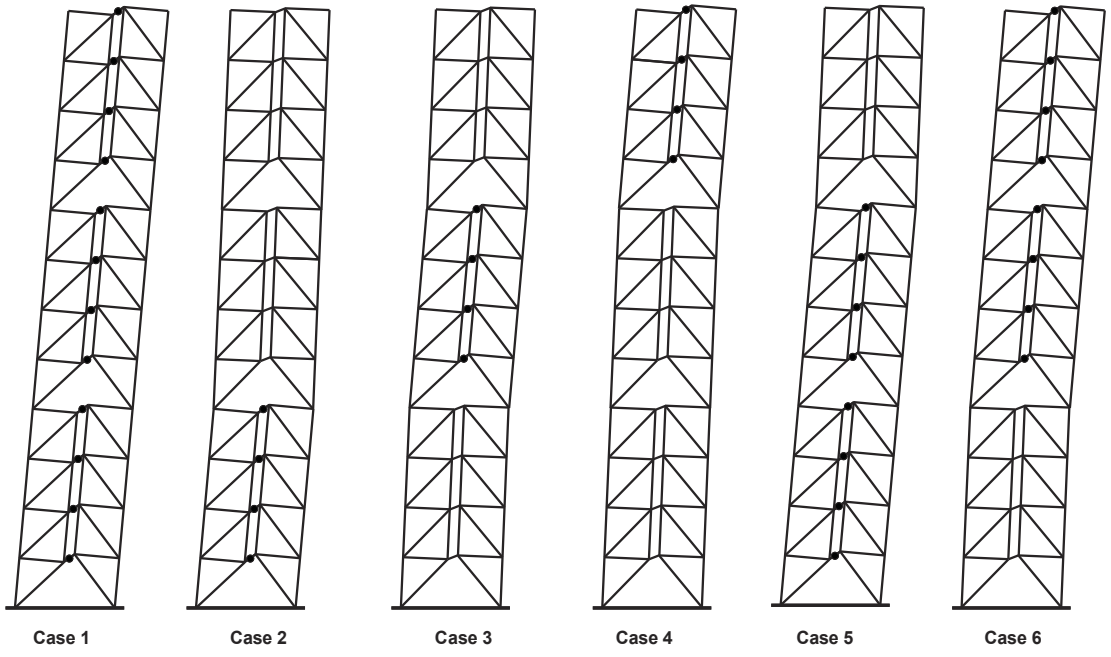

Figure 5-4 Likely yielding pattern cases for a 12-storey SESBF-3 configuration.

a)

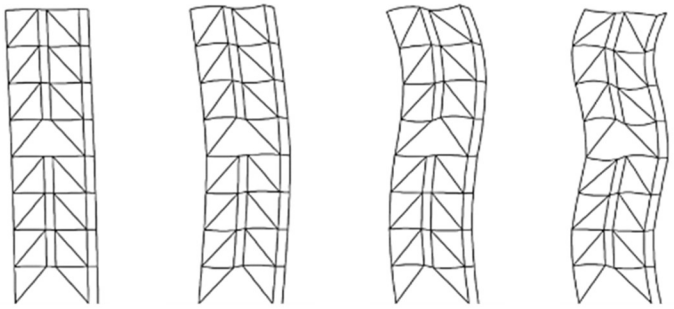

Elastic Mode 1 $T_{1,el} = 2.07s$ | Elastic Mode 2 $T_{2,el} = 0.74s$ | Elastic Mode 3 $T_{3,el} = 0.38s$ | Elastic Mode 4 $T_{4,el} = 0.27s$

b)

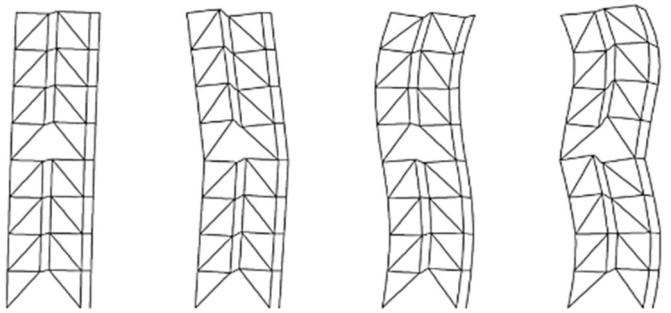

Inelastic Mode 1 $T_{1,in} = 6.20s$ | Inelastic Mode 2 $T_{2,in} = 2.32s$ | Inelastic Mode 3 $T_{3,in} = 0.42s$ | Inelastic Mode 4 $T_{4,in} = 0.31s$

c)

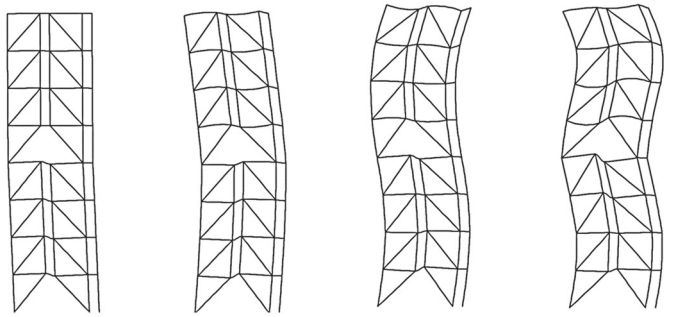

Inelastic Mode 1 $T_{1,in} = 5.07s$ | Inelastic Mode 2 $T_{2,in} = 0.97s$ | Inelastic Mode 3 $T_{3,in} = 0.40s$ | Inelastic Mode 4 $T_{4,in} = 0.29s$

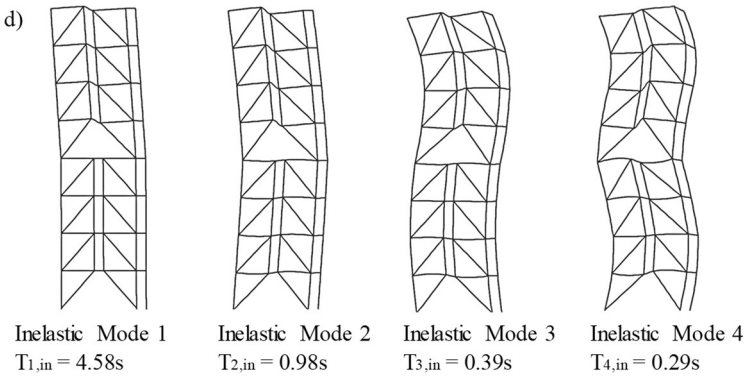

Figure 5-5 Mode shapes and periods of 8-storey SESBF-2 configuration: a) Elastic modes; b) Inelastic modes, Case1: links yielding in both segments; c) Inelastic modes, Case 2: links yielding in bottom segment; and d) Inelastic modes, Case 3: links yielding in second segment only ($\alpha = 0.01$).

5.2.2 Proposed design procedure

In actual applications, it is anticipated that SESBFs will need to be designed in accordance with the applicable building code and steel design standard prescribing minimum earthquake design force levels as well as ductile detailing and capacity design requirements. This can be satisfied by selecting ductile links to achieve the required minimum lateral resistance at every level. As done for conventional steel braced frames, force demands in the links of SSBFs can be obtained using an equivalent static force procedure (ESFP) or response spectrum analysis together with design parameters specified in codes. If response spectrum analysis is used, as is often required by codes for tall braced frames as discussed here, link design becomes iterative as the dynamic properties of the frame will likely change when member sizes are progressively adjusted in previous iterations. To initiate the analysis/design process, member sizes are needed that can be obtained from preliminary design done with the ESFP or from previous similar projects.

As discussed, all links of the truss segments in SESBFs are likely to yield at the same time during an earthquake and it is therefore recommended that all links of each segment be same and designed for the average link force obtained from analysis. This approach also simplifies detailing and fabrication processes. Once the links are designed, Set I member forces can be computed and combined with the forces from gravity loads. Members of the elastic spines can then be designed

for these forces. At this stage, member sizes can be adjusted as necessary to resist wind and other loads or meet lateral wind and seismic drift limits. Once minimum sizes are determined for all elastic truss members are known, Set II member forces can be computed using the updated structure model with reduced link stiffness and the truncated design spectrum. The design of the elastic spine members is then reviewed and modified as needed to resist the total force demand from gravity loads plus Sets I and II. RSA of the elastic frame can then be redone to verify and adjust as required the size of the ductile links selected in the previous iteration.

For segmental SESBFs, the number of spine truss segments and/or number of storeys per segment are additional parameters that must be determined in design. As observed from previous studies, forces in truss members generally diminish when increasing the number of segments but this is generally at the expense of larger and less uniform storey drifts (Chen et al. 2018a). This behaviour can only be assessed through nonlinear response history analysis and a procedure is proposed by Chen et al., (2018b) to conduct such nonlinear analyses in a timely manner using simplified structure models such that an appropriate elastic truss segment arrangement can be determined.

5.3 Case Study

5.3.1 Buildings studied

The buildings studied are 8-storey and 16-storey office buildings of the normal importance category located on a site class C in Vancouver, British Columbia. The floor plan, design gravity loads, and elevations of the seismic force resisting systems are shown in Figure 5-6. The lateral load resisting system of the buildings consists of four identical braced frames acting along each orthogonal direction. The response of the structure in the E-W direction was examined. Frame design was performed for both wind and seismic loads but the latter governed for the braced frames in the E-W direction. In the seismic analysis, P-Δ effects and notional loads were considered but accidental torsion was neglected for simplicity. As shown in Figure 5-6b and 6c, SESBF-1 and SESBF-2 configurations were considered for the 8-storey building while SESBF-2 and SESBF-4 were examined for the 16-storey building. The 8-storey frames are used to illustrate the application of the proposed design method. The response of 16-storey braced frames with then be examined to validate the accuracy of the design method.

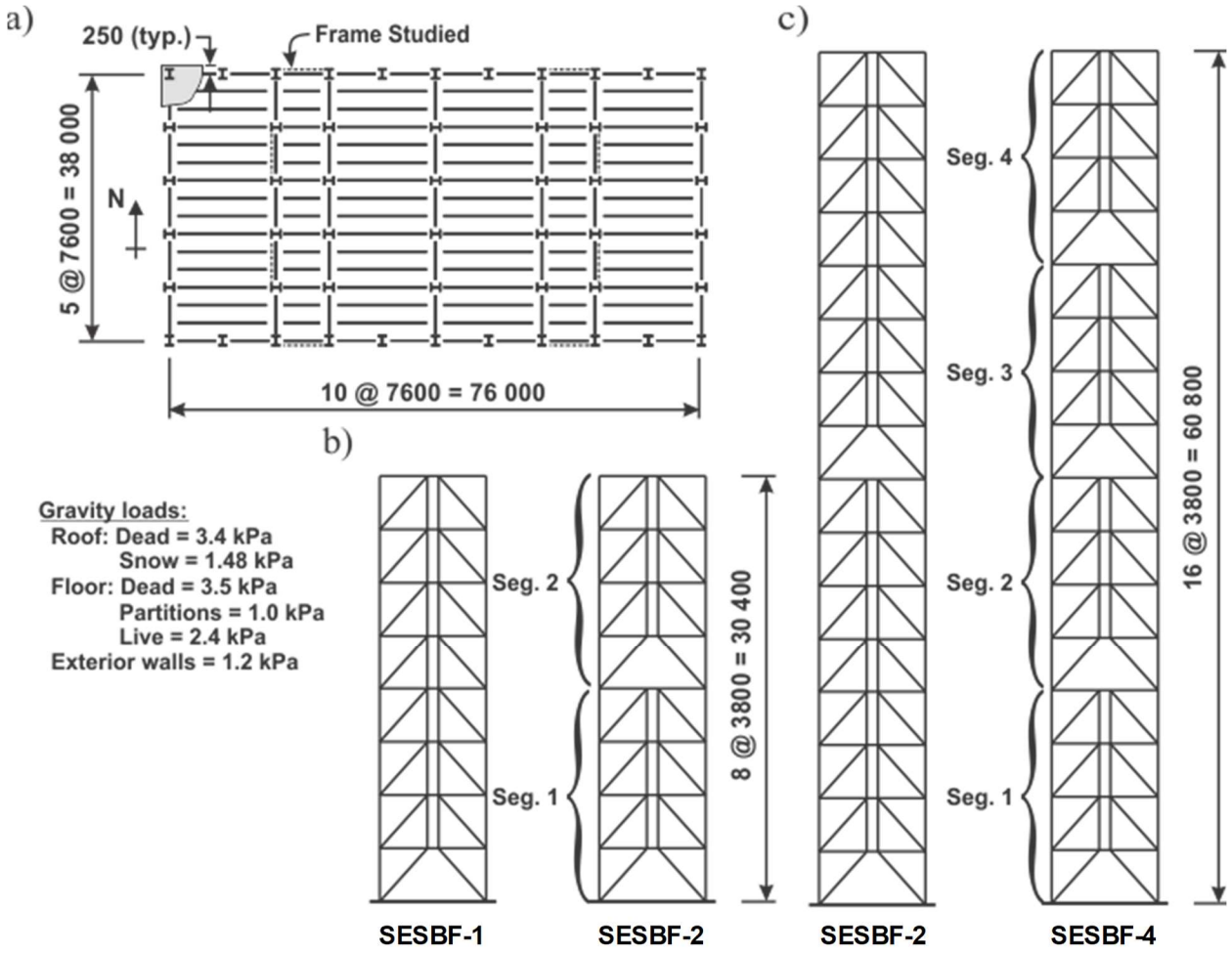

Figure 5-6 Building studied: a) Plan view; b) Elevation of 8-storey configurations SESBF-1 and SESBF-2; and c) Elevation of 16-storey configurations SESBF-2 and SESBF-4.

5.3.2 SESBF Design

5.3.2.1 Design of ductile links

The structures were designed in accordance with the provisions of the National Building Code of Canada (NBCC) (NRCC, 2015) and the CSA S16-14 steel design standard (CSA, 2014). In the NBCC, the design base shear V is obtained from $V = S(T_a)M_vI_EW/R_dR_o$, where $S(T)$ is the design spectrum obtained from uniform hazard spectral (UHS) ordinates computed for a 2% in 50 years probability of exceedance at specific periods, M_V is a factor that accounts for the contribution of higher modes on base shear, I_E is the importance factor, W is the building seismic weight and R_d

and R_o, are respectively the ductility- and overstrength-related force modification factors. The design spectrum ordinates for the site are given in Table 5-2. For the structures studied, the M_V and I_E factors were equal to 1.0, and values of 4.0 and 1.5 were assigned to the factors R_d and R_o, respectively, as specified in the NBCC for ductile EBFs. In the NBCC, the structure period to be used for the calculation of S can be obtained from modal analysis, without exceeding $T_a = 0.05h_n$ for braced frames, where h_n is the total building height expressed in meters. Values of h_n, T_a, $S(T_a)$, W, V are presented in Table 5-3 for the two buildings. For braced steel frames, the base shear V cannot be less than the value computed with T_a = 2.0 s. This minimum base shear requirement applied for the 16-storey building.

Table 5-2 Design spectrum ordinates for site class C in Vancouver, BC

Period (s)	0.0	0.2	0.5	1.0	2.0	5.0	10.0
S_a (g)	0.84	0.84	0.75	0.42	0.26	0.08	0.03

Table 5-3 Parameters used to calculate the design base shear

Number of storeys	h_n (m)	T_a (s)	S (g)	W (kN)	V/Building (kN)	V/Braced Frame (kN)
8	30.4	1.52	0.337	115092	6292	1573
16	60.8	3.04	0.256 [1]	226164	9612	2403

[2] Minimum value at T_a = 2.0 s governs the design.

When RSA is used for design, NBCC requires that the analysis results be adjusted such that the base shear from analysis is at least equal to 80% of the design base shear V. This rule applied for the studied structures and the frames were designed for 0.8 times the seismic forces given in Table 5-3. Scaled shear forces in the ductile links from RSA were added to those induced by notional

lateral loads equal to 0.5% of the gravity loads and the resulting link shears were amplified for P-delta effects as specified in CSA S16-14 to obtain the shears used to select the links. The ductile links, as well as beams and columns, were made from ASTM A992 W shapes. As recommended, the same shape was used for all links of each truss segment. Braces and vertical ties were made from ASTM A500, grade C, square tubing. For all members, F_y was equal to 345 MPa. Column sections were kept constant for two consecutive floors and their splices were designed for shear and axial forces. Beams outside the links were considered as pin-connected to the columns. The braces and vertical ties were also considered as members with pinned end connections.

The design of the SESBFs each required a few iterations. Periods of the elastic and inelastic modes obtained for the last design iteration are given in Table 5-4 for the 8-storey SESBFs with 1 and 2 truss spine segments. Inelastic modes for the two frames are respectively presented in Figure 5-3 and 5. Inelastic modal properties were obtained using $\alpha = 0.01$ for all m link yielding patterns. Elastic and inelastic modal properties for the 16-storey SESBF-2 and SESBF-4 are presented in

Table 5-5. The three yielding link patterns identified for the 16-storey SESBF-2 are same as those for the 8-storey SESBF-2 shown in Figure 5-5, with the exception that each vertical truss segment has 8 storeys in height. For the 16-storey SESBF-4 configuration, the number of yielding pattern cases is $m = 4(4+1)/2 = 10$. The link yielding pattern cases from $m = 1$ to 10 for the 16-storey SESBF-4 are not shown here due to space constraints. They were all developed using the sequences shown for the 12-storey SESBF-3 in Figure 5-4.

Table 5-4 Periods (s) of the elastic and inelastic vibration modes of the 8-storey SESBFs

n	*Case No.*	T_1		T_2		T_3		T_4	
		El.	Inel.	El.	Inel.	El.	Inel.	El.	Inel.
1	1	2.07	**6.33**	0.66	0.83	0.33	0.36	0.23	0.23
2	1	2.07	**6.20**	0.74	**2.32**	0.38	0.41	0.27	0.31
	2	-	**5.07**	-	**0.97**	-	0.40	-	0.29
	3	-	**4.58**	-	**0.98**	-	0.39	-	0.29

Notes: Values of inelastic modes were obtained with $\alpha = 0.01$.

Values in bold are periods of modes considered in IRSA for Set II forces.

Table 5-5 Periods (s) of the elastic and inelastic vibration modes of the 16-storey SESBFs

n	m	T_1		T_2		T_3		T_4		T_5		T_6	
		El.	Inel.	El.	Inel.	El.	Inel.	El.	Inel.	El.	Inel.	El.	Inel.
	1	4.32	**10.9**	1.33	**3.90**	0.68	0.90	0.46	0.64	0.34	0.38	0.27	0.32
2	2		**9.4**		**2.02**		0.89		0.54		0.37		0.30
	3		**7.6**		**1.76**		0.77		0.51		0.36		0.28
	1	4.67	**11.2**	1.54	**4.04**	0.83	**2.31**	0.56	**1.62**	0.39	0.46	0.39	0.39
	2		**7.8**		**2.39**		**0.96**		**0.61**		0.41		0.39
	3		**7.7**		**1.85**		**0.95**		**0.68**		0.41		0.39
	4		**7.2**		**1.76**		**1.08**		**0.66**		0.41		0.39
4	5		**5.6**		**2.37**		**1.03**		**0.60**		0.40		0.38
	6		**9.8**		**2.59**		**1.62**		**0.70**		0.43		0.39
	7		**9.3**		**2.66**		**1.08**		**0.88**		0.43		0.39
	8		**7.7**		**2.49**		**1.61**		**0.66**		0.42		0.39
	9		**11.0**		**3.58**		**1.80**		**1.05**		0.45		0.38
	10		**9.6**		**3.27**		**1.91**		**0.90**		0.44		0.37

[1]Values of inelastic modes were obtained with $\alpha = 0.01$.

[2]Values in bold are periods of modes considered in IRSA for Set II forces.

5.3.2.2 Design of elastic trusses

Analysis under gravity loads was performed as recommended in the previous sections, i.e., with reduced stiffness assigned to all links. Calculation of the Set I forces $r_{I,stat}$ was performed manually assuming two lateral load patterns: inverted triangular load pattern and lateral load distribution

from response spectrum analysis of the elastic frames. Calculations are illustrated in Figure 5-7 for the 8-storey SESBF-1 SESBF-2 systems for the inverted triangular load pattern. For both frames, the calculation is based on the force equilibrium for one-half of the frame width including one vertical truss and the ductile links. Forces in every links are set equal to the probable link strength including strain hardening effect, V_{PL}. In CSA S16-14, V_{PL} of short links yielding in shear is equal to 1.3 times the link shear resistance calculated with probable yield stress $R_y F_y$ = 385 MPa. For the single segment frame, the amplitude of the lateral load F_{max} at the roof level is obtained from moment equilibrium with respect to the pinned base of the truss segment (point "o" in the figure). Forces in the truss members are then calculated from the roof level. The same approach is used for the two-segment frame, starting with the second segment. The force $F_{2,max}$ is obtained from moment equilibrium of the upper segment and member forces are then determined in that segment. The lateral force V_2 from the second segment is then applied at the top level of the first segment and the force $F_{1,max}$ is adjusted to achieve moment equilibrium for the bottom segment. If that force is negative, $F_{1,max}$ is set equal to zero and the V_2 is reduced to reach moment equilibrium.

The same procedure is applied if a lateral force pattern from elastic response analysis of the frame is adopted. In Figure 5-8, Set I member forces computed with both lateral load distributions are compared. Although the two loading patterns in Figure 5-8a are quite different, the resulting brace forces associated to V_{Truss} and tie forces associated to M_{Truss} are nearly same. As shown for the 16-storey SESBF-2 system in Figure 5-9, the differences become more important for taller structures, especially for the forces in the vertical ties. For this frame, using the load distribution from RSA in lieu of the triangular inverted pattern resulted in lower tie forces in the second segment and lower tie forces in the bottom one. For consistency, it is recommended that the vertical distribution of the lateral loads for this analysis be compatible with the one used for the design of the links. Alternatively, a lateral load distribution can be back-calculated from the shear strength of the selected links. These approaches should result in lateral load patterns representative of the conditions prevailing when yielding is reached in all links of the structure. For the frames examined in this study, link design forces were obtained from response spectrum analysis and lateral loads for the determination of the r_I forces were distributed based on the storey shears obtained from RSA.

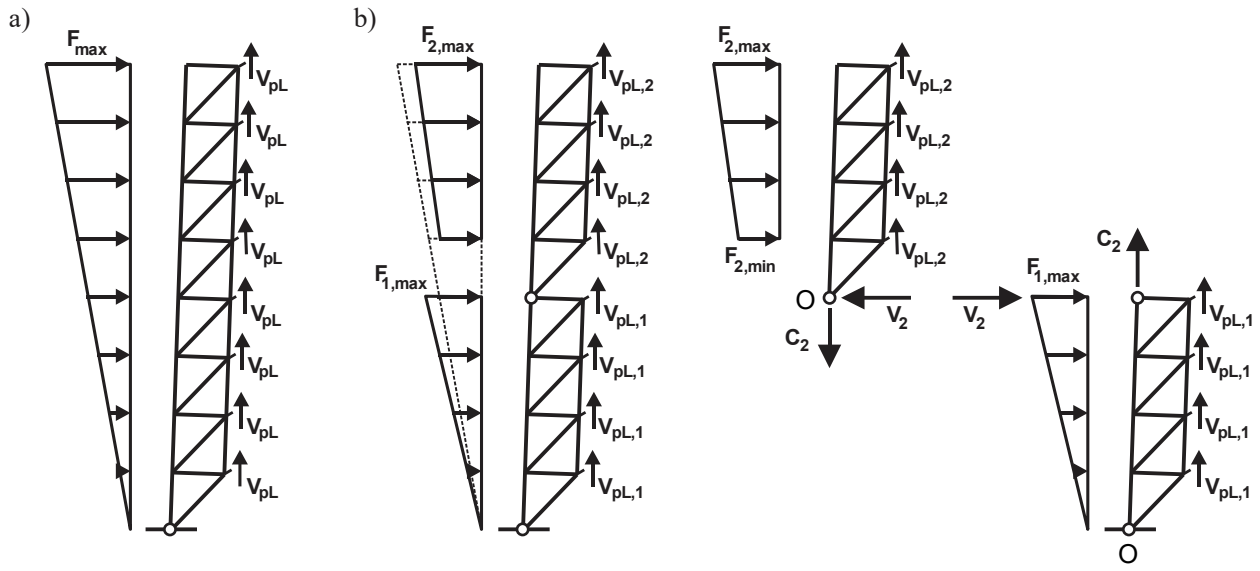

Figure 5-7 Calculation of the Set I member forces for the 8-storey frames assuming an inverted triangular lateral load pattern: a) SESBF-1 configuration; b) SESBF-2 configuration.

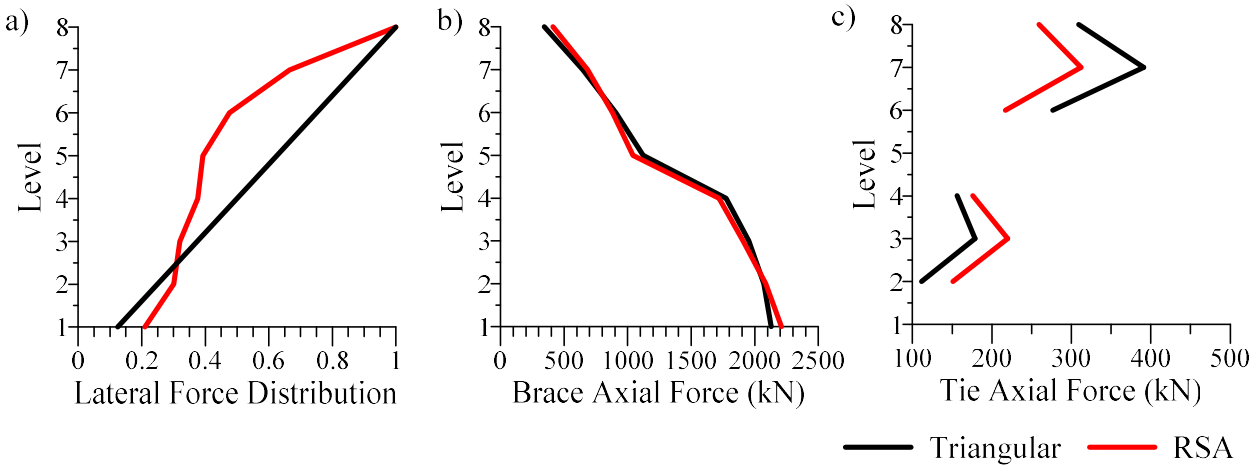

Figure 5-8 Comparison between inverted triangular and RSA lateral load patterns used for the calculation of Set I member forces for the 8-storey SESBF-2 configuration: a) Lateral load patterns; b) Brace axial forces; c) Tie axial forces.

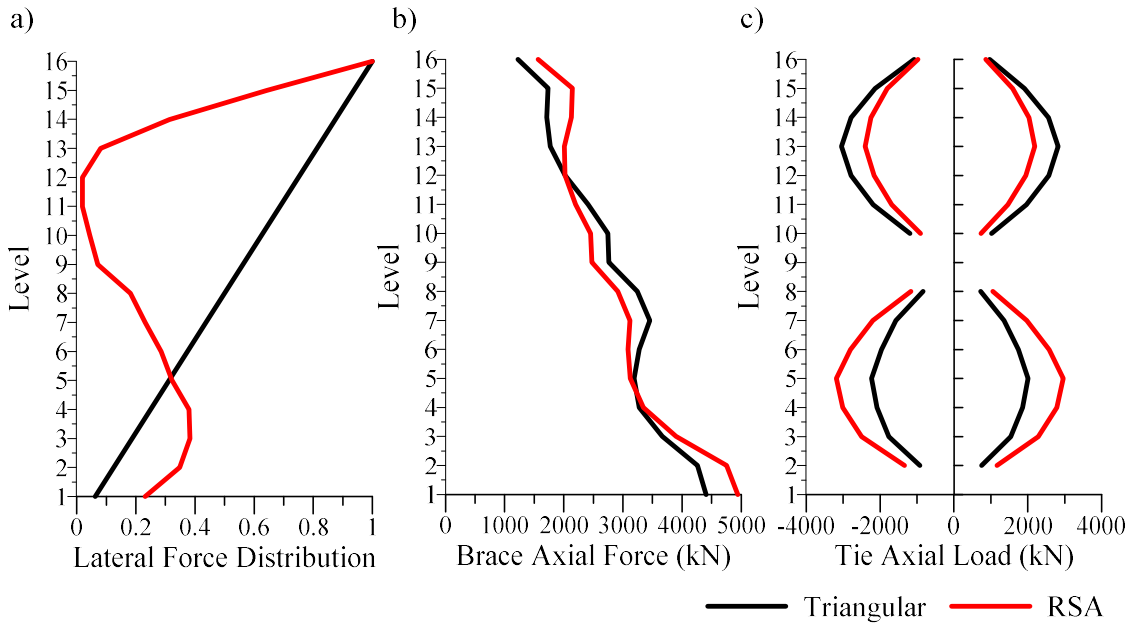

Figure 5-9 Comparison between inverted triangular and RSA lateral load patterns used for the calculation of Set I member forces for the 16-storey SESBF-2 configuration: a) Lateral load patterns; b) Brace axial forces; c) Tie axial forces.

The last phase for the design of the truss members is the calculation of the Set II member forces. The structure models were modified to include reduced stiffness properties with $\alpha = 0.01$ in accordance with the various yielding pattern cases. The truncated design spectra used for the 8-storey SESBF-1 and SESBF-2 structures are shown in Figure 5-10a and 10b, respectively. For SESBF-1, the spectrum was set equal to zero for periods longer than 1.0 s to eliminate the contribution from inelastic mode 1 ($T_{1,in}$ = 6.33 s from Table 5-4, not shown in the figure) and include that from inelastic modes 2 and 3 with periods $T_{2,in}$ = 0.83 s and $T_{3,in}$ = 0.36 s. For the SESBF-2 frame, the spectrum was cut at a period of 0.5 s so that the contribution of the inelastic mode 3 with period $T_{3,in}$, which corresponds to the first relevant inelastic mode, and that of the higher inelastic modes be considered. For this structure, inelastic periods in mode 3 in Table 5-4 are nearly the same (= 0.39 to 0.41s) for all three yielding pattern cases i = 1 to 3. The same modified design spectrum truncated at T = 0.5 s could then be used to include these modes in all three IRSA while eliminating the contribution from the inelastic mode 2 with periods equal to 2.32, 0.97 and 0.98 s for cases 1 to 3.

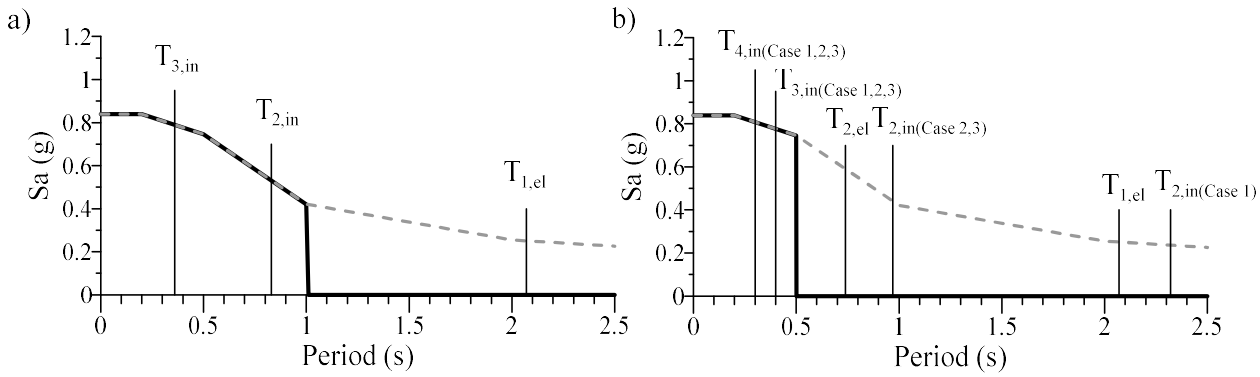

Figure 5-10 Truncated design spectra for: a) 8-storey SESBF-1 configuration; and b) 8-storey SESBF-2 configuration.

Set II forces on braces, ties and columns of the 8-storey SESBF-2 and 16-storey SESBF-2 frames are plotted in Figure 5-11. As depicted, different yielding link cases governed the magnitude of $r_{\text{II,IRSA}}$ forces in braces, ties, and columns along the building height, which indicates that all cases must be considered in the design. The $r_{\text{II,IRSA}}$ axial forces in ties and columns are maximum at mid-height of each vertical truss segment, indicating that M_{Truss} is also maximum at that location. Brace axial forces are associated with V_{Truss}. In the plots, brace forces are maximum at the top and lower ends of the truss segments and minimum near their mid-heights, which is consistent with the distribution of M_{Truss}.

In Figure 5-12, Set II forces obtained from IRSA performed on structures models with different reduced link stiffness ratios α are compared for the 8-storey SESBF-1 configuration. As expected, the results are not sensitive to the assumed α value, as was predicted from the small variations in inelastic periods shown in Table 5-1.

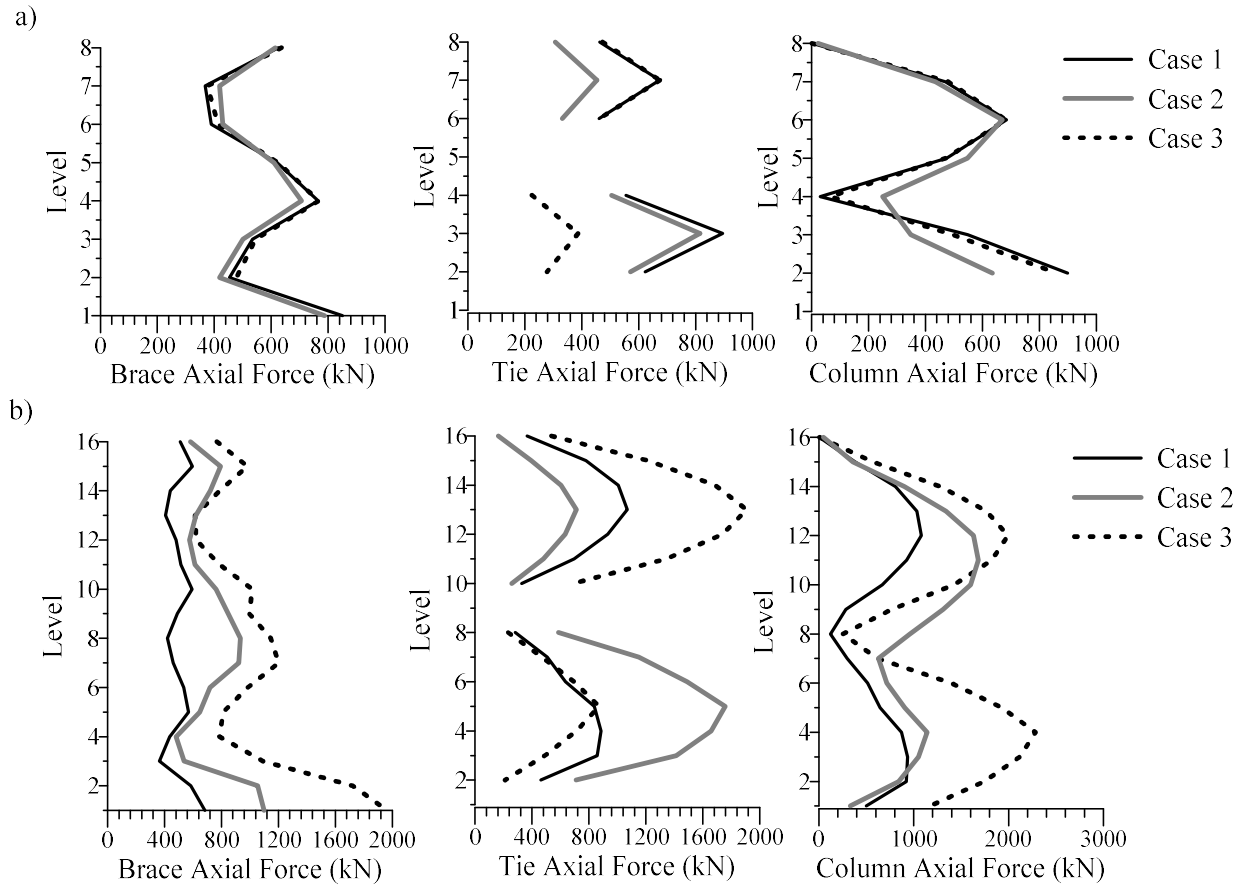

Figure 5-11 Set II axial forces in braces, ties and columns for cases i = 1, 2, and 3 for: a) 8-storey SESBF-2 configuration; and b) 16-storey SESBF-2 configuration.

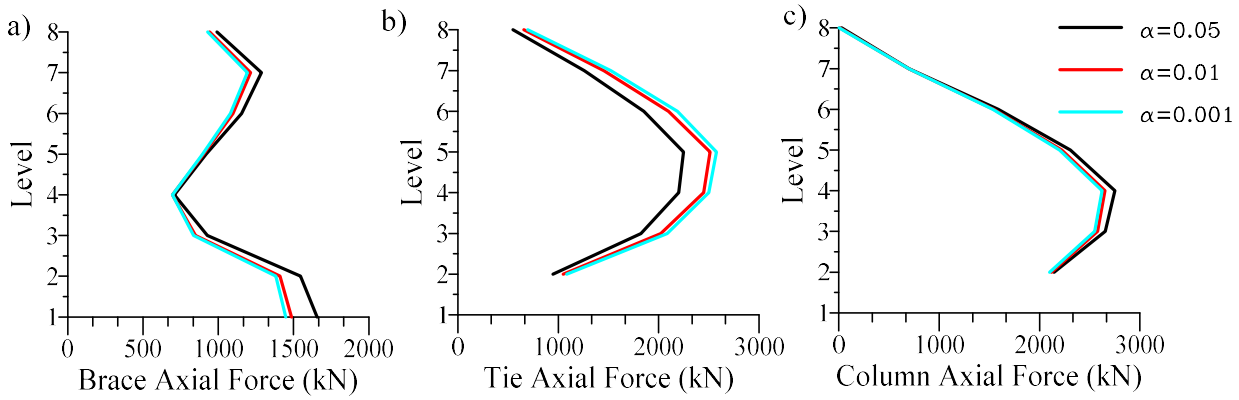

Figure 5-12 Influence of reduced link stiffness on Set II forces of 8-storey SESBF-2 configuration.

Total design forces for braces, ties, and columns of the 8-storey SESBF-1 and 8-storey SESBF-2 configurations are shown in Figure 5-13. Gravity load effects on braces and ties are small. Axial forces in braces are similar for both frame configurations but the relative contribution from Set I and Set II varies with the number of truss segments (e.g. Set I forces in SESBF-2 are larger than those in SESBF-1). Axial forces in the ties are largely dominated by Set II forces for both frame configurations. This was expected as ties, in comparison with braces, beams and columns, are not required to resist lateral loads associated considered in the determination of Set I forces. It must be recalled that tie members are added in the EBF system to create the vertical elastic trusses and are therefore mainly involved in the resistance of the moment M_{Truss}. The figure also shows that axial loads in ties reduce significantly when adopting a segmental truss configuration, which is also expected in view of their role in the structure. Axial forces in columns are largely contributed by Set I forces. However, interrupting the continuity of the vertical trusses also has a considerable effect on Set II axial forces in columns. Axial forces at columns bases are induced by global overturning moments associated with Set I forces and are not affected much by the continuity of the vertical trusses.

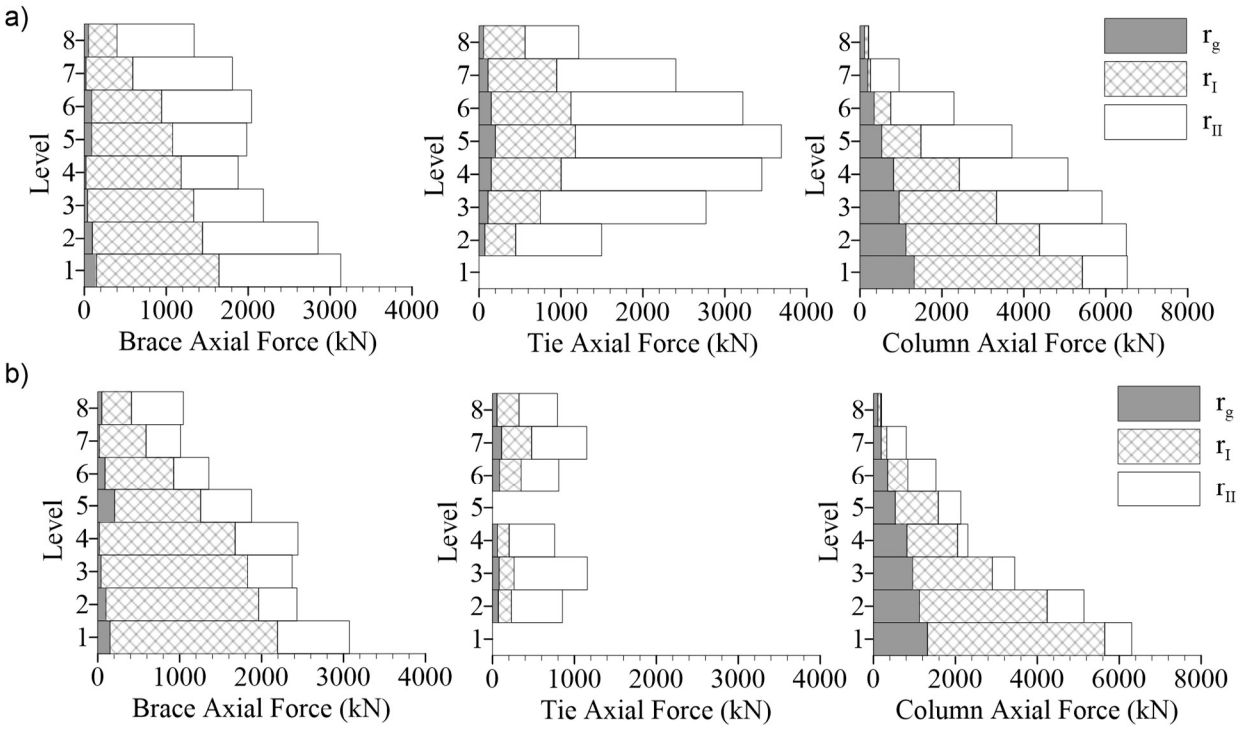

Figure 5-13 Axial forces in braces, ties, and columns of 8-storey seismic force resisting system: a) SESBF-1 configuration; and b) SESBF-2 configuration.

5.3.3 Validation of the method through nonlinear dynamic analysis

5.3.3.1 Selection and scaling of seismic ground motions

Ground motion records were selected and scaled in accordance with the guidelines included in Commentary J of NBCC 2015. For Vancouver, seismic hazard for a probability of exceedance of 2% in 50 years is contributed by three major earthquake sources (Goda and Atkinson 2011, Tremblay et al. 2015): M6.5-7.0 shallow crustal earthquakes (C) at close distances (10-20 km), M6.5-7.0 subduction inslab events (SIS) expected to occur at a depth of 50-70 km under the site, and M>8.5 subduction interface (SIF) earthquakes at 130-150 km. According to NBCC guidelines, the ensemble of records included a suite of 5 representative ground motion time histories for each seismic source. In addition to magnitude and distance properties, ground motions of each suite were selected to reflect local site conditions and match the design spectrum over scenario-specific

period ranges T_{RS} over which they contribute most to the hazard. The records of each suite were scaled individually to match, on average, the design response spectrum over their respective period ranges T_{RS}. Additional scaling was then applied to all records of a suite when the mean spectrum for the suite was less than 90% of the target spectrum over the suite scenario-specific period range.

The spectra of the scaled ground motions of each suite are presented in Figure 5-14. The scenario-specific period ranges are indicated in the figure. As shown, crustal and SIS ground motions have short dominant periods, whereas SIF records have energy distributed over a wide period range up to long periods. For the structures studied, the former two suites were expected to excite the higher modes contributing most to Set II member forces. The SIF suite was expected to affect both Set I and Set II forces while also imposing large displacement demand on frames.

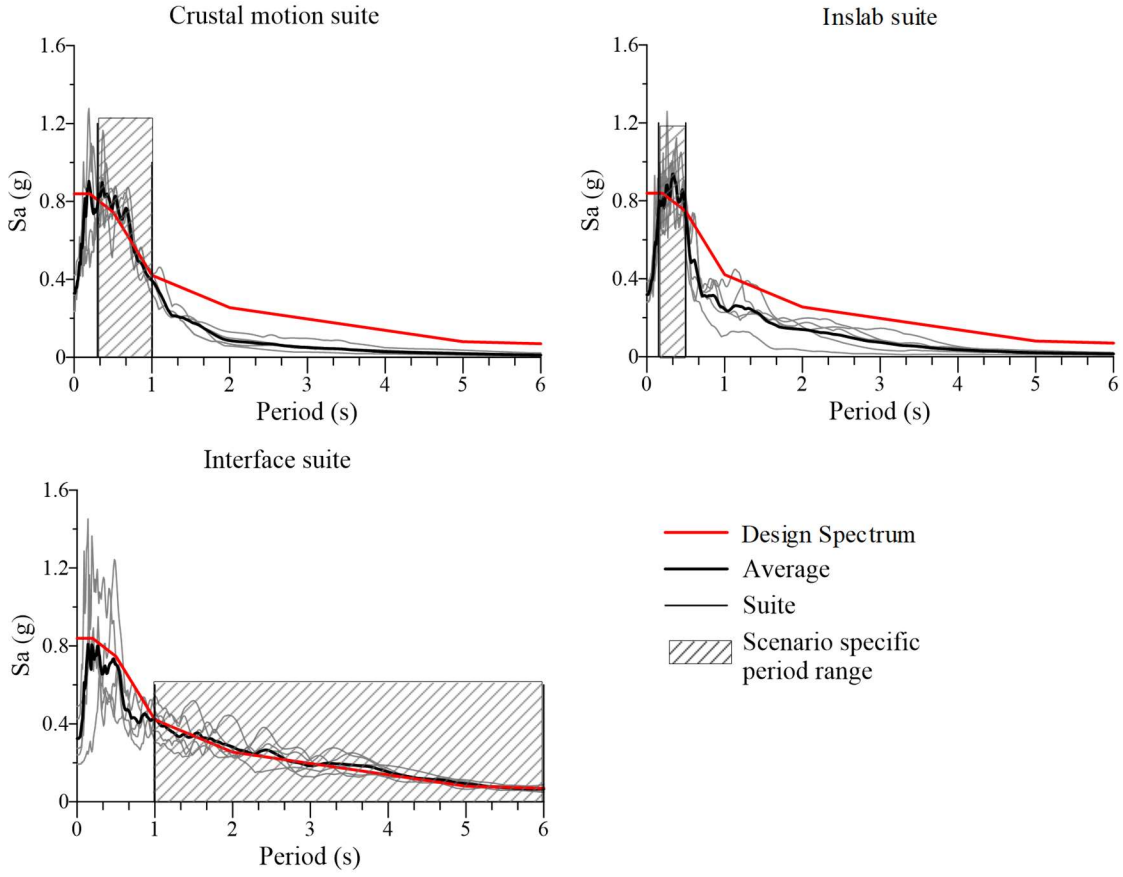

Figure 5-14 Scaled response spectra and the scenario-specific period range for each ground motion suite for Vancouver, Site Class C: a) crustal suite, b) subduction inslab (SIS) suite, and c) subduction interface (SIF) suite

5.3.3.2 Numerical modeling

NLRHA was performed using the OpenSees platform (McKenna and Fenves, 2004). Two-dimensional models were used that included one bracing bent acting in the E-W direction. The models included a leaning column carrying ¼ of the gravity loads carried by the gravity columns laterally supported by the braced frame studied. The shear links were modelled using elastic beam-column elements with zero-length elements replicating the elastic and inelastic shear responses of the links (Koboevic et al. 2012). The Steel02 material was assigned to the zeroLength element to simulate the link hysteretic response including isotropic and kinematic strain hardening, together with the Min-Max material to capture link failure. The Min-Max material was calibrated against the results of experimental tests conducted by Okazaki and Engelhardt (2006). Additional information on the OpenSees model and its calibration can be found in Chen et al. (2018a).

Although the truss members were expected to remain elastic, all members were modelled using nonlinear beam-column elements with distributed plasticity and fiber cross-section discretization to detect possible member yielding or buckling limits states. The Steel 02 material was assigned to these elements and initial out-of-straightness was assigned to the braces, columns and ties to accurately predict buckling response. Probable steel yield strengths of 385 and 460 MPa were assigned to the W-shapes and HSS members, respectively. Rayleigh damping of 3% of critical was assigned in the first and third vibration modes for the 8-storey structures and the first and fifth modes for the 16-storey structures. Stiffness proportional damping was assigned only to the structural members responding in the elastic range. P-Δ effects were considered in the analyses with tributary gravity loads from dead load plus 50% of the floor live load and 25% of the roof snow load. Gravity loads were applied to the braced frame and the leaning column.

5.3.3.3 Seismic Response of the 8-storey *SESBF*-2

The behaviour assumed for the development of the analysis method is first validated by observing time histories of the forces induced in the ductile links, braces, and ties of the 8-storey SESBF-2 frame. Results are presented in Figure 5-15 and 16 for the structure subjected to the SIF3 subduction interface and C2 crustal ground motions, respectively. Drift ratios for both elastic truss segments, obtained by dividing the relative horizontal displacements at top and bottom ends of the

segment by the segment height, are also plotted in the figures. The elastic first mode period of the frame is 2.07 s but this period can elongate significantly when links experienced yielding, as shown in Figure 5-5.

In Figure 5-15a, both segments oscillate in phase with long periods approximately equal to 3-4 s. The segment drift response is also larger drifts developed in the second segment, sufficient to trigger large yielding excursions in links at the 5^{th} (L5) and 8^{th} (L8) levels, i.e., bottom and top floors of segment 2, as shown in Figure 5-15b. Shear force responses in these two links are well synchronized with each other as well as with the drift response of the segment, confirming the assumption made in design for segment response. The drift demand in segment 1 is less and link L1 just reached yielding. For time between 70 and 80 s, the response of first segment is essentially elastic, as revealed by the high frequency characterizing the shear force signal in link L1. During that same time window, yielding occurred in segment 2, which corresponded to the yielding pattern case 3 considered in design (Figure 5-5). For time greater than 80 s, yielding developed in both segments, thus reflecting yielding case 1. The comparison between shear link force responses in links L1 and L5 shows that the latter generally lags behind the former, which is seen as a result of seismic demand propagating upward in the structure.

As expected, forces in braces and ties are contributed by both first mode (r_I) and higher modes (r_{II}). In Figure 5-15c, the brace at 7^{th} level in segment 2 is more influenced by higher modes when segment 1 is mostly elastic and stiffer ($t < 80$ s), thus more capable of transmitting high frequency demand to the top segment. Later, when yielding case 1 is observed, the force demand on the brace is governed by r_I contribution. In Figure 5-15e, the brace force history at level 3 in the bottom segment if dominated by first mode response (r_I), as predicted in Figure 5-13b. As was also expected in design, maximum forces in braces of both segments are in phase with maximum forces (and yielding) in ductile links. In both segments, the analysis results show that peak force demand in braces is well predicted by the design method (r_I+r_{II}). Because the main function of the vertical tie members is to provide continuous flexural stiffness for the vertical trusses, axial loads in ties in Figure 5-15d and 15f are significantly influenced by higher mode (high frequency) response in both segments. Both force signals also contain oscillations at longer periods (3-4 s), revealing a contribution from first inelastic mode, especially when yielding occurs in both segment at $t > 80$ s. This is also supported by the fact that peak tie forces for $t < 80$ s correspond well with the total

force from Sets I and II (r_I+r_{II}) whereas those after that time match well Set I (r_I) forces. This excellent correlation also validates the method used to predict axial load demand in the vertical ties.

Contrary to ground motion SIF3 that had energy at short, intermediate and long periods, energy in crustal earthquake motions is concentrated in the short period range less than 1.0 s. This difference can be observed when examining the response of the frame to the C3 ground motion in Figure 5-16. As shown, the two vertical truss segments consistently drift towards opposite directions before t = 7.5 s, i.e., before significant yielding occurs in the ductile links. Between t = 7.5 and 8.0 s, large yield excursions are observed in the links of both segments and the response progressively changes to one characterized by the two segments oscillating in phase. As shown, the fore demand in braces and ties for this ground motion is less, likely because r_I forces predicted in design did not develop under this ground motion having limited energy in the periods close to the elastic and inelastic first modes (T > 2.07 s).

Peak storey drifts, peak storey shears, and peak axial loads in braces, columns and ties at every level of the SESBF-2 structure are presented for each individual ground motion in Figure 5-17. In the figure, envelopes of the demand from each ground motion type are represented using thicker lines. Design forces in braces, columns and ties as predicted with the proposed method are also plotted for comparison. Peak responses for each earthquake source are presented individually in Figure 5-18. The figures show that the SESBF-2 system could exhibit uniform storey drift along each vertical truss segment under all ground motions, as intended in design. For this structure, larger drifts developed in the upper segment. As anticipated, ground motions from subduction interface events (SIF) imposed larger storey drifts with maximum values reaching up to 2.45% h_s. In Figure 5-18, maximum mean storey drift values along the frame height are respectively 1.05, 1.32 and 1.93% h_s for the crustal, SIS and SIF ground motions. The largest value (1.93% h_s) is smaller than the 2.5% h_s limit specified in the NBCC for buildings of the normal importance category and the response of the frame would classify as satisfactory. The lower drift demand imposed by the ground motions from crustal and SIS events is explained by their much lower energy in the vicinity of the structure fundamental period (mean acceleration response spectra ordinates of the scaled ground motions at T_1 = 2.07 s are 0.07, 0.12 and 0.23 g for crustal, SIS and SFI records). The relatively greater energy of the crustal and SIS records at short vs long periods

also explains the larger differences between peak storey drifts in segments 1 and 2 for these two ground motions.

Although storey drifts vary significantly among the three ground motion types, very consistent storey shears and axial forces in truss members are observed in Figure 5-17 and 18. For all braces, vertical ties and columns, peak forces are generally very well predicted by the analysis and design procedures and all members could sustain the imposed seismic demand without yielding in tension and buckling in compression. Except for the brace forces in the top two levels, mean force demands imposed by the three ground motion types in Figure 5-18 are all lower than the design values, confirming that the proposed method can produce realistic and safe force estimates for design purposes.

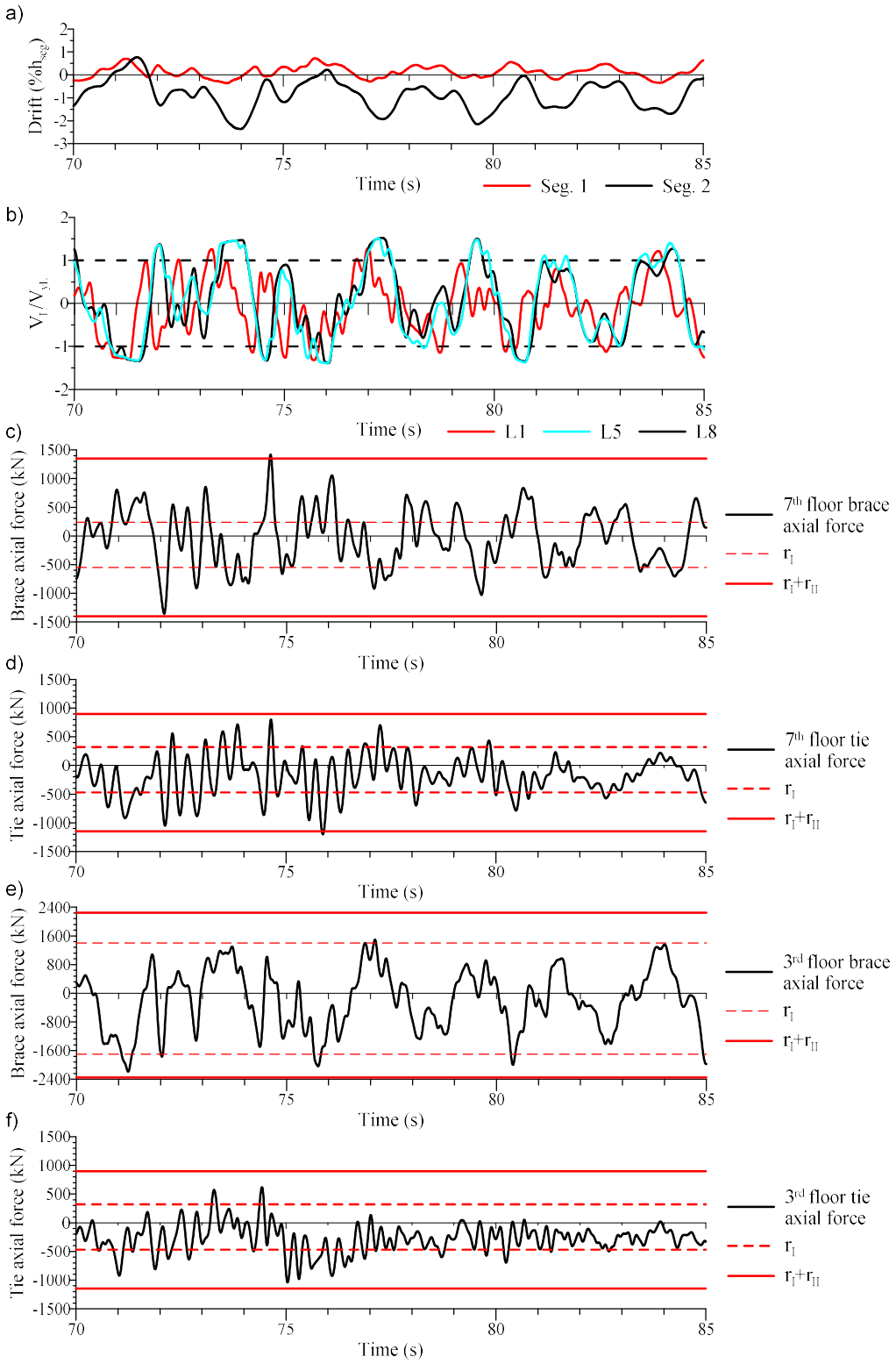
a)
Drift (%ℎ_seg)
Time (s)
Seg. 1
Seg. 2
b)
V_i/V_y1
Time (s)
L1
L5
L8
c)
Brace axial force (kN)
Time (s)
7th floor brace axial force
r_I
r_I+r_II
d)
Tie axial force (kN)
Time (s)
7th floor tie axial force
r_I
r_I+r_II
e)
Brace axial force (kN)
Time (s)
3rd floor brace axial force
r_I
r_I+r_II
f)
Tie axial force (kN)
Time (s)
3rd floor tie axial force
r_I
r_I+r_II

Figure 5-15 Time-history response series of 8-storey SESBF-2 configuration under ground motion SIF3: a) Segment drifts; b) Link shear forces; c) Axial force in brace at 7th floor; d) Axial force in tie at 7th floor; e) Axial force in brace at 3rd floor; and f) Axial force in tie at 3rd floor.

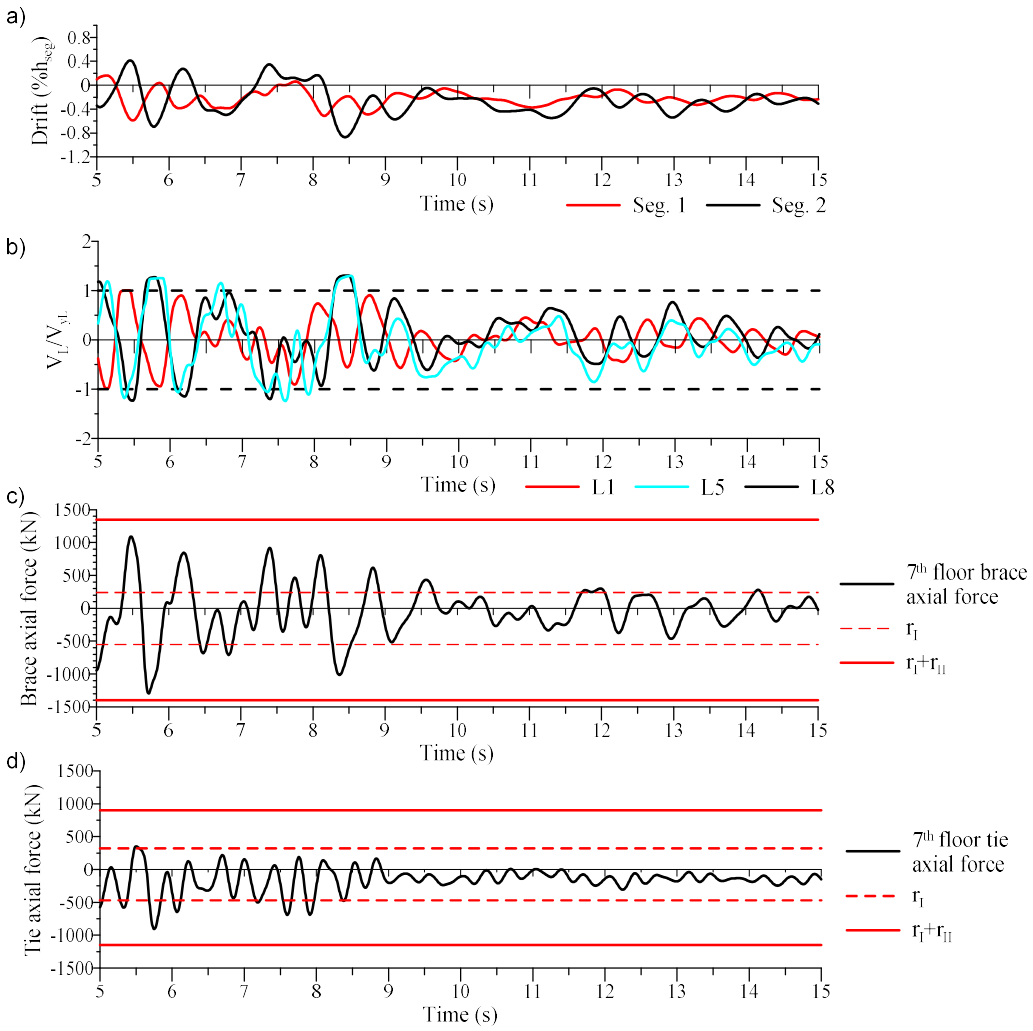

Figure 5-16 Time-history responses of 8-storey SESBF-2 configuration under ground motion C2: a) Segment drifts; b) Link shear forces; c) Axial force in brace at 7th floor; and d) Axial force in tie at 7th floor.

In Figure 5-18, design brace forces in compression and tension in the top tow levels are slightly lower than mean force demands from the three ground motion suites. Axial compression predicted for the vertical tie members are slightly exceeded in the first segment for one crustal earthquake

ground motion and in the second segment for one SIS motion. As shown in Figure 5-11a and 13b, maximum forces in the upper level braces and in the tie members of both segments are mainly contributed by Set II forces that are induced by the elastic response of the elastic vertical trusses. That response is weakly bounded by yielding of the ductile links and may therefore be sensitive to the actual demand from ground motions relative to the design input, as illustrated in Figure 5-19. Figure 5-19a shows an enlarged view of the design spectrum (DS) for the 0.3-0.5 s period range, together with 5% damped spectra for one record of each type. In Table 5-4, the inelastic periods $T_{3,in}$ for the frame range between 0.39 and 0.41 s. As shown in the figure, the spectra of the three records are close to or exceed the design spectrum in the vicinity of this period range, which can explain why the design tie force at level 3 in the lower segment is exceeded under record C2 in Figure 5-19b and the brace design forces at levels 7 and 8 in the second segment are exceeded under all three motions in Figure 5-19c. In addition, IRSA used to determine Set II member forces is performed using the 5% damped design spectrum whereas NLRHA is conducted assuming 3% damping. These effects, together with the simplifications inherent to the method (combination of elastic and inelastic modal contributions, model with reduced link stiffness, etc.), may result in some unavoidable inaccuracies for some members and caution should therefore be exercised when using Set II force predictions.

Brace forces in the lower levels of the frame and axial forces induced in the columns are mostly contributed by Set I forces and, thereby, strongly depend on the first mode response of the frame. For this structure, the SIF ground motions match well the design spectrum for long periods corresponding to the frame elastic and inelastic first mode periods and axial demands in the columns and lower braces from these ground motions correspond well to and are well bounded by the design values obtained assuming yielding of all links over the frame height. Design predictions become more conservative in the bottom levels due to the reduced likelihood that all links in the levels above develop simultaneously their strain hardened capacities, a behaviour that has been observed in past studies on braced frames. As was the case for drifts, the crustal and SIS ground motions did not govern axial loads in columns as a result of their limited energy in long periods.

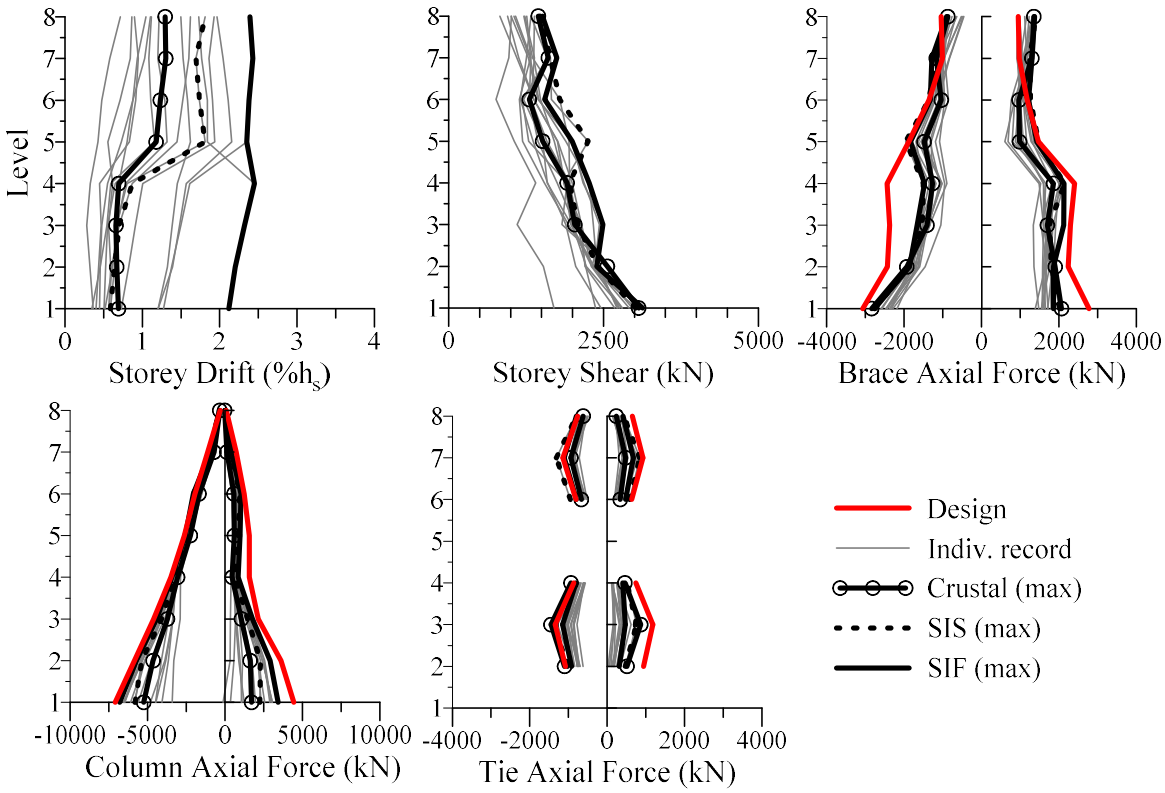

Figure 5-17 Peak values of storey shears, drifts, and axial forces in braces, columns, and ties along the height of the 8-storey SESBF-2 configuration.

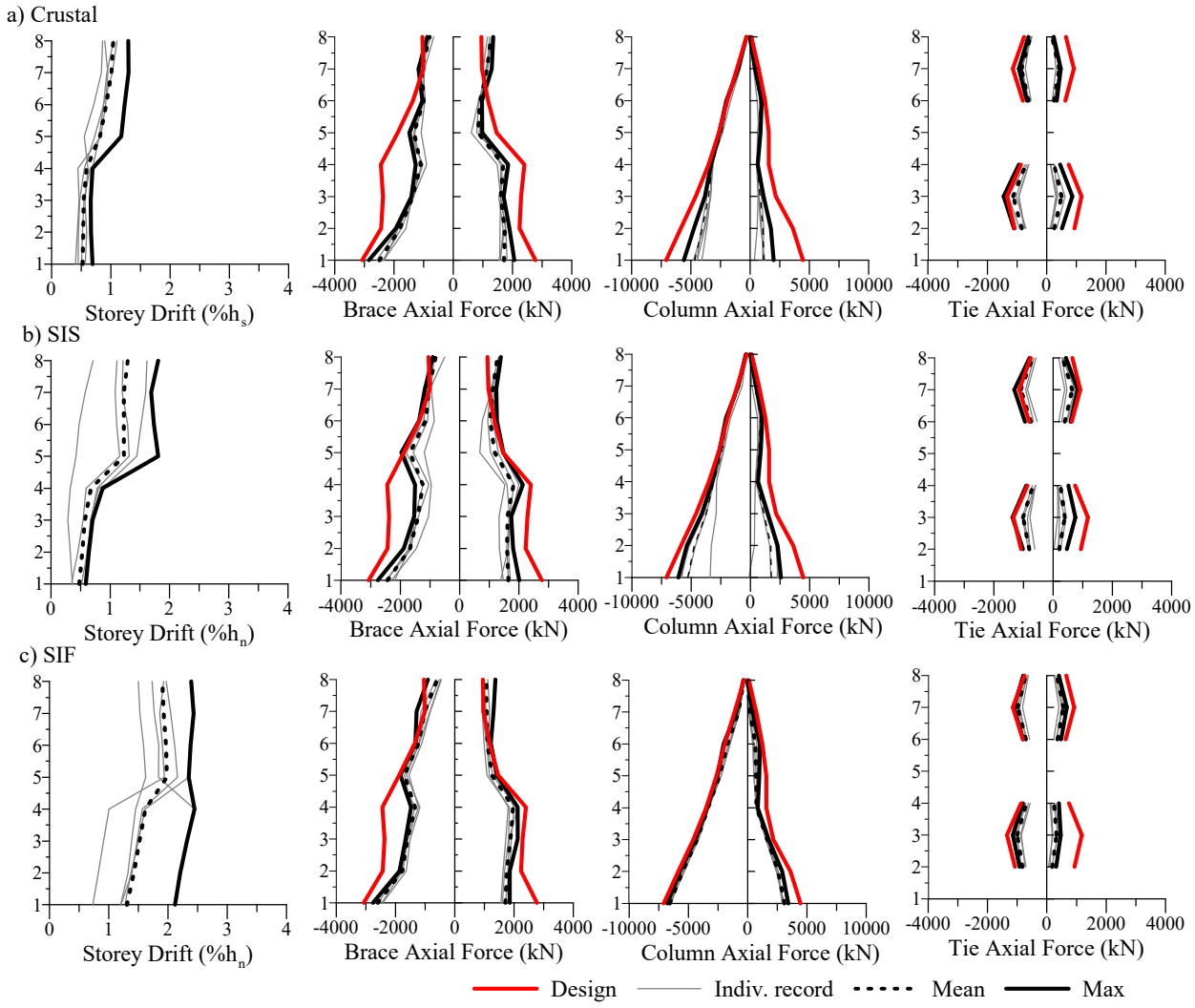

Figure 5-18 Peak values of storey drifts and axial forces in braces, columns and ties for the 8-storey SESBF-2 configuration under: a) Crustal records; b) SIS records; and c) SIF records.

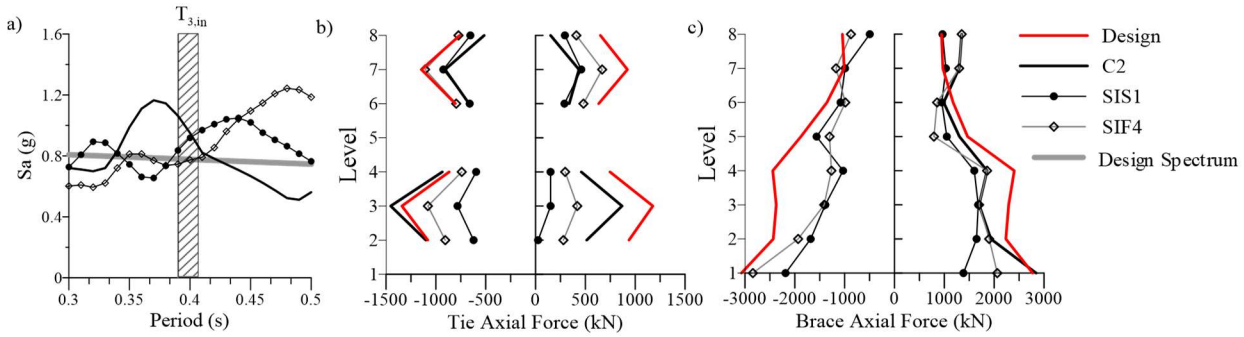

Figure 5-19 Spectra and member forces from records C2, SIS1, and SIF4 for the 8-storey SESBF-2 configuration: a) Response spectra; b) Axial forces in ties; c) Axial forces in braces.

5.3.3.4 Seismic Response of the 8-storey *SESBF*-1

Seismic response parameters are given in Figure 5-20 for the 8-storey building with SESBF-1 configuration. As expected, a more uniformly distributed storey drift response was achieved at the cost of much larger tie axial forces and slightly larger brace and column axial forces, especially at intermediate levels of the structure where moments M_{Truss} are maximum. When compared to drifts observed for the SESBF-2 configuration, maximum storey drifts under crustal, SIS, and SIF ground motions reduced to 1.13, 1.18 and 1.71% h_s, respectively. Axial compression forces induced in the tie members of the SESBF-1 system reached 3347 kN and 3220 kN at the 4th and 5th floors, which compare well with the corresponding design values of 3452 kN and 3691 kN at these levels. These values are significantly higher than the maximum values of 1453 and 1312 kN obtained in the first and second segments of the SESBF-2 system. On the tension side, the estimates from the design method are slightly conservative for both configurations consisting of one or two segments. For this SESBF-1 structure, axial compression and tension forces in braces and columns are also well predicted by the proposed method, with the exception of the brace forces in the upper two levels, similar to the behaviour observed for the SESBF-2 configuration.

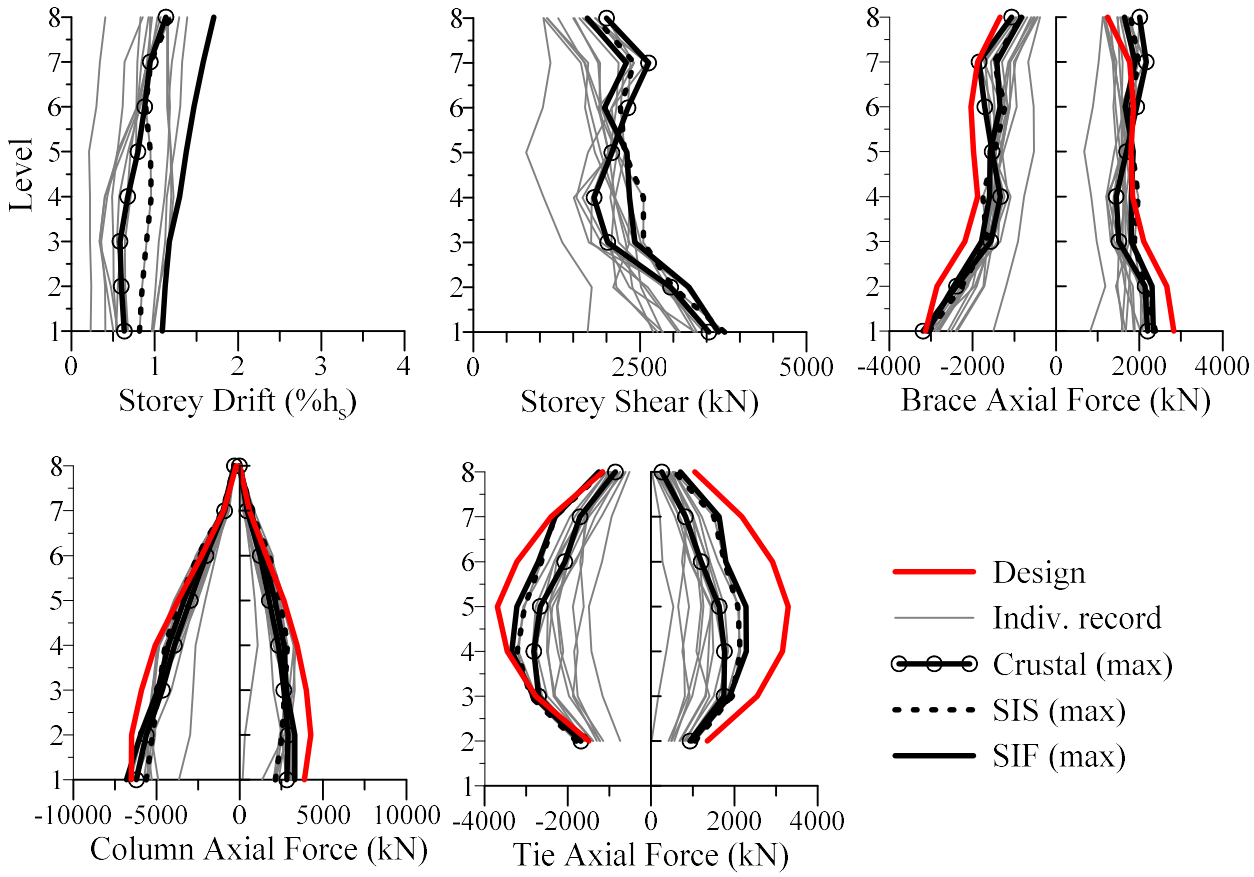

Figure 5-20 Peak values of storey drift, shears, and axial forces in braces, columns, and ties along the height of the 8-storey SESBF-1 configuration.

5.3.3.5 Seismic Response of the 16-storey *SESBFs*

NLRHA results for the 16-storey buildings with the SESBF-2 and SESBF-4 configurations are presented in Figure 5-21 and 22, respectively. Note that the SESBF-1 configuration was also investigated in the study initially but the axial load demand in the vertical ties reached 7000 kN which was deemed excessive for implementation in practice for the building braced frame geometries and that configuration was then discarded.

In Figure 5-21 and 22, both frame configurations exhibit uniformly distributed storey drift responses along their heights. Maximum storey drifts reached 1.97% h_s and 2.30% h_s for the SESBF-2 and SESBF-4 configurations, respectively, which is adequate. The larger deflections observed for the SESBF-4 structure were expected because of the lower restrain offered by the

shorter elastic truss segments, as was noted by comparing drifts of the 8-storey SESBF-1 and SESBF-2 systems. As also anticipated, adopting the SESBF-4 system would results in reduced fore demands in the truss members, especially for the vertical tie members. The proposed analysis method could predict well the forces in the braces and columns of the two frames as well as the forces in the vertical ties of the SESBF-4 system. For some of these braces and ties, the analysis method marginally underestimated maximum force demand from the ground motions, as was observed and explained for the 8-storey frames.

In Figure 5-21, the method predicted overly conservative forces for the vertical ties of the SESBF-2 structure. Examination of the time history response of that frame showed that yielding of the links did not develop simultaneously over the length of the 8-storey tall truss segments, contrary to the behaviour assumed for design. This behaviour is illustrated in Figure 5-23 for the upper segment of the structure when subjected to the C5 crustal earthquake record. It is noted that record C5 is the one that imposed the largest force demand in the ties of the upper segment. As shown, forces in the links progressively develop from the lower to the upper end of the segment such that yielding propagates over the segment height: links that have developed yielding in the first place no longer yield when yielding initiates in the last link. Near t = 11 s, links are even yielding in opposite directions at both ends of the segment. This behaviour is attributed to the dynamic lateral response of the truss segments inducing large flexural deformations over their heights. For this frame, that flexural response is associated to elastic modes 3 and 4 with periods of 0.68 and 0.46 s, respectively, or inelastic modes 5^{th} and 6^{th} with periods ranging from 0.37 to 0.46 s, depending on the yielding case pattern (see

Table 5-5). These periods fall within the period ranges where ground motions of all three types have high energy. Stiffer truss segments would be needed or ground motions capable of imposing relatively large response to obtain deformation profiles that more closely correspond to the ones assumed in design. Conversely, it is much easier to develop simultaneous yielding of all ductile links of the shorter 4-storey segments of the SESBF-4 structure that was assumed in design, which results in a closer match between predictions and ground motion demand for the tie forces.

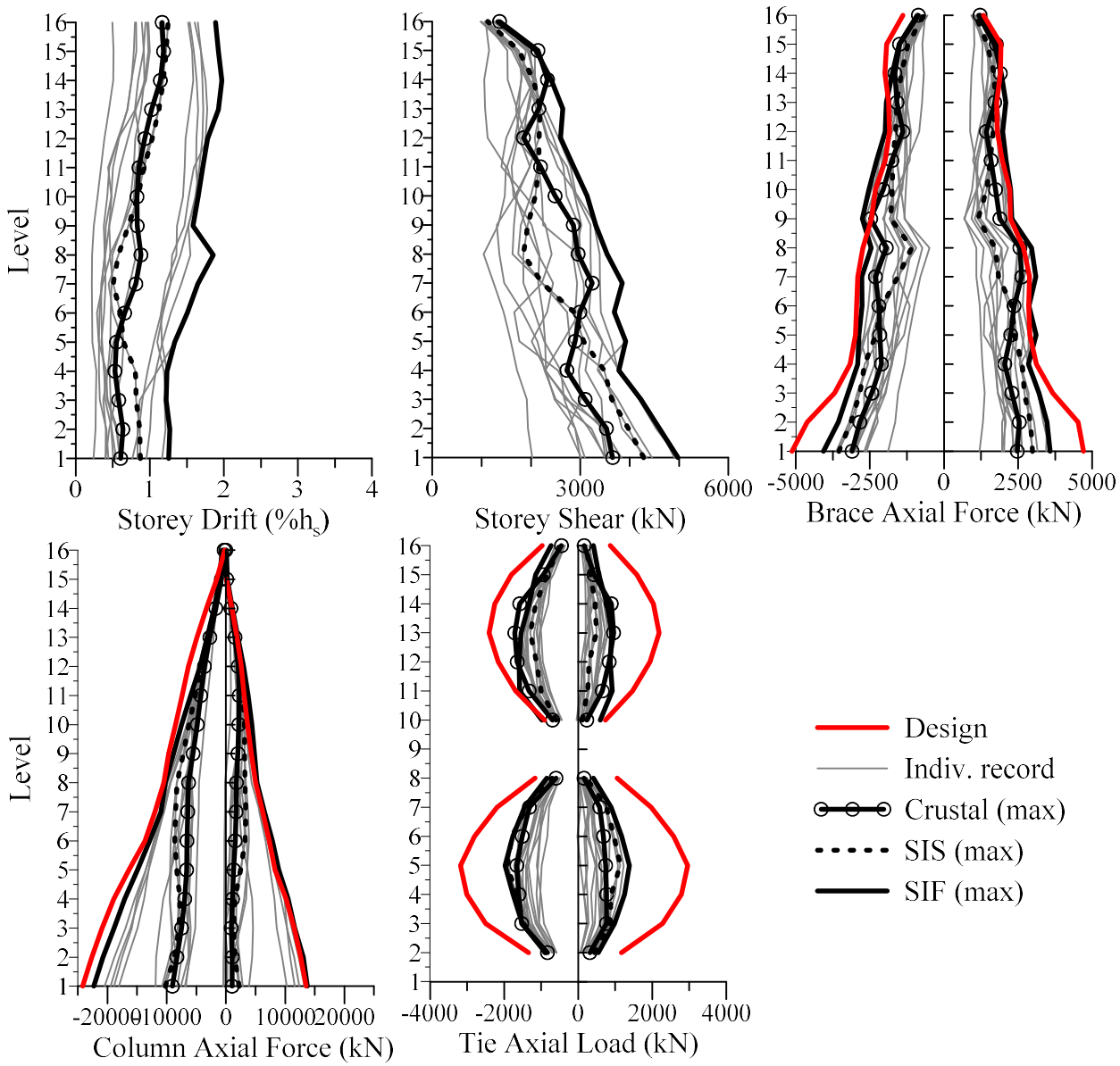

Figure 5-21 Peak values of storey drifts, storey shear, and axial forces in braces, columns and ties along the height of the 16-storey SESBF-2 configuration.

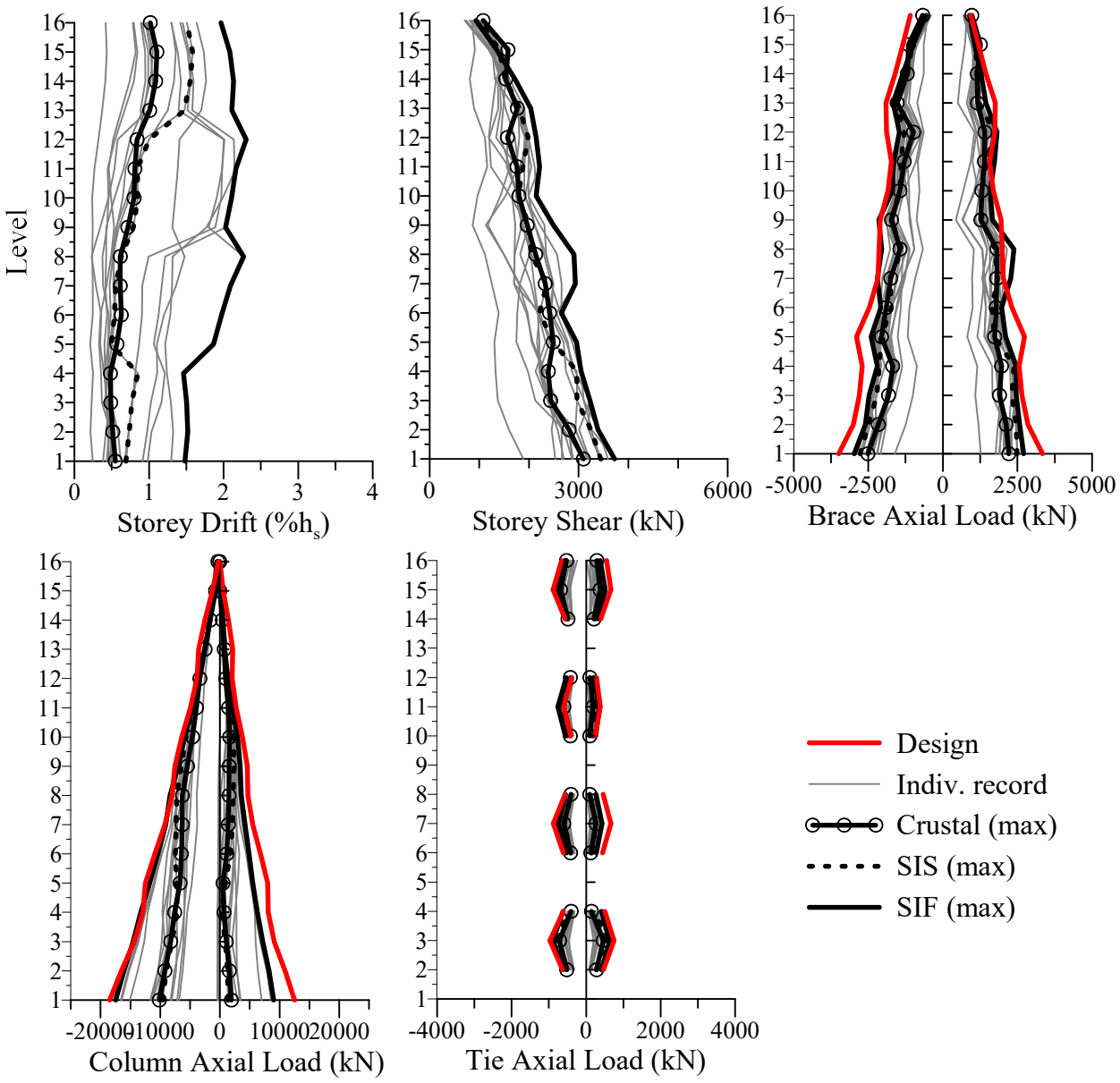

Figure 5-22 Peak values of storey drifts, storey shears, and axial forces in braces, columns and ties along the height of the 16-storey SESBF-4 configuration.

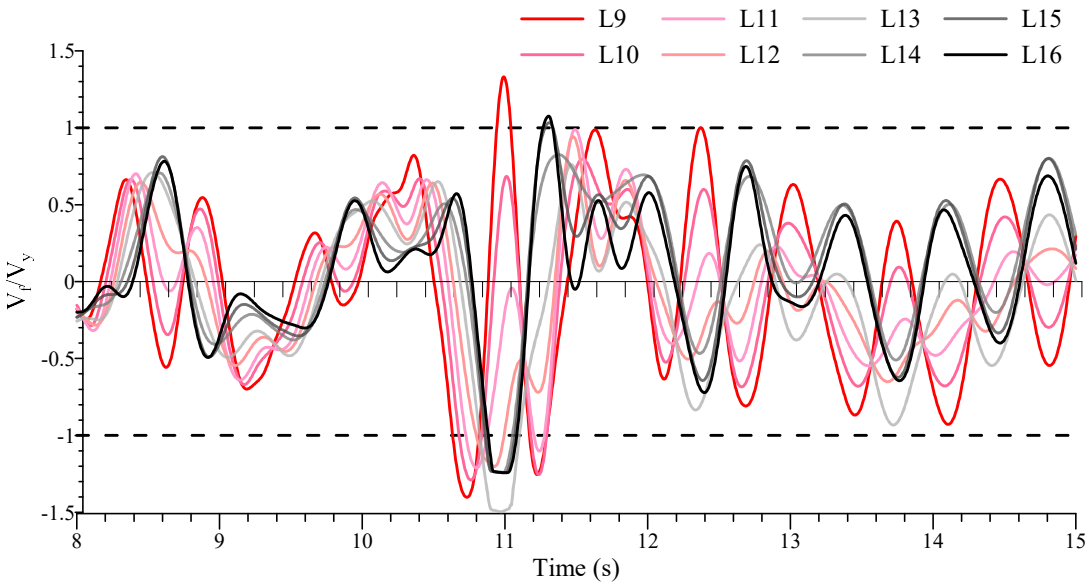

Figure 5-23 Shear force time-history in the links of the upper segment of SESBF-2 configuration under C5 ground motion.

Further NLRHA of the SESBF-2 structure was performed to examine the influence of the ground motion signature on the frame dynamic behaviour and truss member forces. The shear response of the links of the second segment when the frame was subjected to the SCT record of the 1985 Mexico City earthquake is shown in Figure 5-24. This record is not representative for the site studied but, as shown in Figure 5-25, it was selected because it has a marked dominant period of approximately 2 s, close and just above the elastic second mode period ($T_{2,el}$ = 1.33 s) and inelastic second mode periods ($T_{2,in}$ = 2.02 and 1.76 s) in

Table 5-5. For the analysis, a scaling factor of 2.2 was applied to the ground motion to obtain spectral accelerations comparable to the design spectrum near the first elastic mode period and the third and fourth inelastic mode periods. Large energy at periods close to the frame second periods is expected to mobilize uniform deformation demand on the individual segments that should favor simultaneous and uniform yielding of all links in each segment. As shown in Figure 5-24, this response was in fact activated with forces in all 8 links being nearly perfectly in phase in every oscillation. The demand in that second mode was however excessive and failure occurred in the links at t = 36 s, which reduced the link strength to 50% of original. Nevertheless, as shown in

Figure 5-26, the analysis showed that peak forces in the vertical tie members could be adequately predicted with the proposed analysis method for a ground motion capable of triggering the behaviour assumed for the method. Brace force demands on the columns and the braces in the lower levels are less than those are predicted in design because the response of the structure to that particular ground motion was mainly in the second mode.

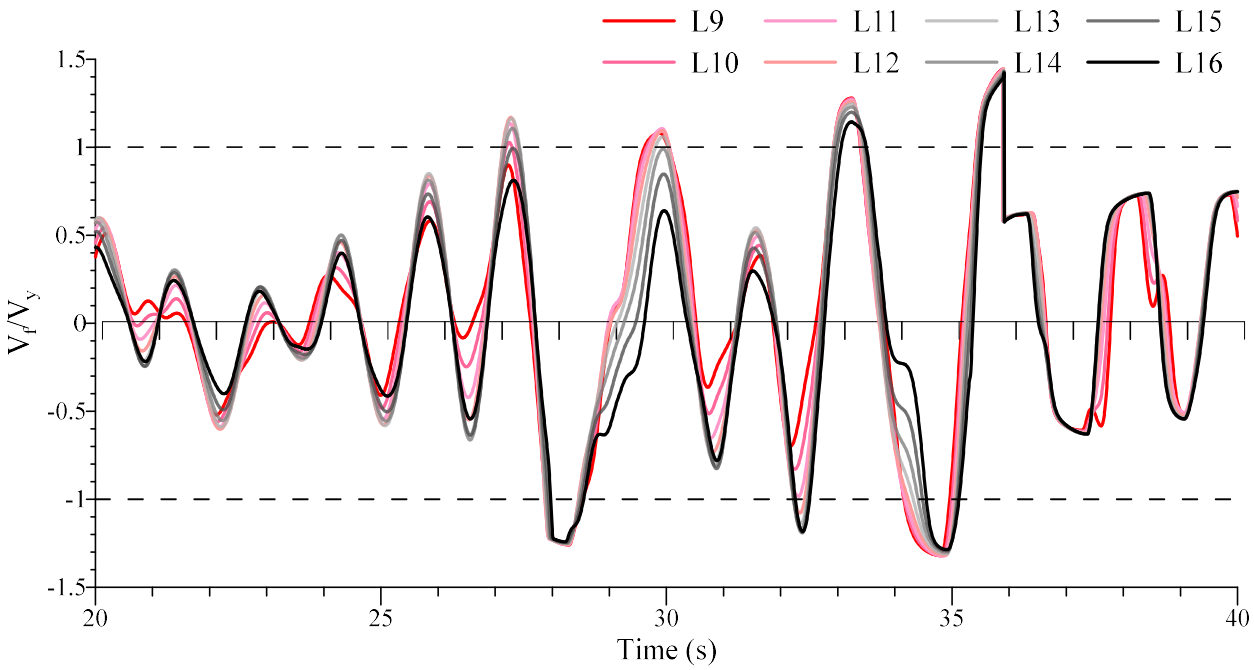

Figure 5-24 Shear force time-history developed in links of upper segment of SESBF-2 configuration under Mexico City, 1985, ground motion.

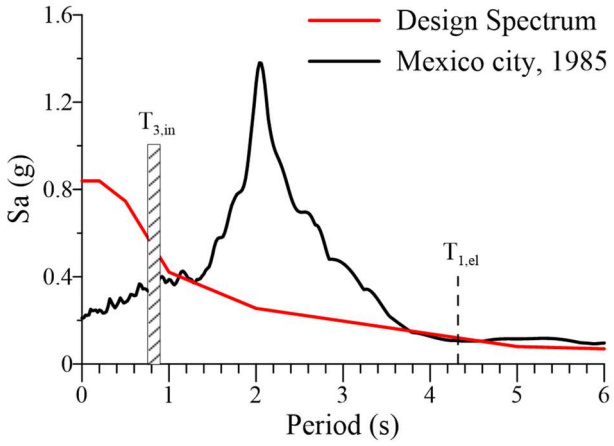

Figure 5-25 Design spectrum and response spectrum of the 1985 Mexico City earthquake (SCT, S00E record).

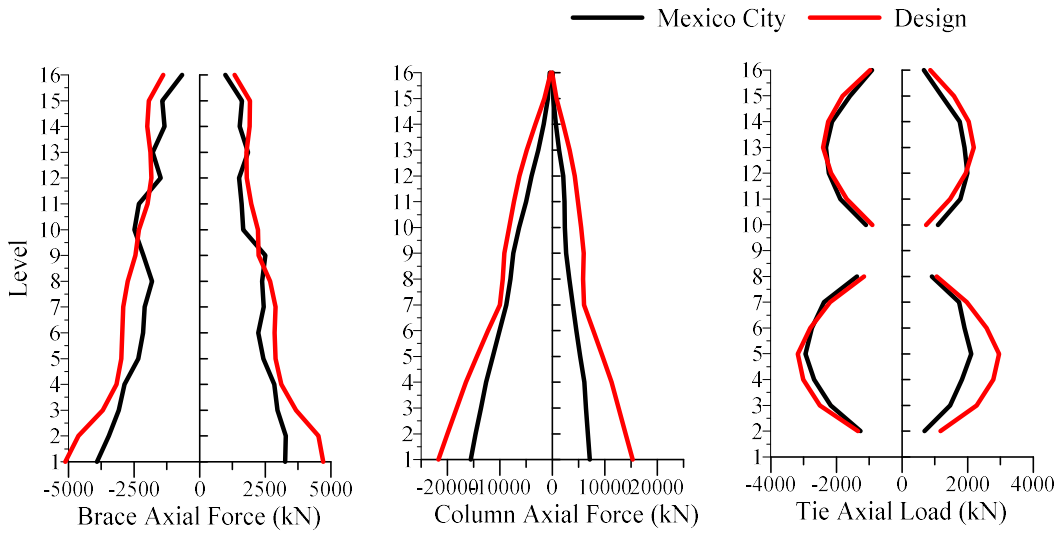

Figure 5-26 Peak values and distribution of axial forces in braces, columns and ties along the height of 16-storey SESBF-2 configuration under the 1985 Mexico City earthquake (SCT, S00E record).

5.4 Conclusions

A practical analysis method has been proposed for the design of tall steel braced frames with vertical segmental elastic trusses (SESBF) that are used to achieve uniform drift response while limiting forces in the elastic truss members under earthquake ground motions. The proposed method aims at determining maximum seismic axial forces induced in the members of the elastic vertical truss segments. The method combines the forces arising from yielding of the ductile elements along the braced frame height to the forces resulting from higher modes involving flexural dynamic response of the elastic truss segments. Forces of the first set are determined from static analysis assuming a realistic vertical distribution of the lateral loads. Forces of the second set are determined from a response spectrum analysis performed on a structure model with reduced stiffness assigned to the yielding elements and a design response spectrum truncated to only include the contribution from the modes with flexural response of the truss segments. For frames with

segmented vertical trusses, the response spectrum analysis is performed for different yielding pattern cases likely to develop under earthquake ground motions and the maximum value is retained for design. The proposed method is simple and can be readily implemented in day-to-day practice using commercially available structural analysis software.

The method was applied and validated for 8-storey and 16-storey SESBFs created from conventional EBFs. SESBF configurations including one, two and four elastic truss segments were examined. The structures were located in Vancouver, BC, and their behaviour was examined through NLRHA under ground motions generated by three different sources of earthquakes. Except for the two cases discussed below, the proposed method provided excellent predictions of the peak force demand imposed on the truss members.

Seismic forces in some braces and vertical tie members were slightly underestimated by the proposed method. Forces in these members are dominated by elastic flexural response of the truss segments. This response is not bounded by yielding of the ductile elements of the system and is therefore sensitive to possible differences between ground motion and design spectra as well as damping assumed in analysis. Additional studies could be performed to account for this behaviour in the proposed method. For the 16-storey frame with two 8-storey segments, forces in the vertical ties were overpredicted by the method because simultaneous and complete yielding of the links within the individual truss segments that was assumed in design was not observed in the analyses. For such tall frames with long truss segments, typical dominant ground motion periods are closer to the periods of the modes associated with individual flexural response of the truss segments, rather than the structure modes that could trigger uniform drift and yielding of all links in the truss segments. Further studies are needed to adapt the method for such SESBF applications.

In this study, the method was validated for conventional EBFs modified to include elastic truss spines. Further validation is necessary for other SESBF configurations such as the dual BRB system shown in Figure 5-1b. Experimental validation of the SESBF system and the analysis method is also needed for tall braced frame applications.

Acknowledgements

This project was funded by the Natural Sciences and Engineering Research Council of Canada and the Fonds de recherche Nature et technologies (FRQNT) of the Government of Québec.

References

AASHTO. (2014). *Guide Specifications for Seismic Isolation Design*. American Association of State Highway and Transportation Officials (AASHTO), Washington, DC.

Aoki, K., Fukuyama, K., Okumoto, H., Ukai, K.,and Taga, K. (1998). "Design of a High-Rise Building Using Unbonded Braces with Varying Cross Section." *Journal of Constructional Steel*, 6, 139-144, (*in Japanese*)

Balazadeh-Minouei, Y., Tremblay, R., and Koboevic, S. (2017). "Seismic Retrofit of an Existing 10-Storey Steel Chevron Braced Frame." *Journal of Structural Engineering*, (Submitted)

Blakeley, R.W.G., Cooney, R.C., and Megget, L.M. (1975). "Seismic shear loading at flexural capacity in cantilever wall structures." *Bulletin New Zealand National Society for Earthquake Engineering*, 8(4), 278-290.

Buckle, I., Al-Ani, M., and Monzon, E. (2011). *Seismic Isolation Design Examples of Highway Bridges*. Report no. NCHRP 20-7 / Task 262(M2), University of Nevada, Reno, NV.

Chen, C.H. and Mahin, S.A. (2012). *Performance-based seismic demand assessment of concentrically braced steel frame buildings*. Report No. PEER-2012/103, Pacific Earthquake Engineering Research Center, Univ. of California, Berkeley, CA.

Chen, L., Tremblay, R., and Tirca, L. (2012). "Seismic Performance of Modular Braced Frames for Multi-Storey Building Application." *Proc. 15th World Conference on Earthquake Engineering*, Lisbon, Portugal, Paper No. 5458.

Chen, L., Tremblay, R., and Tirca, L. (2018a). "Modular tied eccentrically braced frames for improved seismic response of tall buildings." *Journal of Constructional Steel Research* (Submitted)

Chen, L., Tremblay, R., and Tirca, L. (2018b). "Optimized Design of Steel Braced Frames with Segmental Elastic Spines using Simplified Analysis Models." *Journal of Constructional Steel Research* (Submitted)

Chopra, A.K., and Goel, R.K. (2001). *A Modal Pushover Analysis Procedure to Estimate Seismic Demands for Buildings: Theory and Preliminary Evaluation*. Report No. PEER 2001/03, Univ. of California, Berkely, CA.

Chopra, A.K., Goel, R.K., and Chintanapakdee, C., (2004). "Evaluation of a Modified MPA Procedure Assuming Higher Modes as Elastic to Estimate Seismic Demands." *Earthquake Spectra*, 20(3), pp. 757-778.

CSA. (2014). *CSA S6-14, Canadian Highway Bridge Design Code*. Canadian Standards Association (CSA), Toronto, ON.

CSI. (2017). SAP2000, v19. Computer and Structures, Inc., Berkeley, CA.

Eberhard, M.O., and Sozen, M.A. (1993). "Behavior-based Method to Determine Design Shear in Earthquake-Resistant Walls." *Journal of Structural Engineering*, 119(2), 619-640.

Eibl, J. and Keintzel, E. (1988). "Seismic shear forces in RC cantilever shear walls." *Proc. 9th World Conference on Earthquake Engineering*, Tokyo-Kyoto, Japan, VI, 5-10.

Ghersi, A., Neri, F., Rossi, P.P., and Perretti, A. (2000). "Seismic response of tied and trussed eccentrically braced frames." *Proc. Stessa 2000 Conf.,* Montreal, Canada, 495-502.

Ghersi, A., Pantano, S., and Rossi, P.P. (2003). "On the design of tied braced frames." *Proc. Stessa 2003 Conf.,* Naples, Italy, 413-429.

Goda, K., and Atkinson, G.M. (2011). "Seismic performance of wood-frame houses in south-western British Columbia", *Earthquake Engineering and Structural Dynamics*, 40, 903-924.

Khatib, I.F., Mahin, S.A., Pister, K.S. (1988). *Seismic behavior of concentrically braced frames*. Report. No. UCB/EERC-88/01, Earthquake Engineering Research Center, Univ. of California, Berkeley, CA.

Koboevic, S., Rozon, J., and Tremblay, R. (2012). "Seismic performance of low-to-moderate height eccentrically braced steel frames designed for North-American seismic conditions." *Journal of Structural Engineering*, 138(12), 1465-1476.

Laghi, V., Palermo, M., Gasparini, G., and Trombetti, T. (2017). "Strong-Back System Coupled with Framed Structure to Control the Building Seismic Response." *Journal of Civil & Environmental Engineering*, 7(2). DOI: 10.4172/2165-784X.1000274

Lai, J-W. and Mahin, S.A. (2015). "Strongback System: A Way to Reduce Damage Concentration in Steel Braced Frames." *Journal of Structural Engineering*, 141(9). DOI: 10.1061/(ASCE)ST.1943-541X.0001198.

Mar, D. (2010). "Design examples using mode shaping spines for frames and wall buildings." *Proc. 9th U.S. National Conference and 10th Canadian Conference on Earthquake Engineering.* Toronto, ON, Paper No. 1400.

Martini, K., Amin, N., Lee, P.L., and Bonowitz, D. (1990). "The Potential Role of Nonlinear Analysis in the Seismic Design of Building Structures." *Proc. 4th National Conference on Earthquake Eng.*, Palm Springs, CA, 2, 67-76.

McKenna, F. and Fenves, G.L., (2004). Open System for Earthquake Engineering Simulation (OpenSees). Pacific Earthquake Engineering Research Center (PEER), University of California, Berkeley, CA. (http://opensees.berkeley.edu/index.html)

Merzouq, S. and Tremblay, R. (2006). "Seismic Design of Dual Concentrically Braced Steel Frames for Stable Seismic Performance for Multi-Storey Buildings." *Proc. 8th U.S. National Conference on Earthquake Eng.*, San Francisco, CA, Paper 1909.

NRCC. (2015). National Building Code of Canada 2015, 14th ed., National Research Council of Canada, Ottawa, ON.

Okazaki, T., and Engelhardt, M.D. (2006), "Cyclic Loading Behaviour of EBF links constructed of ASTM A992 Steel." *Journal of Construction Steel Research,* 63, 751-765.

Panian, L., Bucci, N., and Janhunen, B. (2015). "BRBM Frames: An Improved Approach to SeismicResistant Design Using Buckling-Restrained Braces." *Proc. Second ATC & SEI Conference on Improving the Seismic Performance of Existing Buildings and Other Structures*. San Franscisco, CA, 632-643. Doi: 10.1061/9780784479728.052.

Panian, L., Bucci, N., and Tipping, S. (2017). "BRBM Frames: An Improved Approach to Seismic-Resistant Design Using Buckling-Restrained Braces," *Proc. Structures Congress 2017: Buildings and Special Structures*, ed. J.G. Soules, Denver, CO, 60-71.

Priestley, M.J.N., and Amaris, A.D. (2002). *Dynamic amplification of seismic moments and shears in cantilever walls*. European School for Advanced Studies in Reduction of Seismic Risk. Research Report No. ROSE-2002/01, Pavia, Italy.

Pollino, M., Slovenec, D., Qu, B., and Mosqueda, G. (2017). "Seismic Rehabilitation of Concentrically Braced Frames Using Stiff Rocking Cores." *Journal of Structural Engineering,* 143(9). Doi: 10.1061/(ASCE)ST.1943-541X.0001810.

Rodriguez, M.E., Restrepo, J.I., and Carr, A.J., (2002). "Earthquake-induced floor horizontal accelerations in buildings," *Earthquake Engineering and Structural Dynamics*, 31 (3), 693–718.

Rossi, P.P. (2007). "A Design Procedure of Tied Braced Frame. *Earthquake Engineering and Structural Dynamics*, 36 (14), 2227-2248.

Sabelli, R. (2001). *Research on Improving the Design and Analysis of Earthquake-Resistant Steel-Braced Frames*. NEHRP Fellowship Report No. PF2000-9, Earthquake Engineering Research Institute, Oakland, CA, 2001.

Simpson, B.G., and Mahin, S.A. (2018). "Experimental and Numerical Investigation of Strongback Braced Frame System to Mitigate Weak Story Behavior." *Journal of Structural Engineering*, 144(2). DOI: 10.1061/(ASCE) ST.1943-541X.0001960.

Slovenec, D., Sarebanha, A., Pollino, M., Mosqueda, G., and Qu, B. (2017). "Hybrid Testing of the Stiff Rocking Core Seismic Rehabilitation Technique," *Journal of Structural Engineering*, 143(9). DOI: 10.1061/(ASCE) ST.1943-541X.0001814.

Speicher, M.S. and Harris III, J.L. (2016). "Collapse prevention seismic performance assessment of new special concentrically braced frames using ASCE 41." *Engineering Structures*, 126, 652-666.

Sullivan, T.J., Priestley, M.J.N., and Calvi, G.M. (2008). "Estimating the Higher-Mode Response of Ductile Structures." *Journal of Earthquake Engineering*, 12(3), 456-472. DOI:10.1080/13632460701512399

Taga, K., Kato, M., Tokuda, Y., Tsuruta, J., and Wada, A. (2004). "Hints on How to Design Passive Control Structure Whose Damper Efficiency is Enhanced, and Practicality of This Structure. *Proc. Passive Control Symposium 2004*, Tokyo Institute of Technology, Yokohama, Japan, 105-112. (*in Japanese*)

Takeuchi, T., Chen, X., Matsui, R. (2015). "Seismic performance of controlled spine frames with energy-dissipating members." *Journal of Constructional Steel Research,* 114, 51-65.

Tirca, L., Chen, L., Tremblay, R. (2015). "Assessing collapse safety of CBF buildings subjected to crustal and subduction earthquakes." *Journal of Constructional Steel Research*, 115, 47-61.

Tremblay, R., Robert, N., and Filiatrault, A. (1997). "Tension-Only Bracing: A Viable Earthquake-Resistant System for Low-Rise Steel buildings?" *Proc. SDSS '97 Fifth Int. Colloquium on Stability and Ductility of Steel Structures*, Nagoya, Japan, 2, 1163-1170.

Tremblay, R. (2000). "Influence of Brace Slenderness on the Seismic Response of Concentrically Braced Steel Frames," *Proc. STESSA 2000 Conf.*, Montréal, QC, 527-534,

Tremblay, R. (2003). "Achieving a stable inelastic seismic response for multi-story concentrically braced steel frames." *Engineering Journal*, 40(2), 111–129.

Tremblay, R. and Merzouq, S. (2004). Dual Buckling Restrained Braced Steel Frames for Enhanced Seismic Response. *Proc. Passive Control Symposium 2004*, Tokyo Institute of Technology, Yokohama, Japan, 89-104.

Tremblay, R. and Merzouq, S. (2005). Assessment of Seismic Design forces in Dual Buckling Restrained Braced Steel Frames. *Proc. First Int. Workshop on Advances in Steel Constructions*, Ischia, Italy, 739-746.

Tremblay, R., Atkinson, G.M., Bouaanani, N., Daneshvar, P., Léger, P., and Koboevic, S. (2015). "Selection and scaling of ground motion time histories for seismic analysis using NBCC 2015," *Proc. 11th Canadian Conference on Earthquake Engineering*, Victoria, BC, Paper No. 99060.

Tremblay, R. and Poncet, L. (2007). Improving the Seismic Stability of Concentrically Braced Steel Frames. *Engineering Journal*, 44(2), 103-116.

Tremblay, R., Chen, L., Tirca, L. (2014). "Enhancing the seismic performance of Multi-storey Buildings with a Modular Tied Braced Frame System with added energy dissipating devices." *International Journal of High-Rise Building*, 3(1), 21-33.

Whittaker, A.S., Uang, C.M. and Bertero, V.V. (1990). *An Experimental Study of the Behavior of Dual Steel Systems.* Report. No. UCB/EERC-88/14, Earthquake Engineering Research Center, Univ. of California, Berkeley, CA.

Zaruma Ochoa, S.R. (2017). *Seismic stability of buckling-restrained braced frames*, M.Sc. Thesis, University of Illinois at Urbana-Champaign, Illinois, 178 p.

CHAPTER 6 ARTICLE 3: DETERMINATION OF OPTIMUM CONFIGURATIONS FOR STEEL BRACED FRAMES WITH SEGMENTAL ELASTIC SPINES

L. Chen[1], R. Tremblay[2], and L. Tirca[3]

[1]Graduate Student. Dept. of Civil, Geological and Mining Engineering, Ecole Polytechnique de Montreal, 2500, chemin de Polytechnique, Montreal, Quebec, Canada H3T 1J4 Email: liang.chen@polymtl.ca

[2]Professor. Dept. of Civil, Geological and Mining Engineering, Ecole Polytechnique de Montreal, 2500, chemin de Polytechnique, Montreal, Quebec, Canada H3T 1J4 Email: robert.tremblay@polymtl.ca

[3]Associate Professor. Dept. of Building, Civil and Environmental Engineering, Concordia University, 1515, St. Catherine W., Montreal, Quebec, Canada H3G 1M8 Email: lucia.tirca@polymtl.ca

The article was submitted to the *Journal of Structural Engineering (ASCE)* on August 8, 2018.

Abstract

A simplified analysis method is proposed to predict the response of Segmental Elastic Spines Braced Frames (SESBFs) and select the most appropriate truss segment configuration for a given frame. The method relies on a simplified structure model that can reproduce both the elastic flexural response and inelastic shear response of the braced frame system. The proposed simplified model is described, and a flowchart is presented to illustrate the steps leading to the frame properties required to achieve the optimum seismic drift response for a given truss segment configuration. In design, the process is repeated for different potential truss segment configurations and their seismic responses are compared to select a suitable configuration for the structure. The application of the proposed procedure is illustrated for a 24-storey building structure located in Vancouver, BC. Five different truss segment arrangements were investigated, and two configurations were identified as appropriate for the structure. Final design of the four most promising candidates was performed to

confirm the findings from preliminary design and the comparison confirmed that the proposed method and simplified analysis model are suitable tools for the preliminary design of SESBFs.

Keywords

Segmental elastic spine, simplified model, storey drift, drift concentration factor

6.1 Introduction

Elastic vertical truss spines can be introduced in tall steel braced frames to mitigate the development of soft-storey response and increase the redundancy for tall braced frame applications (Tremblay et al. 1997, Ghersi et al. 2000, 3003, Tremblay 2003, Merzouq and Tremblay 2006, Rossi 2007, Tremblay and Poncet 2007, Mar 2010, Lai and Mahin 2015, Simpson and Mahin 2018). Figure 1a shows a non-uniform inelastic drift profile anticipated for a conventional EBF structure. In the tied braced frame (TBF) system shown in Figure 6-1b, vertical tie members are added to the original EBF to form two stiff elastic vertical trusses that can prevent storey drift concentrations over the frame height. To improve cost-efficiency of the system, the elastic vertical truss can be segmented along the frame height to reduce the force demand on the truss members while partially retaining the restraining beneficial effect of the elastic truss (Chen et al. 2012, Tremblay et al. 2014, Chen et al. 2018a). This modified frame configuration, shown in Figure 6-1c, is referred to herein as a braced frame with segmental elastic spine, or SESBF. The use of vertical elastic trusses has also been investigated for the retrofit of seismically deficient steel braced frames (Pollino et al. 2017, Balazadeh-Minouei et al. 2018).

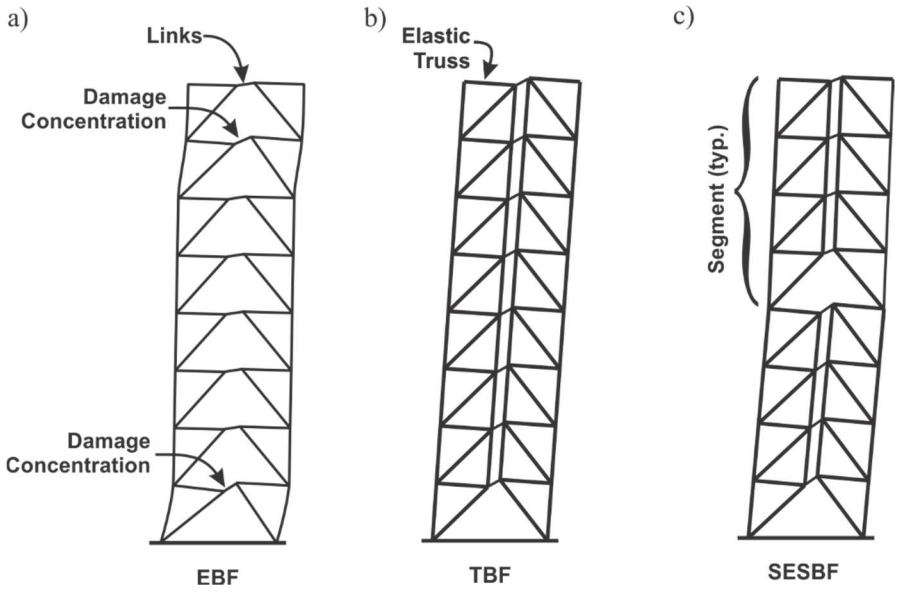

Figure 6-1 Evolution of braced frame systems to mitigate the soft-storey response: a) Eccentrically braced frames prone to damage concentration; b) TBF; c) SESBF

Chen et al. (2018b) have recently proposed a detailed analysis and design procedure for the elastic truss members of SESBFs having one or more truss segments. The method is based on the superimposition of the member forces that are expected to develop upon yielding of the ductile elements of the SESBF to the forces that are generated by the dynamic flexural response of the individual truss segments. That dynamic is due to the floor horizontal masses present along the truss segments and the shear-flexure flexibility of the elastic trusses. The first set of forces can be determined from static analysis whereas response spectrum analysis is used to estimate the second one. The authors validated the proposed method through nonlinear response history analyses (NLRHA) for 8- and 16-storey buildings having different truss segment configurations. The study confirmed the reduction in truss member forces obtained when interrupting the flexural continuity of the elastic truss spine. However, the proposed method does not inform on the maximum number of segments (or minimum height) of truss segments required to achieve stable inelastic response with acceptable storey drifts. For a given structure, design and NLRHA must then be performed for the different potential solutions such that an informed decision can be made for the most suitable configuration, which represents a lengthy and ineffective task.

This article presents a simple and effective procedure that can be used to perform the preliminary design of SESBFs for the selection of the most appropriate truss segment configuration. The method involves, in sequence, static analysis, response spectrum analysis and nonlinear response history analysis of the potential SESBF configurations. In the process, the frame properties are progressively adjusted to achieve the optimum storey drift response for each frame configuration. The method relies on a simplified structure model (SM) used to conduct in a timely manner the nonlinear response history analyses required to obtain inelastic seismic response. The article introduces the proposed methodology and the procedure is then applied and illustrated for a 24-storey office building located in Vancouver, British Columbia. Five different truss segment arrangements are examined to select the appropriate solutions for the structure. Final design of the most promising candidates is performed to verify the adequacy of the method and simplified analysis model that are proposed for preliminary design purposes. Results from NLRHA from the SM of the structures after preliminary design are compared to those obtained using a refined finite element model of the structures after final design. In the article, the design method is applied for SESBFs derived from conventional steel EBFs. It is also used in combination with Canadian seismic design provisions. The method can be easily adapted for other braced frame configurations and for design requirements applicable in other countries.

6.2 Proposed Methodology

6.2.1 Simplified structural model (SM)

A lumped mass-spring model as shown in Figure 6-2 is generally used to perform simplified nonlinear dynamic analysis of seismic force resisting systems (SFRSs) The model consists of lumped masses, m_x, assigned at every floors and shear springs that represent the storey shear stiffness, K_x, and the storey shear resistance of the system, F_{yx}. The model is suitable for SFRSs that deform and yield essentially in shear, as is the case for most steel SFRSs. For tall and slender braced frames, global flexural deformations can be included in the analysis by using springs that deform both in shear and flexure while yielding in shear only. P-delta effects can also be included by adding a leaning column and modelling actual storey heights between floors.

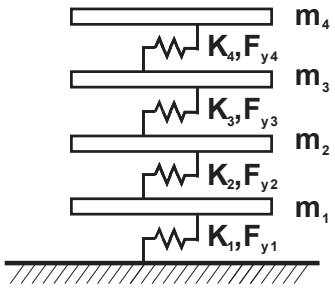

Figure 6-2 Typical lumped mass-spring structural model for 4-storey frame

Lateral response of an SESBF-2 (SESBF with two truss segments) is schematically illustrated in Figure 6-3a. Shear deformation of the system is due to axial deformations in braces and beams plus shear and flexural deformations of the ductile links. These shear deformations increase when yielding takes place in the ductile links. Lateral deformations are also caused by overall bending of the braced frame resulting for axal deformations of the exterior columns. Past studies have shown that peak storey drifts in each truss segment of properly proportioned SESBFs are nearly same (Chen et al. 2018a, b). For the purpose of selecting an appropriate truss arrangement in preliminary design, it is deemed acceptable to assume a unique storey drift amplitude per truss segment and this assumption was used to develop the proposed simplified model shown in Figure 6-3b.

The model includes an elastic column with flexural stiffness EI_b representing the bending stiffness of the braced frame which is essentially provided by the outer columns. That stiffness would therefore vary with column sizes along the frame height. One elastic column is used for each truss segment. The first column is rigidly connected at the base of the structure and a rotational constraint is assigned between the node located at the upper end of the column and the first node at the lower end of the subsequent column to achieve a continuous bending deformation profile along the frame height (θ_b in the figure). Vertical displacements of these two nodes are blocked and a nonlinear spring is used to connect the nodes horizontally. That spring replicates the shear flexibility of the braced frame as well as the yielding response of the truss segments that occurs upon yielding of the ductile links (K_s, F_{ys} in the figure). Hence, drifts due to overall bending and shear deformations are considered in the lateral fame response (Δ_b and Δ_s in the figure). The model also includes a P-delta column which is pinned at the base, has a pinned joint at every segment joint and infinite flexural and shear stiffness properties. Gravity loads contributed by the building floors and

horizontal seismic masses at floor levels (P_x and m_x in the figure) are assigned to this column. In this way, P-delta effects are properly accounted for assuming lateral displacements linearly varying along each truss segment. Parameters involved in the formulation of the preliminary design using the SM are: floor masses m_x, flexural stiffness of the braced frame EI_{bx}, elastic stiffness $K_{s,j}$ and yield strength $F_{ys,j}$ of the horizontal spring for each truss segment j.

The simplified mode presented here can be easily constructed using commercially available computer programs as most components are elastic and inelasticity is concentrated in the springs reproducing yielding of the ductile links. In this study, all the analyses with the SM were performed using SAP2000 analysis software (CSI 2016).

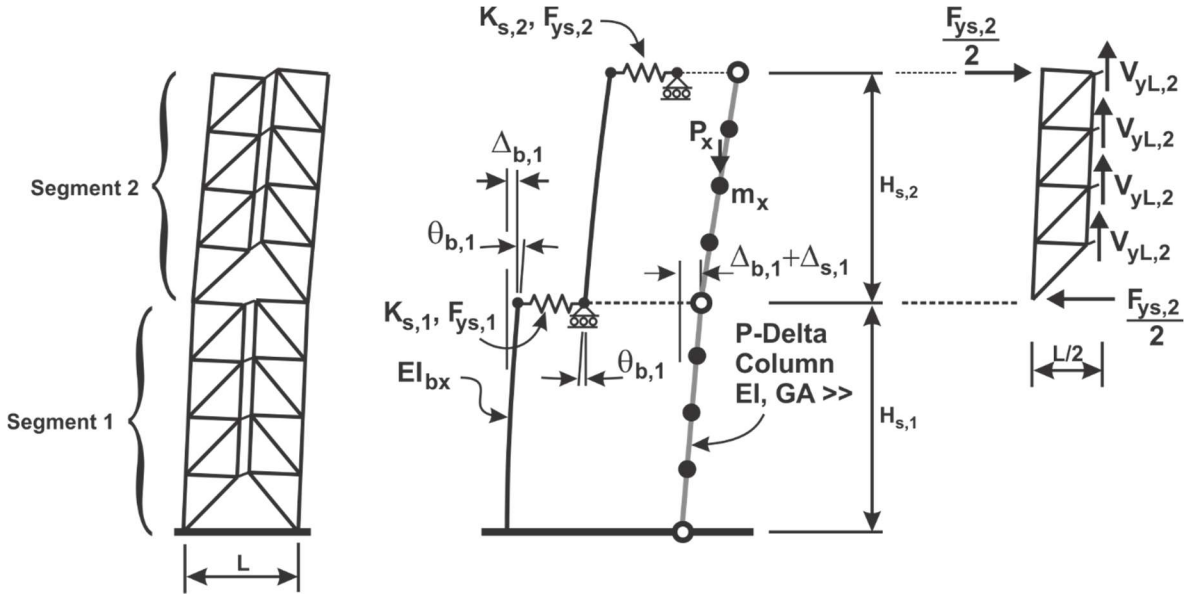

Figure 6-3 SESBF-2 system and its deformed shape: a) Actual frame; b) Simplified model (SM)

6.2.2 Stiffness and strength properties

At the beginning of the design process, gravity loads P_x and masses m_x can usually be determined but stiffness and strength parameters $EI_{b,x}$, $K_{s,j}$ and $F_{ys,j}$ are not known and a first estimate can be obtained from available sources of information, such as code proposed values for periods and code requirements for minimum lateral strength and drift limits under seismic and wind loads. As indicated, the SM is used to perform NLRHA to assess and compare the seismic responses obtained for various truss segment configurations and, eventually conclude on the most promising

configuration which will then be retained for final design. Relying on NLRHA conducted with a simplified model developed with approximate stiffness and strength properties may not be sufficient to give a realistic view of the actual potential of the various truss configuration options.

In the procedure described herein, it is proposed to use the SM within an iterative design process where the model properties are gradually improved to incorporate more realistic and relevant information on the structure and its response generated in the process and, also, to enhance the seismic inelastic response of the structure. In this way, SM analysis will be used to develop a sound preliminary design of each truss segment configuration such that the comparison can be made on more realistic structural options that would be closer to final design. The information generated during the preliminary design would then be used for initiating the final design phase of the selected configuration using the detailed design procedure proposed by Cheng et al. (2018b). The main steps that are proposed to complete the preliminary design phases are briefly summarized in the next paragraph. These steps are also presented in the flow chart of Figure 6-5. Thereafter, a comparison is made between the stiffness properties that are obtained at the end of the preliminary design and those that exhibited by the structures after final design. This comparison is performed for 4 structures that are described in detail in later in the article. It is presented herein to provide an overview of the capacity of the method and appreciate the level of accuracy sought in this preliminary design phase.

Typically, for structures located in high and moderate seismic regions, the process would start with the calculation of the seismic loads from simple equivalent static force procedures (ESFPs) proposed in codes using a structure fundamental period from code empirical equations. Using this seismic demand, preliminary design of key structural components can be performed that are used to obtain preliminary estimates for $EI_{b,x}$ and $K_{s,j}$. The shear strength $F_{ys,j}$ can also be determined from this calculations. Stiffness estimates can be refined by comparing the resulting structure period to code values. Seismic drift limits are also used to adjust as necessary the structure stiffness. Drifts under wind loading can also be verified at this step to ensure the frame has sufficient stiffness. Once the stiffness properties have been verified for all these cases, the process is repeated except that response spectrum analysis (RSA) is recommended to obtain seismic load pattern that better reflects the expected dynamic seismic response of the structure. In Figure 6-4, distribution of storey shears from ESFPs of the NBCC (NRCC 2015) and ASCE 7 (ASCE 2016) for EBFs for

8-, 16- and 24-storey buildings are compared to that obtained from RSA. As shown, static demand from both codes are comparable for all three frames, but RSA gives drastically different results for the 16- and 24-storey frames. After stiffness and strength properties of the SM are adjusted based on RSA, including period and drift verifications, NLRHA is conducted with the SM to examine the storey drift response of the structures. At this step, the amplitude and vertical distribution of the strength F_{ys} are typically refined as necessary to achieve the best storey drift response with the truss segment configuration pattern studied.

Figure 5 presents the ratios between the stiffness $EI_{b,}$ and K_s at the end of the preliminary design to the same values at the end of the final design. Results are presented for four different 24-storey SESBFs configurations: six 4-storey segments (SESBF-6), four 6-storey segments (SESBF-4), three 8-storey segments (SESBF-8), and 5 segments consisting of two 6-storey segments plus three 4-storey segments (SESBF-5). As shown, for both stiffness parameters, the method used to estimate the stiffness in preliminary design gave good predictions of the values obtained at the final design, with differences that are generally less than 20%, except for the flexural stiffness in the building top storeys. It is noted that, for simplicity, the flexural stiffness in the SM was kept constant over the height of each truss segment, using the value determined at the base of the segment. In the final design, column sizes were selected at every other level, which explains why the EI_b ratios between the two models are larger in the upper part of each segment in Figure 6-5a. Smoother variations in the shear stiffness ratios are seen in Figure 6-5b because uniform shear properties were assumed in each truss segment for both the SM and the final structure design, which is typical for SESBFs (Cheng et al. 2018b).

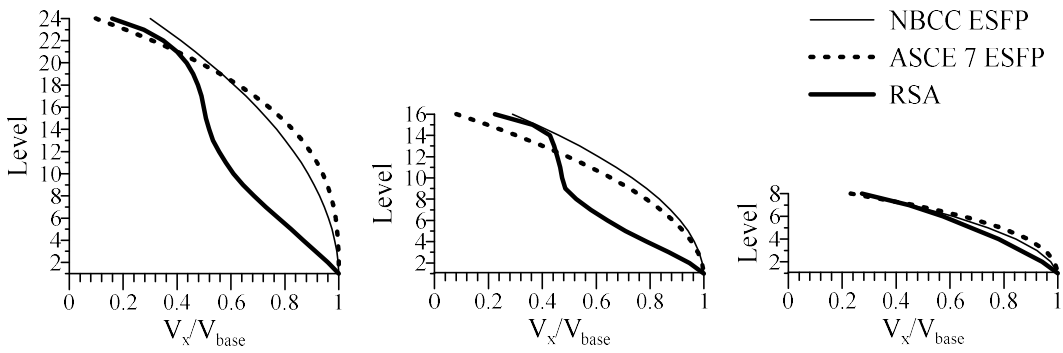

Figure 6-4 Vertical distribution of seismic storey shears from NBCC and ASCE 7 ESFPs and RSA.

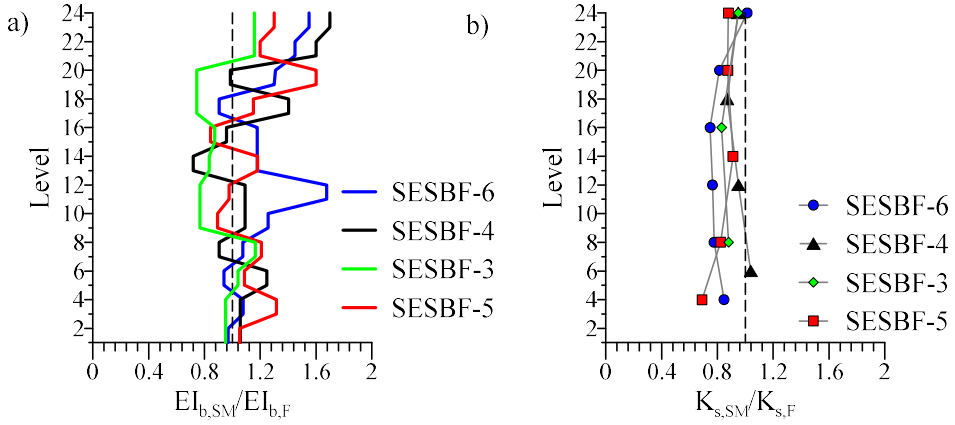

Figure 6-5 Comparison between stiffness values from preliminary design (SM) and after final design (F): a) Flexural stiffness; and b) Shear stiffness.

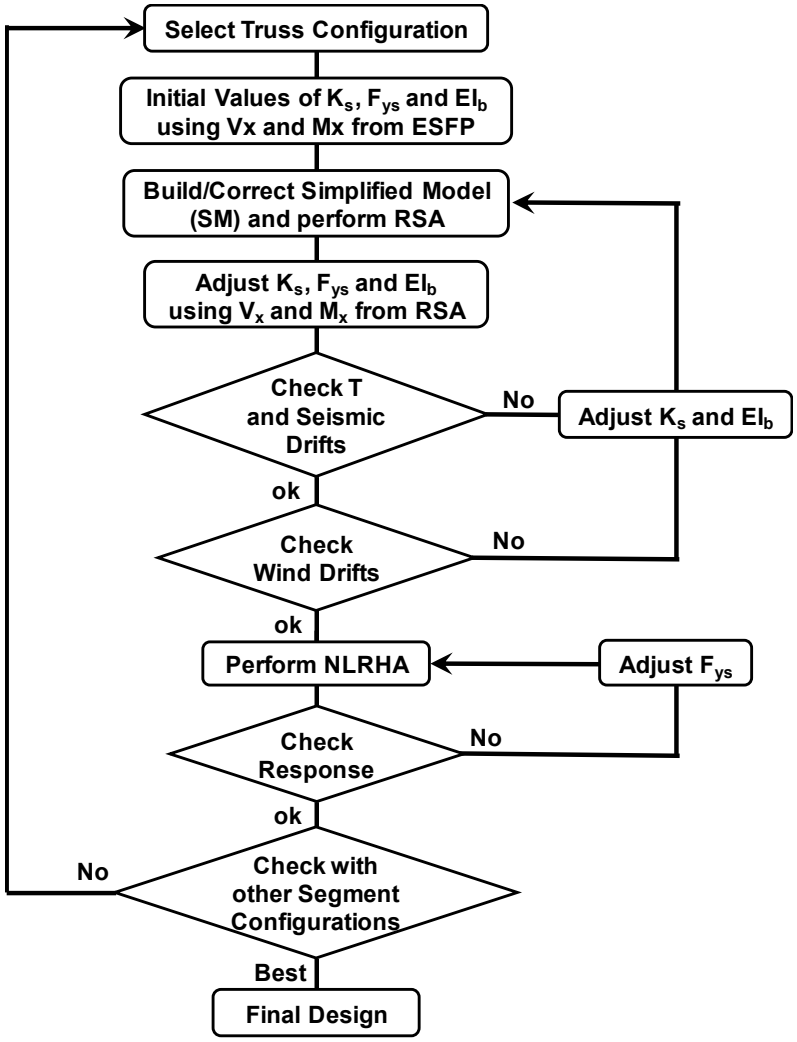

Figure 6-6 Flowchart of the preliminary design process for SESBFs using the SM

6.3 Detailed Procedure

This section presents with greater details the main steps of the preliminary design performed with the SM. In each step, details are provided on how to obtain the required member sizes and/or frame properties and, eventually refine these values. The steps are summarized in the flow chart of Figure 6-6. The procedure is presented for application in Canada when following the provisions of NBCC 2015 and the requirements of the CSA S16-14 steel design standard (CSA 2014). It can be easily adapted to comply with other code documents.

6.3.1 Selection of a truss segment configuration

As discussed, preliminary design is performed to identify among realistic solution candidates one or two truss segment configurations that would be more appropriate for the project. Possible solutions vary from SESBFs with a single continuous elastic truss to braced frames with short segments spanning over only 2 or 3 storeys. More uniform and smaller drifts are expected with the former, but the solution would likely require higher steel tonnage because truss members will be subjected to higher forces. Member forces can be reduced when using shorter truss segments, but this strategy generally results in larger, more variable storeys drift response or, even, structural collapse. Past studies have shown that a good compromise can be obtained with 3- to 6-storey truss segments. The optimum solution also depends on other factors such as the frame height and seismic characteristics of the region. The process can therefore be initiated by starting from one extreme and progressing towards the other one until a suitable configuration is found or starting from an intermediate solution which is then subsequently modified based on the response obtained for the previous configurations.

6.3.2 Determining initial SM properties using ESFP

For a given configuration, preliminary design starts by determining initial values for the strength and stiffness properties for the nonlinear springs of the simplified model. Those are obtained from seismic design storey shears V_x obtained from the code ESFP. In the NBCC, the design base shear V is calculated from:

$$V = S(T_a)WM_vI_E/(R_dR_o) \quad (1)$$

In this equation, S is the design spectrum defined using uniform hazard spectral ordinates established for a probability of exceedance of 2% in 50 years, T_a is the building fundamental period for design, M_v is a factor that accounts for higher mode amplification on base shear, an importance factor I_E, the building seismic weight W, and the ductility- and overtrength-related force modification factors R_d and R_o. In this study, the period Ta was taken equal to the upper limit prescribed for braced steel frames, i.e., $T_a = 0.05h_n$, where h_n is the total height of the structure in meters. NBCC also requires that the design base shear V be not less than the values computed at T_a

= 2.0 s, i.e., $V = S(2.0)M_v I_E W/R_d R_o$, a limit that applies to taller structures. The distribution of the seismic lateral forces F_x along the building height is determined from:

$$F_x = (V - F_t)\frac{w_x h_x}{\sum_{i=1}^{n} w_i h_i} \quad (2)$$

where F_t is a concentrated load applied at the roof level to account for higher mode effects on storey shears, and w_x and h_x are the floor seismic weights and the elevations of the floor levels from the ground, respectively. For structures with T_a longer than 0.7 s, $F_t = 0.07 T_a V$, without exceeding $0.25V$; $F_t = 0$ when $T_a \leq 0.7$ s. Storey shears V_x obtained from forces F_x are used to determine the yield resistance of the ductile links, V_{yLx}:

$$V_{yL,x} = V_x \frac{h_{sx}}{L} \quad (3)$$

where h_{sx} is the storey height. Note that short links yielding in shear are used in the structures studied. The same procedure would apply to longer links yielding in flexure. As shown in Figure 6-3, yield forces $F_{ys,j}$ for each truss segment j can then be calculated by moment equilibrium of the free body diagram of half the braced frame width:

$$F_{ys,j} = 2\sum V_{yL,x}\frac{L/2}{H_{s,j}} \quad (4)$$

where $H_{s,j}$ is the height of the truss segment. An initial estimate of the stiffness $K_{s,j}$ in the SM could be set proportional to the link shear strengths. Richard et al. (2010) developed and validated an expression to predict the storey shear stiffness k_{sx} of EBFs based on the design storey shear V_x and the geometry of the frame:

$$k_{sx} = 1.35\, V_x \left(\frac{E}{F_y}\right)/[0.72(1.19 - 0.092L_d)\left(\frac{L_d^2}{a}\right) + \left(\frac{0.13La}{h_{sx}}\right) + \left(\frac{1.71\ \ sxe}{L}\right) + \left(\frac{0.21eh_{sx}}{d}\right)] \quad (5)$$

In this equation, F_y and E are the steel yield strength and Young's modulus, L_d is the length of the braces, a is the beam length outside the link, h_{sx} is the storey height, e is the length of the shear link, d is the depth of the I-shape link, and L is the width of the braced frame. Note that the values in Eq. (5) are in SI units. The equation accounts for the deformation of the beams, braces and links. It can be also used to calculate the stiffness $K_{S,j}$ for each truss segment assuming an average shear stiffness corresponding to $V_x = F_{ys,j}/n$, where n is the number of links in the truss segment:

$$K_{s,y} = 1.35\frac{F_{ys,j}}{n}(\frac{E}{F_y})/[0.72(1.19 - 0.092L_d)\left(\frac{L_d^2}{a}\right) + \left(\frac{0.13La}{h_{sx}}\right) + \left(\frac{1.71\ \ _{sx}e}{L}\right) + \left(\frac{0.21eh_{sx}}{d}\right)] \quad (6)$$

The flexural stiffness EI_b is directly related to the cross-sectional area of the braced frame exterior columns, A_c, and the distance between the columns (L):

$$EI_b = \frac{2EA_c}{(L/2)^2} \quad (7)$$

A preliminary estimate of EI_b can therefore be obtained by determining the minimum required value for A_c to resist axial compression forces from gravity, C_{grav}, plus seismic loads. Seismic induced axial loads can be taken obtained from the overturning moment M_x from code specified seismic loads amplified by the ratio between factored and probable resistances of the ductile links. In CSA S16-14, the latter is equal to the link nominal shear resistance augmented by 1.1 (difference between probable and nominal yield strengths) and 1.3 for strain hardening effects. For the design of columns in multi-storey EBFs, it is permitted in CSA S16 to apply a reduction factor of 0.9 to link probable resistances to account for the lower likelihood of having all links developing simultaneously their strain hardened resistances. When combining all the applicable factors, the link probable resistance is 1.3/ϕ times the factored link resistance, with ϕ = 0.9, which means that the column cross-section A_c can be obtained from:

$$A_c = \frac{1}{0.8Fy}\left(C_{Grav} + \frac{1.3\ M_x}{0.9\ L}\right) \quad (8)$$

In this expression, the 0.8 factor accounts for resistance factor (0.9) and slenderness effects in column design. It also accounts for additional column axial loads resulting from higher mode response of the truss segments that are not included in Eq. 8 (Chen et al. 2018b). In CSA S16, columns in EBFs must be designed as beam-columns to resist accidental bending moments equal to 20% of their plastic moment capacities. This allowance is not considered here as moments in columns of SESBFs are limited by the stiffness of the elastic vertical truss.

Values of EI_b from Eqs. 7 and 8 only need to be performed at levels where column splices are expected in the structure. These column properties are then used up to the next column splice. For simplicity, the same column properties can be assigned at all columns of each truss segment.

6.3.3 Construct the SM model and perform RSA

The initial properties are introduced in the simplified model (SM) and a response spectrum analysis (RSA) is performed to obtain more realistic estimates of Vx and M_x that are used to refine the amplitude and vertical distribution of the strength and stiffness properties of the structure. In NBCC, results from RSA must be scaled such that the base shear from analysis is at least equal to $0.8V$ from Eq. 1 (or V for structures with irregularities). This scaling requirement is expected to affect the design of taller frames for which code prescribed minimum base shear values may control. In NBCC, this is the case for frames having a fundamental period longer than 2.0 s and this scaling was applied in the examples presented later. Using the RSA results, strength and stiffness properties are adjusted using Eqs. 3 to 8. Because RSA results depend on the structure stiffness, this step may need to be repeated until convergence is reached. The verifications in the following two steps may be included in these iterations.

Figure 6-7 compares distributions of V_x obtained from ESFP and RSA for the 24-storey SESBF-6 structure example discussed later. Storey shears from the SM are obtained for each of the 6 truss segment (forces in the horizontal springs linking the truss segments). In this figure, the SM analysis was performed using properties based on the final design of the structure. Results from RSA performed with a refined finite element model of the final SESBF design is also plotted for comparison. As shown, the proposed SM can predict well the dynamic seismic demand for SESBFs.

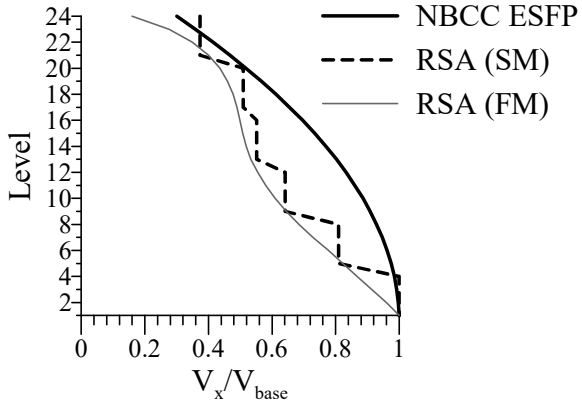

Figure 6-7 Storey shear distribution pattern for the 24-storey SESBF-6 configuration.

6.3.4 Verification of the fundamental period and seismic drifts

Stiffness values in previous steps were indirectly obtained from ultimate limit states and may not reflect the actual properties after final design, especially if serviceability limit states affect the design. To ensure that RSA and, subsequently, NLHRA, are performed with realistic stiffness properties, it is therefore recommended that values of EI_b and K_s be adjusted as needed early in the process. One parameter that can be first examined is the fundamental period of the structure. The period obtained from the SM can be compared to the code upper limit on design period and/or fundamental periods obtained for comparable braced frames in similar seismic conditions. For instance, Figure 6-8 compares the fundamental period from dynamic analysis (T_d) to the NBCC upper limit on T_a for braced frames (= 0.05 h_n) for 48 EBFs in western Canada studied in previous research (Koboevic and David 2010, Mansour et al. 2011, Faucher 2017, Chen et al 2018a, 2018b). The figure shows that the fundamental period of a Tied EBF is expected to be approximately equal to 1.3 times the code upper limit on T_a. Stiffness values from the previous step should be adjusted if the period obtained from the SM deviates significantly from this value.

Storey drifts obtained from RSA performed with the SM should also be used to adjust as necessary the stiffness properties of the structure. Shear stiffness K_s should be augmented if drifts from analysis consistently exceed the code limit over the frame height. Adjusting the flexural stiffness EI_b at the structure base is more appropriate when excessive drifts are concentrated in the upper floor levels.

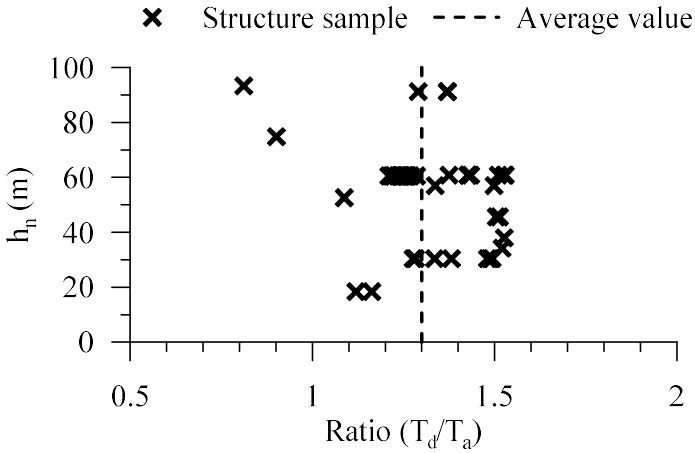

Figure 6-8 T_d/T_a for braced frames in past studies

6.3.5 Verification of the wind drifts

For tall frames or regions where wind loading is high, drift limits or peak horizontal accelerations under wind loading may govern the design of the braced frame. In this case, it is advisable to use the SM to perform an analysis under wind loading and adjust the stiffness properties to satisfy the applicable code limits. Under wind loading, storey drifts in the upper part of the structure are often critical and those can be effectively controlled by augmenting the braced frame flexural stiffness in the lower storeys.

6.3.6 Performing NLRHA

Once stiffness and strength properties of the SM have been adjusted as described in the previous steps, the model can be used to perform preliminary nonlinear response history analyses (NLRHA) to verify the inelastic seismic response of the frame with the truss segment configuration studied. The analyses can be performed using a limited number of ground motions selected among the ones imposing more critical demand. In the SM, the F_{ys} values assigned to the nonlinear springs must be the ones obtained from RSA performed on the SM model with the latest adjusted stiffness properties. In the SM, a suitable hysteretic model should be assigned to the nonlinear springs to properly reproduce the expected cyclic inelastic response expected for the ductile elements of the system.

6.3.7 Verification of NHLRA results

Storey drift response from NLHRA is compared to code seismic drift limit. Uniformity of the drift response over the frame height (variation of storey drifts between truss segments) can also be used to evaluate the adequacy of the response. If deemed appropriate, the strength assigned to truss segments can be adjusted to correct excessive nonlinear storey drifts. A few analysis-adjustment iterations can then be performed at this step to obtain the best possible response for the truss segment configuration studied. For consistency, the corrections made to F_{ys} can also be made to K_s values as both properties are not independent. Marked deviations in the required vertical strength profile compared to RSA analysis may indicate that the truss segment arrangement examined is not appropriate for the structure.

6.3.8 Comparison with other truss segment configurations

The process is repeated for other potential truss segment configurations and responses obtained for all chosen solutions are compared to select the most promising candidate(s) for final design.

In this article, storey drift response is used to evaluate and compare truss segment configurations, which is a natural choice for evaluating and comparing the merits of various truss spine designs. As indicated, steel tonnage generally reduces as the number of truss segments is increased, whereas storey drifts typically increase and become less uniform when taking this direction. Hence, a cost-effective solution is often selected as the case that utilizes the largest number of truss segments while exhibiting an acceptable drift response. This objective forms the basis of the selection of the second and subsequent truss segment configurations to be examined.

6.3.9 Final Design

The design procedure presented in Chen et al. (2018b) can be used for the final design of the SESBF with the selected configuration(s). A frame design is needed to initiate this design procedure and rapid convergence can be achieved by using a design that has the stiffness and strength properties obtained at the end of the preliminary design phase. The ductile link segments in each truss segment would therefore be selected to develop the required F_{ys} values and beam and bracing members would be selected to resist forces induced by these links, according to capacity design. Similarly, column sizes would be selected to resist axial loads from gravity loads plus forces imposed by the ductile links while also satisfying the required flexural stiffness EI_b determined in the preliminary design process.

6.4 Design Example

This section illustrates the choice of the truss segment configuration for a 24-storey building example. Preliminary design is performed for 5 different SESBF configurations and final design is carried out for 4 of these configurations to confirm the findings of the preliminary design.

6.4.1 Buildings studied

The building studied in an office building of the normal importance category located on a class C site in Vancouver, British Columbia. The structure floor plan and specified gravity loads are shown in Figure 6-9. The building is regular in plan and its seismic force resisting system consists of four identical braced frames acting along each orthogonal direction. For simplicity, accidental torsion effects were neglected in design. The storey height is 3.8 m at every floor level, giving a total building height h_n = 91.2 m.

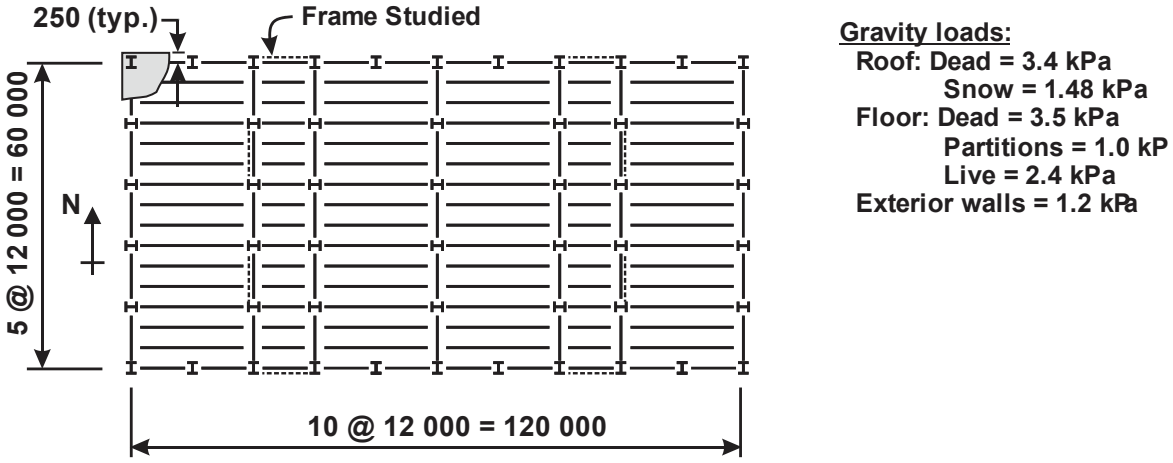

Figure 6-9 Plan view and specified loads of the building studied.

The braced frames acting in the E-W direction were examined and the five different SESBF configurations considered are shown in Figure 6-10. For this example, the process started with a liberal solution with eight 3-storey tall segments and evaluated towards more robust systems having four 6-sorey segments. At the end, an intermediate solution lying between the previous two ones, was also examined.

For this example, a modular (replaceable) link system was adopted, which gives more latitude to the design engineer as the links can be selected independently from the beam segments outside of the links (Mansour et al. 2011). When using modular links, the link length can also be easily varied as needed by extending the beam segments beyond the brace-to-beam connections, but this option was not retained in this study. For simplicity, all links were assumed to have a length of 1.5 m. All beams and columns were assumed to be W shapes conforming with to ASTM A992 whereas ASTM A500, grade C, square tubing was used for the brace and vertical tie members.

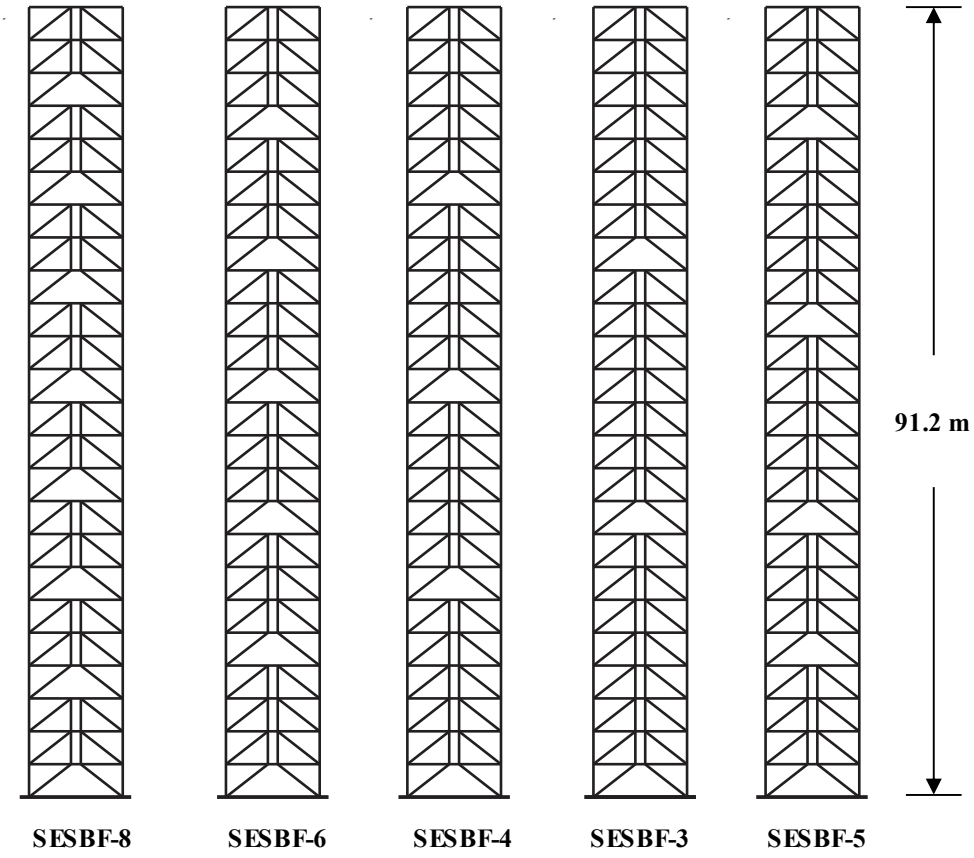

Figure 6-10 The studied SESBF-*n* configurations of the 24-storey building

6.4.2 Preliminary design

The procedure followed for preliminary design for the SESBF-8 configuration is explained hereafter. The same approach was used for the other four configurations. The seismic design base shear V from the NBCC ESFP is first determined using Eq. 1. Spectral ordinates specified for the site are given in Table 6-1 and the period T_a was taken equal to the upper limit permitted by the code, i.e., 0.05 h_n = 0.05 x 91.2 m = 4.56 s. This period is much longer than 2.0 s and the minimum base shear force at calculated with T_a = 2.0 s must be used, which gives S(2.0 s) = 0.26 g. For this structure, M_V and I_E = 1.0 and factors R_d and R_o were set equal to 4.0 and 1.5, respectively, as specified for steel EBFs. The resulting force V was therefore equal to 0.0433 W. The storey shear distribution from ESFP (Eq. 2) is plotted in Figure 6-11a. For each segment, forces F_{ys} for the SM

were determined using the mean V_x value over the height of the segment, as also shown in Figure 6-12a (stepwise increasing curve).

Table 6-1 Design spectrum ordinates for Site Class C, Vancouver

Period (s)	0.0	0.2	0.5	1.0	2.0	5.0	10.0
S_a (g)	0.84	0.84	0.75	0.42	0.26	0.08	0.03

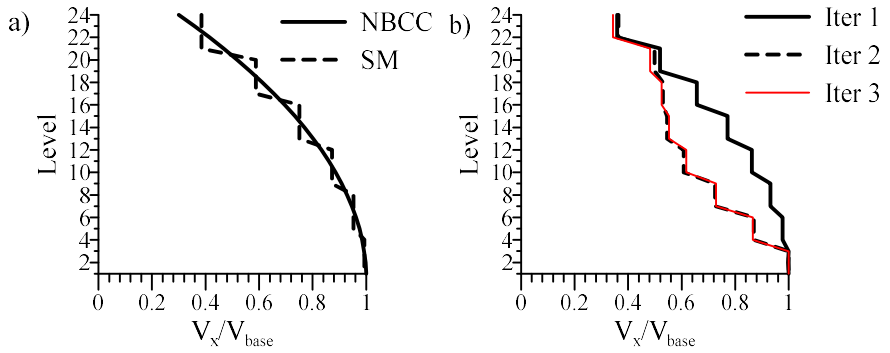

Figure 6-11 Storey shear distributions for the SESBF-8 configuration: a) From ESFP; b) From RSA using the SM.

Values of shear stiffness per storeys and K_S for each segment were obtained using V_x in Eqs. 5 and 6, respectively. The required column sizes were obtained with Eq. 7 from computed seismic overturning moments M_x and gravity induced axial loads C_{Grav} at every level. As indicated in Figure 6-5, values of EI_b were computed at the base of each truss segment and were kept constant over the height of the segments. Masses m_x and total tributary gravity loads P_x for P-delta effects were computed and assigned to the nodes located at every level along the P-delta leaning column of the SM.

Prior to performing RSA with the SM, the fundamental period of the structure was verified against the target value of $1.3T_a$ discussed previously. For this frame $1.3T_a$ = 1.3x4.56 = 5.93 s. From the SM with the calculated K_s and EI_b stiffness properties, the computed fundamental period was found equal to 6.13 s and the SM stiffness properties were increased by $(6.13/5.93)^2 = 1.07$ to obtain more realistic lateral stiffness for the frame.

RSA was then conducted using the SM and the site-specific design spectrum described in Table 6-1. The storey shear distribution in Figure 6-11b (Iteration 2) was obtained from this analysis. The vertical distribution of strength and stiffness in the SM model were adjusted using this seismic demand and the stiffness values were further adjusted to meet the target period. RSA was repeated with the revised values and, as shown in Figure 6-11b (Iteration 3), these changes had nearly no effect on storey the shear distribution.

Seismic and wind induced lateral displacements were both computed using the SM and displacements were computed. Stiffness properties were then adjusted until all applicable drift requirements were met. For the SESBF-8 configuration examined in this example, as well as for SESBF-8, SESBF-6, SESBF-5 and SESBF-4 only required slight increase of the frame flexural stiffness EI_b. For the SESBF-3 configuration, the shear stiffness K_S had to be increased by 10% to satisfy the seismic drift limits in addition to the increasing the frame bending stiffness.

6.4.3 NLRHA

The nonlinear springs were assigned a bi-linear hysteretic (Wen) model for the NLRHA. In the model, the post yielding stiffness and the transition between elastic and inelastic regimes were adjusted to mimic the strain hardening response of ductile EBF links yielding in shear.

The ground motions employed to assess the seismic performance of the structure were selected in accordance with the guidelines of the NBCC 2015 for Vancouver, BC. Three suites of 5 ground motion time histories were selected, one for each of the three earthquake sources contributing to the hazard at the site for a probability of exceedance of 2% in 50 years: M6.5-7.0 shallow crustal (C) earthquakes at short (10-20 km) distance, M6.5-7.0 subduction deep inslab earthquakes (SIS) at a depth of 50-70 km, and M>8.5 subduction interface earthquakes (SIF) at 130-150 km (Goda and Atkinson 2011, Tremblay et al. 2015). Scaling was performed for each suite over their respective scenario-specific period ranges T_{RS} where they dominate the hazard. Response acceleration spectra of the scaled records are plotted in Figure 6-12 against the design spectrum. Nonlinear dynamic analyses were conducted on the SM using a direct integration scheme. P-Delta effects were included in the analyses.

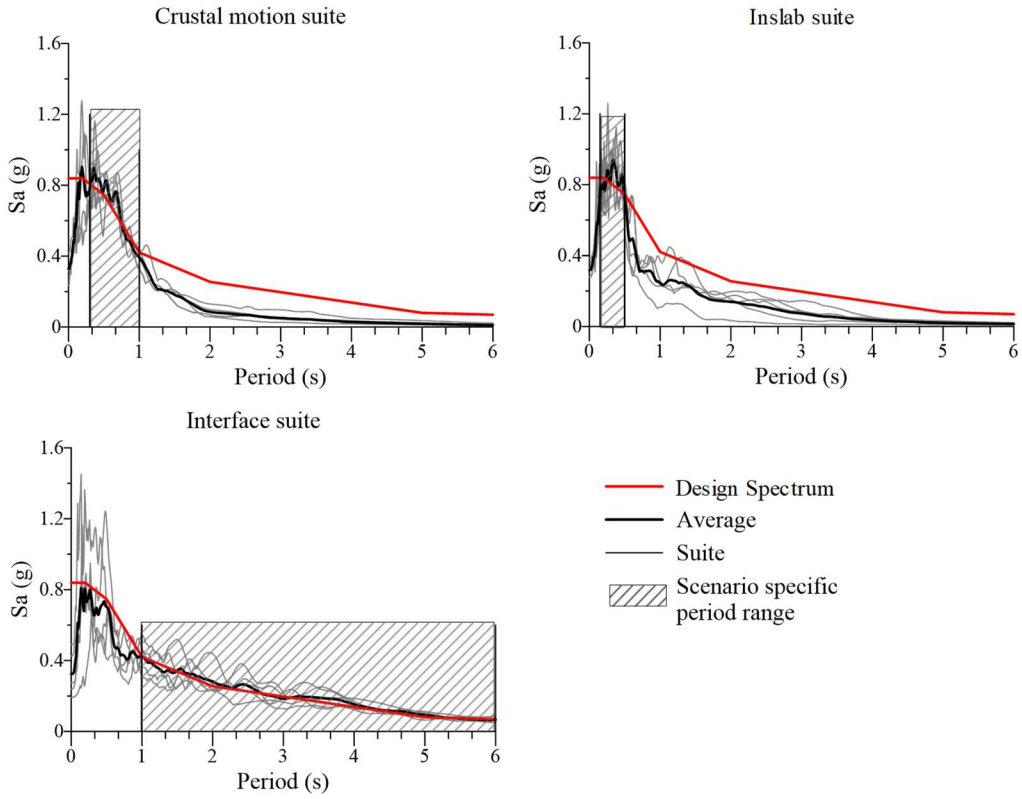

Figure 6-12 Acceleration response spectra of the scaled ground motion records.

Table 6-2 selected ground motions

No.	*Date*	*Event Name*	*Station*	*Component*	M_w	*SF*
C1	1989-10-18	Loma Prieta	BRAN	0	6.93	0.52
C2	1994-1-17	Northridge-01	Simi Valley –Katherine Rd	0	6.69	0.53
C3	1994-1-17	Northridge-01	Canyon Country- W Lost Cany	270	6.69	0.68
C4	1994-1-17	Northridge-01	Sun Valley –Roscoe Blvd	0	6.69	1.16
C5	1994-1-17	Northridge-01	LA - Saturn St	110	6.69	0.8
SIS1	2001-02-28	USA, Nisqually	Gig Harbor Fire Station	270	6.8	2.4
SIS2	1949-04-13	USA, Olympia	Olympia Hwy Test Lab	356	6.7	1.65
SIS3	1949-04-13	USA, Olympia	Olympia Hwy Test Lab	86	6.7	1.35
SIS4	2001-03-24	Japan, Geiyo	SMN012	N-S	6.8	2.31
SIS5	2001-01-13	El Salvador	HSRF	0	7.7	0.66
SIF1	2011-03-11	Japan, Tohoku	AOM028	NS	9	3.8
SIF2	2011-03-11	Japan, Tohoku	FKS021	EW	9	3.46
SIF3	2003-09-26	Japan, Tokachi-Oki	HDKH01	NS2	8	2.6
SIF4	2011-03-11	Japan, Tohoku	TCGH09	NS2	9	2.82
SIF5	2011-03-11	Japan, Tohoku	YMTH12	NS2	9	3.97

Peak storey drifts from NLRHA are plotted in Figure 6-13 for the SESBF-8 configuration. In this example, the 84% percentile value from the 15 ground motions was used to assess the seismic response. As shown, this frame exhibited storey drifts consistently increasing towards the roof level. In the top storey, the maximum 84th percentile value exceeds the limit of 2.5% h_s specified in the NBCC for buildings of the normal importance category. For this frame, an attempt was made to improve the reduce the storey drifts in the upper level by slightly increasing the strength F_{ys} in of the upper segment. This change resulted in much larger drifts in the lower truss segment, indicating that this configuration with short segment was sensitive to variations in lateral resistance similar to a conventional EBF. Because of the excessive storey drifts and high sensitivity of the response to slight modification in strength properties, this configuration was discarded and the preliminary design process was pursued for the other configurations.

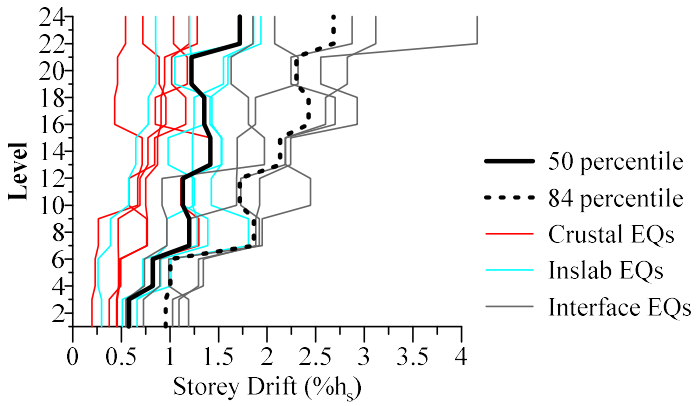

Figure 6-13 Storey drift profiles from NLRHA with the SM for the SESBF-8 configuration.

To investigate the benefits gained by using fewer and taller truss segments, configurations SESBF-6, SESBF-4, and SESBF-3 were proposed and preliminary designed as described above. The storey drifts response obtained for each configuration are plotted in Figure 6-14a to 14c, respectively. As expected, storey drifts gradually reduce and become more uniform when using more restraining elastic vertical truss segments. The maximum 84th percentile drift meets the 2.5% h_s limit when the number of segments is reduced from 8 to 6. With 4 and 3 segments, it reduces further to 1.8% h_s and 1.0% h_s, respectively. The latter would satisfy the NBCC limit for post-disaster buildings, i.e., a much higher performance level compared to the one generally required for office buildings of the

normal importance category considered in this example. Because this superior response would not be needed and likely require additional steel, it would not be retained for this application.

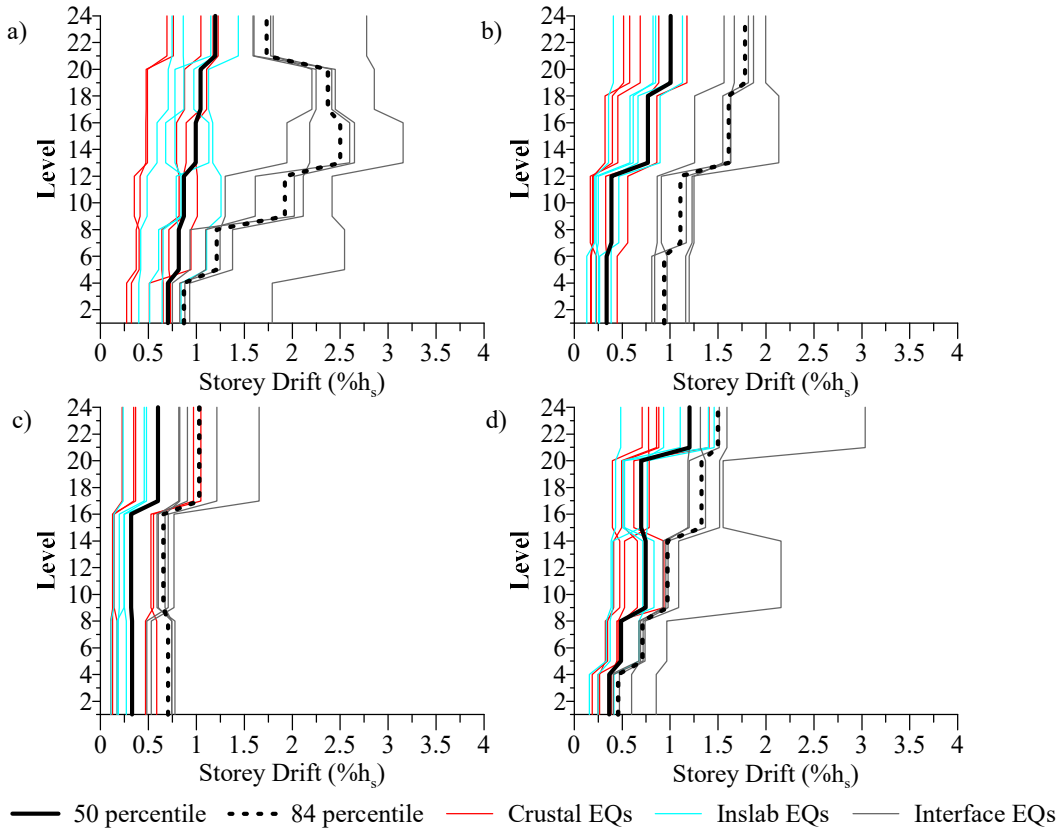

Figure 6-14 Storey drift profiles from SM NLRHA for configurations: a) SESBF-6; b) SESBF-4; c) SESBF-3; and d) SESBF-5.

As indicated, peak storey drifts for the SESBF-6 system just reached the 2.5% h_s code limit. In fact, the storey drifts obtained using storey shears from SM RSA analysis reached 2.6% at levels 13th to 15th corresponding to the 4th truss segment. In the last step of preliminary design, the strength F_{ys} for that 4th segment was increased by 10%, which permitted to reduce the drift to the satisfactory value shown in Figure 6-14a. Considering that this design barely met the NBCC limit and the SESBF-4 configuration exhibited better storey drift response, it was decided to develop an intermediate solution and with 5 truss segments which was expected to achieve a more robust response compared to SESBF-6 structure. For this SESBF-5 configuration, two 6-storey segments as used in SESBF-4 were used from levels 9 to 20 to control the large storey drifts observed in SESBF-6 at these levels. Truss segments covering 4 storeys were kept for levels 1 to 8 and levels

21 to 24. As shown in Figure 6-14d, the peak storey drift response for this hybrid truss configuration was clearly improved compared to SESBF-6. Surprisingly, peak storey drifts for this last SESBF-5 design were also smaller than those obtained with the SESBF-4 configuration with four 6-storey truss segments. This shows that the complex nonlinear response of this braced frame system may not always correspond to expectations based on intuitions and experience. In this context, it is important that preliminary design with NLRHA be performed for all plausible configurations so that the best option can be identified. In this context, having access to a simple and effective analysis model that considerably eases NLRHA, as the one proposed herein, represents a very valuable tool for achieving cost-effective solutions in day-to-day practice.

In Figure 6-13 and Figure 6-14, it is noted that the subduction interface earthquake (SIS) records imposed the largest displacement demand for this tall braced frame building. Ground motions from inslab and crustal earthquakes were generally less critical. This difference is attributed to the dominant period exhibited by the ground motions of each suite, as revealed by the spectra presented in Figure 6-12. Maximum peak storey drifts among all floors under each ground motion are presented for each frame in the upper part of Figure 6-15. The figure confirms the greater severity of the ground motions generated by subduction interface earthquakes for this structure (ground motions nos. 11 to 15), clearly indicating that large earthquakes expected to occur in the Cascadia subduction zone must be considered when assessing the seismic performance of structures located in southwest British Columbia and the northwest region of the U.S.

Peak values of drift concentration factors (DCF) for all structures and ground motions are presented in the bottom part of Figure 6-15. DCF is the ratio between the peak storey drift among all floors and the peak roof drift (MacRae et al. 2004). It is an indicator of the distribution of the storey drift along the frame height, with lower values reflecting more uniform response. It can therefore be also utilized when evaluating and comparing the response of the different frame configurations in preliminary design. Figure 15 show that the SESBF-3 system outperformed the other frames for both the amplitude and distribution of peak storey drifts. This confirms the advantage of taller segments for damage distribution. The SESBF-5 and SESBF-4 configurations also exhibit excellent storey drift response under the most demanding interface subduction (SIF) motions. For all frames, satisfactory storey drift amplitudes were imposed by the crustal and inslab subduction earthquakes. These records however produced relatively higher DCF values compared to the SIF

motions, likely because of their shorter dominant periods generating more pronounced contributions from higher modes and, thereby, greater differences in storey drifts. Under these ground motions, the SESBF-4 configuration offered better DCF response than the SESBF-5 one because of the taller truss segment limiting localized storey drift response.

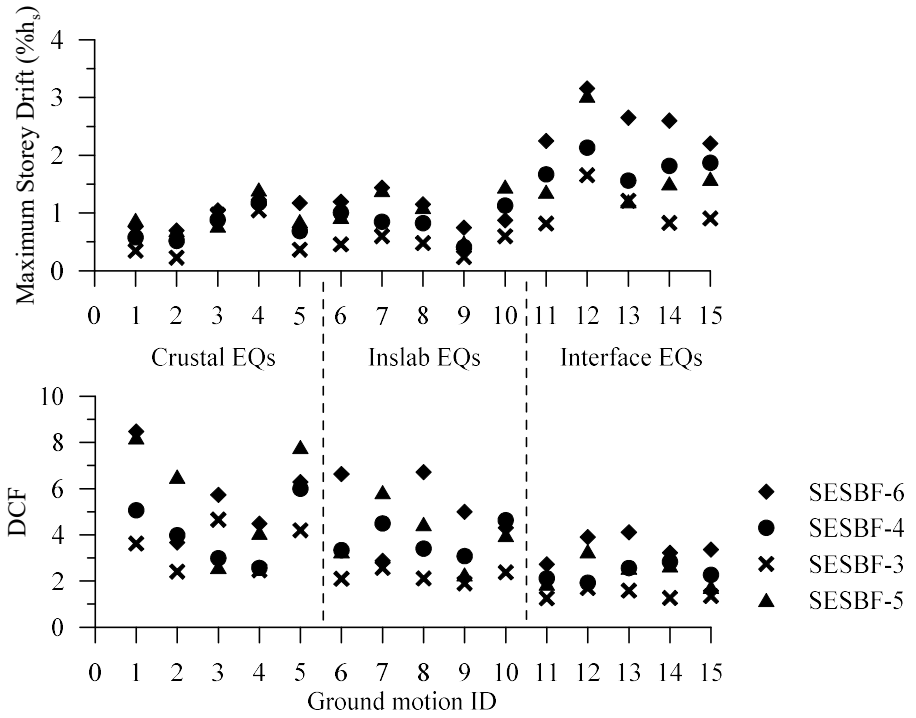

Figure 6-15 Peak storey drifts and drift concentration factor (DCF) from SM NLRHA.

6.4.4 Final Design

Final design was performed for the four SESBF configurations that displayed adequate response in preliminary design. The approach used for the final design is described in Chen et al. (2008b) and is briefly summarized herein for completeness. NLRHA of the final designs was then performed using a refined finite element structure model (FM) developed on the OpenSees platform (McKenna and Fenves, 2004). Final design solutions are presented and the findings are compared with the expectations from preliminary design. Storey drift responses from NLRHA performed with the SM in preliminary design are compared to those obtained for the final design solutions with the FM.

6.4.4.1 Design Procedure

The first step in design consists in selecting W sections for the links using the link force demand from the RSA performed in the last iteration of the preliminary design. As discussed, the same section was used for all links within each segment and the average force demand per truss segment was therefore considered in design. Because link sections are selected from a discrete set of available shapes, some degree of overstrength is created when using actual shapes in the final design compared to the theoretical F_{ys} values considered in the SM mode. The overstrength for the selected links is illustrated in Figure 6-16 using ratios between design factored shear V_f and factored shear resistances of the links V_r. As shown, similar and consistent levels of overstrength, not exceeding 10%, were introduced in all four frames.

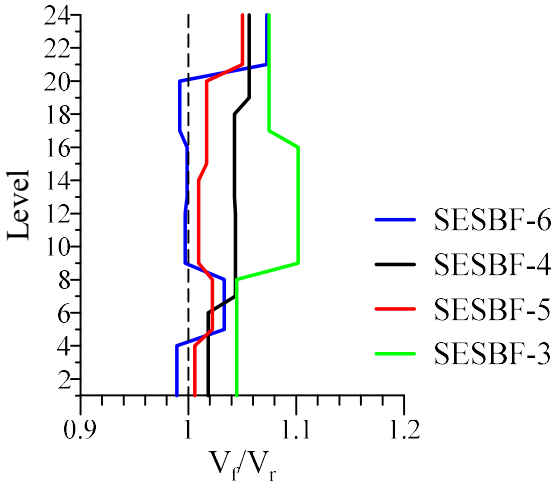

Figure 6-16 Link overstrength for the SESBF-6, SESBF-4, SESBF-5 and SESBF-3 configurations.

The design of the truss members is performed in a second step. Member forces from gravity and seismic effects are combined to obtained design forces. In the method proposed by Chen et al. (2018b), seismic induced forces are divided into two components: r_I forces arising upon simultaneous yielding of all links over the frame height, i.e., assuming first mode response in the nonlinear range, and, r_{II} forces resulting from elastic dynamic response in flexure of the truss segments associated with higher modes. The first set of forces is obtained from static analysis under lateral loads triggering yielding of all links, as commonly done in capacity design. The second set

is determined using RSA performed using a structure model with reduced stiffness assigned to the links and a truncated design spectrum to only include effects from higher mode response.

Axial forces in the bracing members, vertical tie members and columns from all three sources (gravity, r_I, and r_{II}) are presented in Figure 6-17 for configurations SESBF-4 and SESBF-6. As shown, r_I forces largely dominate column design and r_{II} forces only impact the design of the braces and tie members. In preliminary design, gravity and r_I forces were considered when determining column cross-section areas A_c for the calculation of EI_b used in the SM model (see Eq. 8). Hence, flexural stiffness properties in preliminary design represented well the values from final design as was shown in Figure 6-5a. Conversely, r_{II} forces affecting brace (and beam) sizes and, thereby, storey shear stiffness, were not considered in preliminary design. For instance, Eq. 5 was developed for conventional EBFs for which r_{II} forces do not exist. This may have contributed to the differences observed in Figure 6-5b between shear stiffness (K_s) values estimated in preliminary design and obtained after final design. Figure 6-17 also shows that the forces in columns and braces of both frame configurations are very similar. Only the forces in the vertical ties are increased when reducing the number of truss segments from 6 to 4. The force demand for the SESBF-5 configuration (not shown in the figure) is nearly identical to that of the SESBF-6 structure.

Properties of the frames after final design are given in Table 6-3. Period values from SM are within 5% of the values computed for the frame final design, which is deemed acceptable considering the much simpler approach used to obtain the SM. As expected, the steel tonnage for the SESBF-3 surpasses the ones required for all other configurations. The SESBF-5 solution required less steel than its SESBF-4 counterpart and only slightly more than the SESBF-6 configuration.

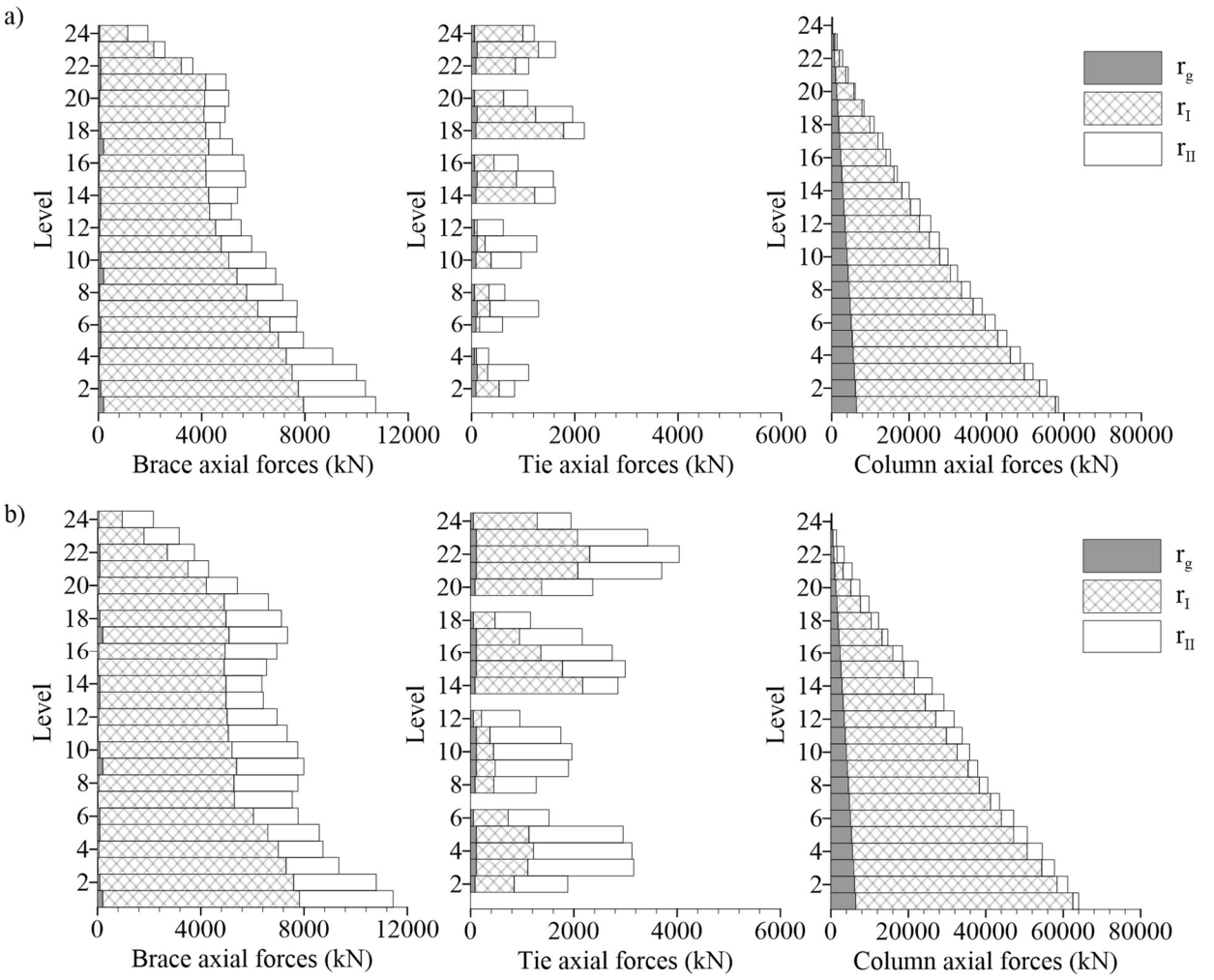

Figure 6-17 Axial force demands in truss members for configurations: a) SESBF-6; and b) SESBF-4.

Table 6-3 Characteristics and storey drift response of the SESBF configurations

Segment type	T_d (SM)	T_d (FM)	Steel tonnage /frame	SM		FM	
				Max drift (84^{th} perc.)	DCF (84^{th} perc.)	Max drift (84^{th} perc.)	DCF (84^{th} perc.)
	(s)	(s)	(t)	(% h_s)	-	(% h_s)	-
SESBF-6	5.92	6.25	274	2.50	6.60	2.52	5.38
SESBF-4	5.93	6.26	308	1.78	4.60	1.60	3.82
SESBF-3	5.54	5.88	371	1.03	3.37	1.36	3.05
SESBF-5	5.96	6.24	277	1.50	6.36	1.61	4.25

6.4.4.2 NLRHA using FM

To verify the accuracy of the storey drifts predicted with SM in preliminary design, detailed finite element models (FM) of the braced frames were developed and used to carry out NLRHA with the OpenSees computer program. The models used Steel02 material for all steel sections. Nonlinear beam-column elements with initial imperfections were used to model the beams, columns, braces and ties. Ductile links were modeled with nonlinear shear springs, elastic beam-column elements and min-max material calibrated against past test results. All gravity columns were included and gravity loads were applied to the structure to account for P-delta effects. Additional information regarding the FM can be found in Chen et al. (2018b).

The FM were subjected to the ground motions given in Table 6-2 and the storey drift demands for all four frame configurations are given in Figure 6-18. Maximum peaks storey drifts among all floor levels and DCF values are summarized in Table 6-3. Values obtained with the SM are also given in the table for comparison. The similitudes between the plots of Figure 6-14 and Figure 6-18 and the excellent agreement between the SM and FM values in Table 6-3 demonstrate that the SM can predict with high accuracy the complex nonlinear seismic response of SESBFs. These results also show that the stiffness and strength properties determined in the preliminary design phase are representative of the properties exhibited by the same frames after final design. For this 24-sorey building example, the FM analyses therefore confirmed the findings from preliminary design that

the SESBF-5 would represent an appropriate braced frame solution with peak storey drifts of 1.5-1.6% h_s. The final design also permitted to conclude that this design would also represent a suitable solution in terms of steel tonnage.

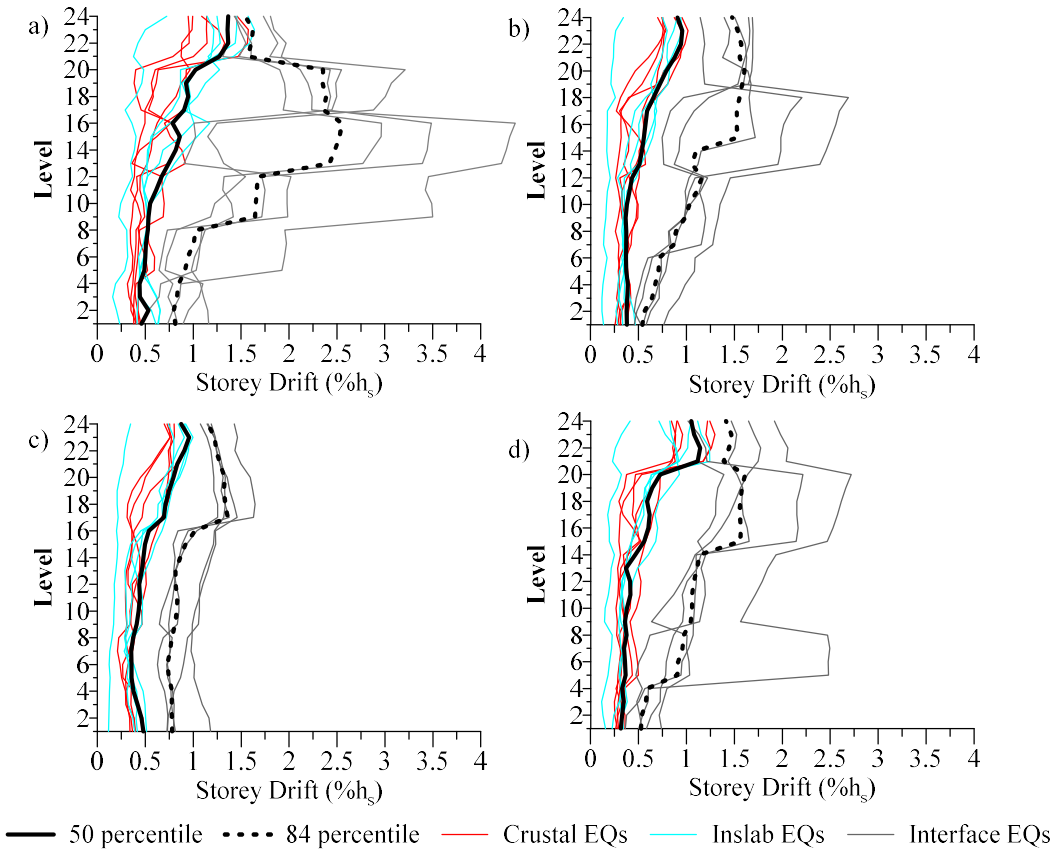

Figure 6-18 Storey drift profiles from FM NLRHA for configurations: a) SESBF-6; b) SESBF-4; c) SESBF-3; and d) SESBF-5.

6.5 Conclusion

A simple method was proposed to perform the preliminary design and estimate the inelastic seismic response of tall steel braced frames with segmental elastic trussed spines (SESBFs) used in building structures. The method is intended to be used for determining the most appropriate configuration for the vertical truss segments. The preliminary design process includes several steps that involve, in sequence, code equivalent static force procedure, response spectrum analysis (RSA) and, finally, nonlinear response history analyses (NLRHA). The method utilizes an easy-to-build and

computationally efficient simplified numerical model (SM) to conduct the required RSA and NLRHA of SESBFs. In the process, the properties of the braced frame are progressively improved such that the seismic response obtained at the end is the best that can be achieved for the truss segment configuration studied. The process can include the analysis under wind loading to ensure that the frame can meet drift and acceleration related serviceability limit states with the stiffness properties used in seismic analysis. The preliminary design method would be applied to all potential elastic truss segment configurations so that a selection for final design can be made by comparing their respective seismic responses.

The application of the proposed method was illustrated for a 24-storey building example. SESBFs with five different configurations were examined and two configurations were identified as appropriate solutions after completion of the preliminary design. Final design was performed for those plus two other configurations to confirm the findings from preliminary design. Stiffness and strength properties determined in preliminary design matched well the values obtained after final design. Storey drift responses from NLRHA performed with the SM model in preliminary design also agrees with those obtained using a refined finite element model of the final design, so that the same conclusion on the most suitable configuration could be drawn after both preliminary and final designs. These results confirm the adequacy of the proposed method and simplified analysis model for the preliminary design of SESBFs.

This study was limited to only one braced frame example and further investigation is needed to confirm its appropriateness for braces frames having different height and geometries.

References

ASCE. 2016. *ASCE/SEI 7-16 Minimum Design Loads for Buildings and Other Structures*. American Society of Civil Engineers. Reston, Virginia, USA.

Chen, L., Tremblay, R., and Tirca, L. (2012). "Seismic Performance of Modular Braced Frames for Multi-Storey Building Applicaton." *Proc. 15th World Conference on Earthquake Engineering*, Lisbon, Portugal, Paper No. 5458.

Chen, L., Tremblay, R., and Tirca, L. (2018a). "Modular tied eccentrically braced frames for improved seismic response of tall buildings." *Journal of Constructional Steel Research* (Submitted)

Chen, L., Tremblay, R., and Tirca, L. (2018b). "Enhanced Seismic Design Procedure for Tall Steel Braced Frames with Segmental Elastic Spines." *Journal of Constructional Steel Research* (Submitted)

CSI. (2016). *SAP2000 - Integrated Software for Structural Analysis and Design*. Computer& Structures, Berkeley, CA.

Ghersi, A., Neri, F., Rossi, P.P., and Perretti, A. (2000). "Seismic response of tied and trussed eccentrically braced frames." *Proc. Stessa 2000 Conf.,* Montreal, Canada, 495-502.

Ghersi, A., Pantano, S., and Rossi, P.P. (2003). "On the design of tied braced frames." *Proc. Stessa 2003 Conf.,* Naples, Italy, 413-429.

Faucher, L.A. (2017). Concept and performance of modular steel eccentrically braced frames. Master thesis. Ecole polytechnique de Montreal.

Goda, K., and Atkinson, G.M. (2011). "Seismic performance of wood-frame houses in south-western British Columbia", *Earthquake Engineering and Structural Dynamics*, 40, 903-924.

Lai, J-W., and Mahin, S.A. (2015). "Strongback System: A Way to Reduce Damage Concentration in Steel Braced Frames." *Journal of Structural Engineering*, 141(9).

MacRae, G., Kimura, Y., Roeder, C.W. (2004). "Effect of Column Stiffness on Braced Frame Seismic Behavior." *Journal of Structural Engineering*, 130(3).

Mansour, N., Christopoulos, C., Tremblay, R. (2011). "Experimental Validation of Replaceable Shear Links for Eccentrically Braced Steel Frames." *Journal of Structural Engineering*, 137(10).

Mar, D. (2010). "Design examples using mode shaping spines for frames and wall buildings." *Proc. 9th U.S. National Conference and 10th Canadian Conference on Earthquake Engineering.* Toronto, ON, Paper No. 1400.

McKenna, F. and Fenves, G.L., (2004). Open System for Earthquake Engineering Simulation (OpenSees). Pacific Earthquake Engineering Research Center (PEER), University of California, Berkeley, CA. (http://opensees.berkeley.edu/index.html)

Merzouq, S., and Tremblay, R. (2006). "Seismic Design of Dual Concentrically Braced Steel Frames for Stable Seismic Performance for Multi-Storey Buildings." *Proc. 8th U.S. National Conference on Earthquake Eng.*, San Francisco, CA, Paper 1909.

NRCC. (2015). *National Building Code of Canada, 14th ed.*, National Research Council of Canada, Ottawa, ON.

Richards, P.W., (2010). Estimating the stiffness of Eccentrically Braced Frames. *Pract. Period. Struct. Des. Contr.*, 15(1): 91-95.

Rossi, P.P. (2007). "A Design Procedure of Tied Braced Frame." *Earthquake Engineering and Structural Dynamics*, 36 (14), 2227-2248.

Koboevic, S. and David, S.O. (2010). "Design and seismic behaviour of taller eccentrically braced frames." *Canadian Journal of Civil Engineering*, 2010, 37(2): 195-208.

Simpson, B.G., and Mahin, S.A. (2018). "Experimental and Numerical Investigation of Strongback Braced Frame System to Mitigate Weak Story Behavior." *Journal of Structural Engineering*, 144(2). DOI: 10.1061/(ASCE) ST.1943-541X.0001960.

Takeuchi, T., Chen, X., Matsui, R. (2015). "Seismic performance of controlled spine frames with energy-dissipating members." *Journal of Constructional Steel Research,* 114, 51-65.

Tremblay, R., Robert, N., and Filiatrault, A. (1997). "Tension-Only Bracing: A Viable Earthquake-Resistant System for Low-Rise Steel buildings?" *Proc. SDSS '97 Fifth Int. Colloquium on Stability and Ductility of Steel Structures*, Nagoya, Japan, 2, 1163-1170.

Tremblay, R. (2003). "Achieving a stable inelastic seismic response for multi-story concentrically braced steel frames." *AISC Eng. J.*, 40(2), 111–129.

Tremblay, R., Atkinson, G.M., Bouaanani, N., Daneshvar, P., Léger, P., and Koboevic, S. (2015). "Selection and scaling of ground motion time histories for seismic analysis using NBCC 2015," *Proc. 11th Canadian Conference on Earthquake Engineering*, Victoria, BC, Paper No. 99060.

Tremblay, R. and Poncet, L. (2007). Improving the Seismic Stability of Concentrically Braced Steel Frames. *Engineering Journal*, 44(2), 103-116.

Tremblay, R., Chen, L., Tirca, L. (2014). "Enhancing the seismic performance of Multi-storey Buildings with a Modular Tied Braced Frame System with added energy dissipating devices." *International Journal of High-Rise Building*, 3(1), 21-33.

CHAPTER 7 EXPERIMENTAL TEST PROGRAM

7.1 Introduction

Chapter 4 investigated the possibility of framing configurations with segmental elastic trusses. The superior seismic response of SESBFs comparing with that of conventional EBFs was demonstrated. Chapter 5 and Chapter 6 presented and validated a practical design and optimization procedure. This chapter describes the design of a set of two large-scale shake table tests. The first test aims to examine the seismic resistance medium-rise chevron braced frames in eastern Canada designed according to NBCC 1980. The second test intents to examine the seismic performance of a SESBF as a retrofitting strategy to the chevron braced frame, while validate the design procedure proposed in chapter 5. A complete report will be available upon the completion of tests.

7.2 Test program

The test program consists of two sets of large-scale shake table tests. The first test is a 30% scale 8-storey chevron braced frame located in Montreal, Eastern Canada. The second test is a 30% scale 8-storey SESBF with 2 4-storey segments. Both specimens will be tested against 4 sets of historical ground motion records that are scaled to match the Uniform Hazard Spectrum of Montreal region defined in NBCC 2015. If a frame survives all tests, the intensity of the input motion will be increased gradually until a pre-defined interstorey drift value is reached. Montreal is selected for the building location because the author wants to investigate the efficiency of the proposed SESBFs for building located in regions with lower seismicity.

7.2.1 Overview

The test program will be carried out in the structural laboratory of Ecole Polytechnique de Montreal. The equipment available in the lab is shown in Figure 7-1 Structural laboratory The primary machine that will be used is the shaketable which is shown as the seismic simulator in the figure.

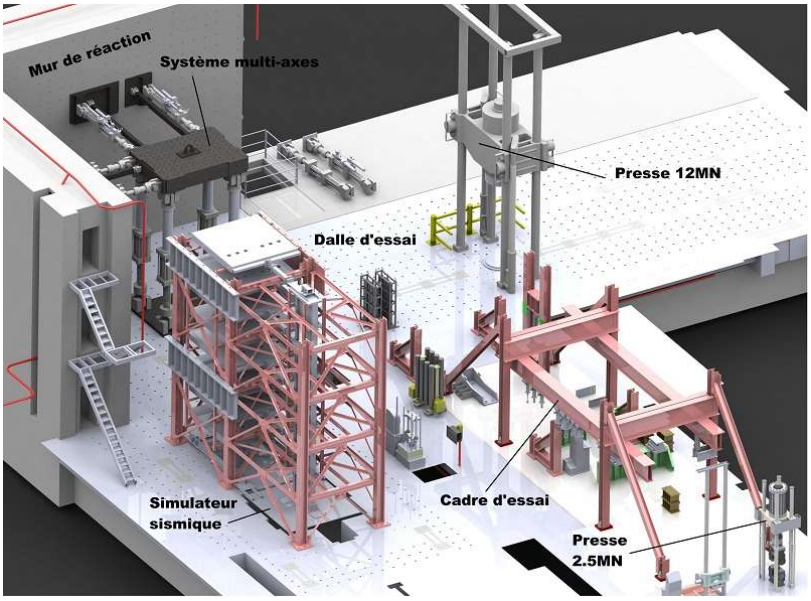

Figure 7-1 Structural laboratory (navigator.innovaton.ca, *École Polytechnique de Montréal*)

The test program designed herein has to adapt to the existing components in the lab, specifically the mass unit which is 62.5 kN each. The heights of floors are also fixed as 4.6m for the ground floor and 3.75m for floors above. Maximum number of storeys are set as eight based on the height limit of the parameter frame.

As stated in the previous section, this test program involves testing of two 30% scale braced frames with seismic simulator as well as other material and member tests that will be required to conduct the shaketable tests. The design of the test specimens will be demonstrated in the section below.

7.2.2 Design of original frames

This section describes the design of both frames in their original geometry.

7.2.2.1 Frame geometry and loads

The prototype building is an 8-storey office building located Montreal region. The height of all storeys except first floor is 3.8 m. The height of first floor is 4.6 m. The building consists 5 bays on both N-S and E-W directions. The width of each bay is 9 m. Dead load is 2.4 kPa for roof and 3.1 kPa for floors. Note that the dead load of floors intentionally assigned so that the seismic weight

of floors is the same as that of roof. This assignment is made due to the limitation of available masses in laboratory.

Snow load on the roof is 1.62 kPa. Live load is 2.4 kPa for floors. Dead load of both partition walls and exterior walls is 1.0 kPa. The plan view and elevation view of the prototype building are shown in Figure 7-2.

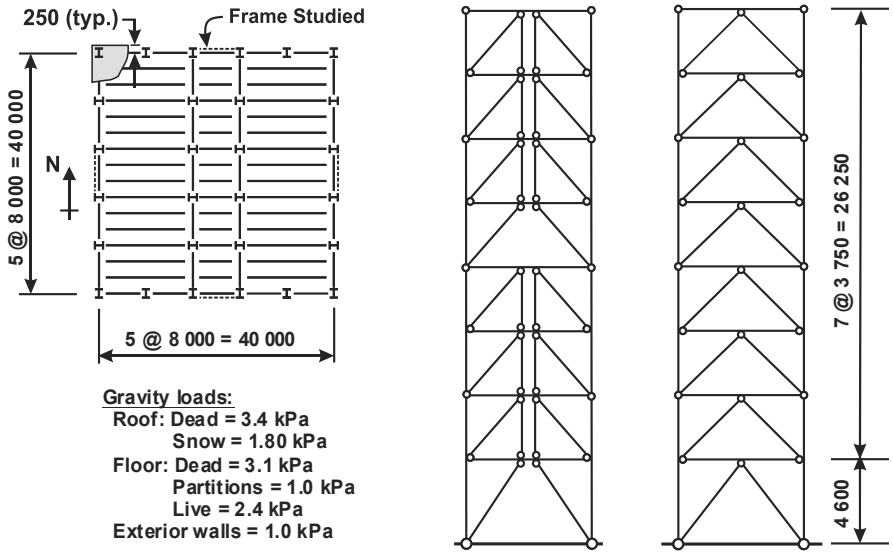

Figure 7-2: Plan view and elevation view of prototype structures

7.2.2.2 Design of chevron braced frame

This section highlights the design considerations and details for designing the chevron braced frame.

The chevron braced frame is designed according to NBCC 1980. There are three main differences between NBCC 1980 and NBCC 2010 for chevron braced frames. Firstly, the equation for calculating the induced lateral load has been changed.

According to NBCC 1980, the base shear of buildings V is calculated as:

$$V = AKI_EFSW \qquad \text{Eq. 7.1}$$

where A is the peak ground acceleration, which equals to 0.04 for hazard zone 2, K equals 1.0 for braced frames, I_E is the importance factor, F is the site-specific modification factor, which is 1.0 for Site Class C and 1.5 for Site Class E, W is the seismic weight of the building. S is related to

the fundamental period T_a of the structure. S is taken as the minimum value of 1 and $\frac{0.5}{\sqrt{T_a}}$. The suggested T_a for steel buildings is calculated as $\frac{0.09h_n}{L^2}$, where h_n is the height of the structure and L is the width of the structure. The suggested period is used for the preliminary design, more accurate period can be calculated with Rayleigh method. Besides the equation itself, seismic forces for buildings located on different site is differentiated by one factor F. From Class C site to Class E site, the induced seismic load for the same structure increased by a flat 50%.

In NBCC 2015, the equation to calculate the base shear of the structure is modified as:

$$V = \frac{S(T_a)I_E M_v W}{R_d R_o} \qquad \text{Eq. 7.2}$$

where $S(T_a)$ is the spectral acceleration of the design spectrum at period T_a, I_E is the importance factor, M_v is the higher modes factor, R_d and R_o are the reduction factor for ductility and overstrength respectively. For conventional frame, Rd and Ro are 1.5 and 1.3. For Type LD (limited ductility) CBF, they are 2.0 and 1.3. In addition, NBCC 2015 also specified the upper and lower bound of V. V shall not be less than $\frac{S(2.0)I_E W}{R_d R_o}$ or greater than $\frac{\frac{2}{3}S(0.2)I_E M_v W}{R_d R_o}$. The code also suggests for Ta, it shall be taken as $0.025h_n$ for braced frames. If the period obtained from dynamic analysis is smaller than the value, Ta can be increased to $0.05h_n$. The site-specific modification factors F_a and F_v are applied at the spectrum level. If dynamic analysis is conducted, the base shear V can be reduced to $0.8V$ but greater than the base shear obtained from dynamic analysis.

As a result, design seismic loads specified in the 1980 code edition are much lower than those prescribed today. For conventional CBF, the base calculated with equations provided by NBCC 2015 is more than twice as the one calculated with NBCC 1980. The storey shear and its distribution alone the building height calculated for the studied structure is shown in Figure 7-3.

The second main difference between the two versions of NBCC is specific for chevron braced frames. In NBCC 1980, the beams in the chevron braced frame are not designed according to strong beam scenario, i.e. the beams are not required to withstand the unbalanced load created by the buckled of braces. Therefore, the frames are prone to fail in a “weak beam storey mechanism”.

The connection design also has been developed to guarantee a ductile failure mechanism over the years. Nowadays, the building code requires all brace connections in the lateral force resisting frame designed with 1.3 times the probable yield strength of braces. While in 1980s, the connections were designed with the factored load.

In additional, the load combinations used for design are also changed. In NBCC 1980, the load combination involves seismic load are listed as below:

$$U = 1.25D + 0.7(1.5L + 1.5E)$$

$$U = 1.25D + 1.5E$$

The factors used for seismic load E are changed to 1.0 in later editions.

Knowing these differences between the two version of codes, four different chevron braced frames were designed according to NBCC 1980 at this stage in order to select the most appropriate frame for experimental test. 2 of them are located on site Class C, with an importance factor of 1.0 and 1.3 respectively. The other 2 are located on site Class E, also with an importance factor of 1.0 and 1.3. The periods calculated from Rayleigh method for all four buildings are shown in Table 7-1.

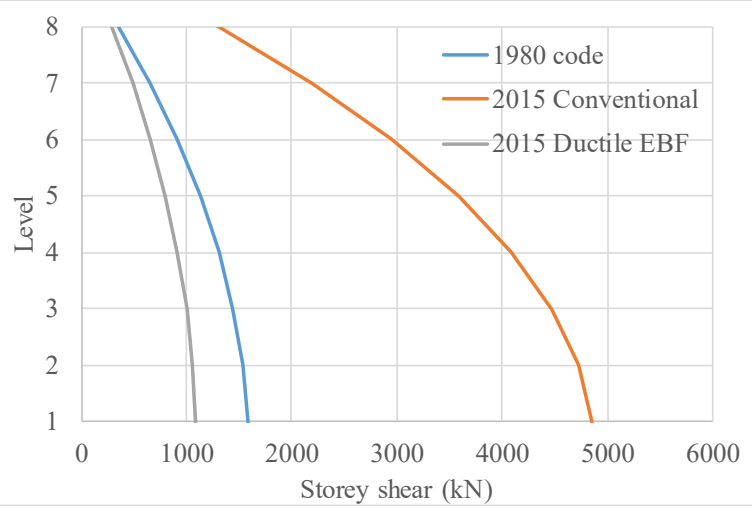

Figure 7-3: Comparison between storey shear of buildings of different configurations

Table 7-1 Periods of structures (sec)

Structure	Tdesign	T1	T2	T3
C-1.0	2.37	2.54	0.88	0.46
C-1.3	2.32	2.49	0.83	0.45
E-1.0	2.26	2.35	0.80	0.43
E-1.3	2.07	2.22	0.76	0.43

7.2.2.3 Selection of the studied frame for test

With limited resource for the experimental test, only one of the four designed chevron braced frames can be selected. The criteria of the selection are the following:

1. The selected frame should be able reflect the critical failure mode of the frame. The inherent limitation of this test program is that the test is performed on a 30% scaled frame. The size of connections makes it very difficult to replicate the connection failure modes in real buildings. Consequently, the primary failure mode that will be investigated in this test is the failure of beams in the chevron braced frame.
2. Due to the limited selection of steel sections, it is preferable to have higher seismic forces that are induced into the frame so that after scaling, most of the members can still be purchased directly.

To select the most representative frame, finite element models of all four frames are built in OpenSees. To assess the performance of the structure more accurately, nonlinear beam column elements are used extensively in these models. The beams, columns and braces all consist of 10 to 20 nonlinear beam column elements with initial imperfections to allow buckling and yielding of these members. Rotational springs that replicate the response of gusset plates are also included. However, since the connection failure is not a concern in this study, no failure conditions were set for these springs. Steel02 material is assigned to all members. The hysteresis response of brace members is calibrated in Chapter 3. For columns, the initial imperfection is set to L/1000, where L

is the unsupported length of the columns. Gravity loads are applied at the top of columns, which is the condition in the tests. Detailed description of the numerical models is discussed in 7.3.1.

Nonlinear dynamic analyses are conducted with these models. The ground motion records used herein are discussed in Sections 7.2.4. The storey drift profiles of frames with importance factor of 1.0 under the selected ground motion records are illustrated in Figure 7-4. Frames with importance factor of 1.3 experienced less damage and are not considered for future discussions. Comparing the seismic response of the two frames, CBF on Class E site experienced greater damage, which makes the frame a good candidate for the experiment.

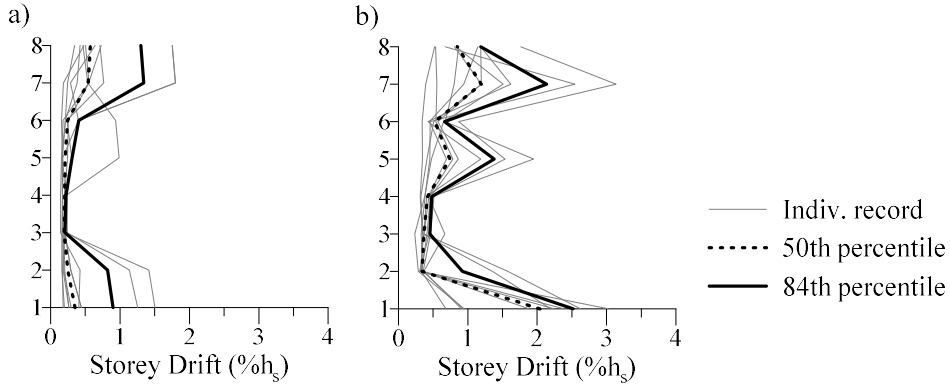

Figure 7-4 Storey drift profile of 8-storey chevron braced frame: a) Class C site; b) Class E site

Therefore, the 8-storey chevron braced frame designed for the building with regular importance and located on Class E site is selected as the target frame in this study. The member sections of the selected frame are shown in Table 7-2.

Table 7-2 Member sections of selected CBF

Floor	Brace	Beam	Column
8	HSS114.3X114.3X6.4	W200X35.9	W310X32.7
7	HSS152.4X152.4X4.8	W200X35.9	W310X32.7
6	HSS152.4X152.4X4.8	W310X60	W310X32.7
5	HSS152.4X152.4X6.4	W310X60	W310X32.7
4	HSS152.4X152.4X7.9	W360X91	W310X32.7
3	HSS152.4X152.4X7.9	W360X91	W310X32.7
2	HSS152.4X152.4X7.9	W360X122	W310X32.7
1	HSS152.4X127X12.7	W360X122	W310X32.7

7.2.2.4 Design of SESBF with 2 segments

With the target frame selected, corresponding SESBF is also designed based on the code requirement today. Based on the experience acquired from the previous studies, it is understood that 4-storey segments generally yield better results for 8-storey SESBFs. Thus, the SESBF is designed to have two equal length 4-storey segments. At the time this program was initiated, the design method was not finalized yet. To have a robust and cost-efficient system without knowing a sophisticated method to design it, the 8-storey SESBF is designed based on the results obtained from time-history analysis.

The design is an iterative procedure. Initial member sizes were selected as per a conventional EBF while the tie members are selected based on experience. For a conventional EBF, a preliminary design is carried out with the storey shear forces calculated from equivalent static procedure as introduced in 7.2.2.2 while considering the R_d, R_o for conventional Type D (ductile) EBFs, which are 4.0 and 1.5 respectively.

Starting from there, time-history analyses were performed to obtain a more accurate design force for each structural member. This step is repeated until the difference between the results obtained from past two steps is within a tolerance. This tolerance is set as 5% of the member design force.

The selected member sizes are listed in Table 7-3. Note that in SESBFs, because all links in a segment works together, there is no need to have one link on each floor. In this case, the upper segment only has two links and they are located on the 5th and 7th floor.

Table 7-3 Member sections for 8-storey SESBF with 2 segments

Floor	Link	Beam	Brace	Tie	Column
8	-	W360X39	HSS152.4X152.4X6.4	HSS152.4X152.4X4.8	W200X41.7
7	W360X39	W360X39	HSS152.4X152.4X6.4	HSS139.7X139.7X6.4	W200X41.7
6	-	W360X39	HSS152.4X152.4X7.9	HSS139.7X139.7X4.8	W310X79
5	W360X39	W360X39	HSS177.8X177.8X9.5	-	W310X79
4	W360X39	W460X52	HSS177.8X177.8X9.5	HSS139.7X139.7X4.8	W360X110
3	W360X39	W460X52	HSS177.8X177.8X9.5	HSS139.7X139.7X6.4	W360X110
2	W360X39	W460X60	HSS177.8X177.8X9.5	HSS139.7X139.7X4.8	W360X147
1	W360X39	W460X60	HSS203.2X203.2X9.5	-	W360X147

7.2.3 Scaling of testing frames

Three types of models are generally considered in structural modeling, the true model, the adequate model, and the distorted model. The true model means a model maintains complete similarity, which reflects the real properties of the structural response. The adequate model, which maintains "first order" similarity. The distorted model, that may violate one or more of the first-order stipulations.

The true model is the most desirable model type; however, it is usually not economical or not realistic to build, in which case, an adequate model is preferred. In this case, an adequate model is adopted for the study. In the adequate model stress, strain and modulus of elasticity are selected as the identical quantities.

The prototype frame is scaled based on the Table 7-4. Length and mass are selected as the controlling parameter due to the limitations in the laboratory. All other parameters are scaled accordingly.

Table 7-4: Scaling factors for shaketable specimens

Quantity	Symbol	Derivation	Ratio
Length	l_r	selected	0.3
Modulus of Elasticity	E_r	selected	1.00
Mass	m_r	$= \frac{62.5\ kN}{\frac{1}{n} wA}$	0.019
Horizontal Accelerations	α_r	$= \frac{E_r I_r^2}{m_r}$	4.69
Vertical Accelerations	g_r	gravity	1.00
Time	T_r	$= \sqrt{\frac{m_r}{E_r I_r}}$	0.253
Strain	ε_r	selected	1.00
Stress	σ_r	$= E_r$	1.00
Force	F_r	$= \sigma_r l_r^2$	0.09
Moment	M_r	$= \sigma_r l_r^3$	0.027
Area	A_r	$= l_r^2$	0.09
Moment of Inertia	I_r	$= l_r^4$	0.0081
Axial stiffness	K_r	$= \frac{A_r E_r}{l_r}$	0.3

*note n: number of frames per direction; *w* distributed seismic weight; A: floor area

7.2.3.1 Scaling of beams of chevron braced frame

To accurately scale the beam sections is one of the most important tasks for the test of chevron braced frame. Due to the large ratio between the original structure and the scaled one, even a slight change in beam strength could lead to a different failure mechanism of the test specimen.

Moreover, the small bending capacity of the scaled beam makes it impossible to utilize an existing section.

Consequently, the scaled beam is built with 5 parts as shown in Figure 7-6. A plate with the same flexure stiffness and bending capacity as the beam is added to each side of the beam-to-brace connection. All the other parts are designed to remain essentially elastic so that all the inelastic action happens within the plates. To replicate response of the shear tabs, the beam-to-column connections are built with two L-shapes. The connection is welded to the column face.

To verify the response of the beam, an ABAQUS model is built. The deformed shape and the stress distribution after applying the unbalanced load created by brace buckling is shown in Figure 7-6. The specimen is subjected to both the in-plane and out-of-plane forces induced by the connected braces. Plastic hinge is formed in the plate right beside the center connection. No out-of-plane buckling is observed, which suggests that no lateral bracing is needed for the built-up beam.

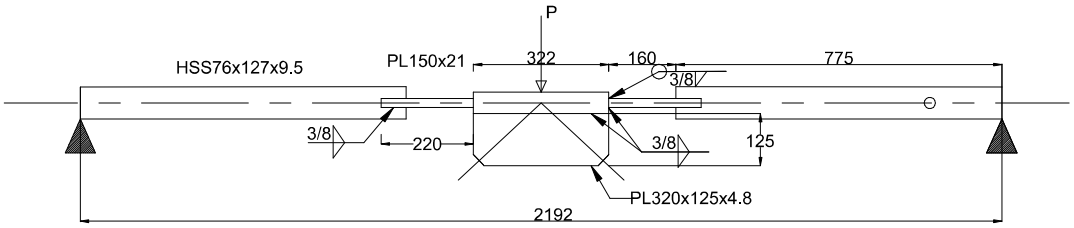

Figure 7-5 Drawing of the composite beam

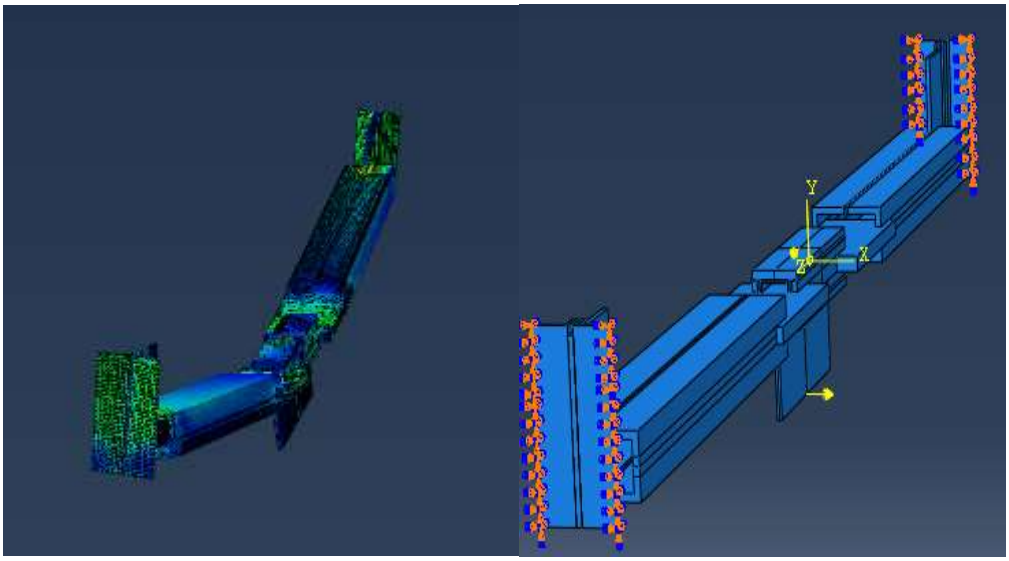

Figure 7-6: ABAQUS model of the scaled beam

7.2.3.2 Scaling of ductile links

Links in the scaled model are also replaced with steel plates due to their small shear stiffness and capacity. The plates possess the same stiffness and yield strength as the ductile links in the original structure.

For easier assembly process, the plates that replicating the ductile links are welded to a 20 mm thick end plate on each side. Then, the part is bolted to the frame as a removable link. Details of the connection is shown in Figure 7-7.

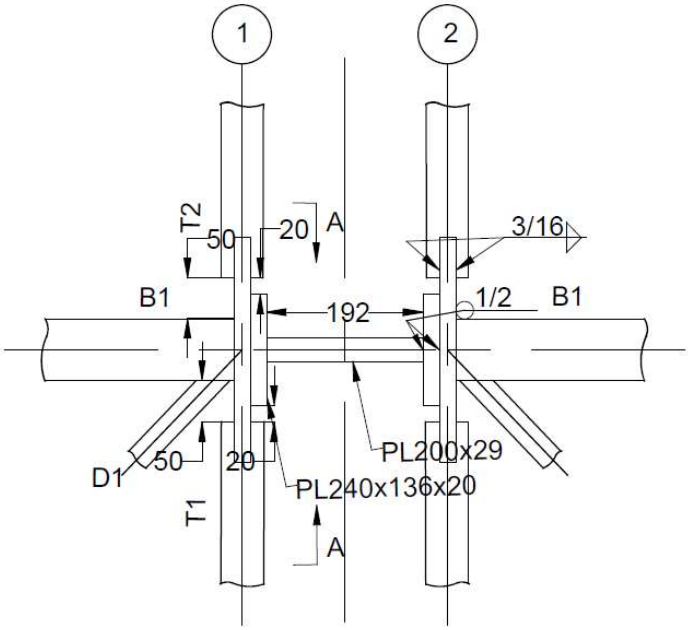

Figure 7-7 Detail of the link assembly

7.2.4 Selection of ground motions

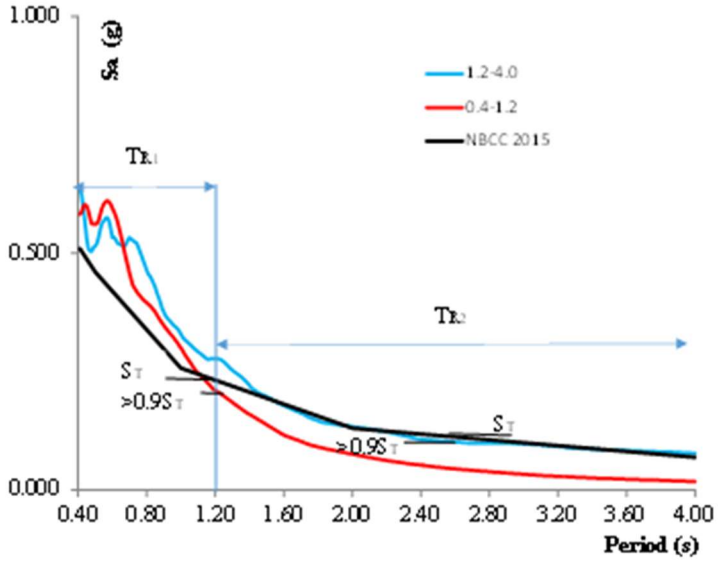

Figure 7-8: Ground motion scaling

At the time when the program was planned, the complete scaling process suggested by NBCC 2015 was not published. However, the principles of ground motion selection and scaling are applied here. Simulated ground motion records produced for Montreal region are adopted. The ground motion records are then divided into two categories: the ones with high energy in short period range and the ones in long period range, noted as set 1 and set 2. The period ranges for set 1 and set 2 records is between 0.4s to 1.2s and 1.2s to 4s respectively. Both ground motion sets are scaled in their respective period range to ensure the lowest spectral acceleration on the average spectrum within that period range is at least 90% of that of the design spectrum. The average value of the spectrums of the scaled ground motion sets are illustrated in Figure 7-8. Set 1 and set 2 are colored as red and blue respectively. The spectrum of all selected records after scaling is plotted in Figure 7-9.

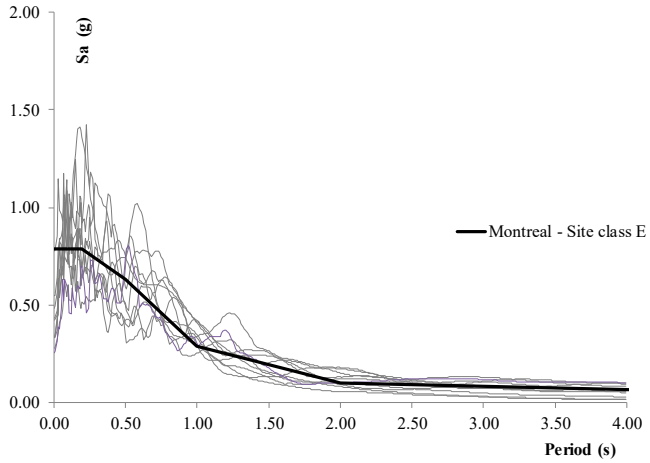

Figure 7-9 Spectrum of scaled ground motion records

7.3 Numerical models and simulation results

7.3.1 Modeling details

The structural model is built in OpenSees simulation platform. Braces, columns and beams are all modeled using force based nonlinear beam-column elements with fibre sections. All gravity columns, a total of 16, are simulated in the model connected by link beams. Both frame columns

and gravity columns are modeled with $1/1000h_s$ out-of-straightness to allow buckling in these columns. Due to the fact that both columns are continuous for two-storeys which are the common practice at that time, all of the columns are simulated as a sinusoidal shape with the cross-point located at each floor level. To justify the results of column models, a W360x134 column is modelled in OpenSees with above parameters. The length of the column is set to 3.8 m. It is pin connected on both end and axial compression load is applied to one end while the other end is pinned to the ground. The F_y of the material is set to 350 MPa. The result in terms of displacement and axial force is shown in Figure 7-10.

According to NBCC 2015, the ultimate compression resistance of a member shall be taken as 1.2 times the probable compression resistance of the member. In this regard, the ultimate compression resistance is calculated as 5806 kN. The difference between the ultimate compression resistance and the result of analysis is 1.9%. It proves that the column model is able to replicate the buckling response of a column accurately.

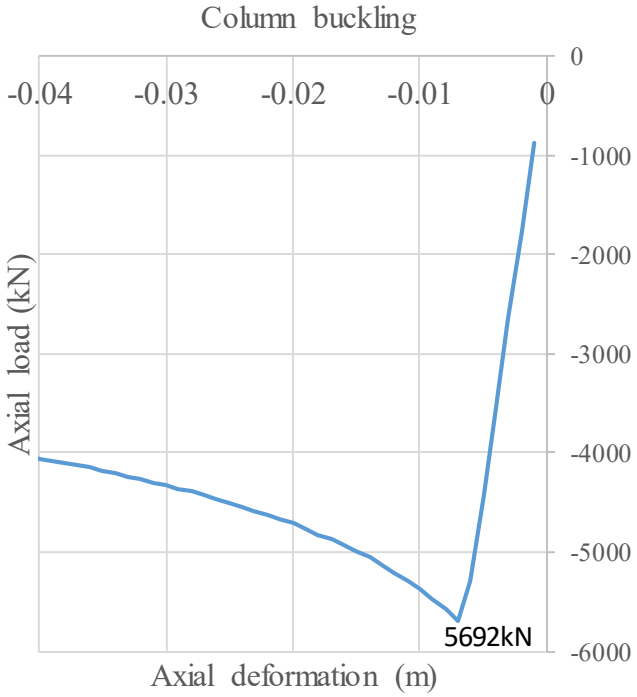

Figure 7-10: Result of column analysis

Gravity load and 25% snow load are applied at floor and roof level of each column to account for P-Delta effect. The seismic weight of the structure is applied at the top of both energy columns at each level. Rigid links, which accounts for the rigid offset due to connections, are added to both ends of each brace.

Steel02 material is assigned to all members while the yielding strength of W sections and HSS sections is set to 350MPa. Steel material for brace is wrapped with Fatigue material (Uriz,2005) to take account of low-cycle fatigue fracture of brace members.

Beams are modeled with 4 force-based beam-column element with fibre sections, assigned with corotational transformation method to allow possible large displacement due to the large unbalance forces between tension brace and compression brace after buckling, which is not required to account for in 1980 NBCC.

7.3.2 Modeling of connections

Beam-to-column connections, column splices and gusset plate connections are all modelled as rotational springs in the OpenSees models. The location of these springs is demonstrated in Figure 7-11.

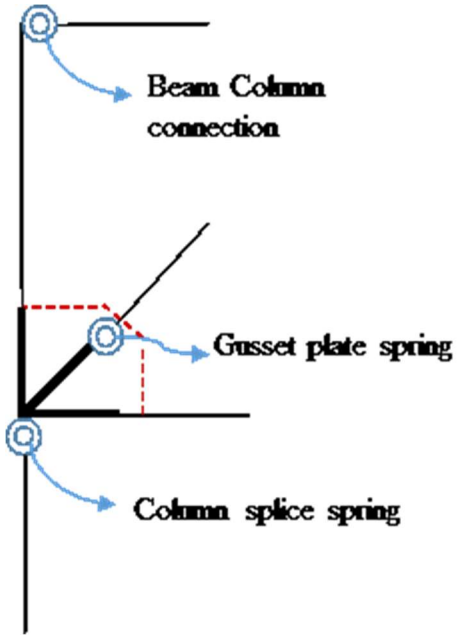

Figure 7-11: Modeling of connections

For gusset plates with simple shapes such as rectangular shape, the flexure stiffness and the yield strength can be directly calculated. For more complex shapes, finite element models are built in SAP2000 to obtain the corresponding stiffness and strength.

For beam to column connections, shear tab connections are assumed in this scenario. Tests have shown that the simple shear tab connection possesses 30-50% of the plastic moment of the connected beam (Kyriakos, 2012). In this study, the shear tab connections are assumed to able to carry 30% of the plastic moment of the connected beam.

7.4 Expected results

7.4.1 Possible failure modes:

7.4.1.1 Possible failure modes of 1980 CBF

Connection failure

The most common failure mode in old buildings. Connections were not designed to carry the probable tensile strength of the connected bracing elements, instead, they were designed to carry the seismically induced forces calculated from either spectrum analysis or static equivalent method.

This failure mode can be inspected based on calculation and is not implemented in the model.

Brace fracture

Braces are modeled with fatigue material to test the influence of brace fatigue failure. However, the common ground motion type in eastern Canada has high frequency but small amplitude, which induces less damage in bracing members. The brace fracture due to fatigue may not be seen.

Beam failure

Chevron bracing systems solely depend on the beams to carry the unbalanced forces induced by tension brace and buckled compression brace. This was not required in old design practice. This will be the most common failure type in the analyses. Figure 7-12 illustrated the typical deformed shape.

Column buckling

Columns would buckle in their weak axis due to excessive drift demand.

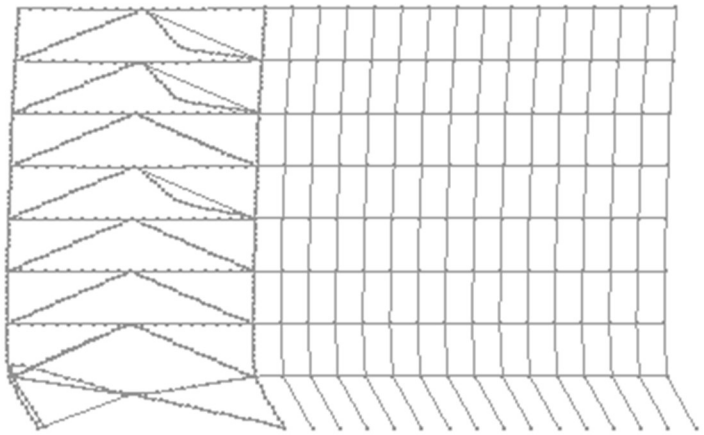

Figure 7-12: Deformed shape

7.4.1.2 Possible failure modes of SESBF

Link failure

Links fracture after a maximum plastic rotation angle is reached. This effect is included in the structural model. Min-max material has been utilized in the link model. The maximum rotation selected for the min-max material is obtained by studying the past experiment results. Details of the calibration process is already discussed in 4.3.1. This failure mode is considered as one of the primary failure mode of the SESBFs.

Connection failure

Connections in ductile structures are required to undertake the maximum strength of the connected members. Thus, connection failure is not supposed to be an issue for SESBFs.

Column buckling

Excessive storey drifts greatly increase the axial forces induced in the columns due to P-Delta effect. If a soft segment is formed in the frame, column buckling could be observed in the response.

Tie buckling

If the axial forces in the tie member exceed the design axial force of the ties, the tie members may undergo buckling or yielding.

7.4.2 Seismic response of the scaled models

Time-history analysis are performed on both the scaled CBF model and the scaled SESBF model. The ground motion records used in the analyses are also scaled according to Table 7-4: Scaling factors for shaketable specimensTable 7-4. The results of the analyses are presented in the following sections.

7.4.2.1 Seismic response of the scaled CBF

Seismic performance of the CBF is relatively poor as expect. The most critical failure mode for the CBF is yielding of beams after brace buckling. The unbalanced vertical projection of the tensive and compressive forces in the braces forces the connected beam to yield prematurely, which significantly reduces the lateral stiffness of that storey. The reduced lateral stiffness combined with P-Delta effect leads to extreme story drifts on the ground floor of the frame. This type of structural response is observed in 7 out of 10 cases. Storey drift profile of the model under selected ground motion records are presented in Figure 7-13. According to the analyses, the beam located on the ground floor of the frame is the most critical member.

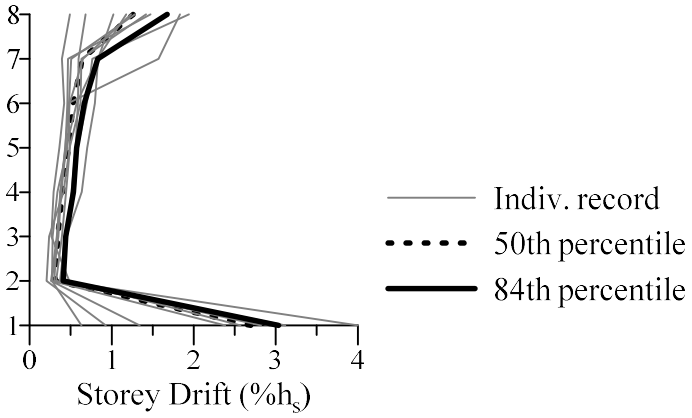

Figure 7-13 Storey drift profile of the scaled 8-storey CBF

7.4.2.2 Seismic response of the scaled SESBF

Storey drift profiles of the SESBF-2 are plotted in Figure 7-14. Overall storey drift values are greatly reduced when compared to the CBF. The maximum storey drift is 1.95% h_s, while the 84th percentile value of the storey drifts is below 1.3% h_s. In general, the maximum storey drifts of the SESBF-2 is evenly distributed alone the building height. No excessive storey drift is observed during the ground excitations. In case of "E7E1-32F", the bottom segment experienced larger storey drift demand compared to the top segment. The same ground motion with higher intensity could lead to the formation of a soft segment. This is expected in the SESBF design. It is foreseeable that an 8-storey SESBF with one segment (SESBF-1) could potentially delay the formation of soft segment (or global collapse mechanism in case of SESBF-1) until an even higher ground motion intensity level with a higher cost. The analyses suggest that the SESBF-2 is able to achieve the design goals and provide a stable seismic response to the structure.

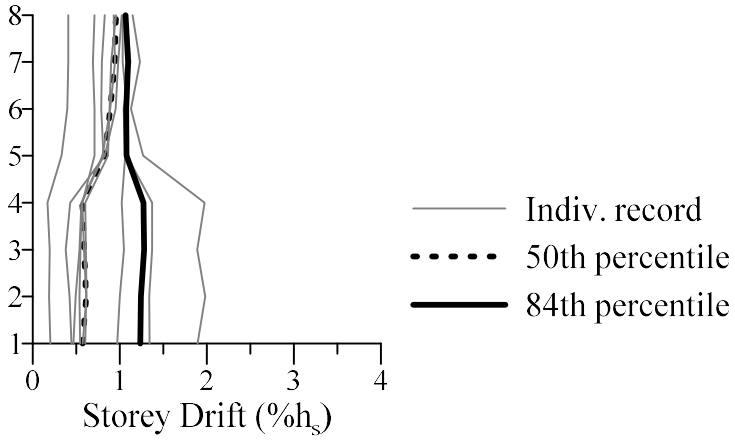

Figure 7-14 Storey drift profile of the scaled 8-storey SESBF-2

The maximum axial forces of the ties and braces of the scaled model are plotted in Figure 7-15. The compression resistance of the members used in the scaled model is shown in red. Due to the limitations of the availability of steel sections, some of the members are adjusted. It is expected that all members in the SESBF-2 remain essentially elastic during the analysis. However, for extreme cases, possible yielding and buckling are also expected.

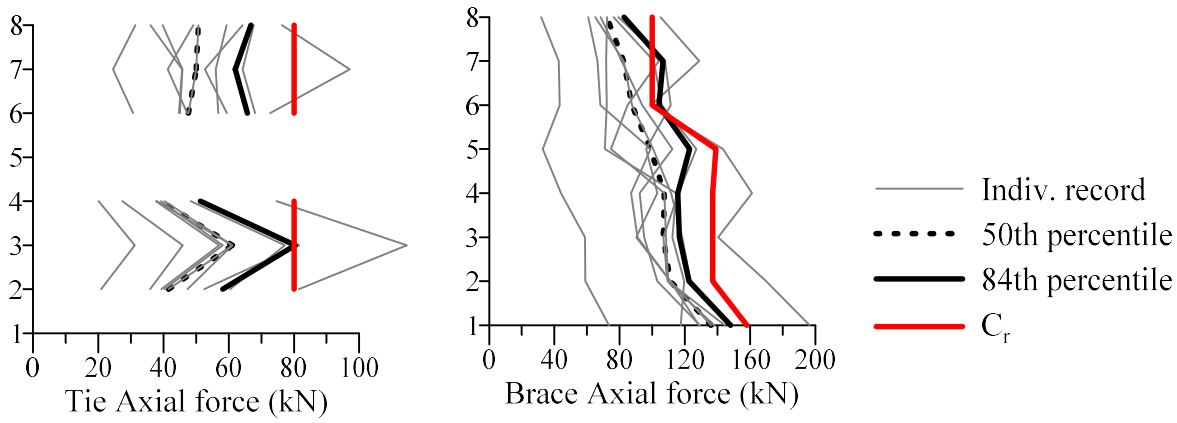

Figure 7-15 Axial forces of ties and braces

CHAPTER 8 GENERAL DISCUSSION

During this Ph.D. research, an understanding of the seismic behaviour of framing systems with segmental and full elastic spines is developed. Majority of the findings and knowledge gained throughout the studies are presented in the articles.

Article 1 investigates the seismic performance of the fully tied EBFs and SESBFs with multiple segments in comparison to conventional EBFs. 8-, 16- and 24-storey buildings with different configurations are designed and analyzed using selected and scaled ground motion records. It is found that, although the fully tied EBFs exhibit the best seismic performance in terms of maximum drifts and drift distribution, SESBFs with two or four segments can achieve similar level of seismic performance.

Article 2 provides a design method for SESBFs with known segmental configuration. The proposed design method combines the traditional capacity design principle with a modal superposition approach. The vibration modes of a SESBF are categorized into two sets. The forces imposed by vibration modes of each set are separately calculated. Set I forces are calculated with the shear strength of the strain hardened ductile links of each segment. Set II forces are obtained through spectrum analyses using a modified response spectrum which includes only the spectrum coordinates corresponding to the Set II modes. These two sets of forces in corporation with the forces induced by gravity loads provide the force envelopes of the members of the segmental trusses. These envelopes are adopted as the design forces to ensure an elastic response of the trusses. The design method is demonstrated for 8- and 16-storey SESBFs with various configurations. It is found that the proposed design method is able to predict the envelops of forces in the structural members accurately. However, using the force envelopes to design the members can be conservative, especially for the tie members, when the selected ground motion records do not provide enough time for the yielding of links in each segment to fully develop.

Article 3 presents a simple method to assess the performance of SESBFs with different segmental configurations using a simplified model (SM). The SM can be easily built without designing the structure. A procedure to develop the SM is also provided. This procedure utilizes modal analyses and spectrum analyses performed on the SM to imitate the stiffness and the strength of the structure. With the SM, time-history analyses are performed with properly selected and scaled ground motion records. The results are used to predict and assess the seismic performance of a SESBF with

corresponding segmental configuration. The accuracy of the proposed method is demonstrated with a 24-storey SESBF with various segmental configurations. Similar maximum storey drifts and drift distribution are obtained between the SM and the models of SESBFs that are properly designed. Therefore, the SM can be used to determine the best segmental configuration of a given SESBF structure within a reasonable time frame.

The three articles highlight the promising seismic performance and the economical advantage of the innovative SESBF system and develop a design procedure that is able to select the most suitable case-specific segmental configuration and provide accurate predictions of member forces. It was also noted that the member forces, especially the forces in the ties, may not reach the maximum when the selected ground motion record does not provide enough time to yield all links in each segment. The relationship between the ground motion period and the maximum forces in the tie members can be further studied to improve the proposed design method.

CHAPTER 9 CONCLUSIONS AND RECOMMENDATIONS

9.1 General

In this chapter, the main findings and conclusions of the study are highlighted and recommendations for future studies are introduced.

This Ph.D. study had four main objectives:

1) Develop an efficient and economic seismic resisting system that is preventive to the soft-storey formation.
2) Develop a robust and simple design methodology for such system. The proposed design method will be tightly connected to the current Building Code Provisions to make it easy to apply in for Canadian applications.
3) Verify the newly developed system and design method with numerical analysis.
4) Develop an experimental test program to validate the proposed design method. The experimental program will include a test on a sub-standard CBF and a test on a SESBF. The objective is to confirm the deficiencies of the sub-standard CBF and verify if the newly proposed system can be used as a seismic retrofit strategy. The test program will be conducted for buildings located in Montreal, Quebec.

The primary original contributions of the thesis work are:

1) Development of a new structural system to improve the seismic performance of steel braced frames
2) Development of a comprehensive step-by-step design procedure for the SESBF system in the context of NBCC 2015
3) Development of a procedure and a simplified, efficient numerical model to determine the optimum configurations for a SESBF structure at the preliminary design stage
4) Development of an integrated experimental program to confirm the deficiencies in existing CBFs and validate the design method proposed for SESBF for an 8-storey structure

The main conclusions of the submitted journal articles are reviewed in Section 9.2. Preliminary conclusions from the work accomplished for the experimental program are also presented in this section. Recommendations for future research are presented in Section 9.3.

9.2 Summary and conclusions

Steel braced frame configurations are widely adopted world-wide as a lateral force resisting system. Conventional CBFs and EBFs are both found to be prone to collapse due to soft-storey formation. In these frames, after the initial yielding of the energy dissipating component, inelastic demand has a tendency of concentrate in the storey and cause excessive storey drift which eventually lead to collapse of the structure.

Various researchers have attempted to solve this problem by adding a continuous vertical elastic spine (SBS) or vertical links (ZBF/SZBF) to the structure that is able to prevent damage concentration. Although the system and its alternatives are proven numerically and experimentally to successfully eliminate the formation of soft-storey, it is found that the force induced to the elastic spine grows exponentially while the number of storeys in the structure increases.

The first objective pursued in this study was to develop a structural system that is able to prevent soft-storey formation while preserving the benefit offered by SBSs or ZBF/SZBFs. To fulfill this objective, a comparative study was performed on various existing steel braced frames including CBF, EBF, TBF, ZBF, and SZBF. 8- and 16-storey building employing these structural configurations were designed. Computational models that can accurately simulate the yielding and fracture of both braces and links were developed and validated through parametric studies. NLRH analysis was performed on 2D frame models incorporating out-of-plane buckling of braces, yielding of ductile links, and P-Δ effect. SZBF and TBF exhibited the most satisfactory seismic response. In order to reduce the force demand of the members in the elastic spine while preserving its functionality in terms of soft-storey prevention, an innovative segmental elastic spine system was proposed. This system comprises multiple segments of elastic spines distributed vertically along the building height and pin connected at intersection joints. The concept was applied to SZBF and TBF systems, referred to as M(modular)-SZBF and M-TBF systems, respectively. The seismic response of these systems was also compared with systems proposed by others in the literatures.

In the M-SZBF, the presence of hat-trusses at intermediate levels introduced a drastic change in terms of stiffness along the building height, which had negative effects on the seismic response of the structure. In the case of the M-TBF, however, excellent seismic performance was exhibited whereas the force demands in the structure members outside of links could be reduced significantly, especially for the tie members.

A more detailed investigation was carried out to examine and compare the seismic response of the EBFs, TBFs, and M-TBFs. Structures having 8, 16, and 24 storeys were designed and analyzed with static pushover analysis and NLRH analysis. Although no collapse was observed in NLRH analysis, soft-storey formation occurred in the EBFs. TBFs experienced the least damage and the inelastic demand was evenly distributed in all storeys along the building height. A drastic increase of axial force demand in the tie members was however observed for the 8-storey to 24-storey buildings. M-TBFs, as expected, showed a much-improved seismic performance compared to that of EBFs comparable to the response observed for TBFs. For M-TBFs, the additional force demands in the structural members from truss actions were minimum with the 4-storey segment configuration. From this investigation, it was realized that TBFs and M-TBFs, instead of being simply improved versions of conventional EBFs, in fact are braced frames with elastic truss spines and should be considered and treated as such in design. Therefore, the M-TBF system was renamed as braced frame with segmental elastic spines (SESBF). The nonlinear response of this system is restricted within the ductile links, while the beams outside of links, columns, ties, and braces form two vertical elastic trusses on either side of the links.

While the enhanced seismic response of SESBFs was numerically proven, SESBF examples studied at this point of the research were designed using the results from nonlinear dynamic analyses because no design method existed for that new configuration. The second objective of this study was therefore to develop a robust and practical design method for the system. Several different approaches were investigated to predict the seismic force demand in the truss member for design purposes.

In this investigation, the structural response in terms of storey drifts and force demands were studied thoroughly in both time domain and frequency domain to identify the sources and contributions for the forces induced in the structural members. It was found that the forces in the

members of the elastic trusses are highly influenced by the higher vibration modes of the structure that involves bending of the truss spines. Furthermore, it was found that the vibration modes with highest impact on member forces were different depending on the number of truss segments of SESBFs. That higher mode response was also found to develop upon yielding of the ductile components in the structure. To identify these modes in modal analysis, the structural model had to be modified by reducing the stiffness of the ductile links to reproduce their inelastic response. It was found that these higher inelastic modes were not significantly different compared to their elastic counterparts in terms of periods, but the inelastic ones must be used together with consistent yielding patterns in the structure to adequately predict member forces. Based on these observations, the seismic design method used for conventional structural systems should be expanded to account for the contribution of these higher inelastic vibration modes. A practical design method for SESBFs was then developed to include those effects. This method is based on capacity design principles under the assumption that the required links capacity in SESBFs is the same as that of conventional EBFs. Structural members in the elastic spines are then designed for two sets of seismic induced forces: 1) the forces induced by strain-hardened links assuming yielding of links occurs simultaneously within each segment over the frame height, and 2) the forces resulting from higher inelastic vibration modes that introduces bending to the spines. A modified response spectrum method is employed to obtain the second set of forces: reduced stiffness is assigned to the ductile links and the spectrum is truncated to include only the spectrum coordinates associated with the inelastic modes of the structure that induce bending action on the elastic spines. Gravity induced forces are added and the truss members can be designed in accordance with the applicable codes or standards.

SESBFs for 8- to 16-storey buildings having different truss segment configuration were designed and analyzed to verify the adequacy of the design method. Good match was found between the maximum forces resulted from nonlinear dynamic analysis and the force demands predicted with the proposed design method.

With the knowledge gained in the process, it was understood that the optimum segmental configuration is structure-specific. To achieve a cost-effective SESBF design, it was also necessary to develop a method and an effective analysis tool to identify the optimum segmental truss configuration for a given structure. One such procedure was developed in this thesis research. The

procedure employs a simplified model that can effectively predict the nonlinear seismic response of a given SESBF configuration with sufficient accuracy without knowing the exact member sizes of the structure. With this tool, design engineers can select a target performance level and perform a series of nonlinear dynamic time-history analyses in a timely fashion to determine the preferable segmental configuration. The simple analysis model was validated through numerical simulations against the nonlinear dynamic analysis results obtained with refined finite element models. In design, the use of the simplified model also gives realistic SESBF strength and stiffness properties to achieve satisfactory seismic response. Therefore, the method can be used at the preliminary design to select the best configuration candidates for final design.

An experimental program that utilizes the SESBF as a retrofit scheme for sub-standard CBFs was developed and initiated. The program is comprised of two parts. The first part is a shake table test on an 8-storey CBF designed in accordance with codes of the 1980s. The second part is a shake table test performed on an 8-storey SESBF with two segments. Both specimens are 30% scaled models of the prototype structures. Numerical analysis was conducted for the prototype frames and the scaled frames to validate the accuracy of the scaling rules that were used. The analyses also demonstrated the enhance seismic performance that can be achieved with the SESBF used as a retrofit scheme. At the time of writing, the specimens have been designed, fabricated and instrumented and are ready to be installed on the shake table. It is expected the results from the testing will be used to improve the accuracy of the numerical model used in the study and to further validate the design procedure proposed herein.

9.3 Recommendations for future studies

Further research is needed on the following topics:

- Analyses on SESBFs with long truss segments showed that the yielding sequence of the links may differ from what was assumed in the proposed design method. Further research is needed to improve the method to account for such possible behaviour.

- The TBF was selected to study the SESBF response and developed the seismic design methods. Further studies should be performed on SESBFs derived from other effective bracing systems such as braced frames with buckling restrained braces.
- This study showed that superior seismic performance can be achieved with SESBFs. In this context, further studies could be performed to propose new values for the R_d and R_o factors that better reflect the robustness of the system.

BIBLIOGRAPHY

AISC. (1992). *Seismic Provisions for Strucutral Steel Buildings.* Chicago, IL.: American Institute of Steel Construction.

Alekar, J., Jain, S., & Murty, C. (1997). Seismic Response of RC frame buildings with soft first storeys. *Proceeding of Central Building Research Institude Golden Jubilee Year Conference on "Natural Hazard in the Urban Habitat"*, (pp. 13-24). New Dehli, India.

Allahabadi, R., & Powell, G. (1988). *Drain 2Dx User Guide.* Earthquake Engineering Research Center. Richmond: California University, Richmond. Earthquake Engineering Research Center.

Archambault, M. (1995). *Etude du Comportement Seismique des Contreventements Ductile en X avec Profiles Tubulaires en Acier.* Montrea, Canada: Ecole Polytechnique.

Beck, J., & Skinner, R. (1974). The Seismic Response of Reinforced Concrete Bridge Pier. *Journal of Earthquake Engineering and Structural Dynamics, 2*, 343-358.

Bosco, M., & Rossi, P. (2009). Seismic behaviour of eccentraically braced frames. *Engineering Structure Vol 31, Issue 3*, 664-674.

Bruneau, M., Engelhardt, M., Filiatrault, A., Goel, S. C., Itani, A., Hajjar, J., . . . Uang, C.-M. (2005). Review of Selected Recent Research on US Seismic Design and Retrofit Strategies for Steel Structures. *Progress in Structural Engineering and Materials*, 7:103-114.

Cassis, J., & Cornejo, E. (1996). Influence of Vertical Irregularities in the Response of Earthquake Resistant Structures. *Proc. 11th World Conf. on Earthquake Eng.* Acapulco, Mexico.

Chen, C., & Mahin, S. (2012). *Performance-based seismic demand assessment of concentrically braced steel frame buildings.* Berkeley, CA.: Pacific Earthquale Engineering Research Center, Univ. of California.

Chen, L. (2011). *Innovative Bracing System for Earthquake Resistant Concentrically Braced Frame Structures.* Montreal, Quebec, Canada: Concordia University.

Chen, L., & Tirca, L. (2013). Simulating the Seismic Response of Concentrically Braced Frames Using Physical Theory Brace Models. *Open Journal of Civil Engineering, 3*(2A).

Chen, Z. (2012). *Seismic Response of High-rise Zipper Braced Frame Structures with Outrigger Trusses.* Montreal, Quebec, Canada: Concordia University.

CISC. (2016). *Handbook of Steel Construction.* Ontario: Canadian Instituteof Steel Construction.

Clifton, C., Bruneau, M., MacRae, G., Leon, R., & Fussell, A. (2011). Steel Structures Damage from the Christchurch Earthquake Series of 2010 and 2011. *Bulletin of the New Zealand society for Earthquake Engineering, 44*(4).

Clifton, G., Nashid, H., Ferguson, G., Hodgson, M., & Seal, C. (2012). Performance of Eccentrically Braced Framed Buildings In The Christchurch Earthquake Series of 2010/2011. *15th WCEE.* Lisboa.

Deierlein, G., Krawinkler, H., Ma, X., Eatherton, M., Hajjar, J., Takeuchi, T., . . . Midorikawa, M. (2011). Earthquake Resilient Steel Braced Frames with Controlled Rocking and Energy Dissipating Fuses. *Steel Construction: Design and Research, 4*(3), 171-175.

Eatherton, M., Hajjar, J., Deierlein, G., Krawinkler, H., S., B., & Ma, X. (2010). Controlled rocking of steel-frames buildings with replaceable energy-dissipating fuses. *Proc. 14th World Conf. on Earthquake Eng.* Beijing, China.

Eatherton, M., Hajjar, J., Deierlein, G., Ma, X., Billington, S., & Krawinkler, H. (n.d.). Steel Framed Rocking Structural Systems for Moderate Seismic Zones. *Proceedings of 2009 Structures Congress*, (pp. 804-812). Austin, Texas.

Eurocode 8: Design of Structures for earthquake resistance. (1998).

Fell, B., Kanvinde, A., Deierleine, G., Myers, A., & Fu, X. (2006). *Buckling and Fracture of Concentric Braces under Inelastic Loading.* Moroga, CA.: Steel Tips, Tehnical Information and Product Service, Structural Steel Education Concil.

FEMA. (2009). *FEMA P-695 Quantification of Building Seismic Performance Factors.* Washington, D.C.: Federal Enmergency Management Agency.

Foutch, D. (1989). Seismic behaviour of eccentrically braced steel building. *Journal of Structural Engineering Vol. 115 Issue 8*.

Han, S., Kim, W., & Foutch, D. (2007). Seismic Behaviour of HSS Bracing Members According to Width-thickness Ratio under Symmetric Cyclic Loading. *J. Struct. Eng., 133*(2), 264-273.

Hejazi, F., Jilani, S., Noorzaei, J., Chieng, C., Jaafar, M., & Abang Ali, A. (2011). Effect of Soft Story on Structural Response of High Rise Buildings. *IOP Conf. Ser.:Mater. Sci. Eng.*, *17.*

HERA. (2013). *P4001:2013 - Seismic Design of eccentrically braced frames.* SCNZ Steel Construction New Zealand.

Hsiao, P., Lehman, D., & Roeder, C. (2012). Improved Analytical Model for Special Concentrically Braced Frames. *Journal of Constructional Steel Research, 73*, 80-94.

Ji, X., Ma, Q., Wang, Y., & Okazaki, T. (2014). Cyclic behavior of steel shear links used in replaceable coupling beams. *10th U.S. National Conference on Earthquake Engineering.* Anchorage: Earthquake Engineering Research Institute.

Kanitkar, R., & Kanitkar, V. (2004). Seismic Performance of Conventional Multi-Storey Buildings with Open Ground Floors for Vehicular Parking. *The Indian Concrete Journal, 78*(2), 99-104.

Kelley, J., & Tsztoo, D. (1977). *Earthquake Simulation Testing of a Stepping Frame with Energy Absorbing Devices.* Berkeley, CA: Earthquake Engineering Research Center, College of Engineering, University of California.

Khatib, I., Mahin, S., & Pister, K. (1988). *Seismic Behavior of Concentrically Braced Steel Frames.* University of California, Earthquake Engineering Research Center. Berkeley, CA.: Earthquake Engineering Research Center, University of California.

Kyriakos, T. (2012). *Moment Capacity of Simple Steel Connections.* Nicosia: Department of Civil Engineering, Frederick University.

Lai, J., & Mahin, S. (2015). Strongback System: A Way to Reduce Damage Concentration in Steel-Braced Frames. *Journal of Structural Engineering, 141*(9).

Lee, K., & Bruneau, M. (2005). Energy Dissipation of Compression Members in Concentrically Braced Frame: Review of Experimental Data. *Journal of Structural Engineering, 131*(4), 552-559.

Lee, S., & Goel, S. (1987). *Seismic Behavior of Hollow and Concrete-filled Square Tubular Bracing Members.* University of Michigan, Department of Civil Engineering. Ann Arbor, MI: Department of Civil Engineering, University of Michigan.

Lignos, D., & Karamanci, E. (2013). Predictive Equations for Modeling Cyclic Buckling and Fracture of Steel Braces. *10th International Conference on Urban Earthquake Engineering, March 1-2, 2013.* Tokyo: Tokyo Institute of Technology.

Liu, J. (2017). Strongback Steel-Braced Frames for Improved Seismic Behavior in Buildings. *Engineering Journal, 54*, 297-308.

Mahin, S. A., Bertero, V., Chopra, A. K., & Collins, R. (1976). *Response of the Olive View Hospital Main Building During the San Fernando Earthquake.* University of Berkeley, Earthquake Engineering Research Center. Berkeley, CA.: Earthquake Engineering Research Center, University of Berkeley.

Mar, D. (2010). Design Examples Using Mode Shaping Spines for Frame and Wall Buildings. *Proc. Joint 9th National Conf. on Earthquake Eng. and 10th Canadian Conf. on Eathquake Engineering*, (p. 001400). Toronto, ON.

Martini, K. (1990). The potential Role of Non-linear Analysisi in the Seismic Design of Building Structures. *Proc. 4th U.S. Nat. Conf. on Earthq. Eng. Vol. 2.* Palm Springs, California.

Martini, K., Amin, N., Lee, P., & Bonowitz, D. (1990). The Potential Role of Non-Linear Analysis in the Seismic Design of Building Structures. *Proc. 4th National Conf. on Earthquake Eng.*, *2*, pp. 67-76. Palm Springs, CA.

Mazzolani, F. (1997). Plastic Design of Seismic Resistant Steel Frames. *Earthquake Engineering and Structural Dynamics, 26*, 167-191.

McKenna, F., & Fenves, G. (2004). Open System for Earthquake Engineering Simulation (OpenSees). Berkeley, CA. Retrieved from http://opensees.berkeley..edu/index.html

Merzouq, S., & Tremblay, R. (2006). Seismic Design of Dual Concentrically Braced Steel Frames for Stable Seismic Performance for Multi-Storey Buildings. *Proc. 8th U.S. National Conference on Earthquake Eng.*, (p. 1909). San Francisco, CA.

NRCC. (2010). *National Building Code of Canada, 13th edition.* Ottawa: National Research Council of Canada.

NRCC. (2015). *National Building Code of Canada, 14th Edition.* Ottawa: National Research Council of Canada.

Okazaki, T., Arce, G., Ryu, H.-C., & Engelhardt, M. (2004, August 1-6). Recent Research on Link Performance in Steel Eccentrically Braced Frames. *13th World Conference on Earthquake Engineering, Paper No. 302*.

Panian, L., Bucci, N., & Janhunen, B. (2015). BRBM Frames: An Improved Approach to Seismic-Resistant Design Using Buckling-Restrained Braces. *Second ATC & SEI Conference on Improving the Seismic Performance of Existing Buildings and Other Structures* (pp. 632-643). San Francisco, CA: ASCE.

Pollino, M., Sabzehzar, S., Qu, B., & Mosqueda, G. (2013). Research needs for seismic rehabilitation of sub-standard buildings using stiff rocking cores. *ASCE structures Congress.* Reston, VA: ASCE.

Pollino, M., Slovenec, D., Qu, B., & Mosqueda, G. (2017). Seismic Rehabilitation of Concentrically Braced Frames Using Stiff Rocking Cores. *Journal of Structural Engineering, 14*(9).

Popov, E., Ricles, J. M., & Kasai, K. (1992). Methodology for optimum EBF link design. *Earthquake Engineering, Tenth World Conference.* Balkema, Rotterdam.

Qu, B., Sanchez-Zamora, F., & Pollino, M. (2014). Transforming Seismic Performance of Deficient Steel Concentrically Braced Frames through Implementation of Rocking Cores. *J. Struct. Eng.* doi: 10.1061/(ASCE)ST .1943-541X.0001085, 04014139

Roke, D., Sause, R., Ricles, J., & Gonner, N. (2009). Damage-free seismic-resistant self-centering steel concentrically-braced frames. *Proc. STESSA 2009 Conf.*, (pp. 3-10). Philadelphia, PA.

Rossi, P. (2007). A Design Procesure of Tied Braced Frame. *Earthquake Engineering and Structural Dynamics, 36*(14), 2227-2248.

Sabelli, R. (2001). *Research on Improving the Seismic Behavior of Earthquake-Resistant Steel Braced Frames.* Oakland: Earthquake Engineering Research Inistitute.

Sabelli, R., Mahin, S., & Chang, C. (2003). Seismic Demands on Steel Braced Frame Building with Buckling-Restrained Brace. *Engineering Structures, 25*(5), 655-666.

Salawdeh, S., & Goggins, J. (2013). Numerical Simulation for Steel Brace Members Incorporating a Fatigue Model. *Engineering Structures, 46*, 332-349.

Santagai, S., Bolognini, D., & Nascimbene, R. (2012). Strain Life Analysis at Low-cycle Fatigue on Concentrically Braced Steel Structures with RHS Shape Braces. *J. Earthquake Eng., 16*(S1), 107-137.

Shaback, B. (2001). *Behaviour of Square HSS Braces with end Connections under Reversed Cyclic Axial Loading.* University of Calgary, Dep. of Civil Eng. Calgary: Dep. of Civil Eng., University of Calgary.

Shaback, B., & Brown, T. (2003). Behaviour of Square Hollow Structural Steel Braces with end Connections under Reversed Cyclic Axial Loading. *Canadian J. of Civil Engineering, 30*(4), 745-753.

Simpson, B. (2016). *Reducing Concentrations of Inelastic Demand with a Strongback.* 2016 EERI Graduate Student Paper Competition winner.

Simpson, B., & Mahin, S. (2018). Experimental and Numerical Investigation of Strongback Braced Frame System to Mitigate Weak Story Behavior. *Journal of Structural Engineering, 144*(2). doi:10.1061/(ASCE)ST.1943-541X.000196

Slovenec, D., Sarebanha, A., Pollino, M., Mosqueda, G., & Qu, B. (2017). Hybrid Testing of the Stiff Rocking Core Seismic Rehabilitation Technique. *Journal of Structural Engineering, 143*(9).

Tirca, L., & Chen, L. (2014). Numerical simulation of inelastic cyclic response of HSS braces upon fracture. *Advanced Steel Construction, 10*(4), 442-462.

Tirca, L., & Tremblay, R. (2004). Influence of building height and ground motion type on the seismic behaviour of zipper concentrically braced steel frames. *13th World Conference on Earthquake Engineering.*

Tirca, L., Chen, L., & Tremblay, R. (2015). Assessing collapse safety of CBF buildings subjected to crustal and subduction earthquakes. *Journal of Constructional Steel Research*(115), 47-61.

Tremblay, R. (2002). Inelastic Seismic Response of Steel Bracing Members. *Journal of Constructional Steel Research, 58*, 665-701.

Tremblay, R. (2008). Influence of Brace Slenderness on the Fracture Life of Rectangular Tubular Steel Bracing Members Subjected to Seismic Inelastic Loading. *Proc. 2008 ASCE Structures Congress.* Vancouver, BC.

Tremblay, R., & Merzouq, S. (2004). Dual Buckling Restrained Braced Steel Frames for Enhanced Seismic Response. *Proc. Passive Control Symposium 2004 Tokyo* (pp. 89-104). Yokohama, Japan: Institute of Technology.

Tremblay, R., & Merzouq, S. (2005). Assessment of Seismic Design Forces in Dual Buckling Restrained Braced Steel Frames. *Proc. First Int. Workshop on Advanced in Steel Construction*, 739-746.

Tremblay, R., & Poncet, L. (2007). Improving the Seismic Stability of Concentrically Braced Steel Frames. *Eng. J. AISC, 44*(2), 103-116.

Tremblay, R., & Tirca, L. (2003). Behaviour and design of multi-story zipper concentrically braced steel frames for the mitigation of soft-story response. *Proc. STESSA 2003 Conf.*, (pp. 471-477). Naples, Italy.

Tremblay, R., Archambault, M., & Filiatrault, A. (2003). Seismic Response of Concentrically Braced Steel Frames Made with Rectangular Hollow Bracing Members. *Journal of Structural Eng., ASCE, 129*(12), 1626-1636.

Tremblay, R., Ben Ftima, M., & Sabelli, R. (2004). An Innovative Bracing Configuration for Improved Seismic Response. *Proc. Recent Advances and New Trends in Structural Design International Colloquium*, (pp. 419-430). Timisoara, Romania.

Tremblay, R., Chen, L., & Tirca, L. (2014). Enhancing the Seismic Performance of Multi-storey Buildings with a Modular Tied Braced Frame System with Added Energy Dissipating Devices. *International Journal of High-Rise Buildings*, 21-33.

Tremblay, R., Poirier, L.-P., Bouaanani, N., Leclerc, M., René, V., Fronteddu, L., & Rivest, S. (2008). Innovative Viscously Damped Rocking Braced Steel Frames. *14th World Conference on Earthquake Engineering.* Beijing, China.

Uriz, P. (2005). *Towards Earthquake Resistant Design of Concentrically Braced Steel Buildings, Ph.D. Dissertation.* Berkeley: University of California.

Uriz, P., & Mahin, S. (2008). *Toward Earthquake Resistant Design of Concentrically Braced Steel Frame Structures.* Berkeley, CA.: Pacific Earthquake Engineering Research Center.

Wiebe, L., Christopoulos, C., Tremblay, R., & Leclerc, M. (2012). Shake table testing of a rocking steel frame designed to mitigate higher mode effects. *STESSA 2012: Proceedings of the 7th International Conference on Behaviour of Steel Structures in Seismic Areas*, 703-708.

Yang, T., & Mahin, S. (2005). *Limiting Net Section Fracture in Slotted Tube Braces.* Orinda: Steel Tips Series, Structural Steel Education Council. Retrieved from Steel tips.

APPENDIX A - DRAWINGS FOR TEST SPECIMENS

List	Content
A0	Drawing list
A1	Chevron Frame - Elevation view & Connection forces
A2	Chevron Frame - Brace & Column sections
A3	Chevron Frame - Beams - B1
A4	Chevron Frame - Beams - B2
A5	Chevron Frame - Beams - B3
A6	Chevron Frame - Columns & Gussets - C1
A7	Chevron Frame - Columns & Gussets - C2
A8	Chevron Frame - Columns & Gussets - C3
A9	Chevron Frame - Columns & Gussets - C4
A10	Chevron Frame - Base Plate & Foundation Plate
S1	MTBF Frame - Elevation view & Connection forces
S2	MTBF Frame - Brace, Tie & Column sections
S3	MTBF Frame - Connection Detail - D1
S4	MTBF Frame - Section B & C
S5	MTBF Frame - Detail A, B, C
S6	MTBF Frame - Detail D, E
S7	MTBF Frame - Base Plate
S8	Mass connector

Shake Table Test Drawings A0
Prepared by : Liang Chen
2017-02-11

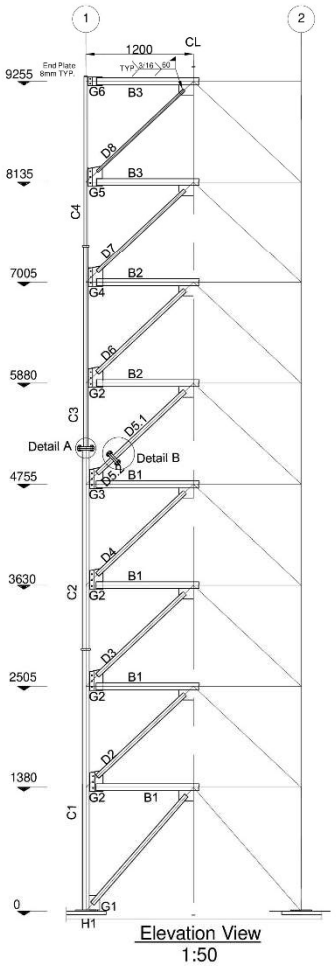

Elevation View
1:50

Note:

1. All columns are continuous for two storeys.
2. Fy 350 MPa.
3. Weld strength 410 MPa.
4. Lateral support for beams and braces must be supplied.
5. B1 is cut from W Section S75x8
6. D4 strain gauge

Shake Table Test Drawings A1
Prepared by : Liang Chen
2017-02-11

Column	Length (mm)	Section
C1	2889	HSS5x3x0.125 A500
C2	2230	HSS4x3x0.125 A500
C3	2218	HSS4x2x0.125 A500
C4	1880	HSS3x1.5x0.1 A500

Brace	Length (mm)	Section
D1	1595	HSS2x1.5x0.125
D2	1328	HSS2x1.5x0.125
D3	1328	HSS2x1.5x0.125
D4	1328	HSS2x1.5x0.125
D5.1	1116	HSS2x1.5x0.10 A500
D5.2	280	HSS2x1.5x0.10 A500
D6	1328	HSS2x1.5x0.10 A500
D7	1328	HSS1.5x1.5x0.10 A500
D8	1328	HSS1.25x1.25x0.1 A500

	Grade
HSS	G40
Plate	A36
L	G40

Shake Table Test Drawings A2
Prepared by : Liang Chen
2017-02-11

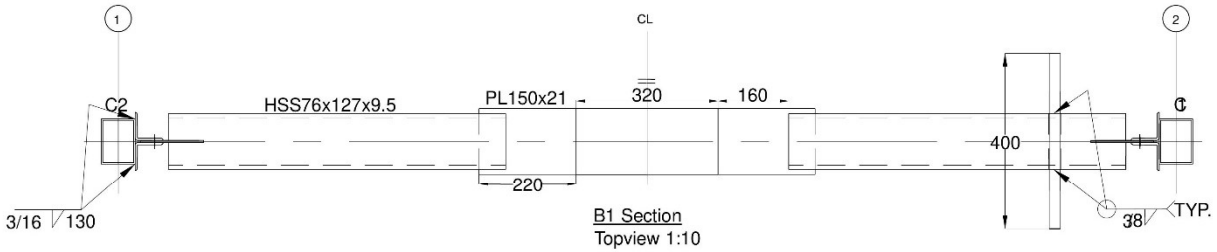

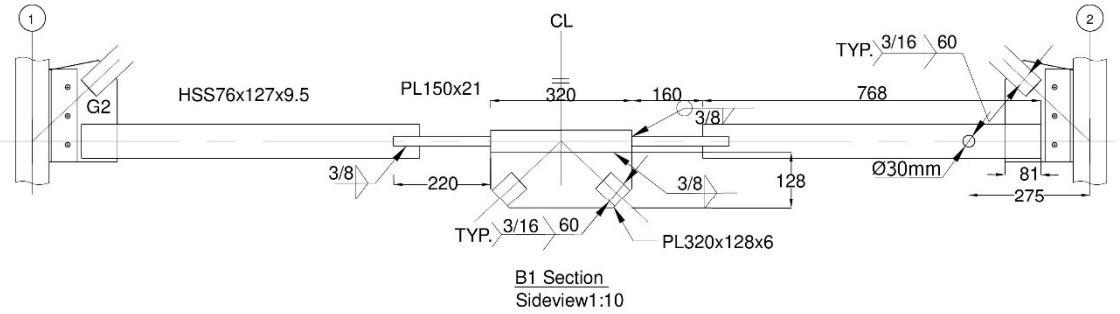

Shake Table Test Drawings A3
Prepared by : Liang Chen
2017-02-11

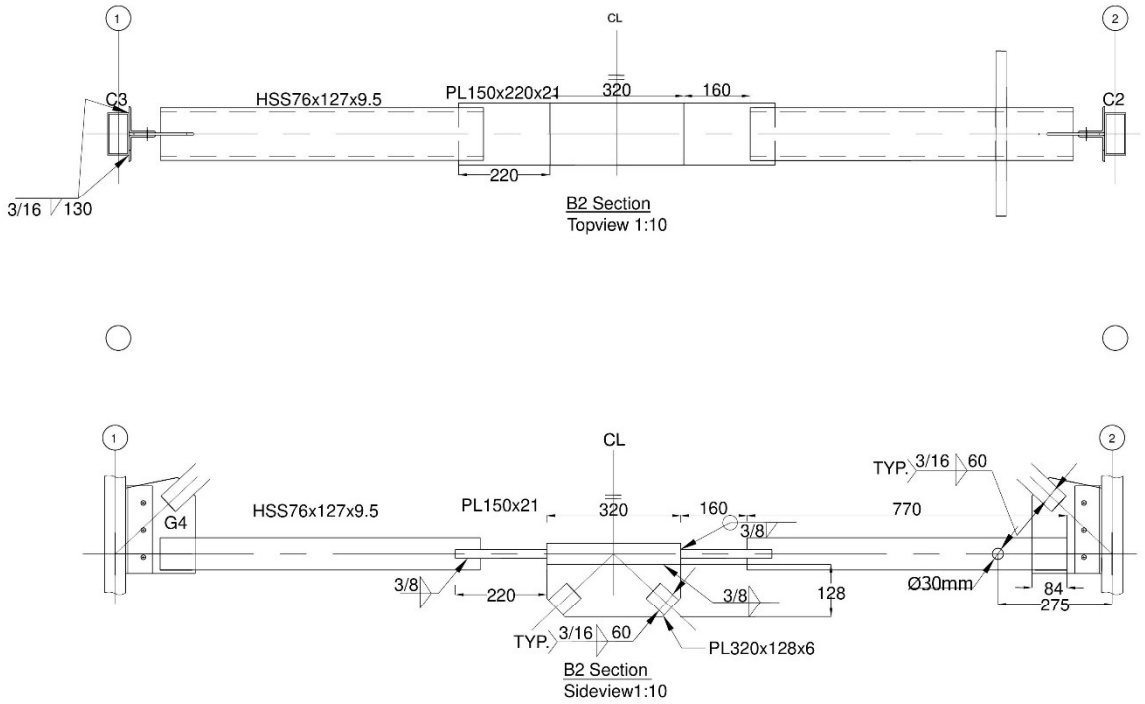

Shake Table Test Drawings A4
Prepared by : Liang Chen
2017-02-11

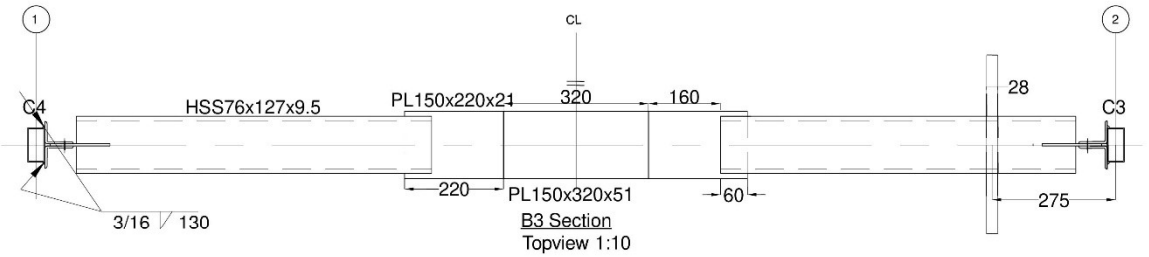

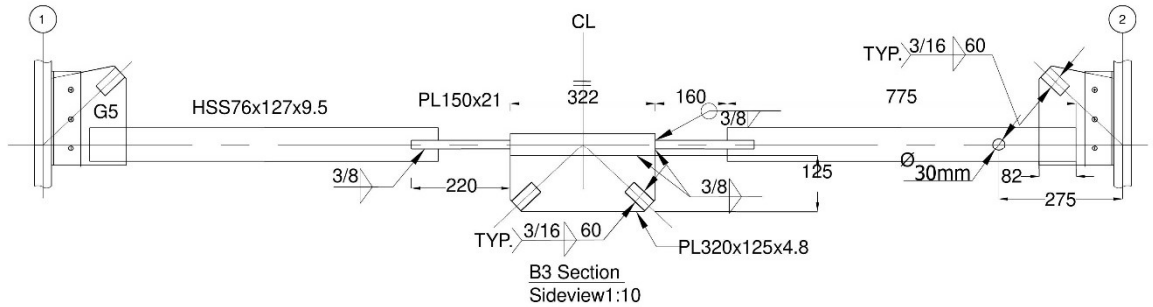

Shake Table Test Drawings A5
Prepared by : Liang Chen
2017-02-11

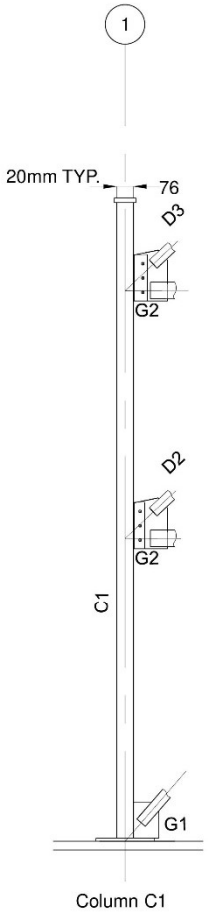

Column C1

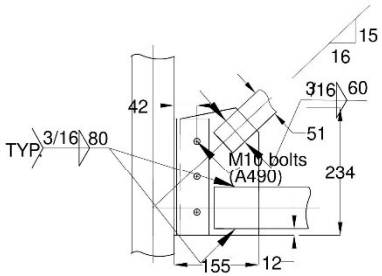

Gusset Detail: G2
1:8

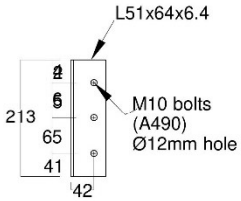

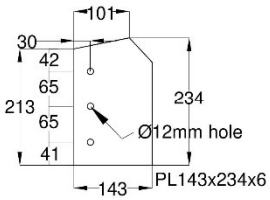

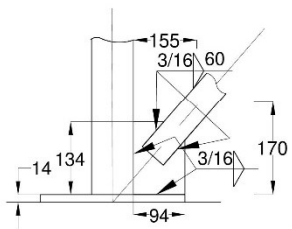

Gusset Detail: G1
1:8

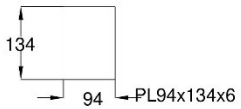

Shake Table Test Drawings A6
Prepared by : Liang Chen
2017-02-11

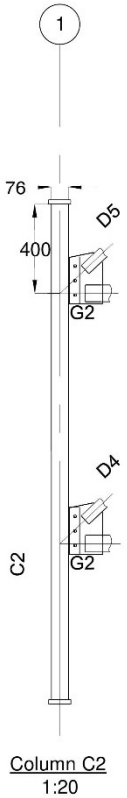

Column C2
1:20

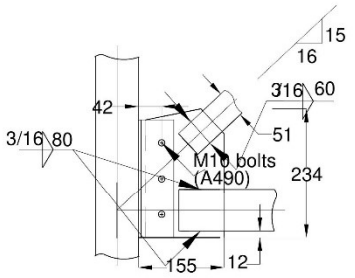

Gusset Detail:
G2 1:8

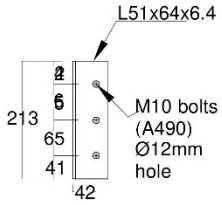

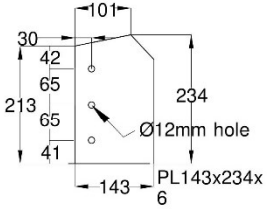

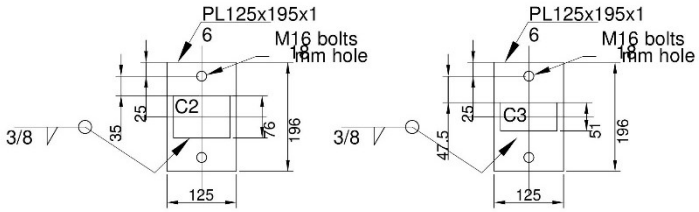

Detail: A
1:8

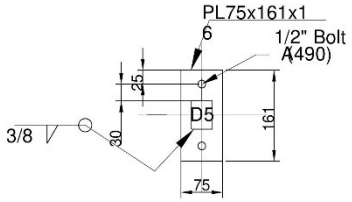

Detail: B
1:8

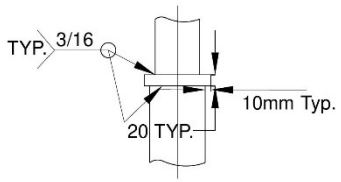

Column
Splices

Shake Table Test Drawings A7
Prepared by : Liang Chen
2017-02-11

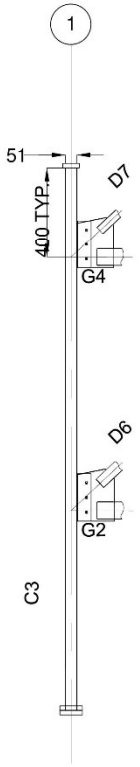

Column C3
1:20

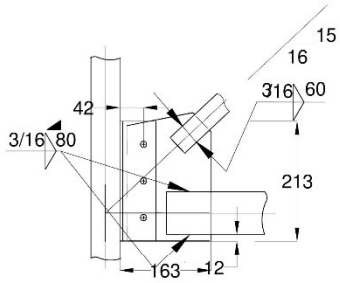

Gusset Detail: G4
1:8

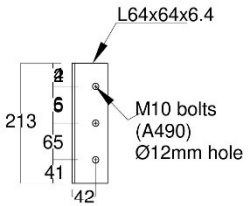

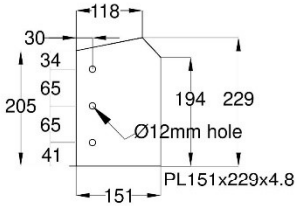

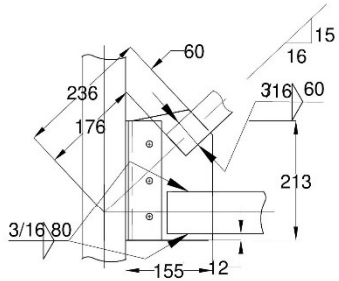

Gusset Detail: G2
1:8

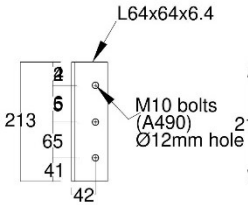

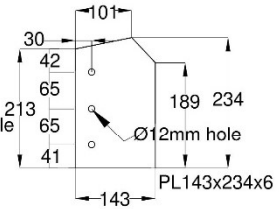

Shake Table Test Drawings A8
Prepared by : Liang Chen
2017-02-11

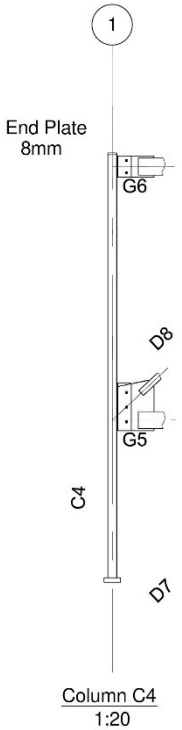

Column C4
1:20

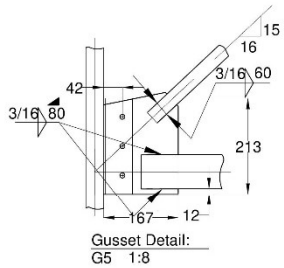

Gusset Detail:
G5 1:8

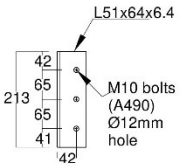

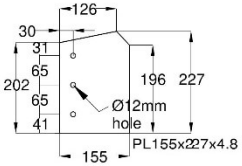

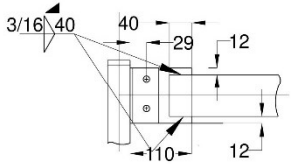

Gusset Detail: G6
1:8

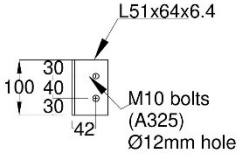

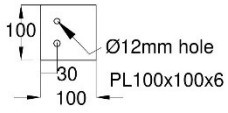

Shake Table Test Drawings A9
Prepared by : Liang Chen
2017-02-11

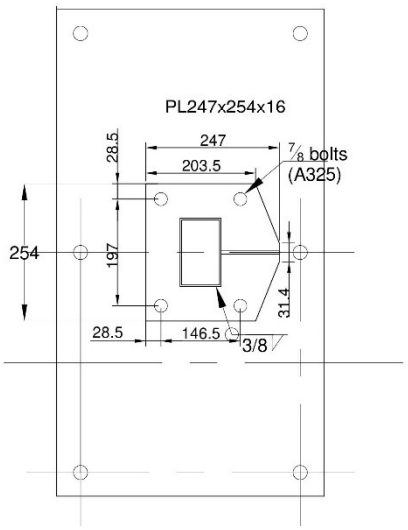

Base Plate Detail
1:8

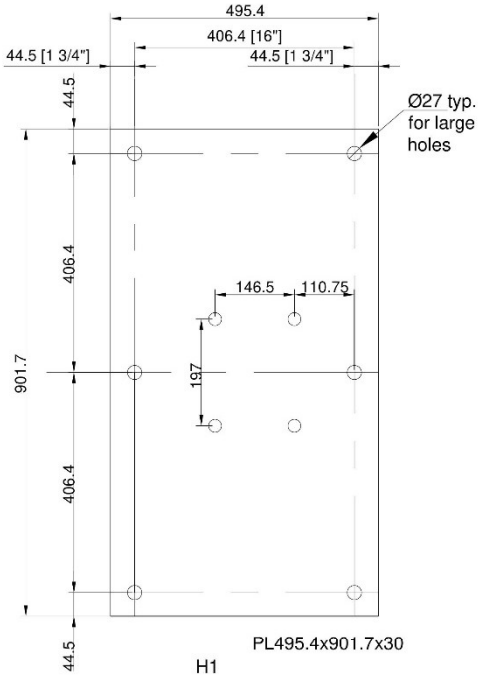

H1

Shake Table Test Drawings A10
Prepared by : Liang Chen
2017-02-11

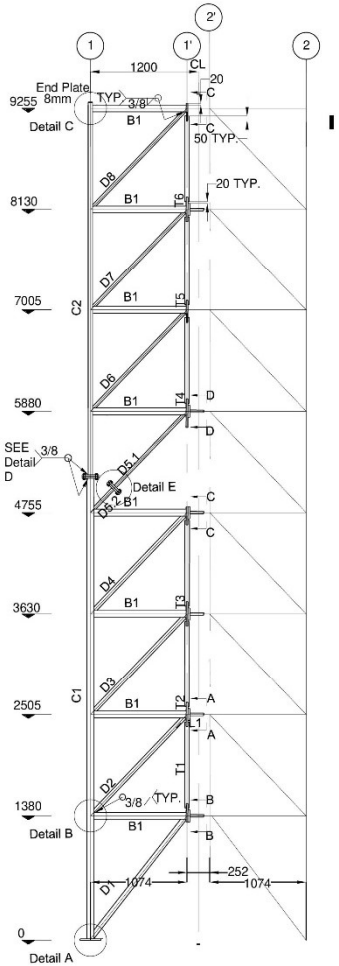

Elevation View
1:50

Shake Table Test Drawings S1
Prepared by : Liang Chen
2017-02-11

Brace	Length (mm)	Section
D1	1670	HSS3x2x0.125
D2	1457	HSS3x2x0.125
D3	1457	HSS3x2x0.125
D4	1457	HSS3x2x0.125
D5.1	300	HSS3x2x0.125
D5.2	1121	HSS3x2x0.125
D6	1474	HSS3x1.5x0.125 A500
D7	1474	HSS2x1.5x0.125 A500
D8	1474	HSS2x1.5x0.125 A500

Tie	Length (mm)	Section
T1	930	HSS1.5x1.5x0.1 A500
T2	930	HSS1.5x1.5x0.1 A500
T3	951	HSS1.5x1.5x0.1 A500
T4	951	HSS1.5x1.5x0.1 A500
T5	981	HSS1.5x1.5x0.1 A500
T6	951	HSS2x1x0.188 A500

Column	Length (mm)	Section
C1	5135	HSS5x3x0.188
C2	4110	HSS5x2x0.125 A500

Beam	Length (mm)	Section
B1	1043	HSS3x5x0.375

	Grade
HSS	G40
Plate	A36

Shake Table Test Drawings S2
Prepared by : Liang Chen
2017-02-11

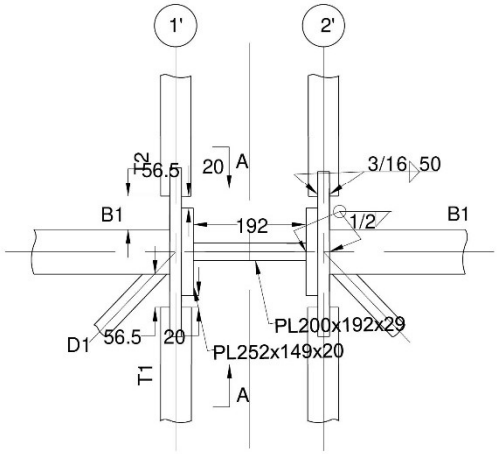

Connection Detail L1
1:8

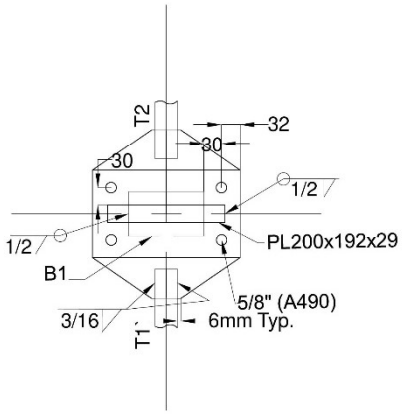

Section A
1:8

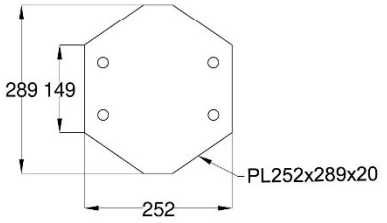

Shake Table Test Drawings S3
Prepared by : Liang Chen
2017-02-11

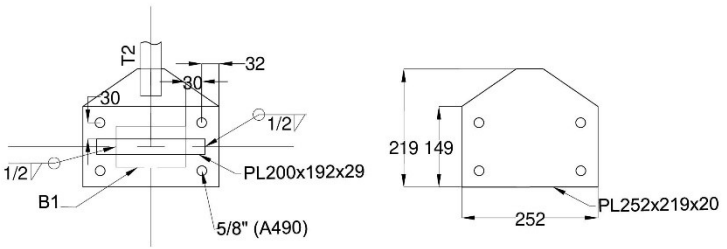

Section B
1:8

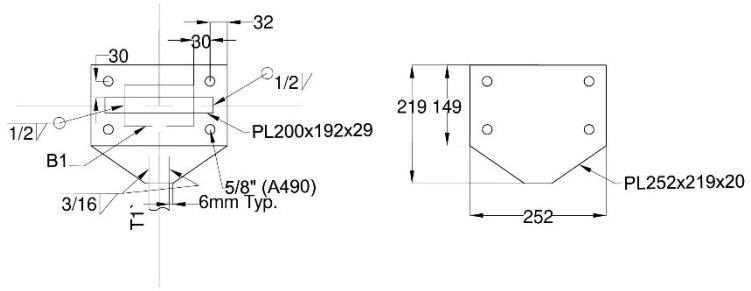

Section C
1:8

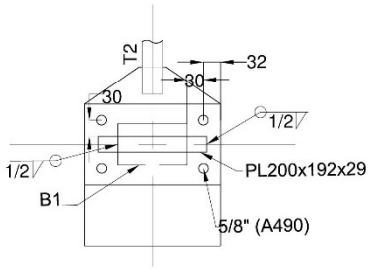

Section D
1:8

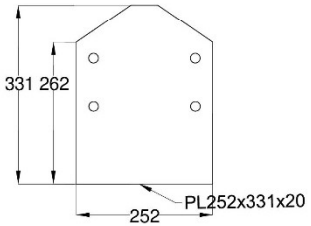

Shake Table Test Drawings S4
Prepared by : Liang Chen
2017-02-11

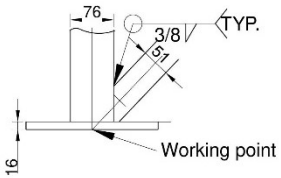

Detail A
1:8

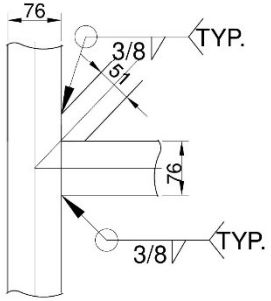

Detail B
1:8

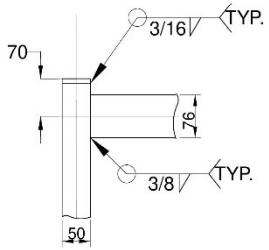

Detail C
1:8

Shake Table Test Drawings S5
Prepared by : Liang Chen
2017-02-11

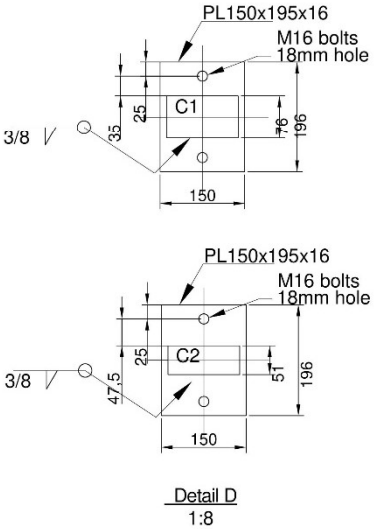

Detail D
1:8

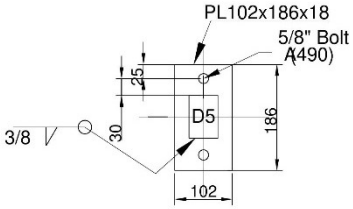

Detail E
1:8

Shake Table Test Drawings S5
Prepared by : Liang Chen
2017-02-11

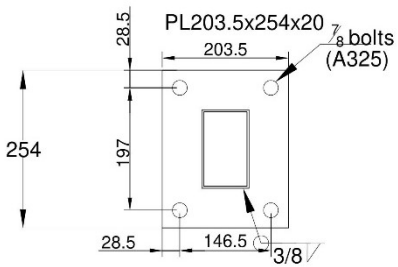

Base Plate Detail
1:8

Shake Table Test Drawings S7
Prepared by : Liang Chen
2017-02-11

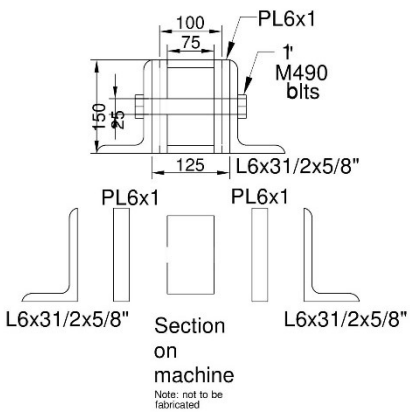

Mass Connector Front View 1:8

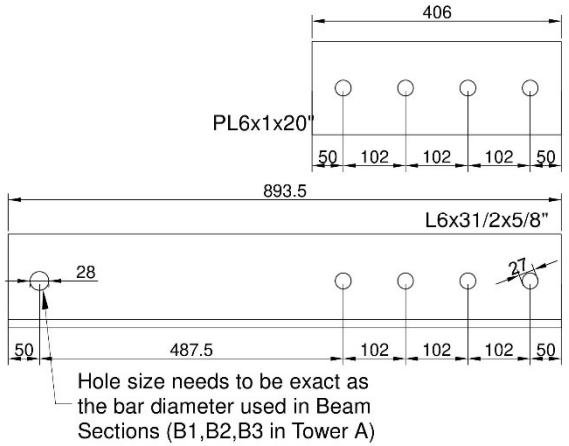

Mass Connector Section View 1:8

Shake Table Test Drawings S8
Prepared by : Liang Chen
2017-02-11